

EFFECT OF THE GREEN TEA POLYPHENOL, EGCG, ON INSULIN SENSITIVITY

by

Huei Leng Helena Ng, BBiotech (Hons)

A thesis submitted in fulfilment of the requirements for the degree of
Doctor of Philosophy (Medical Research)

Menzies Research Institute Tasmania

University of Tasmania

April 2014



Table of contents

Table of contents	i
List of Figures.....	vi
List of Tables	viii
Statement..	ix
Authority of Access	ix
Abstract	x
Acknowledgement	xii
Abbreviations	xiii
Preface.....	xvi
Chapter 1 Introduction.....	1
1.1 Insulin	2
1.1.1 Signalling pathway of insulin.....	3
1.1.2 Haemodynamic actions of insulin	3
1.1.2.1 Insulin signalling in vascular endothelium.....	3
1.1.2.2 Insulin-mediated vasodilation	6
1.1.2.3 Vascular distribution in skeletal muscle.....	7
1.1.2.4 Insulin-mediated microvascular recruitment.....	10
1.1.3 Metabolic actions of insulin	12
1.2 Insulin resistance	13
1.3 Tea derived from <i>Camellia sinensis</i>	16
1.3.1 Health benefits of polyphenols.....	17
1.3.2 Green tea.....	19
1.4 Green tea and type 2 diabetes	21
1.4.1 Epidemiology studies	21
1.4.2 Clinical studies	22
1.4.2.1 Oolong Tea	22
1.4.2.2 Green tea.....	22
1.4.3 Animal studies	24
1.4.3.1 Studies in healthy animals	25
1.4.3.2 Studies in insulin resistant animals.....	26
1.5 Mechanism of action of EGCG	30

1.5.1 Metabolic actions of EGCG	30
1.5.2 Vascular actions of EGCG	31
1.6 Study aims	33
Chapter 2 Methods & materials.....	34
2.1 Materials	35
2.2 Animal care	35
2.3 Isolated constant-flow perfused rat hindlimb procedure	36
2.3.1 Perfusion buffer	36
2.3.2 Animal surgery	37
2.3.3 Perfusion apparatus	37
2.4 <i>In vivo</i> experiment in anaesthetized rats.....	40
2.4.1 Animal surgery	40
2.4.2 Hyperinsulinaemic euglycaemic clamp.....	43
2.4.3 Glucose and lactate determination.....	43
2.4.4 Plasma insulin determination	43
2.4.5 Plasma free fatty acids determination.....	44
2.4.6 Determination of plasma EGCG levels	45
2.4.7 Measurement of muscle microvascular perfusion.....	45
2.4.8 Muscle-specific glucose uptake.....	50
2.5 Akt Western blot.....	51
2.6 Statistical analysis	52
Chapter 3 Direct metabolic and vascular effects of EGCG in rat skeletal muscle.....	53
3.1 Introduction	54
3.2 Methods	55
3.2.1 Animals	55
3.2.2 Constant-flow perfused rat hindlimb: Metabolic studies	56
3.2.2.1 Protocol 1.....	56
3.2.2.2 Protocol 2.....	57
3.2.2.3 Hindlimb glucose uptake.....	59
3.2.2.4 Muscle-specific glucose uptake (R'g)	59
3.2.3 Constant-flow perfused rat hindlimb: Vascular studies	59
3.2.4 Statistical analysis	61
3.3 Results	61

3.3.1 Metabolic effects of EGCG in perfused rat hindlimbs	61
3.3.2 Vascular effects of EGCG in perfused rat hindlimbs	67
3.3.2.1 Low dose NE (0.6 μ M, Type A vasoconstrictor)	67
3.3.2.2 High dose NE (5 μ M, Type B vasoconstrictor)	67
3.3.2.3 5-HT (Type B vasoconstrictor)	68
3.4 Discussion	70
3.4.1 Metabolic studies	70
3.4.2 Vascular studies	71
Chapter 4 Mechanism of EGCG-induced vasodilation in muscle vasculature	75
4.1 Introduction	76
4.2 Methods	79
4.2.1 Animals	79
4.2.2 Experimental protocols	79
4.2.3 Metabolic actions of wortmannin in constant perfused rat hindlimbs	83
4.2.4 AMPK Western blot	85
4.2.5 Statistical analysis	85
4.3 Results	86
4.3.1 Effects of NOS inhibition on EGCG-mediated vasodilation	86
4.3.2 Effects of PI3-K inhibition on EGCG-mediated vasodilation	86
4.3.3 Effects of SFKs inhibition on EGCG-mediated vasodilation	87
4.3.4 Effects of AMPK inhibition on EGCG-mediated vasodilation	88
4.4 Discussion	95
Chapter 5 Acute effects of EGCG in healthy rats <i>in vivo</i>	98
5.1 Introduction	99
5.2 Methods	100
5.2.1 Animals	100
5.2.2 Experiment protocol	101
5.2.3 Pharmacokinetics of intravenously administered EGCG	103
5.2.4 Statistical Analysis	103
5.3 Results	105
5.3.1 Animal characteristics	105
5.3.2 Whole body insulin sensitivity	105
5.3.3 Haemodynamic parameters	107

5.3.4 Microvascular blood volume	110
5.3.5 Muscle insulin sensitivity	110
5.4 Discussion.....	114
Chapter 6 Acute effects of EGCG in insulin resistant rats <i>in vivo</i>	117
6.1 Introduction	118
6.2 Methods	119
6.2.1 Animals	119
6.2.2 Experimental protocol	120
6.2.2.1 Constant-flow perfused rat hindlimb.....	120
6.2.2.2 <i>In vivo</i> study	122
6.2.3 Statistical Analysis	123
6.3 Results	123
6.3.1 Animal characteristics	123
6.3.2 Vascular actions of EGCG in the perfused rat hindlimb.....	124
6.3.3 Acute effects of EGCG in insulin resistant rats <i>in vivo</i>	126
6.3.3.1 Whole body insulin sensitivity	126
6.3.3.2 Haemodynamic parameters	128
6.3.3.3 Muscle microvascular perfusion.....	131
6.3.3.4 Muscle insulin sensitivity	133
6.4 Discussion.....	135
Chapter 7 Chronic effects of EGCG in insulin resistant rats <i>in vivo</i>	139
7.1 Introduction	140
7.2 Methods	141
7.2.1 Animals	141
7.2.2 Experimental protocol	142
7.2.3 Western blot	145
7.2.4 Statistical analysis	145
7.3 Results	146
7.3.1 Animal characteristics	146
7.3.2 Chronic effects of EGCG on whole body insulin sensitivity in insulin resistant rats	150
7.3.3 Chronic effects of EGCG on haemodynamic parameters <i>in vivo</i>	152
7.3.4 Chronic effects of EGCG on muscle microvascular perfusion <i>in vivo</i>	155
7.3.5 Chronic effects of EGCG on muscle insulin sensitivity <i>in vivo</i>	155

7.4 Discussion.....	159
Chapter 8 Discussion	164
8.1 Summary of findings	165
8.2 Vascular actions of EGCG in skeletal muscle.....	165
8.3 Metabolic actions of EGCG in skeletal muscle.....	169
8.4 Implications	174
8.5 Limitations and future directions.....	178
8.6 Conclusion.....	180
References	182

List of Figures

Figure 1.1 Insulin signalling pathway.	5
Figure 1.2 Schematic diagram of nutritive and non-nutritive flow routes in muscle.....	9
Figure 1.3 Natural history of type 2 diabetes.	15
Figure 1.4 Polyphenol classification.	18
Figure 1.5 Major flavan-3-ols and their chemical structure in green tea.	20
Figure 1.6 Mechanism of action of EGCG in various tissues	32
Figure 2.1 Schematic diagram of surgically isolated flow to rat single hindlimb.....	38
Figure 2.2 Perfusion apparatus.	39
Figure 2.3 Schematic diagram of the surgical cannulations for <i>in vivo</i> experiments....	42
Figure 2.4 Example of (A) ultrasound and (B) contrast enhanced ultrasound images of the upper thigh of the rat hindlimb in short axis	47
Figure 2.5 Contrast enhanced ultrasound images at different time points of microbubble infusion.	48
Figure 2.6 Representative microbubble replenishment curve.	49
Figure 3.1 Experimental protocols of perfused rat hindlimb metabolic studies.....	58
Figure 3.2 Experimental protocol of perfused rat hindlimb vascular studies.....	60
Figure 3.3 Dose-response effects of EGCG on hindlimb glucose uptake in 9FD rats ...	63
Figure 3.4 Effect of EGCG on ³ H-2-DG muscle glucose uptake in 9FD rats.....	64
Figure 3.5 Effect of 10 µM EGCG on hindlimb glucose uptake in 5FD rats	65
Figure 3.6 Effect of 10 µM EGCG on ¹⁴ C-2-DG muscle glucose uptake in 5FD rats ...	66
Figure 3.8 Schematic illustration of the two blood flow circulations in skeletal muscle – the nutritive and non-nutritive blood flows	72
Figure 4.1 Potential pathways of EGCG mediated vasodilation in vascular endothelium of skeletal muscle	78
Figure 4.2 Experimental protocols	81
Figure 4.3 Schematic illustration of potential mechanism of EGCG-mediated vasodilation in skeletal muscle.....	82
Figure 4.4 Effects of wortmannin on muscle glucose uptake	84
Figure 4.5 Dose-response effects of EGCG on % vasoconstriction in 5-HT pre-constricted hindlimb during NO synthase inhibition in the presence of L-NAME	89
Figure 4.6 Dose-response effects of EGCG on % vasoconstriction in 5-HT pre-constricted hindlimb during PI3-K inhibition in the presence of wortmannin	90

Figure 4.7 Effects of PI3-K inhibition by 100 nM wortmannin on muscle glucose uptake	91
Figure 4.8 Dose-response effects of EGCG on % vasoconstriction in high dose NE pre-constricted hindlimb during SFK inhibition in the presence of PP2	92
Figure 4.9 Dose-response effects of EGCG on % vasoconstriction in 5-HT pre-constricted hindlimb during AMPK inhibition in the presence of Compound C	93
Figure 4.10 Ratio of pAMPK/AMPK _{total} in common iliac arteries following 10 µM compound C treatments	94
Figure 5.1 Experimental protocol for <i>in vivo</i> study in healthy animals	102
Figure 5.2 Plasma EGCG concentrations following the administration of 50 mg.kg ⁻¹ EGCG bolus.....	104
Figure 5.3 (A) Glucose infusion rate and (B) blood glucose levels during hyperinsulinaemic euglycaemic clamp.....	106
Figure 5.4 Mean arterial blood pressure during hyperinsulinaemic euglycaemic clamp	108
Figure 5.5 Femoral artery blood flow at the end of experiment.....	109
Figure 5.6 Microvascular blood volume before and during hyperinsulinaemic euglycaemic clamp	111
Figure 5.7 Muscle ³ H-2-DG uptake after hyperinsulinaemic euglycaemic clamp.....	112
Figure 5.8 Western blot of pAkt and total Akt in skeletal muscle	113
Figure 6.1 Experimental protocol of perfused rat hindlimb vascular studies.....	121
Figure 6.2 Experimental protocol for <i>in vivo</i> study in insulin resistant animals	122
Figure 6.3 Dose-response effects of EGCG on % vasoconstriction during 5-HT infusions in insulin resistant rat hindlimbs	125
Figure 6.4 Acute effects of EGCG on whole body insulin sensitivity in insulin resistant rats	127
Figure 6.5 Effects of EGCG on haemodynamic parameters in insulin resistant rats ...	129
Figure 6.6 Femoral artery blood flow at the end of experiment in insulin resistant rats	130
Figure 6.7 Microvascular blood volume before and during hyperinsulinaemic euglycaemic clamp in insulin resistant rats	132
Figure 6.8 Muscle ¹⁴ C-2-DG uptake at the end of hyperinsulinaemic euglycaemic clamp in insulin resistant rats	134
Figure 7.1 Experimental protocol for <i>in vivo</i> study in chronic EGCG-treated animals	143
Figure 7.2 An illustration of experimental groups used for Chapter 6 and Chapter 7 .	144

Figure 7.3 Rat body weight during dietary intervention	147
Figure 7.4 Food (A) and energy (B) intake of rats during dietary intervention	148
Figure 7.5 Water (A) and EGCG (B) intake of rats during dietary intervention.....	149
Figure 7.6 Chronic effects of EGCG on whole body insulin sensitivity in insulin resistance rats.....	151
Figure 7.7 Chronic effects of EGCG on haemodynamic parameters	153
Figure 7.8 Chronic effects of EGCG on femoral artery blood flow at the end of hyperinsulinaemic euglycaemic clamp in insulin resistant rats	154
Figure 7.9 Microvascular blood volume during hyperinsulinaemic euglycaemic clamp	156
Figure 7.10 Muscle ¹⁴ C-2-DG uptake after hyperinsulinaemic euglycaemic clamp....	157
Figure 7.11 Western blot of insulin signalling in skeletal muscle	158
Figure 8.1 Vascular and metabolic actions of EGCG in vivo.	177

List of Tables

Table 1.1 Composition of major polyphenols in green tea	20
Table 1.2 Summary of acute and chronic effects of EGCG in human and animal studies	29
Table 2.1 Macronutrient content of experimental diets.....	36
Table 6.1 Animal characteristics following 3 – 4 weeks of HFD treatment	124
Table 7.1 Chronic effects of EGCG on basal characteristics of the rats	150

Statement

The work in the present thesis has exclusively been for the use of a Ph.D. in the area of biomedical research. The data in this thesis has not been used for any other higher degree or graduate diploma in any other university. All experimental and written work is my own, except which has been referenced accordingly and all experimental work abides by the Australian ethical conduct codes regarding animal experimentation.



Helena Ng Huei Leng

Authority of Access

This thesis may be made available for loan and limited copying and communication in accordance with the Copyright Act 1968



Helena Ng Huei Leng

Abstract

Insulin resistance contributes to and precedes the development of type 2 diabetes. Insulin-stimulated microvascular perfusion and glucose uptake in skeletal muscle are important components of glucose homeostasis, and are impaired during insulin resistance. Epidemiological studies suggest that regular green tea consumption may lower the risk for developing type 2 diabetes. Whether green tea or its components could be used as an alternative treatment for type 2 diabetes is not known. The primary aim of this thesis was to investigate the effects of epigallocatechin gallate (EGCG), a green tea polyphenol, on vascular function and glucose metabolism in skeletal muscle.

The direct vascular and metabolic actions of EGCG in skeletal muscle were assessed *in situ* using the isolated, constant-flow perfused rat hindlimb. In this study, four different doses of EGCG were studied: 0.1, 1, 10, and 100 μM . EGCG (1 – 10 μM) caused nitric oxide synthase (NOS)-dependent vasodilation against 5-hydroxytryptamine (5-HT). However, EGCG-mediated vasodilation was independent of PI3-kinase or AMP-kinase activation. EGCG had no direct effects on muscle glucose uptake in the presence or absence of insulin at any of the doses tested. This indicates that EGCG has direct vascular, but not metabolic, actions in skeletal muscle.

Since EGCG had direct vascular effects in muscle its effects on microvascular perfusion and insulin-mediated glucose metabolism *in vivo* were then investigated. The acute and chronic effects of EGCG on vascular function and glucose metabolism were investigated in normal healthy and diet-induced insulin resistant rats *in vivo* under anaesthesia. Hyperinsulinaemic euglycaemic clamp was used to determine the acute and chronic effects of EGCG on whole body insulin sensitivity. In the acute studies, EGCG was infused intravenously to increase plasma EGCG to 10 μM . Acute EGCG stimulated muscle microvascular perfusion in both healthy and insulin resistant rats, but was not additive to insulin-stimulated microvascular perfusion. Acute EGCG did not stimulate muscle glucose uptake or enhance insulin-stimulated muscle glucose uptake. However, acute EGCG treatment improved whole body insulin sensitivity (glucose infusion rate, GIR) by 12% in insulin resistant rats but not healthy rats.

In the chronic studies, high fat-fed rats were given EGCG in their drinking water (200 mg.kg⁻¹.d⁻¹) for 4 weeks to determine whether EGCG could prevent the development of insulin resistance. Chronic EGCG treatment improved whole body insulin sensitivity (GIR) by 21% and insulin-stimulated muscle glucose uptake by 67%. However, chronic EGCG treatment had no effect on muscle microvascular perfusion. This suggests that chronic EGCG treatment improved glucose metabolism, without altering vascular function of insulin resistant rats.

The data from this thesis demonstrate that acute and chronic EGCG treatment exhibit distinct vascular and metabolic effects *in vivo* in rats. Acute EGCG treatment stimulated microvascular perfusion, but not glucose uptake in skeletal muscle. Chronic EGCG treatment improved whole body and muscle insulin sensitivity, but not muscle microvascular perfusion. Together these data provide a mechanistic insight into the potential anti-diabetic effects of chronic EGCG treatment, and support its development as a promising new therapeutic agent for prevention of insulin resistance and type 2 diabetes.

Acknowledgement

First of all, I would like to extend my sincere thanks to my primary supervisor Dr. Michelle Keske for her continual encouragement and advice in these 4 years. This thesis would not have been possible without her help and support. I feel very fortunate to have the opportunity to work with her.

I would also like to thank Prof. Stephen Rattigan for his technical assistance and advice, especially at the beginning of my PhD candidature when Michelle was on maternity leave. I would like to thank Dr. Stephen Richards for his advice and all the help with editing the work in this thesis. “Michelle Keske is awesome! So does Steve(s)!”

I would also like to thank many past and present members of the muscle research group, including Eloise Bradley, Dino Premilovac, Renee Dwyer, Carol Bussey, Hamish Scott, James Peters, Katherine Roberts-Thomson, Sarah Blackwood, Aascha Brown, and Barbara Arnts for their helpful suggestions and friendship. Special thanks also go to the collaborators of this project, Prof. Michael Quon and Dr. Ranganath Muniyappa for their advice and sponsorship of the EGCG. I wish to thank all the staff at the animal facility for their hardwork. Special thanks to Diabetes Tasmania for their support in the past 4 years.

Last but not least, thanks to my family and friends for their never-ending love, support and patience.

Abbreviations

AMP	Adenosine monophosphate
AMPK	Adenosine monophosphate-activated protein kinase
ANOVA	Analysis of variance
APS	Adapter protein with pleckstrin homology and Src homology 2 domains
CAM	Complementary and alternative medicine
CAMK	Calmodulin-dependent protein kinase
CAMKK	Calmodulin-dependent protein kinase kinase
CEU	Contrast enhanced ultrasound
dpm	Disintegration per minute
EGCG	Epigallocatechin gallate
ELISA	Enzyme-linked immunosorbent assay
eNOS	Endothelial nitric oxide synthase
ET-1	Endothelin 1
FBF	Femoral artery blood flow
GIR	Glucose infusion rate
GLUT4	Glucose transporter 4
G6Pase	Glucose-6-phosphatase
HbA1c	Haemoglobin A1c
HDL	High density lipoprotein
HFD	High fat diet
HOMA-IR	Homeostasis model assessment of insulin resistance
HPLC	High performance liquid chromatography
IGF-1	Insulin-like growth factor 1
IRS	Insulin receptor substrate
LDL	Low density lipoprotein

L-NAME	<i>N</i> ^ω -nitro-L-arginine-methyl ester
L-NMMA	<i>N</i> ^G -monomethyl-L-arginine
MAP	Mean arterial blood pressure
MAPK	Mitogen-activated protein kinase
MBV	Microvascular blood volume
mcad	Medium chain acyl coA decarboxylase
NADPH	Nicotinamide adenine dinucleotide phosphate
NE	Norepinephrine
nrf	nuclear respiratory factor
NO	Nitric oxide
NOS	Nitric oxide synthase
OLETF	Otsuka Long-Evans Tokushima Fatty
PEPCK	Phosphoenolpyruvate carboxykinase
PI3-K	Phosphatidylinositol 3-kinase
PPAR γ	Peroxisome proliferator-activated receptor γ
PP2	4-Amino-3-(4-chlorophenyl)-1-(t-butyl)-1H-pyrazolo[3,4-d]pyrimidine
QUICKI	Quantitative insulin sensitivity check index
R'g	Rate of glucose uptake
ROS	Reactive oxygen species
SEM	Standard error of mean
SFK	Src family tyrosine kinases
SHRs	Spontaneously hypertensive rats
SNP	Sodium nitroprusside
TNF α	Tumour necrosis factor α
ucp	Uncoupling protein
V _D	Volume of distribution
ZDF	Zucker diabetic fatty

1-MX	1-methylxanthine
2-DG	2-deoxyglucose
5-HT	5-hydroxytryptamine

Preface

Some of the data obtained in the present thesis has been published or presented at scientific meetings and are listed below.

Publications

Premilovac D, Bradley EA, **Ng HLH**, Richards SM, Rattigan S and Keske MA. Muscle insulin resistance resulting from impaired microvascular insulin sensitivity in Sprague Dawley rats. *Cardiovascular Research*. (2013) 98, 28-36 (Chapter 3)

Premilovac D, **Ng HLH**, Richards SM, Bradley EA, Dwyer RM, Rattigan S, and Keske MA. Role for the microvasculature in glucose uptake in skeletal muscle, in *Glucose Uptake: Regulation, Signaling Pathways and Health Implications*. Nova Science Publishers, Inc., Hauppauge, NY, USA. (2013) 109-139 (Chapter 3)

Oral presentations at conferences

Invited talk at the “*International Conference on Clinical Research*”. San Francisco, CA, USA. July 2011. Keske MA, Premilovac D, **Ng HLH** and Rattigan S. Imaging skeletal muscle microcirculation with contrast-enhanced ultrasound: diagnostic and therapeutic approaches to insulin resistance.

Australian Diabetes Society/Australian Diabetes Educators Association Annual Scientific Meeting, Perth, WA, Australia. September 2011. Premilovac D, **Ng HLH**, Richards SM, Bradley EA, Rattigan R and Keske MA. Moderate increases in dietary fat impair microvascular and metabolic actions of insulin in skeletal muscle of Sprague Dawley rats.

Posters at conferences

Australian Diabetes Society/Australian Diabetes Educators Association Annual Scientific Meeting, Sydney, NSW, Australia. September, 2010. Keske MA, **Ng HLH**, Scott HW, Richards SM, Muniyappa R, Quon MJ and Rattigan S. Vascular actions of EGCG, a green tea polyphenol, in the constant-flow perfused rat hindlimb.

Experimental Biology, San Diego, CA, USA. April 2012. Richards SM, Premilovac D, **Ng HLH**, Bradley EA, Rattigan S and Keske MA. Moderate increases in dietary fat impair microvascular but not myocyte actions of insulin in skeletal muscle of Sprague Dawley rats.

Sharing Excellence in Research, Sandy Bay, TAS, Australia, September 2012. **Ng HLH**, Rattigan S and Keske MA. Acute metabolic and vascular actions of the green tea polyphenol EGCG in rat skeletal muscle.

Drug Discovery & Therapy World Congress 2013, Boston, MA, USA. June 2013. **Ng HLH**, Keske MA. Effects of the Green Tea Polyphenol Epigallocatechin 3-Gallate (EGCG) on Insulin Sensitivity.

American Diabetes Association 73rd Scientific Sessions, Chicago, IL, USA. June, 2013. **Ng HLH**, Rattigan S, Richards SM, Muniyappa R, Quon MJ, and Keske MA. Chronic, but not Acute, Treatment with the Green Tea Polyphenol Epigallocatechin 3-Gallate (EGCG) Ameliorates High Fat Diet (HFD)-Induced Insulin Resistance in Rats

Chapter 1

Introduction

Diabetes is a chronic disease affecting more than 371 million people globally (1). Diabetes is characterised by high circulating glucose levels, which can lead to damage to blood vessels, heart, eyes, kidneys, and nerves. There are three major types of diabetes, including type-1 diabetes, type 2 diabetes, and gestational diabetes. Of all the cases of diabetes, 85 – 95% are type 2 diabetes (1). Type 2 diabetes is associated with older age, physical inactivity, obesity, hypertension, hypercholesterolaemia, hyperlipidaemia, and cardiovascular disease (2). In 2012, the International Diabetes Federation estimated as many as 183 million people worldwide with type 2 diabetes were unaware of their conditions and therefore remained undiagnosed (1). This is mainly due to diabetes being asymptomatic until the later stages of the disease. Appropriate blood glucose management using lifestyle and pharmaceutical approaches in the early stage of diabetes is vital to prevent complications that arise from this disease.

1.1 Insulin

Insulin is a 51-amino acid hormone synthesized and secreted by pancreatic β -cells in response to elevated blood glucose levels. It is responsible for post-prandial fuel storage, which increases glucose uptake into insulin sensitive tissues (skeletal muscle and adipose tissue) and reduces glucose output from liver into bloodstream. Besides its role in regulating glucose and lipid metabolism, insulin also has important haemodynamic actions.

1.1.1 Signalling pathway of insulin

The insulin receptor is a transmembrane receptor with an extracellular ligand binding domain and an intracellular tyrosine kinase domain. Upon activation by binding of insulin, the insulin receptor phosphorylates insulin receptor substrate (IRS) family members, leading to the activation of phosphatidylinositol 3-kinase (PI3-K) signalling pathway (3). Another important action of insulin is the activation of SHC, which in turn activates the mitogen-activated protein kinase (MAPK) branch of insulin signalling pathway (3) (Figure 1.1).

The downstream signalling molecules of the PI3-K branch include PDK and Akt. This PI3-K branch pathway is responsible for the metabolic actions of insulin in liver, adipose tissue, and skeletal muscle, as well as nitric oxide (NO) production by phosphorylation of endothelial NO synthase (eNOS) in endothelial cells to mediate vasodilation. The MAPK branch of the insulin signalling pathway includes RAS, RAF, MEK, and this pathway regulates mitogenesis, differentiation, and cell growth, as well as the endothelin-1 (ET-1) production in endothelial cells to mediate vasoconstriction.

1.1.2 Haemodynamic actions of insulin

1.1.2.1 Insulin signalling in vascular endothelium

The vascular endothelium is the first tissue that insulin encounters after it is secreted by pancreatic β -cells (4). Vascular endothelium acts primarily as a semi-permeable barrier that regulates transport of macromolecules such as insulin into the interstitial space (4).

Furthermore, in the presence of insulin, the endothelium stimulates the production of NO (4; 5), a potent vasodilator, and ET-1 (6), a potent vasoconstrictor (Figure 1.1). It has been proposed that a healthy endothelium has a balanced production of NO and ET-1 for maintaining a healthy vascular tone, and a disruption in this balance is associated with insulin resistance, hypertension and type 2 diabetes (4; 6; 7).

In the early 2000s, Quon and colleagues elucidated the insulin signalling pathway in vascular endothelial cells leading to NO production. To activate NO production in vascular endothelial cells, insulin binds to the insulin receptor, which in turn phosphorylates Tyr kinase (Figure 1.1). Activation of the insulin receptor resulting in stimulation of the signalling cascade, involves IRS, PI3-K, PDK, and Akt. Activated Akt phosphorylates human eNOS at Ser¹¹⁷⁷ (or Ser¹¹⁷⁹ in bovine eNOS), stimulating the activity of eNOS and production NO from vascular endothelium (4; 5; 8-10).

In addition to the NO production, insulin stimulates ET-1, a potent vasoconstrictor. ET-1 production from the vascular endothelium opposes the vasodilator actions of NO. To date, little is known about the mechanisms of insulin-stimulated ET-1 production from the vascular endothelium. Quon and colleagues have reported that ET-1 stimulation by insulin in vascular endothelium is mediated via a distinct pathway from that of the insulin-stimulated NO pathway (11-13). ET-1 stimulated by insulin is MAPK-, but not PI3-K-dependent (11-13). Inhibition of MAPK has been reported to reduce the vasoconstrictor effects of insulin and favour the vasodilation actions by insulin (14).

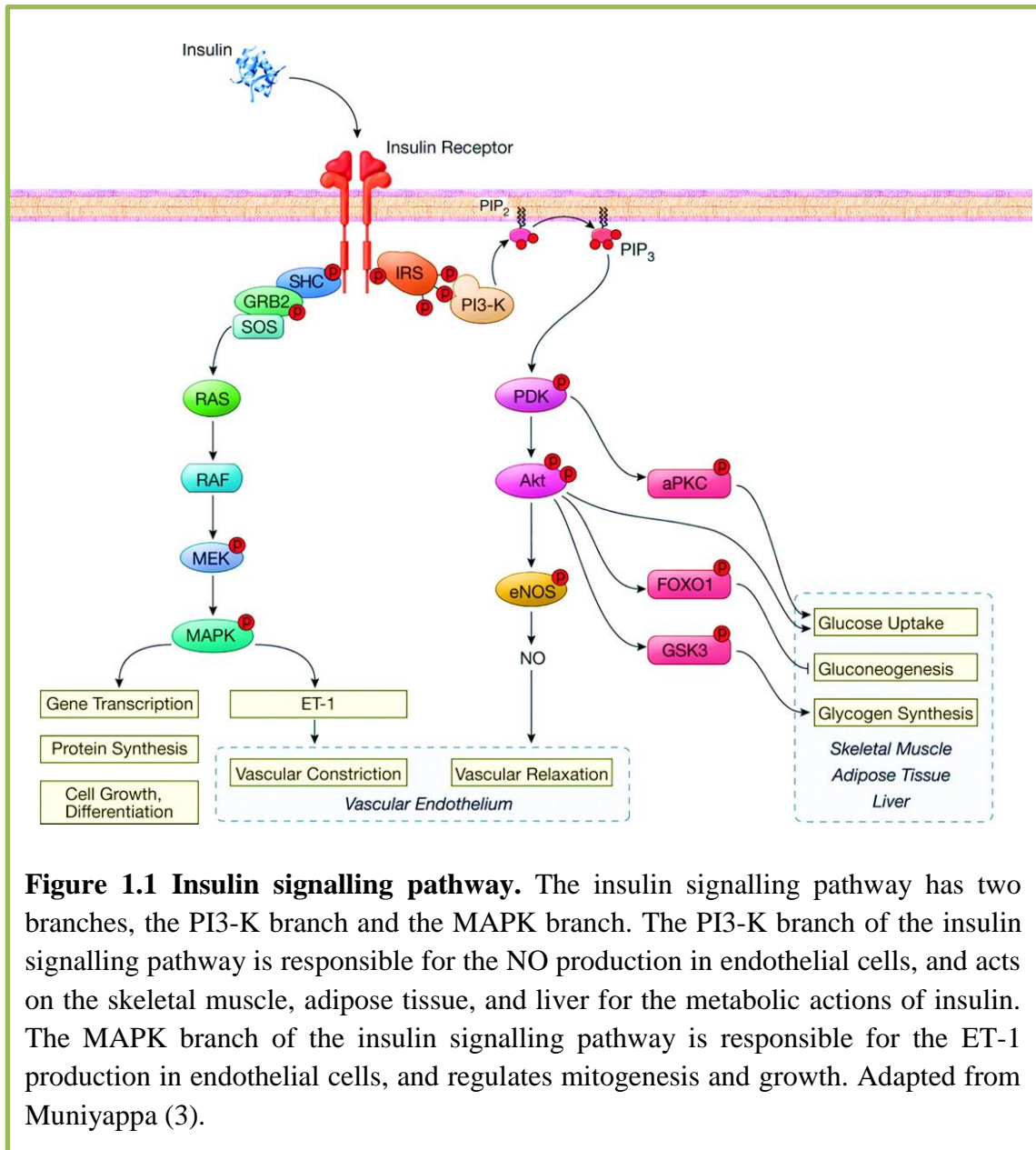


Figure 1.1 Insulin signalling pathway. The insulin signalling pathway has two branches, the PI3-K branch and the MAPK branch. The PI3-K branch of the insulin signalling pathway is responsible for the NO production in endothelial cells, and acts on the skeletal muscle, adipose tissue, and liver for the metabolic actions of insulin. The MAPK branch of the insulin signalling pathway is responsible for the ET-1 production in endothelial cells, and regulates mitogenesis and growth. Adapted from Muniyappa (3).

1.1.2.2 Insulin-mediated vasodilation

The vascular actions of insulin have been documented since the late 1930's (15). Insulin is reported to dose-dependently increase total blood flow in skeletal muscle and this is paralleled by an increase in insulin-mediated muscle glucose uptake (16). NO plays an important role in mediating insulin-stimulated vasodilation in skeletal muscle. Both insulin stimulated increases muscle blood flow and muscle glucose uptake were inhibited when NOS and NO production were inhibited by NOS inhibitors, *N*^ω-nitro-L-arginine-methyl ester (L-NAME) or *N*^G-monomethyl-L-arginine (L-NMMA) (17; 18). Therefore it has been postulated that insulin increases blood flow to skeletal muscle to enhance the delivery of insulin and glucose to skeletal muscle, thereby increasing glucose uptake into the skeletal muscle. Roy *et al.* (19) showed that NOS inhibition by L-NAME reduced whole body glucose disposal rate and muscle glucose uptake by 16% and 50% respectively in rats *in vivo*. It is important to note that NOS inhibition, however, had no effects on basal or insulin-stimulated muscle glucose uptake *in vitro* in both isolated soleus (red fibre type) and extensor digitorum longus (white fibre type) muscles (19), indicating NOS does not play a role in myocyte insulin action.

The importance of vasodilation on glucose uptake was questioned when some vasodilators increased total blood flow to skeletal muscle but did not enhance muscle glucose uptake. These include adenosine (20), epinephrine (21), bradykinin (22; 23), sodium nitroprusside (24), and low dose insulin-like growth factor 1 (IGF-1) (25). To date, the only known vasodilator, besides insulin, that increases both total blood flow to skeletal muscle and muscle glucose uptake was methacholine (23; 26). Baron and colleagues (26) proposed that site-specific vasodilation may be related to the vasodilator's metabolic actions.

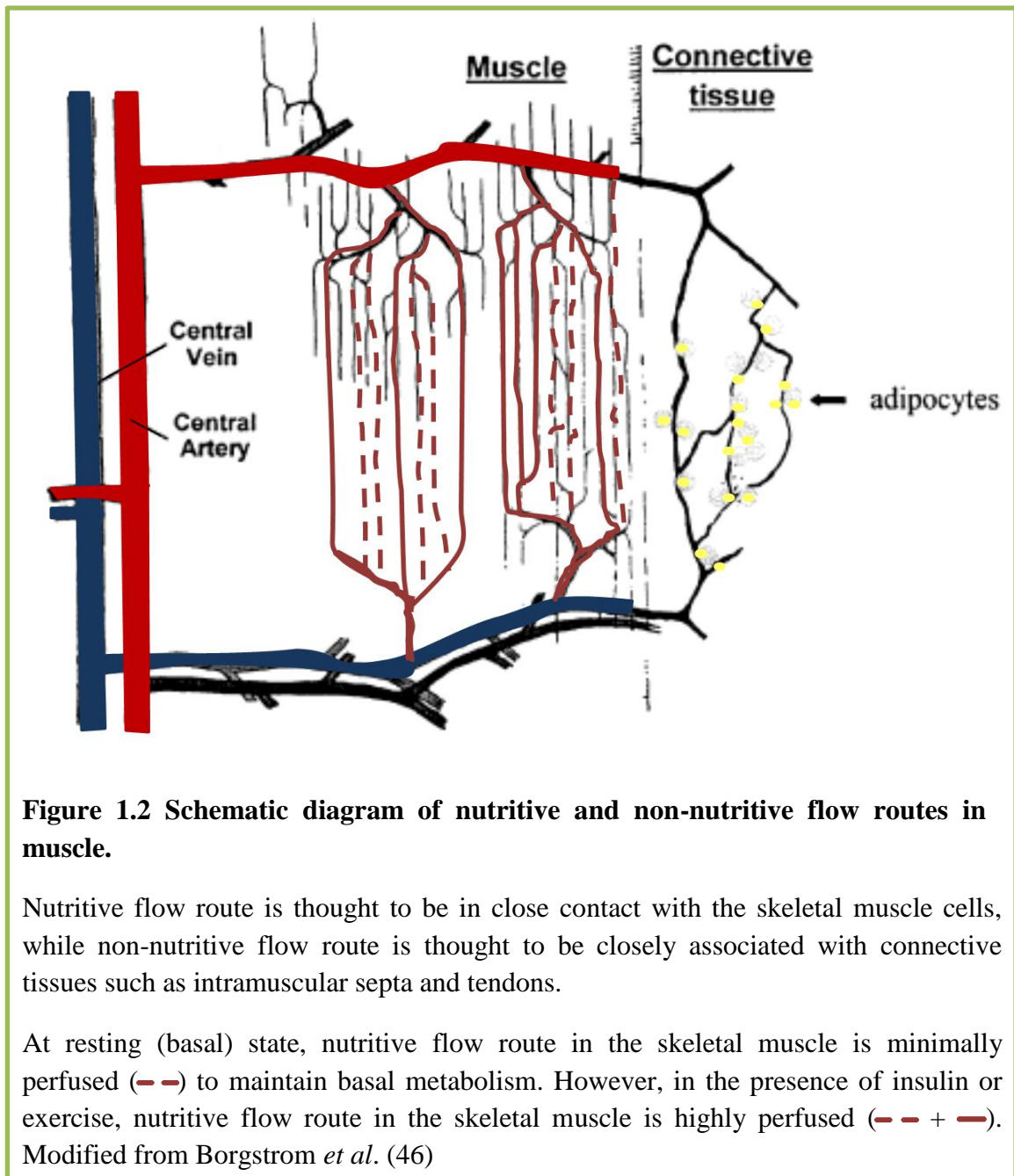
On the other hand, other studies showed that a physiological dose of insulin ($3 \text{ mU} \cdot \text{min}^{-1} \cdot \text{kg}^{-1}$) stimulated muscle glucose uptake without increasing total blood flow in muscle (18; 27). Baron and colleagues proposed that insulin, besides increasing total blood flow, could also increase capillary flow and density of perfused capillaries in skeletal muscle, which in turn increase the perfused muscle mass that was involved in glucose metabolism (28). The increases in capillary flow and density of perfused capillaries have since been known as microvascular (or capillary) recruitment (Figure 1.2). However, microvascular recruitment could not be measured directly in Baron's study due to the lack of available techniques.

1.1.2.3 Vascular distribution in skeletal muscle

It has been generally established that, groups of capillaries, not individual blood vessels, are the fundamental functional unit within the skeletal muscle (29; 30). Terminal arterioles in the skeletal muscle are responsible for regulation of the blood flow distribution of the capillaries unit (instead of each individual capillary) within the muscle microvasculature (31; 32). It has been postulated that larger arterioles ($\geq 50 \mu\text{m}$ diameter) control the resistance, hence flow through the skeletal muscle, while distal arterioles ($\sim 10 - 40 \mu\text{m}$ diameter) function similar to pre-capillary sphincters that regulate flow distribution within the muscle microvasculature (30). It is understood that not all capillaries in a resting muscle are perfused (33; 34), instead the muscle microvasculature undergo vasomotion (35; 36), in which the blood vessels constrict periodically to evenly distribute blood flow through various capillary modules in skeletal muscle. Furthermore, studies have suggested the existence of two distinct

circulatory systems in skeletal muscle (37-41), which are known as the nutritive flow route and non-nutritive flow route.

The flow distribution between the nutritive and non-nutritive flow routes in the skeletal muscle is tightly regulated to meet the metabolic demands. The nutritive flow route is in close contact with the myocytes, and plays an important role to supply nutrients to the myocytes for metabolic needs (42) (Figure 1.2). The non-nutritive flow route supplies the connective tissues in muscle (43) as well as adipocytes (44), and this flow route has been proposed to serve as a functional reserve for the myocytes (41; 45) (Figure 1.2). In the basal or resting states, the blood is shunted through the non-nutritive flow route, during increased metabolic demand it now goes through the nutritive flow route. Flow re-distribution from non-nutritive to nutritive flow routes during an increased metabolic demand is known as microvascular recruitment.



1.1.2.4 Insulin-mediated microvascular recruitment

Insulin appears to increase recruitment of microvascular vessels by either maintaining microvascular perfusion or increasing flow and thus overall increasing microvascular perfusion. In the late 1990s, collaborating researchers from the Universities in Tasmania and Virginia developed two major techniques to assess microvascular perfusion *in vivo* in skeletal muscle (21; 42; 47): metabolism of exogenously infused 1-methylxanthine (1-MX) by xanthine oxidase (21; 27; 48-51), and contrast enhanced ultrasound (CEU) (18; 27; 47; 48; 52; 53).

The metabolism of 1-MX, developed by Rattigan and colleagues (21), was the first technique available for measuring microvascular perfusion. The metabolism of exogenously infused 1-MX was used to measure the perfused capillary surface area in muscle (also known as microvascular perfusion) (21). In the constant-flow perfused rat hindlimb, 1-MX has no vasoactive activity (51). 1-MX is metabolised by the endogenous enzyme xanthine oxidase present in the muscle microvasculature into 1-methylurate (54; 55). Xanthine oxidase is only present in the micro- but not macrovasculature, therefore higher microvascular perfusion will result in higher 1-MX extraction. However, clearance of 1-MX from blood by other tissues (eg. liver) is very rapid, so it is necessary to partially inhibit the endogenous xanthine oxidase activity. Allopurinol is a specific xanthine oxidase competitive inhibitor which is metabolized to form oxypurinol which in turn partially inhibits the xanthine oxidase activity. Oxypurinol also lowers the K_M of xanthine oxidase for 1-MX (56), allowing saturation of xanthine oxidase even at the levels that occur with the arteriovenous difference in 1-MX across the leg muscle vascular bed, thus making 1-MX metabolism independent of flow and only dependent on surface area (exposure to xanthine oxidase amount). Arterial and venous plasma concentrations of 1-MX, 1-methylurate, and oxypurinol are

readily measured by reverse-phase high performance liquid chromatography (HPLC). The disappearance (or metabolism) rate of the 1-MX is an indication of the perfused capillary surface area in skeletal muscle.

Later, studies reported that myocardial (57) and renal (58) capillary blood volume can be measured using CEU technique. This technique involves the simultaneous ultrasound imaging and intravascular administration of gas-filled microbubbles. These microbubbles have similar rheology to that of erythrocytes, and they generate an acoustic signal during their microvascular transit through an ultrasound beam (59). Microbubbles are infused intravenously to reach an arterial steady state concentration before images are acquired. When steady state is achieved, microbubbles within the imaged region are destroyed with pulses of high power acoustic energy. Following this destructive pulse, replenishment of microbubbles provides the information about the capillary flow rate and capillary blood volume (57; 60). This myocardial CEU technique was then adapted for measurement of microvascular flow rate and microvascular blood volume within the skeletal muscle microvasculature (47; 48; 61). The use of CEU for measurement within the muscle microvasculature is described in detail in Chapter 2.

Using these techniques, Rattigan and colleagues have reported that the insulin-mediated microvascular recruitment in skeletal muscle is independent of the increase in total blood flow (21) and occurs before augmentation of total blood flow (48). Furthermore, insulin-mediated microvascular recruitment precedes the activation of insulin signalling pathway in muscle myocytes for its metabolic action as well as insulin-mediated muscle glucose uptake (18). One study (27) also showed that insulin dose-dependently ($1 - 10 \text{ mU} \cdot \text{min}^{-1} \cdot \text{kg}^{-1}$) stimulated muscle glucose uptake, however insulin-stimulated microvascular recruitment reached maximal at the lowest dose of insulin ($1 \text{ mU} \cdot \text{min}^{-1}$

¹.kg⁻¹). Epinephrine increased total blood flow similar to that of the insulin but did not increase 1-MX metabolism and muscle glucose uptake (21). Bradykinin and methacholine both are potent vasodilators, but only the latter increased insulin-mediated microvascular recruitment and muscle glucose uptake (23). These findings indicated that microvascular recruitment was potentially an important event for stimulation of muscle glucose uptake. Studies (18; 53) have shown that when insulin-mediated microvascular recruitment was blocked by a systemically infused nitric oxide synthase inhibitor, L-NAME, there was a 40% reduction of muscle glucose uptake. Taken these together, this research has shown that insulin-mediated microvascular recruitment is NOS-dependent, and it is independent to insulin-mediated vasodilation in larger blood vessels. Insulin-mediated microvascular recruitment significantly contributes to insulin-stimulated muscle glucose uptake.

1.1.3 Metabolic actions of insulin

Skeletal muscle is the largest tissue in the human body and is responsible for 80 – 90% of glucose storage in the postprandial states in healthy humans (62; 63). In order for the muscle to store glucose as glycogen, glucose is required to be transported into muscle cells. In the 1950s, insulin's metabolic actions on muscle became evident when insulin was reported to increase the rate of glucose uptake into muscle and adipose tissues (64; 65). Of all the subtypes of glucose transporters, glucose transporter type 4 (GLUT4) is the major isoform expressed in skeletal muscle and adipose tissue, and is responsible for the uptake of glucose molecules into these tissues (66-70). In the basal state, GLUT4 is pooled and stored within the cell, often referred to as GLUT4 storage vesicles (71). Upon the binding of insulin to its receptor, the PI3-K signalling pathway

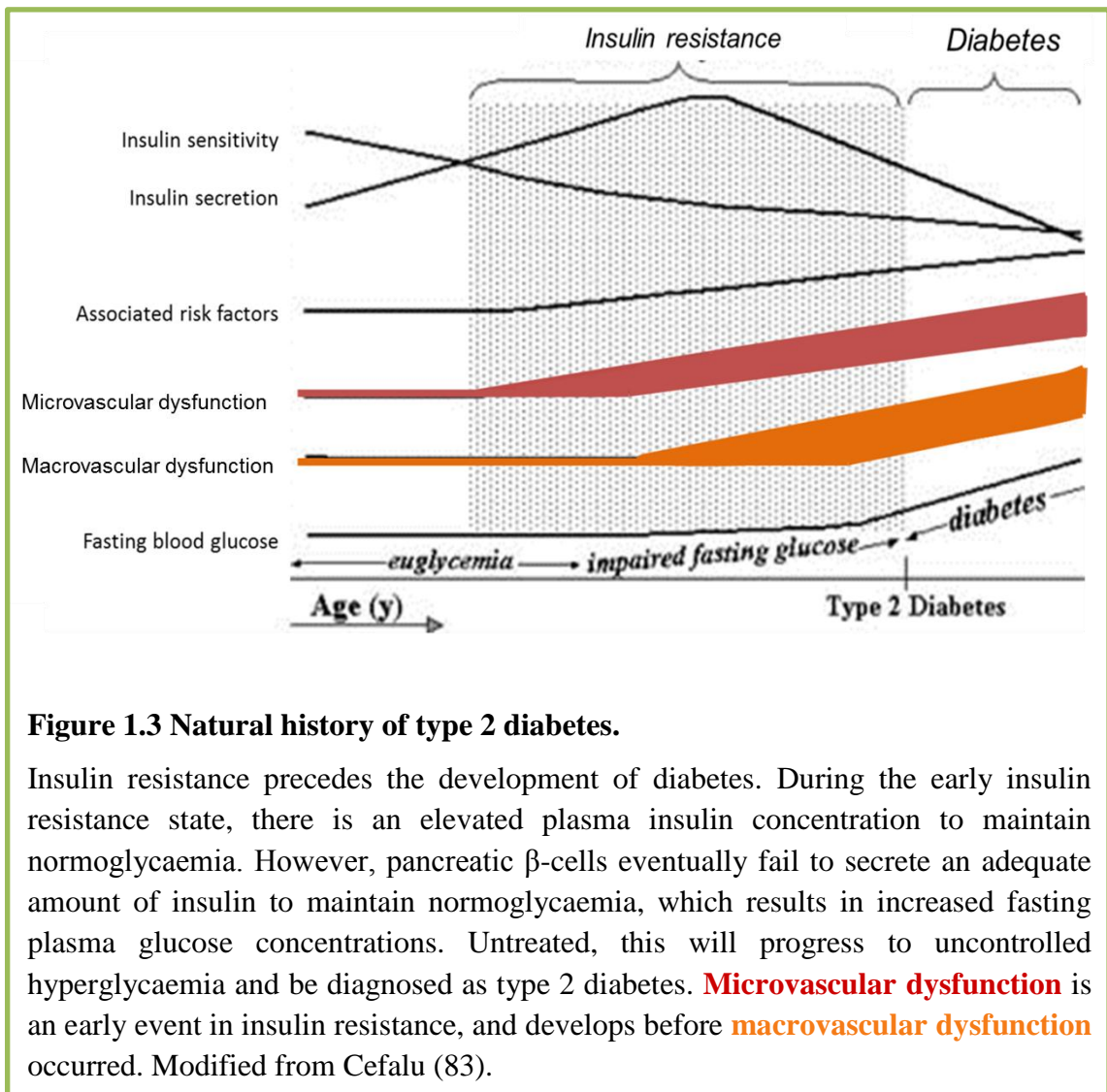
is activated, which includes the activation of downstream signalling pathway PDK1 and Akt. Following the activation of Akt, AS160 is phosphorylated and released from the GLUT4 vesicles, resulting in docking of GLUT4 to the cell membrane (72). In addition to promoting glucose uptake in skeletal muscle and adipose tissues, insulin regulates glucose metabolism by decreasing gluconeogenesis and glycogenolysis in liver. Similar to insulin action on muscle and adipose tissue, insulin action on liver is mediated via the PI3-K signalling pathway. Following the activation of PDK1 and Akt, the CREB/CBP/Torc2 complex is disrupted (73-75), leading to the inhibition of liver gluconeogenic enzymes phosphoenolpyruvate carboxykinase (PEPCK) and glucose-6-phosphatase (G6Pase) (76), resulting in inhibition of liver gluconeogenesis. Interestingly, the pathway by which insulin mediates its metabolic actions overlaps the insulin-mediated vasodilation pathway, suggesting there is an important association between the insulin's vascular and metabolic actions.

1.2 Insulin resistance

In the 1960-70s, the term “insulin resistance” was introduced and defined as a condition where insulin loses its efficiency to stimulate glucose disposal into tissues, in particular skeletal muscle (77). Insulin resistance is characterised by impaired glucose tolerance, in which insulin-sensitive tissues including liver and muscle fail to respond to insulin. Insulin fails to suppress liver glucose production, and fails to increase muscle glucose uptake. Insulin resistance is a fundamental characteristic of type 2 diabetes, and insulin resistance usually precedes the development of type 2 diabetes (Figure 1.3).

As mentioned previously, insulin possesses important haemodynamic actions, where by insulin stimulates microvascular perfusion in skeletal muscle. Research at the Menzies

Research Institute Tasmania has reported that insulin resistance is associated with diminished insulin-mediated microvascular perfusion (or microvascular dysfunction). Acute insulin resistance induced by α -methylserotonin (50) and tumour necrosis factor α (TNF α) (78; 79) reduces insulin-mediated hindleg glucose uptake and this is strongly associated with a reduced microvascular perfusion, and is independent of femoral artery blood flow changes. Furthermore, animal models of insulin resistance, including high fat diet (HFD)-induced insulin resistance rats (80), obese Zucker rats (81), and Zucker diabetic fatty (ZDF) (52) rats display impaired insulin-mediated microvascular recruitment and muscle glucose uptake. More recently, it was reported that impaired insulin-mediated muscle glucose uptake during mild insulin resistance states can result from impaired insulin-mediated microvascular perfusion (82), and impairment in insulin-mediated microvascular perfusion can be developed independently of myocyte insulin resistance (82). Furthermore, it was showed that impaired insulin-mediated microvascular perfusion precedes the development of macrovascular (resistance blood vessels) dysfunction (82) (Figure 1.3).



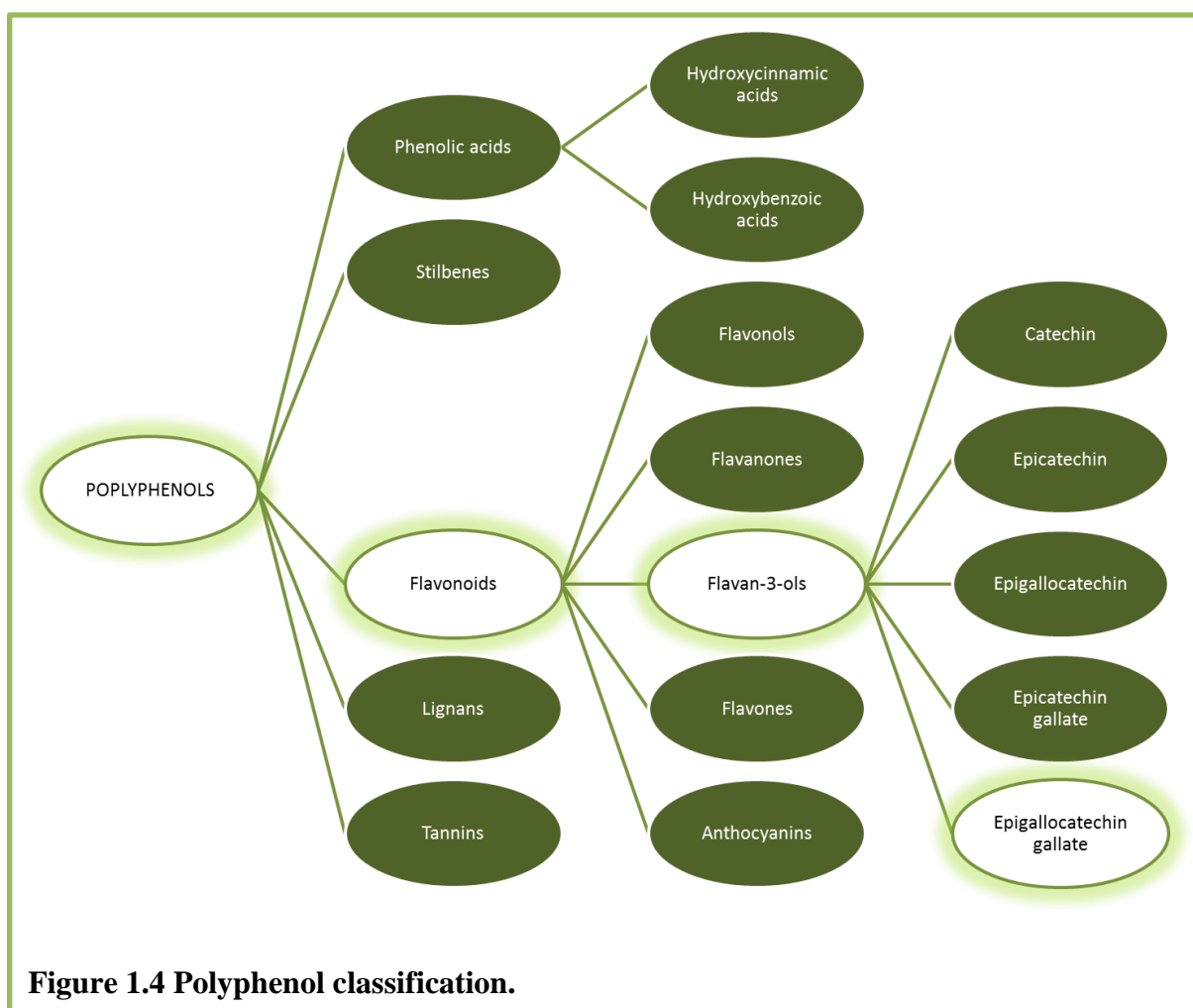
1.3 Tea derived from *Camellia sinensis*

Currently, there are several types of medications and treatments available for blood glucose management in diabetics. Besides the injections of incretin mimetics, in Australia, there are six classes of oral medications used for treating type 2 diabetes, including biguanides, sulphonylureas, thiazolidinediones, meglitinides, α -glucosidase inhibitors, and dipeptidyl peptidase-4 inhibitors (84). However, these medications lose their effectiveness over time, and often the doses are increased and/or used in combination, and eventually insulin injections may be required. More recently, complementary and alternative medicine (CAM) has increased in popularity among the community to prevent or treat a broad range of diseases, including cardiovascular disease, depression, stress, diabetes, etc. Tea has been used to prevent and treat a variety of cancers, including breast (85), liver (86), and prostate (87) cancers. However, whether or not tea should be used as a CAM for diabetes treatment remains debatable.

Tea is one of the most widely consumed beverages in the world, second only to water. There are three major classes of tea, including green, black, and oolong, which are all derived from the plant *Camellia sinensis*. Green tea and oolong tea are widely consumed in Asian countries, while black tea is predominantly consumed in Western countries. Since ancient times, green tea consumption has been lauded for its health-promoting effects. Increasing evidence shows that the health-promoting effects of green tea are attributed to the high polyphenol content.

1.3.1 Health benefits of polyphenols

Polyphenols are found in plants, mainly in fruits (grape, blueberry, cherries, plums, strawberries, cocoa, etc), vegetables (potato, tomato, lettuce, onion, etc) and also tea (88; 89). Polyphenols are essential for plant morphology, growth and reproduction, protection against ultraviolet radiation, and resistance to pathogens (90). There are a number of factors that are known to affect the plant polyphenol content, such as plant variety, soil composition, geographic location, weather condition, and storage conditions (91). Polyphenols are classified according to the number of phenol rings in their chemical structure. The five major classes of polyphenols include phenolic acids, stilbenes, flavonoids, lignans, and tannins (88) (Figure 1.4). Accumulating evidence shows that polyphenol-rich plants possess health-promoting effects, including cancer prevention (92-95), neuroprotection (96; 97), improve cardiovascular and metabolic health (98-100), and lower the risk of type 2 diabetes (101-106). Among all the polyphenol-rich plants, green tea and its flavan-3-ols has been most extensively studied for their health promoting effects.



1.3.2 Green tea

Tea is categorised into different classes based on the degree of tea fermentation (or leaf oxidation) during processing. During tea fermentation, flavan-3-ols, the bioactive polyphenols in tea leaves, undergo polyphenol oxidase-dependent oxidative polymerisation, resulting in the formation of theaflavins and thearubigins (107). Green tea is unfermented and contains the highest concentration of flavan-3-ols. Oolong tea is a partially fermented product and therefore contains a mixture of flavan-3-ols, theaflavins, and thearubigins. Black tea is the most fermented tea, and as a result, contains abundant theaflavins and thearubigins, and limited or no flavan-3-ols. There are five major types of flavan-3-ols in green tea (Figure 1.5), including catechin, epicatechin, epicatechin gallate, epigallocatechin, and epigallocatechin gallate (EGCG). Table 1.1 outlines the composition of the main polyphenols in green tea, where EGCG is the most abundant polyphenols accounting for 33-50% of green tea polyphenols (107; 108).

For decades, research has been focused on the potential anti-cancer activities of green tea and green tea polyphenols (93-95; 109; 110), where encouraging *in vitro* and *in vivo* data have been established. Additionally, much evidence shows that green tea has anti-inflammatory (111; 112), anti-viral (113; 114), and neuroprotective (96; 115) effects. In recent years, extensive research has been carried out to investigate the potential health-promoting effects of green tea in cardiovascular and metabolic health (98; 116-120). Research suggests that the aforementioned health-promoting effects of green tea are attributed mainly to EGCG (110; 112-115).

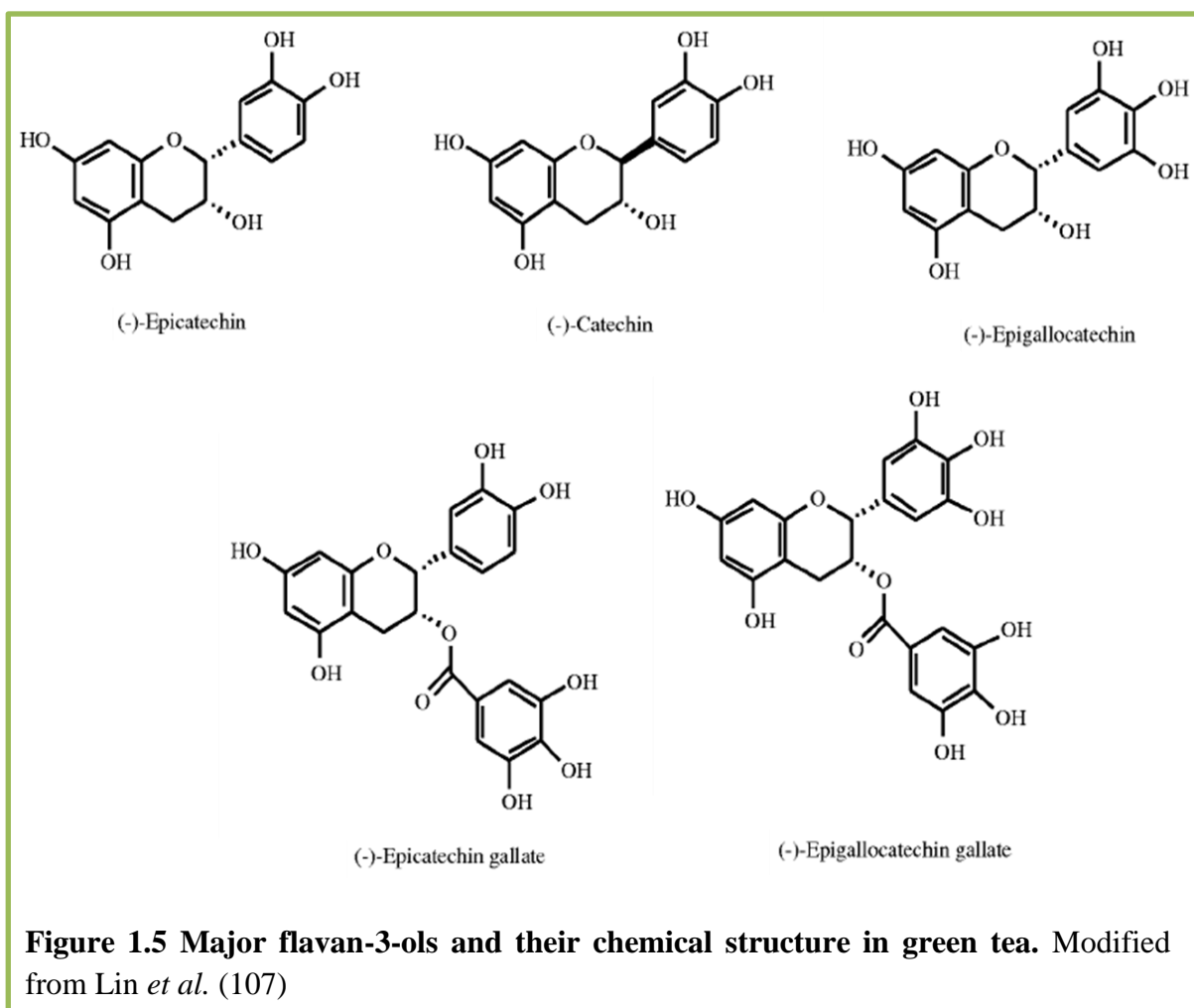


Table 1.1 Composition of major polyphenols in green tea.

Polyphenols	% of total polyphenol
Catechin	2
Epicatechin	6
Epicatechin gallate	6-12
Epigallocatechin	20-30
Epigallocatechin gallate	33-50

1.4 Green tea and type 2 diabetes

1.4.1 Epidemiology studies

Recently, emerging evidence from epidemiological studies show that tea (including both green tea and black tea) consumption is associated with reduced risk for type 2 diabetes (101-106). However, this is debated as not all studies have found this association (121; 122).

In 2009, two meta-analysis by Huxley *et al.* (123) and Jing *et al.* (124) suggested that, compared to non-tea drinkers, tea (green and black tea) consumption of 3 – 4 cups (or more) per day was associated with 17 – 35 % lower risk for type 2 diabetes. Furthermore, a study in a British cohort (102) showed that tea (green and black tea) consumption of > 3 cups per day was associated with a 34% lower risk of diabetes. Among Japanese adults, Iso *et al.* (106) reported an inverse association between green tea consumption and risk for type 2 diabetes. This study suggested that high green tea consumption (≥ 6 cups.d⁻¹) lowers their risk for type 2 diabetes by 33% compared to those who drink < 1 cup per week. Recently, a meta-analysis by Zheng *et al.* (125) reported that green tea catechins treatment for ≥ 12 weeks, but not shorter term (< 12 weeks), was associated with lower fasting blood glucose. On the other hand, Oba *et al.* (121) failed to uncover an association between green tea consumption and reduced risk of diabetes in Japanese. Furthermore, the Singapore Chinese Health Study (122) did not find an association between green tea consumption and the reduced risk for type 2 diabetes. However, these studies are correlative and do not directly address the effect of green tea consumption of metabolic outcomes.

1.4.2 Clinical studies

1.4.2.1 Oolong Tea

Some studies have assessed the metabolic effects of oolong tea in patients with type 2 diabetes. A study by Shimada *et al.* (126) reported that oolong tea treatment for 4 weeks significantly increased plasma adiponectin levels by 9.9% and lowered haemoglobin A1c (HbA1c) levels by 3.3% in patients with various coronary risk factors. There was a slight, but not significant, decrease in the plasma glucose levels. In this study, each patient received 45.4 mg.day⁻¹ of EGCG from the oolong tea for 4 weeks. Hosoda *et al.* (127) used a higher dose of oolong tea treatment (EGCG 386 mg.d⁻¹) for 4 weeks and reported that plasma glucose was significantly lowered in type 2 diabetes patients compared to the control group. The mechanism of the anti-hyperglycaemic effects of the oolong tea is unclear. However, oolong tea seemed to have a concentration-dependent effect on glycaemic control.

1.4.2.2 Green tea

Since the 2000s, numerous clinical studies (116; 128-149) have been undertaken to investigate the metabolic effects of green tea or green tea extracts. In healthy subjects, acute green tea consumption was reported to enhance insulin sensitivity (148) and glucose tolerance (147). However, Josic *et al.* (139) reported that acute green tea consumption (containing 32.4 mg EGCG) did not have glucose and insulin lowering effects. Compared to the previous 2 studies, the EGCG and total polyphenol content in the green tea used in the latter study was markedly lower. Thus, there might be a dose-

dependent effect of green tea (or EGCG) on glycaemic control. Conversely, chronic green tea extract (EGCG 150 mg.d⁻¹) supplementation for 3 weeks lowered the total cholesterol: HDL ratio, but had no other metabolic effects in healthy subjects (135).

Most (116; 130-134; 140-143), but not all (128; 129; 137; 149; 150), studies reported that body weight was reduced following chronic green tea or green tea extract treatment (range from 1 – 6 months of treatment) in overweight and obese subjects. Some studies have reported that following green tea or green tea extract treatment, there were reductions in plasma LDL levels (116; 130; 137; 141; 149; 150) and increased in plasma HDL levels (134; 137; 142; 149; 150). In postmenopausal women with impaired glucose tolerance, EGCG treatment (300 mg.d⁻¹) for 12 weeks reduced plasma glucose by 5% (132). Recent studies have shown that green tea extract treatment (EGCG 208 mg.d⁻¹) for 12 weeks reduced blood glucose (149) and insulin (150) levels significantly in obese subjects. In contrast, EGCG treatment (800 mg.d⁻¹) for 8 weeks had no effects on insulin sensitivity and glucose tolerance in overweight and obese men in another study (129).

In patients with type 2 diabetes, green tea extract (polyphenols 240 mg.d⁻¹, EGCG content not reported) treatment for 8 weeks increased plasma adiponectin levels significantly (144). Another study (138) used a much higher dose of green tea extracts (EGCG 856.8 mg.d⁻¹ for 16 weeks) and reported the homeostasis model assessment of insulin resistance (HOMA-IR), HbA1c, and fasting insulin levels were reduced significantly in type 2 diabetic patients. Furthermore, waist circumferences in the subjects treated with green tea extracts were reduced by 3%. Conversely, Ryu *et al.* (146) showed that metabolic markers including blood lipids, glucose, insulin, and adiponectin levels were not altered following 4 weeks of green tea treatment (polyphenol content not reported). Similarly, another study (136) reported that green tea

treatment (544 mg.d⁻¹ polyphenols, EGCG content unknown) for 2 months had no apparent effects on metabolic markers such as fasting serum glucose and insulin, HbA1c, and HOMA-IR.

Overall, the outcomes from the different clinical trials have not been conclusive. The discrepancies between results are likely due to small study populations, poor diet control during the study period, poor oral bioavailability of catechins (151-155), and/or poor study design. Nonetheless, Brown *et al.* (129) suggested that EGCG supplementation may play a more important role in prevention of insulin resistance and type 2 diabetes rather than as a therapeutic treatment for these conditions. Table 1.2 summarizes the acute and chronic effects of EGCG in human. Taken together, these data indicate that animal studies are essential in order to effectively assess the dosage and mechanism of actions of EGCG to optimally design clinical trials.

1.4.3 Animal studies

Several studies have investigated the anti-diabetic effects of green tea in rodents, including normal healthy (156-158), and insulin-resistant models, such as fructose fed rodents (159; 160), high-fat fed mice (98; 158; 161-163), diabetic (*db/db*) mice (147; 164; 165), ZDF rats (164), spontaneously hypertensive rats (SHRs) (120), and Otsuka Long-Evans Tokushima Fatty (OLETF) rats (166; 167). Table 1.2 summarizes the acute and chronic effects of EGCG in animals.

1.4.3.1 Studies in healthy animals

In healthy rats, green tea treatment for 3 weeks significantly reduced both the epididymal and abdominal adipose tissue weight (157). Besides that, plasma lipid profile, including free fatty acids, total cholesterol, HDL and LDL were significantly lowered by chronic green tea treatment. Interestingly, this study showed that following green tea treatment, muscle glucose uptake and GLUT4 translocation were significantly enhanced (157). In this study, total plasma EGCG levels reached ~40 nM, however, the amount of catechins provided to the rats were not detailed. Another study by Wu and Colleagues (156) showed that following 12 weeks of green tea treatment (mixed catechins 56 mg.d⁻¹, EGCG 37.5 mg.d⁻¹) in rats, significantly lowered fasting plasma glucose, insulin, free fatty acid, and triglyceride levels. In addition, glucose tolerance and insulin sensitivity in these rats were enhanced following the green tea treatment, and this might be in part attributable to the increased insulin sensitivity in adipocytes (156). Interestingly, Ashida *et al.* (157) showed that glucose uptake in adipose tissue was reduced by 80% following green tea treatment, while the former study (156) showed a 40% increase in glucose uptake in adipocytes. In mice fed green tea (EGCG 610 mg.L⁻¹) for 14 weeks, fasting blood glucose levels were lowered while serum lipid levels were not affected (158). In addition, glucose tolerance and muscle glucose uptake in these green tea treated mice were not altered but the adipose tissue glucose uptake was significantly reduced (158). It is too early to draw conclusions on the effects of green tea or EGCG in healthy animals due to the limited studies conducted.

1.4.3.2 Studies in insulin resistant animals

Green tea, green tea extract or EGCG treatments have been reported to ameliorate diet-induced insulin resistance in rodents (98; 158-163) and genetically-derived diabetes in rats (120; 147; 164-167). Green tea treatment (EGCG 1 g.L⁻¹ in drinking water) for 12 weeks improved glucose tolerance in fructose-fed rats (159). Green tea treated fructose-fed rats have lower fasting plasma triglycerides than non-treated rats (159). Besides that, insulin mediated GLUT4 translocation and glucose uptake in adipocytes in the fructose-fed rats were restored by green tea treatment (159). Another study showed that green tea treatment (EGCG 150 or 300 mg.kg⁻¹.d⁻¹) dose-dependently reversed insulin resistance induced by fructose-fed in hamster (160). In this study, animals were fed with fructose for 2 weeks before green tea was administered with the fructose for a further 4 weeks. This study (160) reported that green tea (or EGCG) dose-dependently increased fasting serum adiponectin, reduced fasting serum insulin and triglycerides, while having no effect on fasting glucose levels. Similarly, Bose *et al.* (161) treated insulin resistant mice for 4 weeks with EGCG (3.2 g.kg⁻¹ diet) after 9 weeks of high fat feeding, and reported a significant reduction in fasting blood glucose following the EGCG treatment (insulin levels not reported). However, the food intake of the mice was not reported, and therefore it is unclear how much food (EGCG) was consumed by the mice each day. Studies by Li *et al.* (160) and Bose *et al.* (161) suggested that insulin resistance could be reversed by EGCG treatment in a dose-dependent fashion.

Several studies have assessed the chronic (10 – 24 weeks) metabolic effects of green tea or EGCG in high fat-fed rodents. Chronic green tea treatment in high fat-fed mice for 14 weeks (EGCG 609.7 mg.L⁻¹) (158) and 22 weeks (EGCG 2 mg.kg⁻¹.d⁻¹) (162) have significantly reduced body weight and adipose tissue weight, improved glucose tolerance, GLUT4 translocation in muscle, and muscle glucose uptake, and reduced

fasting plasma glucose. Similar findings were reported (161) where chronic EGCG treatment (3.2 g.kg^{-1} diet) for 16 weeks in high fat-fed mice reduced body weight, adipose tissue weight, fasting plasma glucose, insulin, and HOMA-IR. Body weight and adipose tissue weight reduced significantly in high fat-fed mice following 10 weeks of EGCG treatment ($50 \text{ mg.kg}^{-1}.\text{d}^{-1}$) (163). Besides that, EGCG treatment (163) lowered fasting serum glucose and insulin in high fat-fed mice, thus improved quantitative insulin sensitivity check index (QUICKI, a surrogate index of insulin sensitivity). In these chronic studies (158; 161-163), the effects of green tea or EGCG treatment on body weight and fasting plasma glucose were apparent from week 7 onwards. On the other hand, chronic green tea (polyphenol content not reported) and EGCG ($1 \text{ mg.kg}^{-1}.\text{d}^{-1}$) treatment for 24 weeks in high fat-fed rats did not alter body weight, but increased fat-free mass significantly (98). In the high fat-fed rats, plasma biochemistries including glucose, HDL, LDL and triglycerides were not altered by green tea or EGCG treatment (98). However, green tea or EGCG treatment significantly improved glucose tolerance in the high fat-fed rats (98). Given the similar metabolic effects of the green tea and EGCG in these studies, this suggested that the amelioration of high fat-induced insulin resistance by green tea treatment might be attributed to EGCG.

One study (164) showed that *db/db* mice, a type 2 diabetes mouse model, treated with EGCG ($100 \text{ mg.kg}^{-1}.\text{d}^{-1}$) for 2 weeks improved glucose tolerance, while EGCG treatment at a lower dose ($30 \text{ mg.kg}^{-1}.\text{d}^{-1}$) was not as effective. Wolfram *et al.* (164) also showed that EGCG treatment for 7 weeks could dose-dependently (EGCG $0.25 - 1 \text{ g.kg}^{-1}$ diet) improve glucose tolerance and reduced plasma glucose in *db/db* mice. Another study (165) also reported that *db/db* mice treated with EGCG (1 g.kg^{-1} diet) for 10 weeks significantly improved glucose tolerance and reduced plasma glucose.

Interestingly, acute green tea treatment (mixed catechins 21.6 mg.kg^{-1} , EGCG 16.8 mg.kg^{-1}) lowered the blood glucose in *db/db* mice, but not wild type mice (147).

SHRs (7) and OLETF rats (168) are insulin resistant animal models with endothelial dysfunction. Green tea catechins and EGCG have been reported to improve endothelial function in SHRs (120; 169) and OLETF rats (166; 167). EGCG treatment ($200 \text{ mg.kg}^{-1}.\text{d}^{-1}$) for 3 weeks reduced fasting plasma glucose, increased QUICKI and plasma adiponectin in SHRs (120). EGCG treatment prevented the development of insulin resistance and reduced systolic blood pressure significantly in SHRs (120). Recently, Jang *et al.* (163) showed that EGCG treatment ($50 \text{ mg.kg}^{-1}.\text{d}^{-1}$) for 10 weeks improved high fat diet-induced endothelial dysfunction in mice. In OLETF rats, green tea catechins ($25 - 30 \text{ mg.kg}^{-1}.\text{d}^{-1}$) treatment for 12 weeks lowered blood pressure and fasting blood glucose and insulin in the rats (166; 167). Green tea catechins reduced the reactive oxygen species (ROS) formation and vascular activity of nicotinamide adenine dinucleotide phosphate (NADPH) oxidase in thoracic aorta of OLETF rats (166; 167). TNF α administration, which induces NADPH oxidase and the formation of ROS (170; 171), has been reported to inhibit insulin-mediated microvascular recruitment (78; 79) and impair endothelial function during insulin resistant state (170; 171). These studies implicated that EGCG could prevent the development of insulin resistance by improving endothelial function. A major limitation in most of these aforementioned animal and human studies is the lack of reporting on circulating concentrations of EGCG.

Table 1.2 Summary of acute and chronic effects of EGCG in human and animal studies.

	Treatment	Subjects	Effects	Ref
Human	Acute	Healthy	↑ OGTT	147
			↑ Insulin sensitivity	148
	Chronic	Healthy	--	135
		Obese	↓ Fasting plasma glucose	149
			↓ Fasting plasma insulin ↓ HOMA-IR	150 149; 150
Animal	Acute	Healthy	--	147; 238
		Insulin resistance	↑ OGTT	238
		Type 2 diabetes	↓ Fasting blood glucose	147
	Chronic	Healthy	↓ Fasting plasma glucose ↓ Fasting plasma insulin	156; 158
		Insulin resistance	↓ Body weight	158; 161-163
			↓ Adipose tissue weight	158; 161-163
			↓ Fasting plasma glucose	161; 163; 166; 167
			↓ Fasting plasma insulin ↑ OGTT	160; 161; 163 98; 159
			↑ QUICKI	120; 163
			↑ Endothelial function	120; 163; 166; 167
		Type 2 diabetes	↓ Fasting plasma glucose ↑ OGTT	147; 164; 165 164; 165

Treatment details (eg. dose, length, and animal models) are described in **1.4.2** and **1.4.3**.
OGTT: oral glucose tolerance test; ↑: improve; ↓: reduce; --: no effects

1.5 Mechanism of action of EGCG

1.5.1 Metabolic actions of EGCG

There is mounting evidence from *in vitro* studies suggesting that EGCG has insulin-mimetic metabolic actions on myocytes (157; 172; 173) and hepatocytes (174; 175). In isolated myocytes, green tea and EGCG stimulate GLUT4 translocation and results in increased glucose uptake (157; 158; 172). Similar to insulin, EGCG has been reported to stimulate muscle glucose uptake via the PI3-K/Akt signalling pathway in cultured myotubes (172; 173; 176). However, there is no evidence of EGCG activating the PI3-K/Akt pathway by activating the insulin receptor (172). On the other hand, EGCG at high doses ($> 20 \mu\text{M}$), but not a lower dose ($10 \mu\text{M}$) (173), was shown to stimulate muscle glucose uptake by the activation of adenosine monophosphate-activated protein kinase (AMPK) (176; 177). Interestingly, EGCG could stimulate glucose uptake in cultured myocytes in the absence of insulin (157; 158; 172; 173; 176; 177), indicating that EGCG has an insulin-mimetic action in muscle cells.

EGCG has been shown to suppress hepatic gluconeogenesis in cultured hepatocytes. At high doses ($> 25 \mu\text{M}$), EGCG suppresses hepatic gluconeogenesis through the same pathway as insulin, where EGCG activates IRS-1/ PI3-K/Akt, resulting in inhibition of PEPCK and G6Pase gluconeogenic enzyme activity (175). In contrast, EGCG at a lower dose ($1 \mu\text{M}$) suppresses hepatic gluconeogenesis via the AMPK pathway. In cultured hepatocytes treated with EGCG, AMPK is activated by ROS and Ca^{2+} /calmodulin-dependent protein kinase kinase (CaMKK) pathway (174). Given that EGCG at a dietary dose ($< 10 \mu\text{M}$) acts independent to that of insulin, EGCG might enhance insulin's inhibition of gluconeogenesis (Figure 1.6).

1.5.2 Vascular actions of EGCG

Previous studies have shown that EGCG is a potent vasodilator in isolated aortic ring (178; 179), bovine ophthalmic artery (180), coronary artery ring (181), and mesenteric vascular bed (119). EGCG-mediated vasodilation is endothelium-dependent in isolated vessels including rat aortic ring (178; 182), bovine ophthalmic artery (180), and porcine coronary ring (181). Furthermore, EGCG stimulates NO production in cultured vascular endothelial cells, via the PI3-K/Akt/eNOS pathway (119; 178-181) (Figure 1.6). Interestingly, formation of ROS in endothelial cells is essential for activation of the PI3-K pathway by EGCG (119; 181). In contrast to the vasodilation effects, EGCG at high concentrations ($\geq 100 \mu\text{M}$) induces endothelium-independent vasoconstriction in isolated aortas (178; 183-185). However, it should be noted that plasma EGCG in human is $\sim 1 \mu\text{M}$ following consumption of 8 – 16 cups of green tea (EGCG $800 \text{ mg}\cdot\text{d}^{-1}$) (151; 186). Previous studies (119; 178; 180; 181) showed that EGCG-mediated vasodilation is noticeable within a dietary range ($0.1 - 10 \mu\text{M}$). Taken together, these studies suggested that high doses of EGCG elicit opposing effects to that of low doses of EGCG, and this is important to take into consideration for the design of clinical studies.

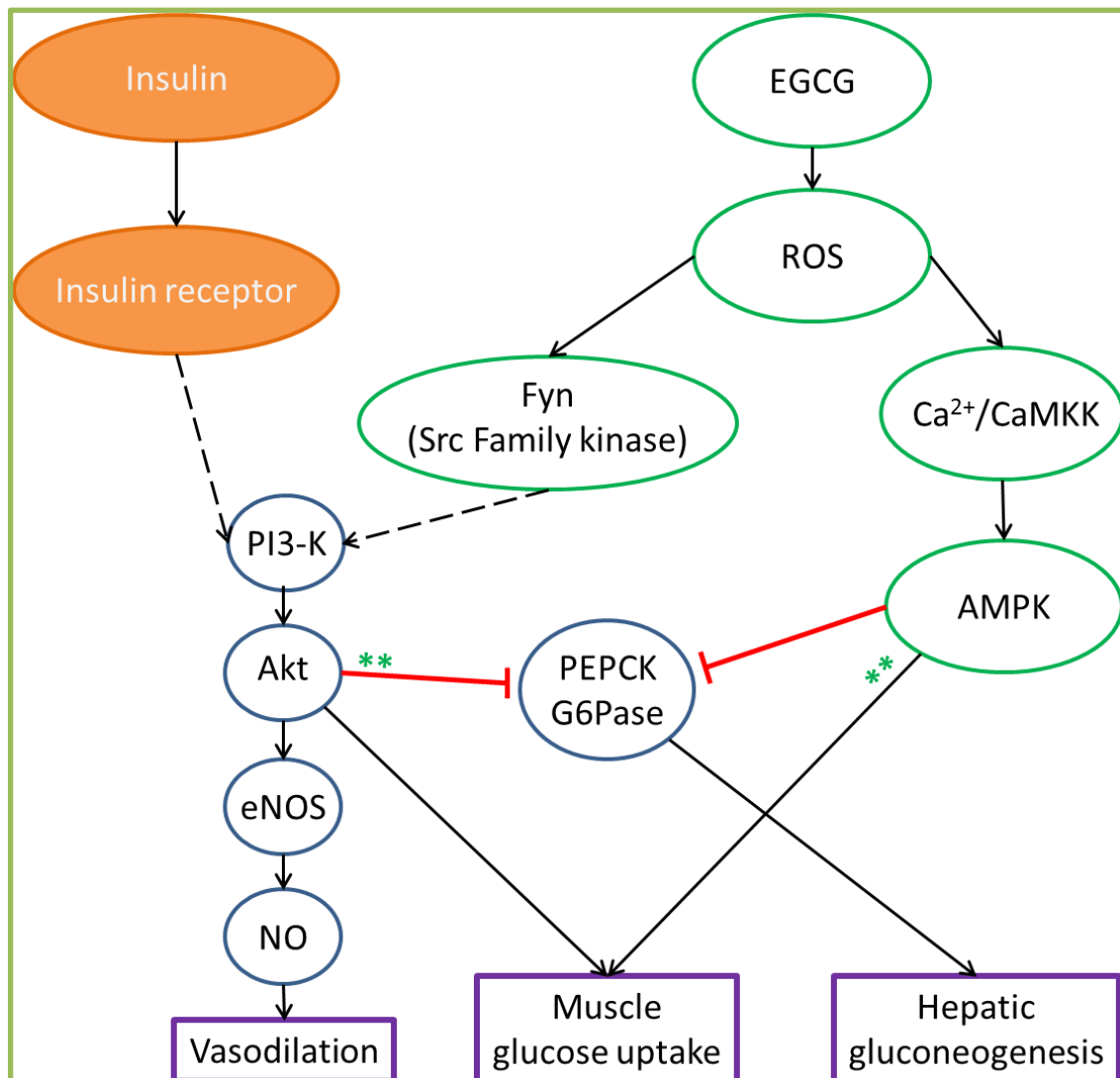


Figure 1.6 Mechanism of action of EGCG in various tissues. Signalling molecules in common for both insulin and EGCG are in blue. Signalling molecules in green are EGCG-specific. Arrows indicate activation while Ts indicate inhibition of the following step in the pathway. ** indicate pathways activated by EGCG at high doses (>20 μM). Some components of the pathways (eg. IRS) have been omitted for clarity.

1.6 Study aims

Skeletal muscle is the largest tissue in the human body and is responsible for 80 - 90% of glucose storage in the postprandial states in healthy humans (62; 63). Insulin-mediated microvascular perfusion contributes to 40% of insulin-stimulated glucose uptake in skeletal muscle *in vivo* (53; 78). Insulin resistance is a fundamental characteristic of type 2 diabetes, and includes impaired insulin action on skeletal muscle, liver and muscle microvasculature.

There is mounting evidence from *in vitro* studies suggesting that EGCG stimulates glucose uptake in cultured myocytes, which are beneficial for the prevention and treatment of insulin resistance and type 2 diabetes. Studies have also suggested that EGCG mimics both vascular and metabolic actions of insulin *in vitro*. Whether EGCG stimulates microvascular perfusion *in vivo* to mediate its metabolic action on skeletal muscle has not been previously investigated.

In the current thesis, the main hypothesis is that EGCG has insulin-mimetic and/or insulin-sensitizing effects *in vivo* on vascular function to improve glucose metabolism in skeletal muscle. Three specific aims were developed in the current thesis to test this hypothesis:

1. To explore whether EGCG has direct vascular and metabolic actions in skeletal muscle *in situ*.
2. To explore whether acute EGCG treatment has insulin-mimetic or insulin-sensitizing actions on microvascular blood flow and glucose metabolism in muscle in healthy and high fat fed insulin resistant rat models *in vivo*.
3. To determine whether chronic EGCG treatment can ameliorate high fat diet-induced insulin resistance *in vivo*.

Chapter 2

Methods & materials

2.1 Materials

EGCG (97% purity) was a kind donation from Tea Solutions, Hara Office Inc., Tokyo, Japan. All chemicals were obtained from Sigma-Aldrich unless otherwise stated.

2.2 Animal care

Male Sprague-Dawley rats (4 weeks old) were obtained from the University of Tasmania Central Animal Facility. Animals were housed at 21 ± 2 °C with a 12h: 12h light: dark cycle. The rats were allowed free access to drinking water and food *ad libitum*. Animals were provided with normal chow from Specialty Feeds, Glen Forest, WA, Australia or Ridley Agriproducts, Corowa, NSW, Australia. Rats were randomly allocated to respective experimental diets at 5 weeks old of age (Table 2.1). Animals' weight, food intake, and water intake were monitored daily during dietary interventions. The animal studies were not carried out in a blinded fashion. However, the animals were randomly assigned to each experimental group. All experimental procedures were approved by the University of Tasmania Animal Ethics Committee (A11282 approved in 2010 and A13384 approved in 2013) and performed in accordance with the Australian Code of Practice for the Care and Use of Animals for Scientific Purposes – 2004, 7th Edition.

Table 2.1 Macronutrient content of experimental diets.

	5FD	9FD	23FD
Protein, % w/w	20	22	19
Fat, % w/w	4.8	9	22.6
Saturated fats, % total fat	17.3	20.4	51.9
Monounsaturated fats, % total fat	38.5	36.6	38.9
Polyunsaturated fats, % total fat	43.8	42.1	9.2
Carbohydrate, % w/w	70.4	65.8	53.7
Crude Fibre, % w/w	5.1	3.2	4.7
Digestable Energy, kJ/g	14.0	13.2	19.9
Source	Specialty Feeds	Ridley Agriproducts	Specialty Feeds

2.3 Isolated constant-flow perfused rat hindlimb procedure

2.3.1 Perfusion buffer

The perfusion buffer used was an erythrocyte-free preparation consisting of Krebs-Ringer bicarbonate buffer (118 mM NaCl, 4.7 mM KCl, 1.2 mM KH₂PO₄, 1.2 mM MgSO₄, 25 mM NaHCO₃, 2.5 mM CaCl₂, and 8.3 mM glucose) containing 4% (w/v) bovine serum albumin (Bovogen Biologicals Pty Ltd, Vic, Australia). Buffer was filtered through a 0.45 µm pore size membrane before use.

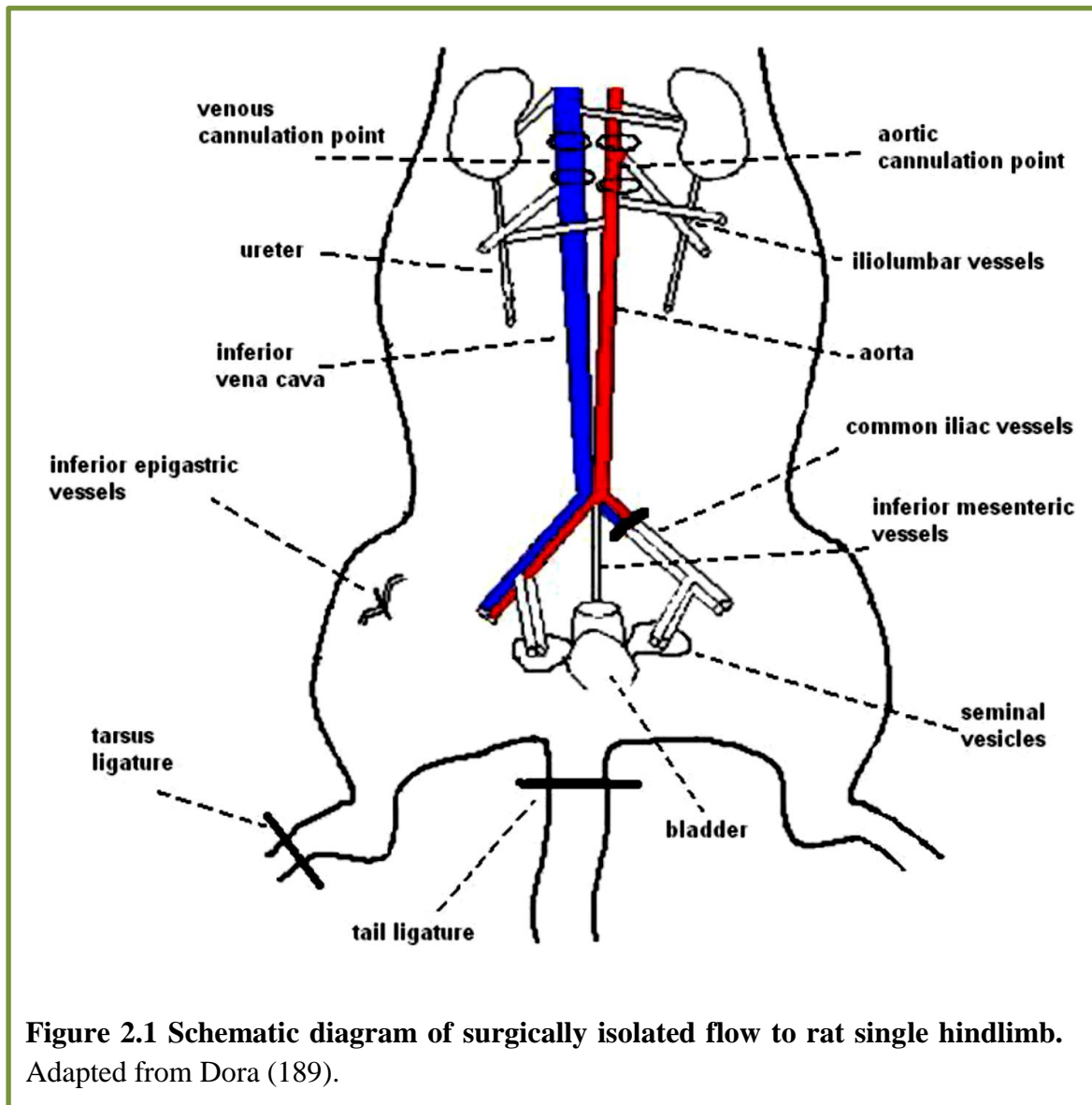
2.3.2 Animal surgery

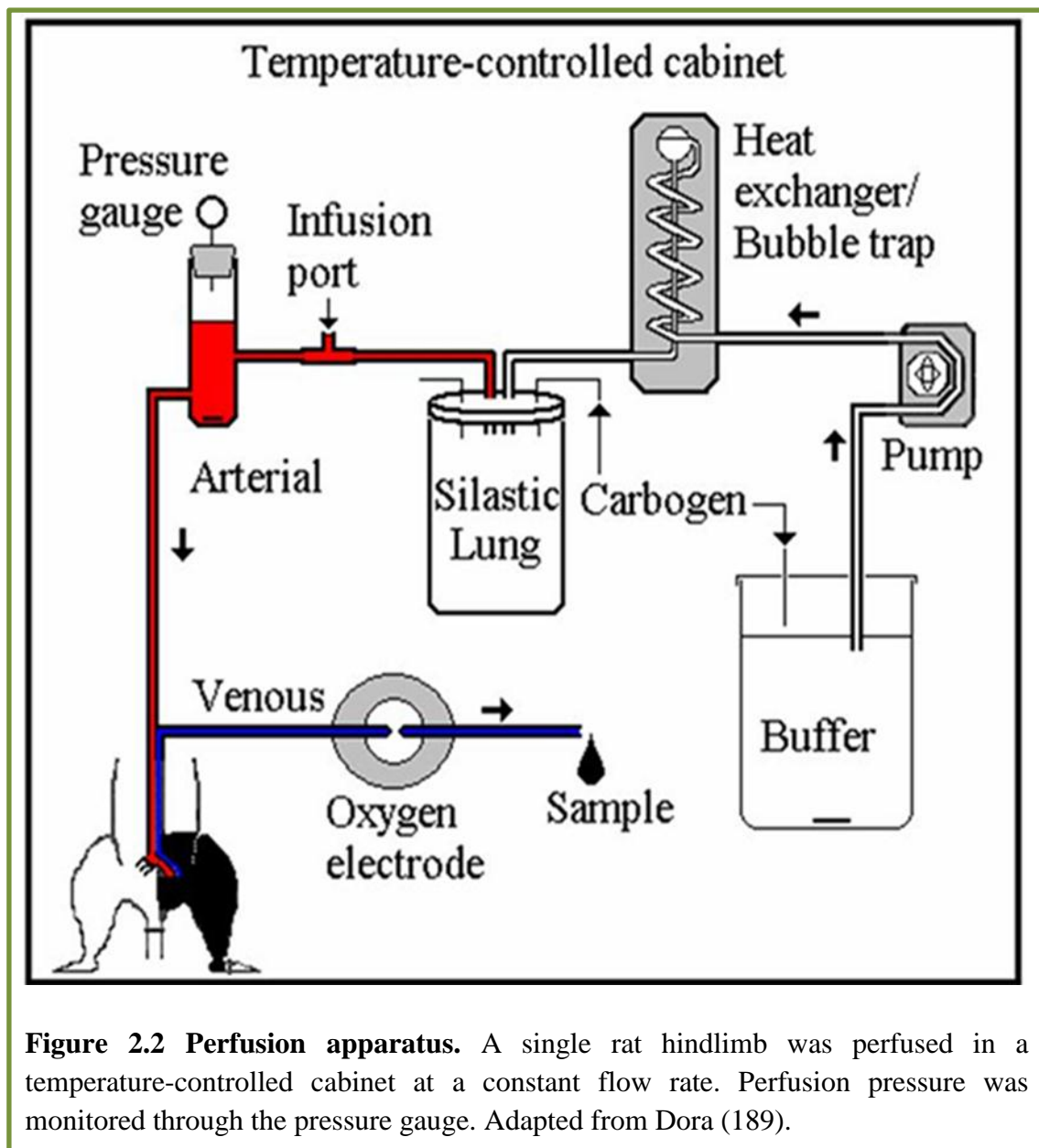
The surgical procedures (Figure 2.1) were essentially as described previously (187), with additional details as outlined elsewhere (188). Male rats were used for perfused rat hindlimb experiments because isolation of flow to one leg is easier due to a less complex blood supply to the genitalia. In brief, an abdominal midline incision was performed, and the abdominal wall was incised from the pubic symphysis to the xipoid process. The following blood vessels and tissues were ligated: superior and inferior epigastric vessels, superficial epigastric vessels, internal spermatic vessels, iliolumbar vessels, left common iliac artery and vein, testicles, and bladder. The descending colon and jejunum were ligated, allowing the removal of the viscera. The descending aorta and vena cava were carefully separated and cannulated in between the renal and iliolumbar vessels with 20G and 18G catheters (Terumo) respectively. The animal was connected to the perfusion apparatus. Lastly, the animal was euthanized with an intra-cardiac injection of pentobarbital sodium at a lethal dose.

2.3.3 Perfusion apparatus

Rat hindlimbs were perfused in a non-recirculating manner with perfusion buffer, using a Masterflex® peristaltic pump (Cole-Parmer, Vernon Hills, IL, USA) to ensure a constant flow rate of $0.5 \text{ mL} \cdot \text{min}^{-1} \cdot \text{g}^{-1}$ of perfused muscle (equivalent to $8 \text{ mL} \cdot \text{min}^{-1}$ for a 200 g rats). The perfusate was gassed with 95% O_2 : 5% CO_2 in a silastic tube oxygenator. Experiments were conducted at 32 °C in a temperature-controlled cabinet, with the buffer temperature maintained by passage through a water-jacketed heat exchange coil. Test substances were infused into a small bubble trap located in the

arterial perfusion line. Perfusion pressure was constantly monitored via a pressure transducer located in the arterial line. The venous effluent was periodically sampled and the remainder discarded. Perfusion pressure was continually recorded using WinDaq data acquisition software (DataQ Instruments, Akron, OH, USA). This apparatus is illustrated in Figure 2.2.





2.4 *In vivo* experiment in anaesthetized rats

2.4.1 Animal surgery

After 4 weeks of dietary treatment, animals were fasted overnight before experiments were conducted. Animals were anaesthetized with an intraperitoneal injection of pentobarbital sodium (5 mg.100g⁻¹ body weight). A tracheostomy was performed to facilitate spontaneous respiration throughout the course of the surgery and experiment. Polyethylene cannulas (PE-58, Intramedic®) were surgically implanted into both left and right jugular veins for continuous infusion of anaesthetic and other intravenous infusions. A third cannula was inserted into the carotid artery for arterial blood sampling and monitoring mean arterial blood pressure (MAP; BLPR2 pressure transducer, World Precision Instruments, Sarasota, FL, USA). Small incisions (~2 cm) were made in the skin of the groin area of the right leg, and the epigastric artery and vein ligated. Then, the femoral artery was separated from the femoral vein and saphenous nerve. An ultrasonic flow probe (Transonic Systems, VB series 0.5 mm) was positioned around the femoral artery of the right leg just distal to the rectus abdominus muscle. The cavity in the leg surrounding the probe was filled with ultrasound conductive gel (Medical Equipment Services Pty Ltd) to provide acoustic coupling to the probe. The probe was then connected to the flow meter (Model T160 ultrasonic volume flow meter, Transonic Systems). This was in turn interfaced with an IBM compatible PC computer which acquired the data at sampling frequency of 100 Hz for femoral artery blood flow, heart rate, and mean arterial blood pressure using WinDaq data acquisition software (DataQ Instruments). Figure 2.3 is a schematic illustration of the surgery performed.

Completion of the surgery was followed by a 60-minute equilibration period to allow cardiovascular parameters to become stable and constant. The rats were maintained under anaesthesia for the duration of the experiment by continuous infusion of pentobarbital sodium ($0.6 \text{ mg} \cdot \text{min}^{-1} \cdot \text{kg}^{-1}$). The rats were placed on the heating block to maintain their body temperature at 37°C throughout the duration of the experiment.

Upon completion of the experiment, the epididymal fat pad of the rats were removed and weighed. Other tissues including whole calf muscle, liver, heart, aorta, and femoral arteries were collected for further analysis. The rats were euthanized by exsanguination.

The majority of our observations on microvascular responses have been obtained in male rats. Given that microvascular responses have the largest coefficient of variance, we continued using male rats to avoid possible gender specific variability. Using males for both types of experiment (perfused hindlimb and *in vivo* experiments) allowed for direct comparison.

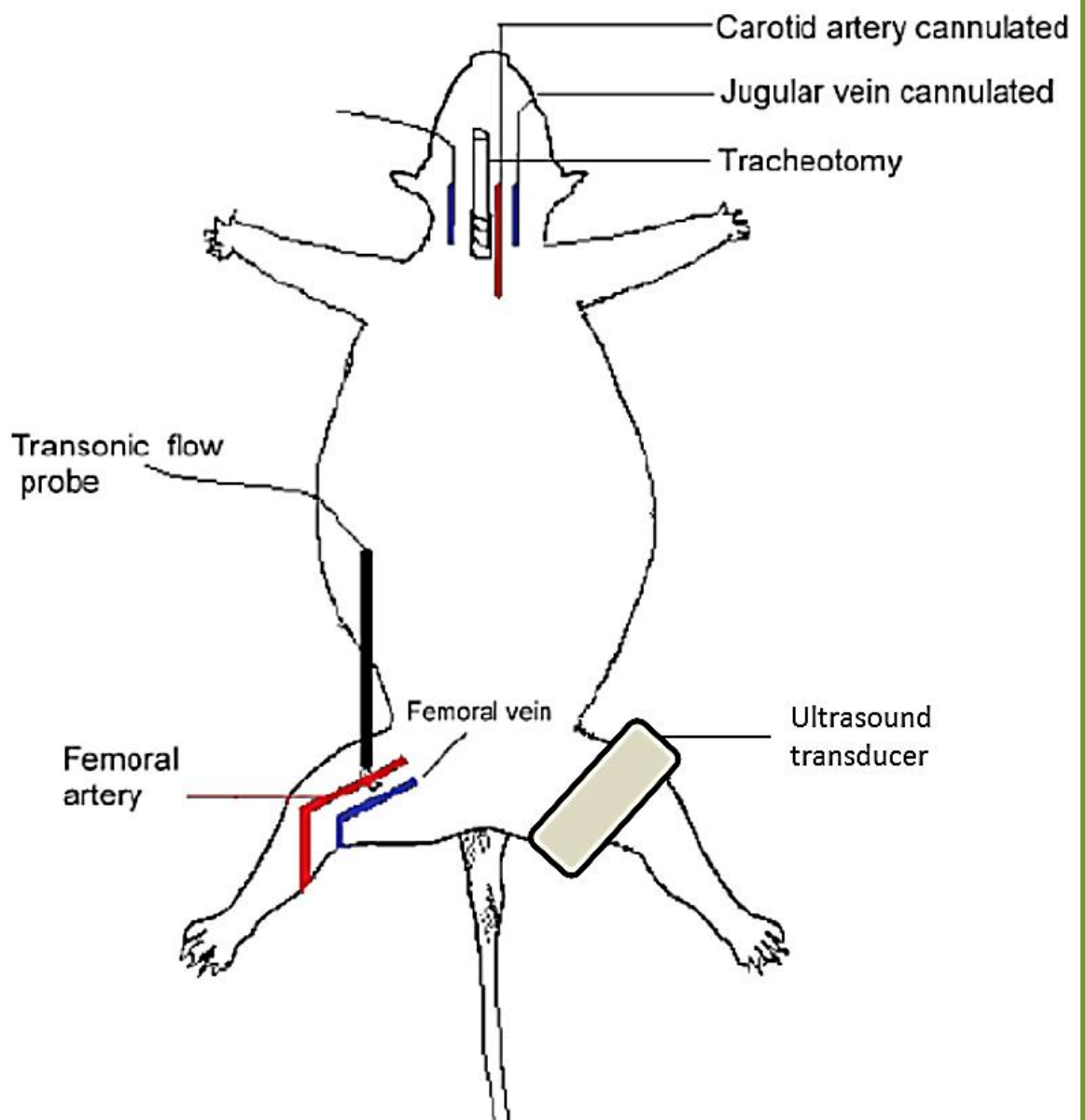


Figure 2.3 Schematic diagram of the surgical cannulations for *in vivo* experiments. Modified from Mahajan *et al.* (23).

2.4.2 Hyperinsulinaemic euglycaemic clamp

The hyperinsulinaemic euglycaemic clamp is a gold standard technique for assessment of whole body insulin sensitivity. Using this method, insulin (Humulin R, Eli Lilly, Indianapolis, IN) was constantly infused ($10 \text{ mU} \cdot \text{min}^{-1} \cdot \text{kg}^{-1}$) while glucose (30% w/v solution) was infused at variable rate to maintain blood glucose level at basal for a period of 120 min. Insulin was diluted freshly prior to the experiment. Steady state glucose infusion rate (GIR) represents the whole body insulin sensitivity.

2.4.3 Glucose and lactate determination

A glucose analyser (Yellow Springs Instruments, Model 2700 Stat Plus) was used to determine blood glucose, blood lactate, plasma glucose and plasma lactate (by glucose oxidase method) concentrations during and at the conclusion of the experiments. A sample volume of 25 μL was required for each determination.

2.4.4 Plasma insulin determination

Rat plasma insulin concentrations before and after the hyperinsulinaemic euglycaemic clamp were determined from arterial blood samples using enzyme-linked immunosorbent assay (ELISA) kit (Mercodia, Uppsala, Sweden) in accordance with the manufacturer's protocol. This ELISA kit has a minimum detectable concentration of $12.18 \text{ pmol} \cdot \text{L}^{-1}$, where the specificity of this ELISA kit was: rat insulin – 100%; human insulin – 167%; human proinsulin – 75%; human C-peptide – < 0.05%; rat proinsulin –

7%; rat C-peptide – < 0.001%; IGF-1 – < 0.02%; IGF-II – <0.02%. The intra-assay variation was between 3.3%, while the inter-assay variation was 2%.

This ELISA kit is a solid phase two-site enzyme immunoassay. The principle of this kit is based on the direct sandwich technique in which two monoclonal antibodies are directed against separate antigenic determinants on the insulin molecule. The microtitration well was coated with anti-insulin antibodies, in which these antibodies bind to the insulin in the samples. The peroxidase-conjugated anti-insulin antibodies then react with the bound insulin. A simple washing step after incubation removes unbound enzyme labelled antibody. The bound conjugate is detected by reaction with a substrate, 3,3',5,5'-tetramethylbenzidine (TMB). The reaction is stopped by adding acid to give a colorimetric endpoint that is read spectrophotometrically at 450 nm.

2.4.5 Plasma free fatty acids determination

Rat plasma free fatty acid levels after dietary intervention was determined from arterial blood samples using a colorimetric assay (NEFA C kit, Wako Pure Chemical Industries, Osaka, Japan) in accordance with the manufacturer's protocol. This kit has a measurable range of 0.05 – 2 mM free fatty acid. The principle of this method based on the enzymatic reactions by Acyl-CoA synthetase (together with coenzyme A and ATP) to convert free fatty acids in the sample to Acyl-CoA, AMP, and pyrophosphoric acid. Acyl-CoA is oxidized by Acyl-CoA oxidase to form 2,3-trans-enoyl-CoA and H₂O₂. H₂O₂ that was produced following the reaction formed a blue purple pigment following reaction with 3-methyl-N-ethyl-N-(β-hydroxyethyl)-aniline, 4-aminoantipyrine, and peroxidase. Free fatty acid levels in the sample are determined from absorbance at 550 nm.

2.4.6 Determination of plasma EGCG levels

Plasma EGCG levels were determined as described by Fu *et al.* (190) with some modifications. Plasma (200 μL) was sampled at the end of the hyperinsulinaemic euglycaemic clamp and stored at $-20\text{ }^{\circ}\text{C}$ until assayed for EGCG levels. 10 μL of resorcinol (0.75 mg.mL^{-1} ; internal standard) and 10 μL of citric acid (20% w/v) were added to each plasma samples. The subsequent mixture was extracted twice with ethylacetate (400 μL) by vortex-mixing for 30 s and then centrifugation at $16,000 \times g$ for 10 min at $4\text{ }^{\circ}\text{C}$. The upper organic phase was collected and evaporated under nitrogen in a $50\text{ }^{\circ}\text{C}$ water bath. The residue was reconstituted in 100 μL of buffer consisting of 0.1 % citric acid and acetonitrile (83:17, v/v), followed by centrifugation at $16,000 \times g$ for 10 min at $4\text{ }^{\circ}\text{C}$. EGCG extraction was $96 \pm 4\%$. The supernatant (50 μL) was subjected to reverse-phase high performance liquid chromatography (HPLC) for analysis. The analytes were eluted on a Gemini[®] 5 μm C18 110Å LC Column (250 x 4.6 mm; Phenomenex) maintained at room temperature using an isocratic mobile phase composed of 0.1% citric acid and acetonitrile (83:17, v/v) running at 1 mL.min^{-1} , and using a detection wavelength of 273 nm. Coefficient of variation for inter- and intra-day assay was 2% and 3% respectively.

2.4.7 Measurement of muscle microvascular perfusion

CEU imaging of skeletal muscle was performed as described previously (191) for determination of microvascular perfusion. A linear array transducer (L9-3) was positioned over the left hindlimb of the rat to image the adductor magnus and semi-membranosus muscle groups. The probe was interfaced with an iU22 ultrasound

(Philips Medical Systems, Australia). Figure 2.4 shows a CEU image of the rat hindlimb. Low mechanical index (0.08) real-time imaging was performed. The acoustic focus and gain settings were optimized and held constant throughout the experiment. Octafluoropropane microbubbles (perflutren lipid microsphere, DEFINITY[®], Lantheus Medical Imaging, Australia) were diluted 1:25 in saline and infused intravenously at 30 $\mu\text{L}\cdot\text{min}^{-1}$ for 15 min to reach steady state before images were acquired. Figure 2.5 shows the ultrasound images obtained at different time point during microbubbles infusion. When steady state was achieved, a high energy destructive pulse of ultrasound (mechanical index = 1.15) was transmitted to destroy microbubbles within the volume of muscle tissue being imaged. Following this destructive pulse, microbubbles replenished the vasculature in the volume of muscle tissue being imaged. Replenishment of microbubbles was captured for 45 s in real-time. This was repeated three times and the acoustic intensity for each time point averaged between the three consecutive loops. Digital images were analysed off-line using QLab (Philips Medical Systems, Australia). Images were background subtracted (0.5 s frames) to eliminate signal from larger blood vessels and tissue *per se*. Analysis of the data was performed identically for all rats. Replenishment curves (Figure 2.6) were used to determine the microvascular blood volume in skeletal muscle. Background-subtracted acoustic-intensity versus time was fitted to the function: $y = A (1 - e^{-\beta \cdot (t - 0.5)})$, where: y is acoustic-intensity at time t , A is plateau acoustic intensity (a measure of microvascular blood volume, MBV), and β is the filling rate by microbubbles (a measure of microvascular flow velocity).

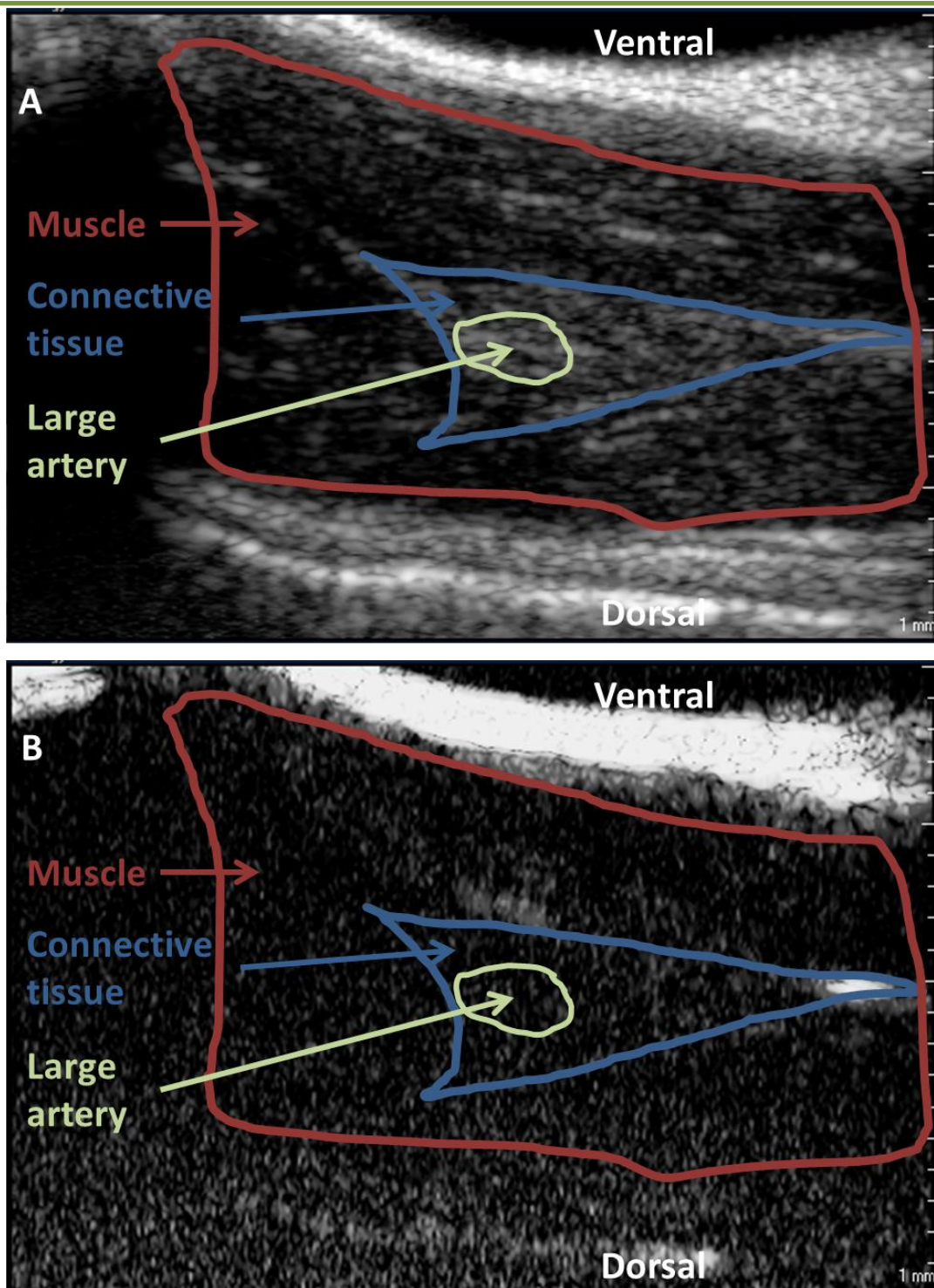


Figure 2.4 Example of (A) ultrasound and (B) contrast enhanced ultrasound images of the upper thigh of the rat hindlimb in short axis. Muscle region is the region of interest during analysis. The connective tissue was used as reference point when positioning the probe.

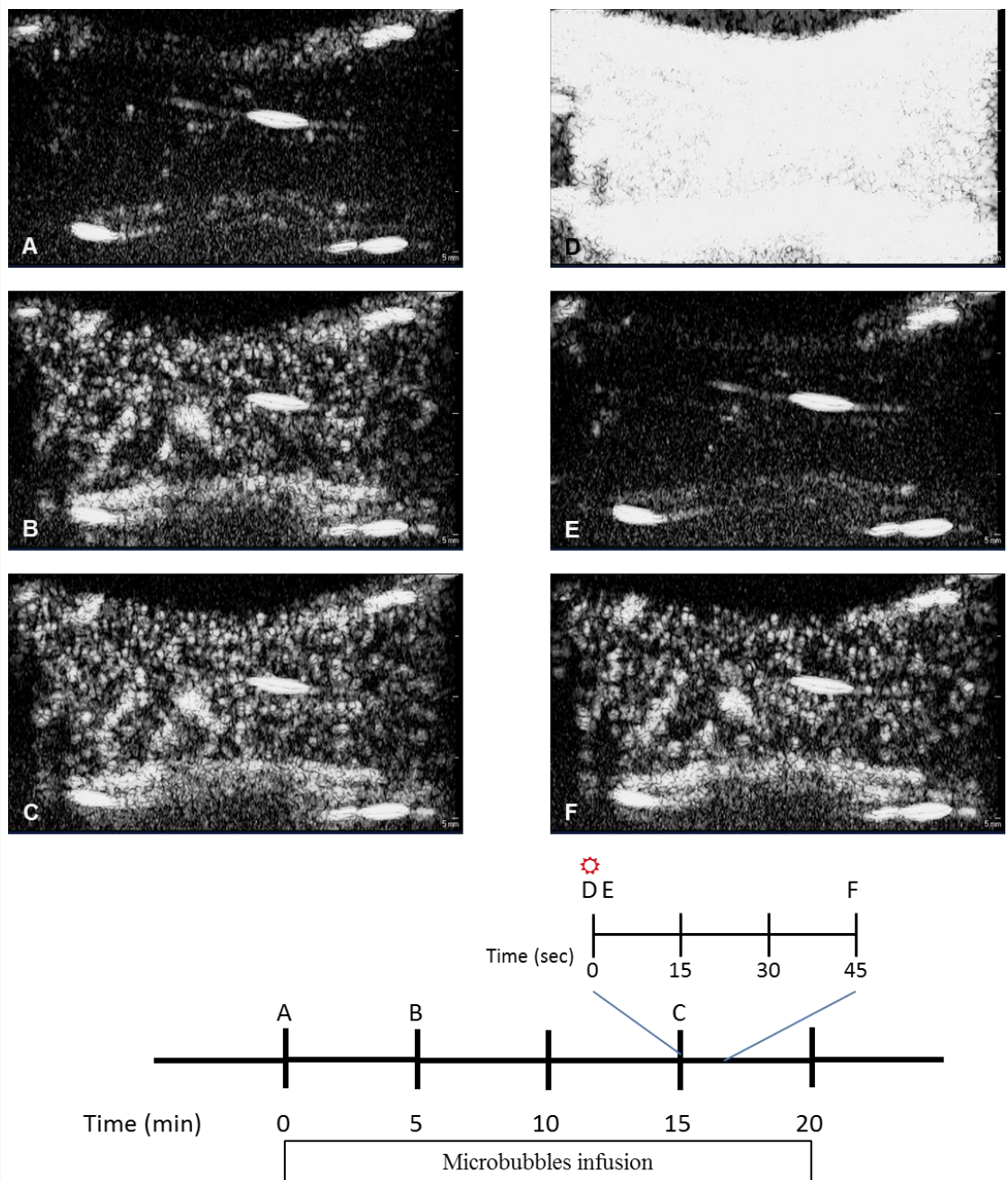

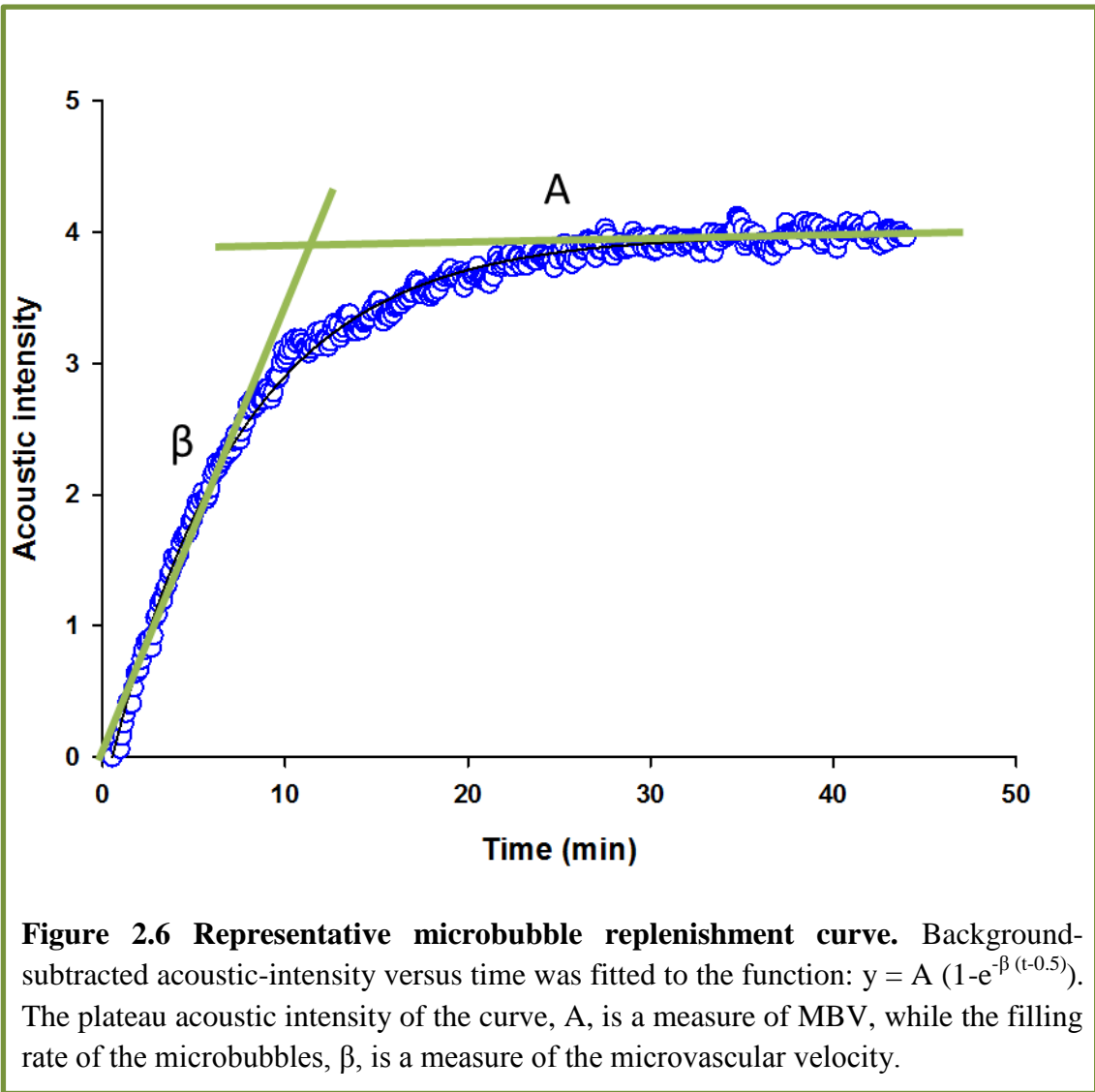


Figure 2.5 Contrast enhanced ultrasound images at different time points of microbubble infusion. Panel A shows the CEU image at 0 min (i.e. no microbubbles). Panel B shows the CEU image at 5 min. Panel C shows the CEU image at 15 min, the steady state of microbubble infusion. Panel D shows the CEU image during the transmission of high energy destructive pulse of ultrasound . Panel E shows the CEU image after the destructive pulse (100 ms following the destructive pulse), few or no microbubbles in the muscle tissue. Panel F shows the CEU image 45 s after the destructive pulse, where the microbubbles have fully replenished the vasculature in the muscle tissue.



2.4.8 Muscle-specific glucose uptake

Radiolabelled 2-[1- ^{14}C]-deoxy-D-glucose (^{14}C -2-DG; specific activity 50 – 60 mCi.mmol $^{-1}$, American Radiolabelled Chemicals, Saint Louis, MO, USA) was used to assess muscle-specific glucose uptake as described previously (192). A 10 μCi bolus of ^{14}C -2-DG in saline was administered 10 min prior to the end of the experiment followed by a continuous 10-minute arterial blood withdrawal at 40 $\mu\text{L.min}^{-1}$. From this 10-minute blood withdrawal sample, 25 μL of plasma was collected to determine the plasma ^{14}C -2-DG level. At the conclusion of the experiment, the whole calf muscle was removed, freeze-clamped in liquid nitrogen and stored at $-80\text{ }^{\circ}\text{C}$ until assayed for muscle ^{14}C -2-DG uptake.

The frozen muscles were ground under liquid nitrogen and approximately 100 mg of ground muscle was homogenized in 1.5 mL distilled water using a Heidolph silent crusher M (4,700 x g, Schwabach Germany). The homogenate was centrifuged at 16,000 x g for 10 min at $4\text{ }^{\circ}\text{C}$, ^{14}C -2-DG levels were determined from the 100 μL muscle aqueous extract after homogenization. Free and phosphorylated ^{14}C -2-DG from muscle aqueous extract (1 mL) was separated using an anion exchange resin (AGI-X8; Bio-Rad Laboratories, CA, USA). Biodegradable counting scintillant (3 mL, Amersham, Arlington Heights, IL, USA) was added to the 25 μL of ^{14}C -2-DG plasma samples and 100 μL of the muscle aqueous extract after homogenization. 16 mL of scintillant was added to the radioactive samples separated by the ion exchange chromatography. Radioactive counts (disintegrations per minute, dpm) were determined using a scintillation counter (LS6500 Beckman CoulterTM, USA). The radioactive counts of these samples which represent the glucose uptake into muscle

(R'g) were calculated as previously described in detail by others (193; 194) and expressed as $\mu\text{g}\cdot\text{g}^{-1}\cdot\text{min}^{-1}$.

2.5 Akt Western blot

Frozen calf muscle tissue were ground into a fine powder under liquid nitrogen. Approximately 50 mg of powered tissue was sonicated (UCD 300, Bioruptor® Plus, Diagenode, Liege, Belgium) at 4 °C for 3 min on high setting in solubilising buffer (1:60 w/v). The solubilising buffer consisted of 25 mM Tris, 2.6 M KF and 250 mM Na₂EDTA at pH 8.0. The homogenate was centrifuged at $16,000 \times g$ for 10 min at 4 °C to remove insoluble material and the protein concentration of the supernatants was determined using Bradford protein assay (Bio-Rad Laboratories, Hercules, CA, USA). An aliquot containing 10 μg protein was heated to 100 °C with an equal volume of SDS sample buffer and electrophoresed on a Novex® 10% Tris-Glycine Mini Gels (Invitrogen, CA, USA). Proteins were electrophoretically transferred to nitrocellulose membranes. After blocking with 5% low fat milk in Tris-buffered saline plus 0.1% Tween 20, membranes were incubated with 1:1000 rabbit anti-phospho-Ser⁴⁷³-Akt (p-Akt, Cell Signalling, Danvers, MA, USA) or 1:1000 rabbit anti-Akt (Cell Signalling) overnight at 4 °C. Following this, the membranes were probed with 1:1000 anti-rabbit secondary antibody (Cell Signalling) for 1 h at room temperature. To visualise the bands equal volumes of West Pico Chemiluminescent Substrate (Thermo Fischer Scientific, Rockford, IL, USA) were mixed together and applied to the membrane. Band intensities were quantified by optical density using DScan EX software version 3.1 (Scanalytics, Rockville, MD, USA).

2.6 Statistical analysis

All data are expressed as means \pm S.E.M. Two-way repeated measures ANOVA with Student-Newman-Keuls post hoc test was used to compare treatment groups over the time course of experiment. An unpaired Student's t-test or a one-way ANOVA with Student-Newman-Keuls post hoc test was used, where appropriate, to make comparisons of differences between endpoint values. All tests were performed using the SigmaPlot 11 (©Systat Software Inc. 2008).

For the constant-flow perfused hindlimb studies, 6 animals in each group will detect a 20% increase in glucose uptake from baseline, or a 20% decrease in perfusion pressure from baseline (power = 0.8, alpha = 0.05). For *in vivo* studies, 8 animals in each group will detect a 30% difference (power = 0.8, alpha = 0.05) in microvascular perfusion.

Chapter 3

Direct metabolic and vascular effects of EGCG in rat skeletal muscle

3.1 Introduction

EGCG has been reported to have insulin-mimetic actions on muscle glucose metabolism and vasodilation *in vitro*. EGCG has been shown to stimulate GLUT4 translocation in skeletal muscle (157; 158; 172) and muscle glucose uptake (157; 172; 173) *in vitro*. On the other hand, EGCG has been demonstrated to be a vasodilator *in vitro*, and EGCG shares a common signalling pathway with insulin in mediating vasodilation (119; 120; 178-182). However, the metabolic and vascular effects of EGCG in an isolated perfused muscle preparation have not been previously characterised.

One of the advantages to assess muscle glucose metabolism in an isolated perfused muscle preparation is to examine the myocyte-specific glucose uptake in the absence of changes in microvascular flow (such as microvascular recruitment). Furthermore, a perfused muscle preparation allows the metabolic actions of EGCG to be assessed in the absence of circulating factors (neural and humoral) that may modify the response to EGCG. It is important to note that isolated cells (C2C12 cells and L6 myotubes) and incubated muscle may possess the same advantages as the perfused muscle preparation. However, isolated cells are not especially insulin sensitive (suprapharmacological insulin concentrations are required to stimulate glucose uptake) (195) and not phenotypically identical to mature myocytes in skeletal muscle *in vivo*. In addition, incubated skeletal muscle receives the nutrients (glucose and insulin) and treatment substances (eg. EGCG) from the bathing incubation buffer through diffusion rather than delivered via vascular network (38; 196).

In contrast, isolated blood vessel systems (eg. aorta, mesenteric vascular bed, and cultured vascular endothelial cells) may not respond to EGCG the same way as skeletal

muscle vasculature. Since skeletal muscle vasculature is the delivery system for myocytes *in vivo*, its responses are the most relevant for assessing the effects of EGCG on glucose delivery and disposal by muscle. Being a non-recirculating and isolated perfused system, it also allows infusion of vasoconstrictors and inhibitors that cannot be used *in vivo* due to secondary effects on other tissues or systems that may indirectly impact on vascular and metabolic actions of EGCG. Thus isolated perfused rat hindlimb system is more useful for dissecting the mechanism of action of EGCG.

The aims of this study were to examine (i) whether EGCG stimulates muscle glucose uptake independent of changes in total muscle blood flow and (ii) whether EGCG has vasodilator properties in muscle vasculature. The constant-flow perfused rat hindlimb preparation was used in the present study to test these aims.

3.2 Methods

3.2.1 Animals

Male Sprague-Dawley rats (n = 101) weighing 222 ± 3 g at 7 – 9 weeks old were used in this study. Animals were housed at 21 ± 2 °C with a 12h: 12h light: dark cycle. The rats were allowed free access to drinking water and food *ad libitum*. Rats were provided with normal chow from Specialty Feeds, Glen Forest, WA, Australia (5FD) or from Ridley AgriProducts, Vic, Australia (9FD) (See Table 2.1). Both 5FD and 9FD fed rats were used in this chapter due to a change in the standard rodent chow at the University of Tasmania animal facility. All experimental procedures were approved by the University of Tasmania Animal Ethics Committee (A11282) and performed in

accordance with the Australian Code of Practice for the Care and Use of Animals for Scientific Purposes – 2004, 7th Edition.

3.2.2 Constant-flow perfused rat hindlimb: Metabolic studies

3.2.2.1 Protocol 1

The dose response effect of EGCG on muscle glucose uptake was assessed using the constant-flow perfused rat hindlimb preparation. The vasculature in the constant-flow perfused rat hindlimb system is fully dilated, making this an ideal preparation for studying muscle glucose uptake in the absence of vasodilation and thus augmentation of glucose delivery by insulin or EGCG. Surgery was carried out in the rats fed with 9FD as described in **2.3.2**. Dose response effects of EGCG on muscle glucose uptake were carried out according to the protocol outlined in Figure 3.1A. Following the surgery, rats were connected to the perfusion apparatus (See **2.3.3**) and allowed a 30-min equilibration period to allow washout of red blood cells. Rat hindlimbs were perfused at a constant flow rate of $0.5 \text{ mL} \cdot \text{min}^{-1} \cdot \text{g}^{-1}$ of perfused muscle. Insulin (final concentration 15 nM) or saline were present in the perfusion buffer reservoir when the rats were connected to the perfusion apparatus. EGCG was infused at 0.1, 1, 10 and 100 μM in 15 min step-wise increments. Muscle glucose uptake was measured using 2-[1,2- $^3\text{H}(\text{N})$]-deoxy-D-glucose (^3H -2-DG; specific activity 5 – 10 $\text{Ci} \cdot \text{mmol}^{-1}$, Perkin Elmer Inc.), where ^3H -2-DG was added into the buffer reservoir (50 $\mu\text{Ci} \cdot \text{L}^{-1}$) after the equilibration period. Perfusate effluent was collected every 15 min before and during the course of the experiment. Whole calf muscle was excised and freeze-clamped at the end of the experiment.

3.2.2.2 Protocol 2

Another set of experiments was conducted to assess the effects of EGCG on muscle glucose uptake over a longer period of time. In this protocol, 10 μM EGCG was infused for a period of 60 min. This dose of EGCG was chosen because EGCG is not toxic to the rats *in vivo* at doses up to 12 μM (500 $\text{mg.kg}^{-1}.\text{d}^{-1}$) (197; 198). Furthermore, EGCG might require a longer period of time to activate the muscle signalling pathway, in which insulin requires ~20 – 30 min to fully activate the signalling cascade in muscle (18; 199). Surgery was carried out in overnight fasted 5FD rats as described in 2.3.2. Figure 3.1B outlines the experimental protocol of this study. In Protocol 2, saline or insulin (15 nM) infusion started after the equilibration period. EGCG was infused to a final concentration of 10 μM during the saline or insulin infusion. Perfusate effluent was collected every 10 min before and during the course of the experiment. ^{14}C -2-DG (25 nCi.min^{-1} ; American Radiolabeled Chemicals Inc.) infusion started 30 min before the end of experiment for the determination of muscle glucose uptake. Whole calf muscle was excised and freeze-clamped at the end of experiment.

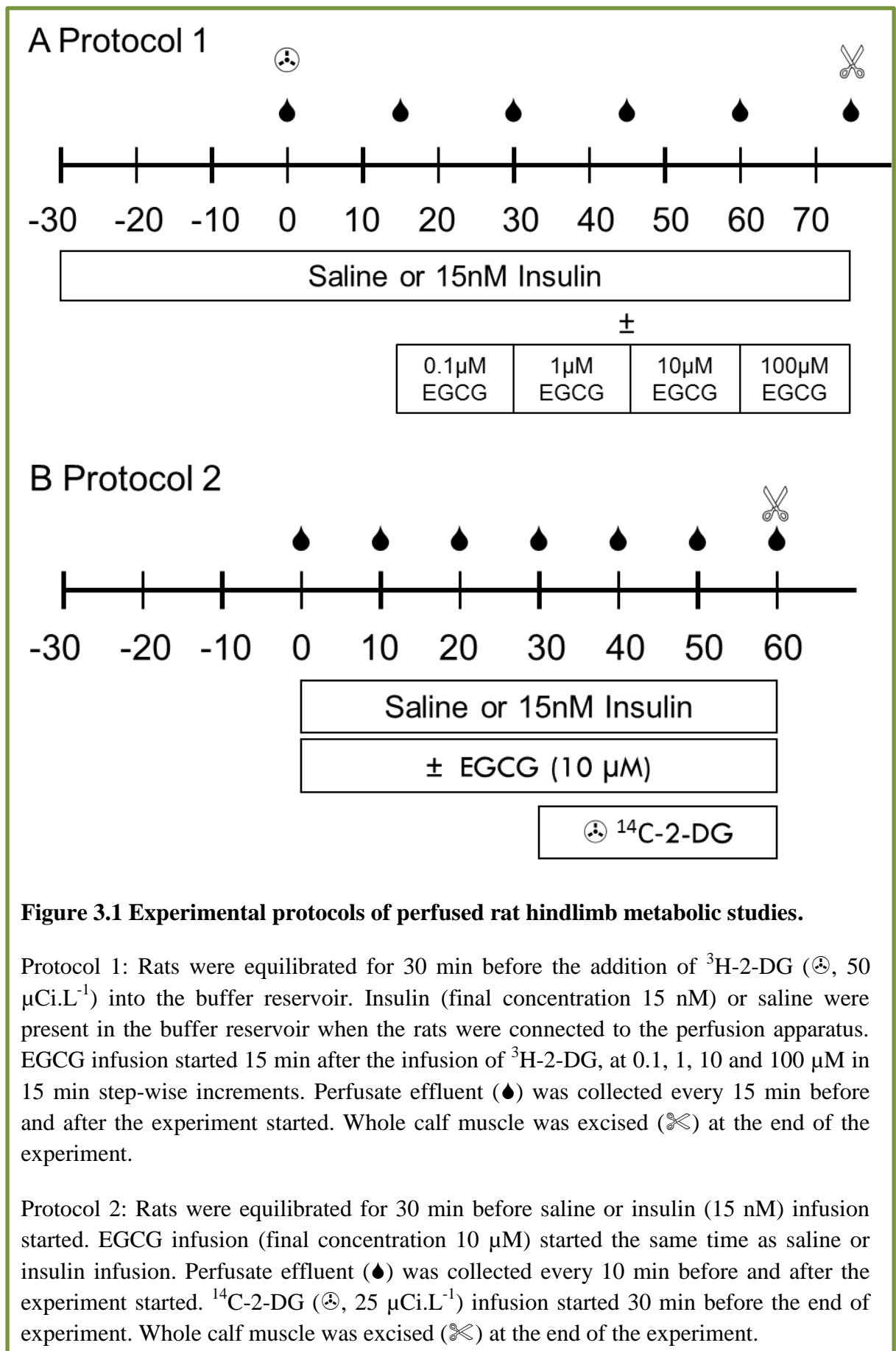


Figure 3.1 Experimental protocols of perfused rat hindlimb metabolic studies.

Protocol 1: Rats were equilibrated for 30 min before the addition of $^3\text{H-2-DG}$ (⊕, 50 $\mu\text{Ci.L}^{-1}$) into the buffer reservoir. Insulin (final concentration 15 nM) or saline were present in the buffer reservoir when the rats were connected to the perfusion apparatus. EGCG infusion started 15 min after the infusion of $^3\text{H-2-DG}$, at 0.1, 1, 10 and 100 μM in 15 min step-wise increments. Perfusate effluent (●) was collected every 15 min before and after the experiment started. Whole calf muscle was excised (✂) at the end of the experiment.

Protocol 2: Rats were equilibrated for 30 min before saline or insulin (15 nM) infusion started. EGCG infusion (final concentration 10 μM) started the same time as saline or insulin infusion. Perfusate effluent (●) was collected every 10 min before and after the experiment started. $^{14}\text{C-2-DG}$ (⊕, 25 $\mu\text{Ci.L}^{-1}$) infusion started 30 min before the end of experiment. Whole calf muscle was excised (✂) at the end of the experiment.

3.2.2.3 Hindlimb glucose uptake

Glucose concentrations of the perfusion buffer and effluent were determined using a glucose analyser as described in 2.4.3. Hindlimb glucose uptake was calculated using the formula: ([Buffer Glucose]-[Effluent Glucose]) x Perfusion Flow Rate, and expressed as $\mu\text{mol}\cdot\text{min}^{-1}$.

3.2.2.4 Muscle-specific glucose uptake ($R'g$)

While hindlimb glucose uptake measures glucose disposal across the whole hindlimb, which consists of muscle tissue, as well as adipose, skin, bone and connective tissue, $R'g$ indicates glucose disposal into muscle specifically. In protocols 1 and 2, ^3H -2-DG or ^{14}C -2-DG was used to measure $R'g$. At the end of experiment, 100 μL of perfusion buffer was collected to determine the influx 2-DG levels. Biodegradable counting scintillant (3 mL; Amersham, Arlington Heights, IL, USA) was added to the 100 μL of perfusion buffer samples. $R'g$ was determined as described in 2.4.8.

3.2.3 Constant-flow perfused rat hindlimb: Vascular studies

Surgery was carried out in the 5FD rats as described in 2.3.2. Vascular studies in hindlimbs were carried out according to the protocol outlined in Figure 3.2. The vasculature in the constant flow perfused hindlimb system is fully dilated. Therefore, in order to study the potential vasodilatory response of EGCG, the hindlimb vasculature was pre-constricted with norepinephrine (NE, 0.6 or 5 μM) or 5-hydroxytryptamine (5-HT, 0.15 – 0.24 μM) to increase perfusion pressure to approximately 70 – 150 mmHg.

These vasoconstrictors were chosen as they constrict at different sites in the vascular tree and each causes blood flow re-distribution through a different vascular pathway, termed nutritive and non-nutritive (38).

The vasoconstrictors were infused 30 min prior to and during infusion of saline (vehicle) or EGCG (0.1, 1, 10, 100 μ M in 15 min stepwise increments). At the end of each experiment, 500 μ M sodium nitroprusside (SNP) was infused to assess maximal vasodilatory capacity of the isolated hindlimb, in order to determine the absence of oedema-mediated vasoconstriction which may mask the vasodilation effects of EGCG. Perfusion pressure was continually recorded using WinDaq data acquisition software (DataQ Instruments, Akron, OH, USA).

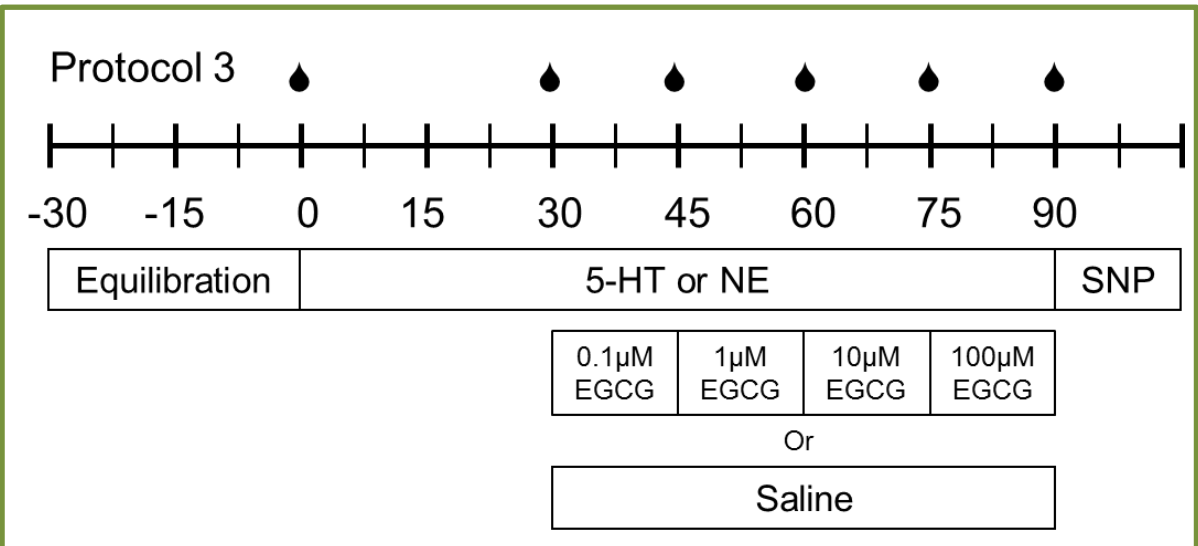


Figure 3.2 Experimental protocol of perfused rat hindlimb vascular studies.

Protocol 3: Rats were equilibrated for 30 min before infusion of vasoconstrictors (5-HT or NE) started. Rats were either infused with saline (vehicle) or EGCG (0.1, 1, 10, 100 μ M in 15 min stepwise increments) 30 min after the infusion of vasoconstrictor. Perfusate effluent (●) was collected before and every 15 min after the experiment started. At the end of each experiment, 500 μ M SNP was infused to assess maximal vasodilatory capacity of the isolated hindlimb.

3.2.4 Statistical analysis

All data are expressed as means \pm S.E.M. Two-way repeated measures ANOVA with Student-Newman-Keuls post hoc test was used to compare treatment groups over the time course of the experiment. A one-way ANOVA with Student-Newman-Keuls post hoc test was used, where appropriate, to make comparisons of differences between endpoint values. All tests were performed using the SigmaPlot 11 ([©]Systat Software Inc. 2008).

3.3 Results

3.3.1 Metabolic effects of EGCG in perfused rat hindlimbs

The effects of 4 different doses of EGCG (0.1, 1, 10, and 100 μ M) on muscle glucose uptake were assessed. Hindlimb glucose uptake at 0 min was not different between saline and EGCG groups (1.51 ± 0.49 and 1.40 ± 0.37 μ mol.min⁻¹ respectively), and none of the EGCG doses (0.1 – 100 μ M) tested stimulated hindlimb glucose uptake (Figure 3.3A and B). As expected, insulin stimulated hindlimb glucose uptake by 3.8 fold (Figure 3.3C, $p < 0.001$ vs. saline), but this response was not altered at any dose of EGCG tested (Figure 3.3D). R'g was assessed at the end of the experiment using the isotopic glucose tracer ³H-2-DG. Compared to saline, insulin stimulated muscle glucose uptake by 3.6 fold (Figure 3.4, $p < 0.001$). EGCG alone did not alter muscle glucose uptake and did not augment insulin-stimulated muscle glucose uptake (Figure 3.4).

Next, the metabolic effects of a single dose (10 μ M) of EGCG was assessed for 60 min (Protocol 2). At the end of the experiment, hindlimb glucose uptake in saline and

EGCG infused rats were not significantly different (2.26 ± 0.31 and 2.60 ± 0.34 $\mu\text{mol}\cdot\text{min}^{-1}$ respectively) and did not change from baseline (Figure 3.5). Insulin stimulated hindlimb glucose uptake by 3.7 fold ($p < 0.001$ vs. saline), and this was not altered by EGCG (Figure 3.5). R'g was assessed at the end of the experiment using the isotopic glucose tracer ^{14}C -2-DG. Compared to saline, insulin stimulated muscle glucose uptake by 7 fold (Figure 3.6, $p < 0.001$). EGCG alone did not alter muscle glucose uptake or augment insulin-stimulated muscle glucose uptake (Figure 3.6).

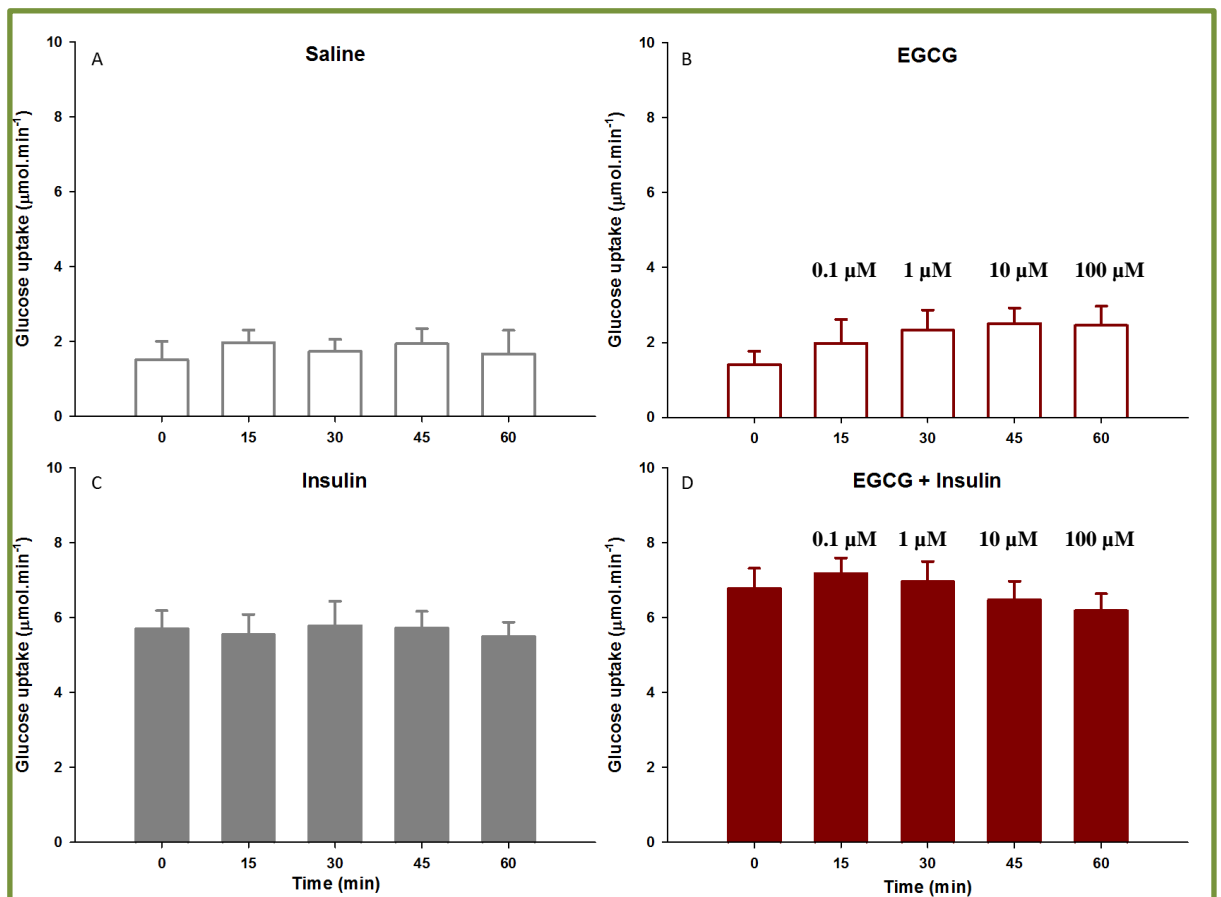


Figure 3.3 Dose-response effects of EGCG on hindlimb glucose uptake in 9FD rats. $n = 8$ in each group. Final concentration of insulin was 15 nM, EGCG was infused into the hindlimb to final concentrations of 0.1, 1, 10, and 100 μM in 15 min increments. Data not statistically significant from 0 min in all groups (repeated measures ANOVA).

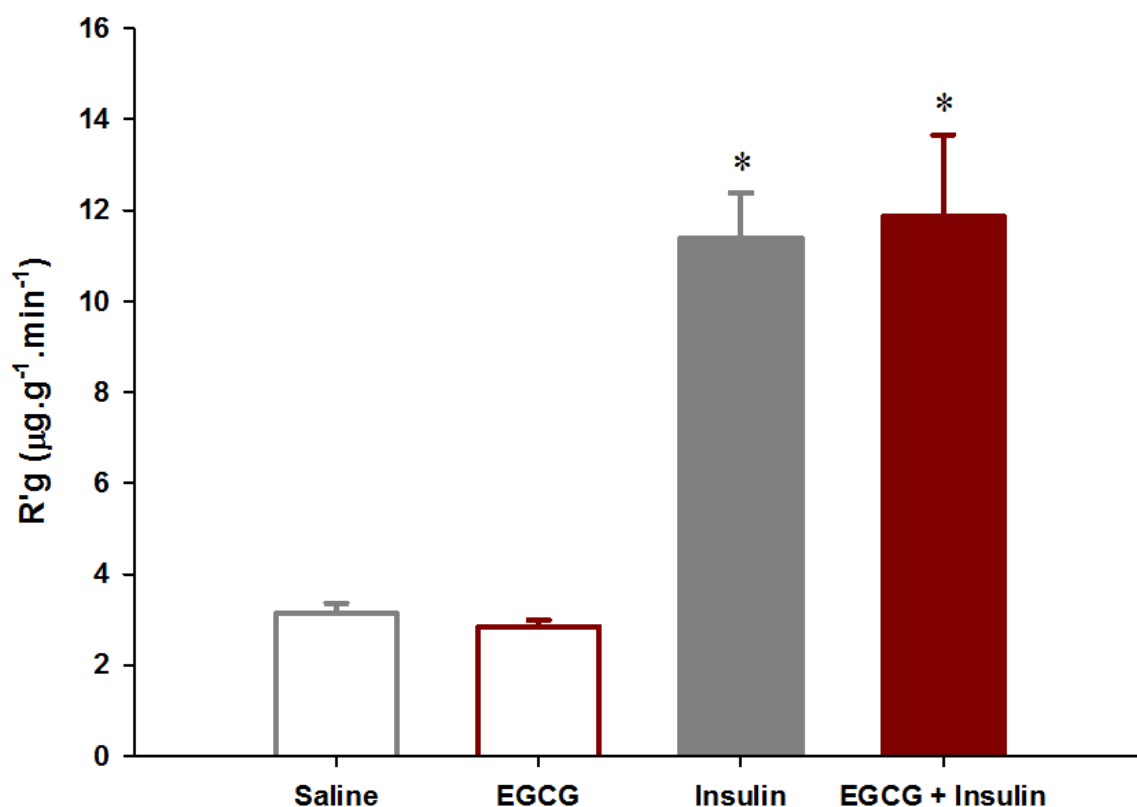


Figure 3.4 Effect of EGCG on ³H-2-DG muscle glucose uptake in 9FD rats. Data represents R'g at the end of experiment, following cumulative of four doses of EGCG in the EGCG and EGCG + Insulin groups. n = 8 in each group. * p < 0.001 vs. Saline and EGCG groups (One-way ANOVA).

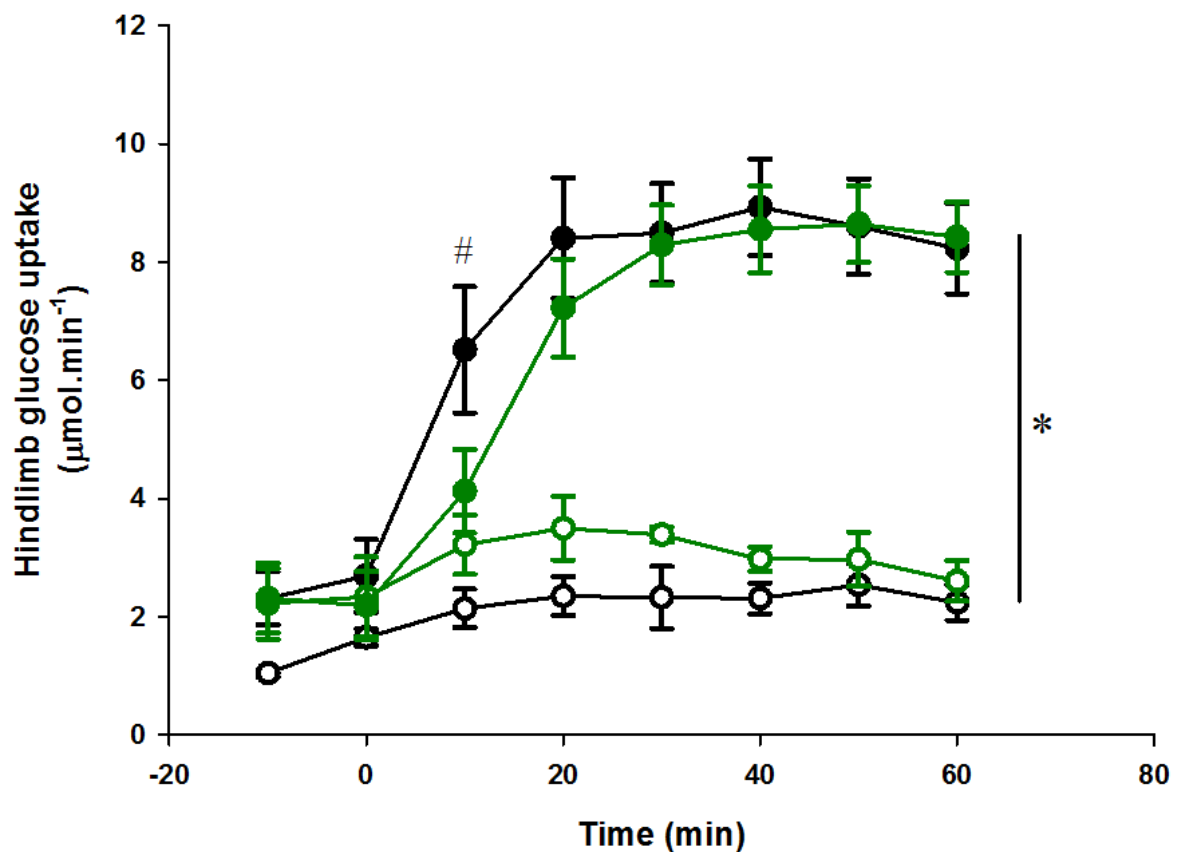
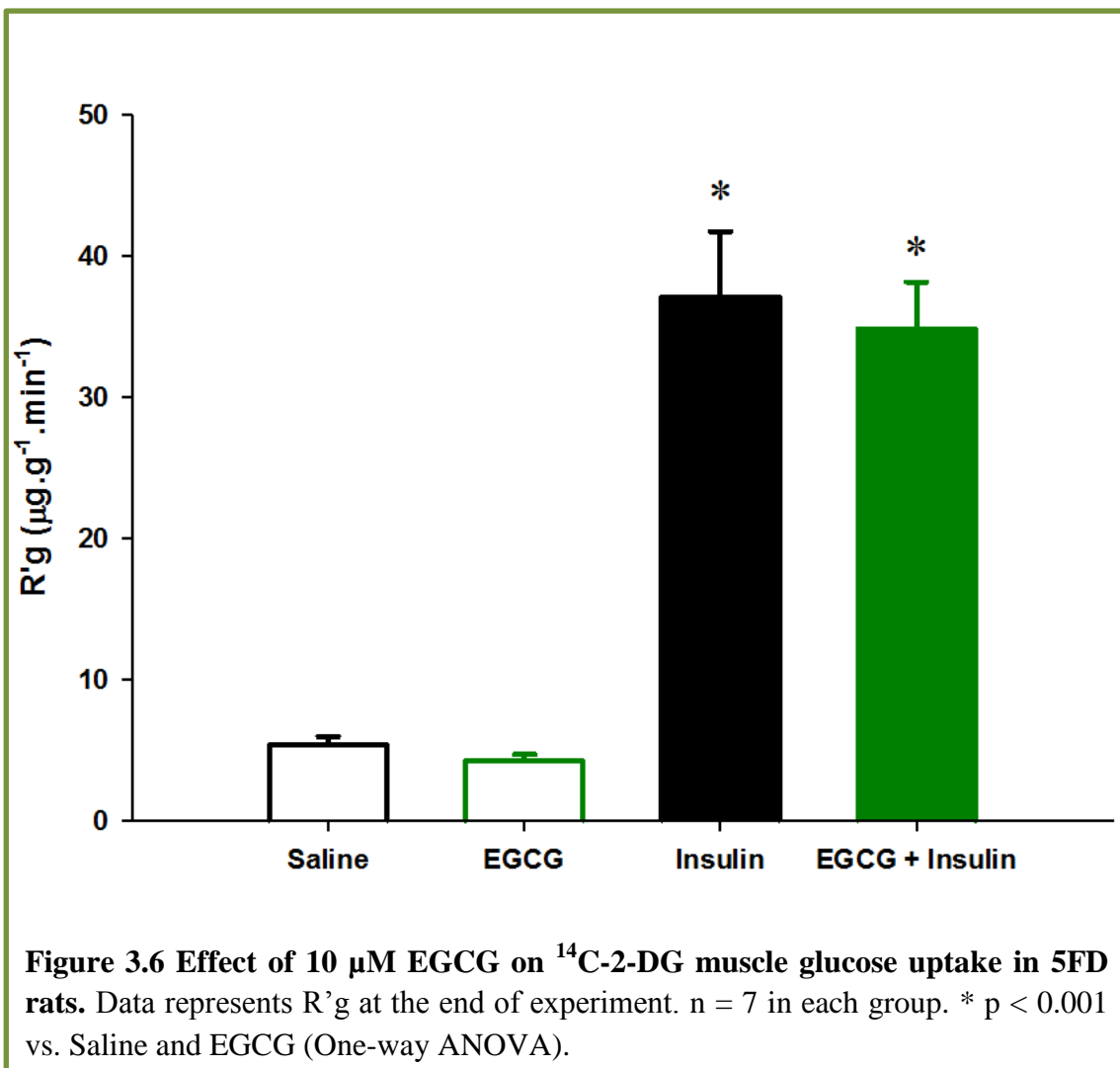


Figure 3.5 Effect of 10 μ M EGCG on hindlimb glucose uptake in 5FD rats. Hindlimb glucose uptake was calculated from the differences in the glucose concentration of the buffer reservoir and perfusate outflow and multiply by the perfusion flow rate. ○ - Saline, □ - EGCG, ● - Insulin, and ■ - EGCG + Insulin, $n = 7$ in all groups. * $p < 0.001$ Insulin and EGCG + Insulin vs. Saline and EGCG (Two-way repeated measures ANOVA). # $p < 0.001$ Insulin vs. all other groups (Two-way repeated measures ANOVA).



3.3.2 Vascular effects of EGCG in perfused rat hindlimbs

3.3.2.1 Low dose NE (0.6 μ M, Type A vasoconstrictor)

The direct vascular actions of EGCG were assessed using the constant-flow perfused rat hindlimb system. Hindlimb perfusion pressure under basal conditions at a flow rate of $\sim 8 \text{ mL} \cdot \text{min}^{-1}$ for a single hindlimb was $40.5 \pm 1.1 \text{ mmHg}$ ($n = 14$). This preparation is fully vasodilated because of the absence of hormonal and neural inputs. Thus, to assess the vasodilatory properties of EGCG, the vasculature preparation was pre-constricted with low dose NE ($0.6 \mu\text{M}$) to increase perfusion pressure to $76.1 \pm 2.5 \text{ mmHg}$ ($n = 14$). Perfusion pressures of EGCG infused at 0.1, 1, 10, and $100 \mu\text{M}$ in 15 min step-wise increments were not different from that of the saline infused NE-pre-constricted hindlimbs (Figure 3.7A). In all hindlimbs, SNP reversed NE-mediated vasoconstriction by $>95\%$, representing maximal vasodilation and return of perfusion pressures to basal levels, indicating absence of oedema-mediated vascular resistance.

3.3.2.2 High dose NE (5 μ M, Type B vasoconstrictor)

Hindlimb perfusion pressure under basal conditions in this set of experiments was $39.5 \pm 1.1 \text{ mmHg}$ ($n = 12$). A high dose of NE ($5 \mu\text{M}$) increased the hindlimb perfusion pressure to $153.8 \pm 5.7 \text{ mmHg}$ ($n = 12$). In the presence of high dose NE, EGCG did not induce vasodilation at 0.1 and $1 \mu\text{M}$. Compared with saline, EGCG induced 14% vasodilation ($p = 0.032$ vs. Saline) at $10 \mu\text{M}$ against high dose NE (Figure 3.7B). However, EGCG did not induce further dilation at $100 \mu\text{M}$ (Figure 3.7B). In all

hindlimbs, SNP reversed NE-mediated vasoconstriction by >95%, representing maximal vasodilation and return of perfusion pressures to basal levels.

3.3.2.3 5-HT (Type B vasoconstrictor)

Hindlimb perfusion pressure during this set of experiments was 39.3 ± 0.9 mmHg ($n = 15$). The vasculature preparation was pre-constricted with 5-HT ($0.15 - 0.24$ μ M) to achieve a comparable perfusion pressure to the low dose NE. Perfusion pressure following 30 min of 5-HT infusion was 76.0 ± 5.4 mmHg ($n = 15$). EGCG infused at 0.1, 1, 10, and 100 μ M in 15 min step-wise increments caused dose-dependent vasodilation in 5-HT pre-constricted hindlimbs (Figure 3.7C). Compared with saline, 1, 10 and 100 μ M EGCG significantly ($P < 0.05$) reduced 5-HT-mediated vasoconstriction. At the highest dose tested (100 μ M), EGCG opposed 5-HT mediated vasoconstriction by $47 \pm 6\%$ ($p < 0.05$ vs. saline). In all hindlimbs, SNP reversed 5-HT-mediated vasoconstriction by >95%, representing maximal vasodilation and return of perfusion pressures to basal levels.

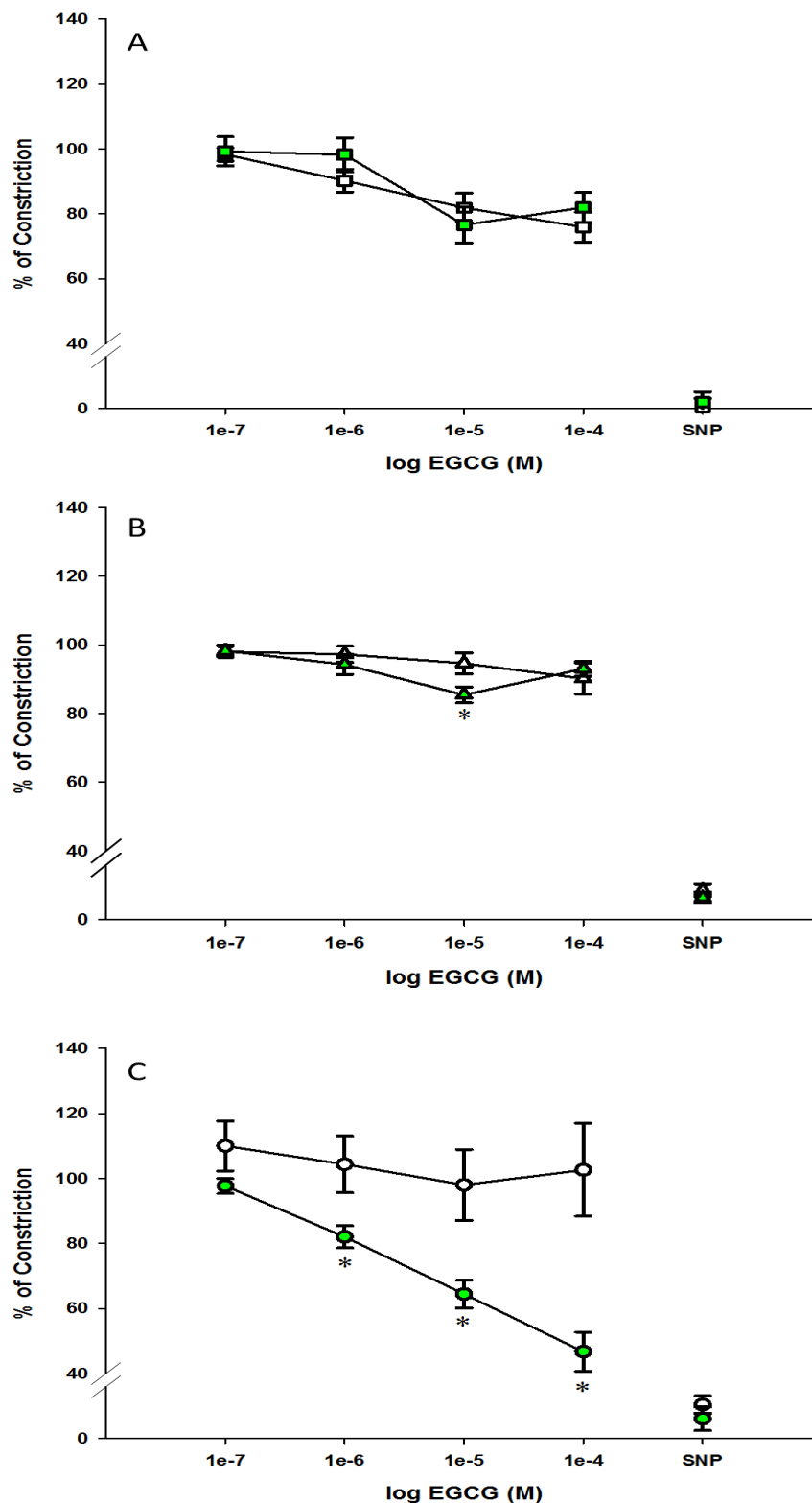


Figure 3.7 Dose-response effects of EGCG on % vasoconstriction during (A) 0.6 μ M NE, (B) 5 μ M NE, and (C) 5-HT infusions. Data represents % of constriction of the perfused rat hindlimb from 30 min after the infusion of vasoconstrictors. White – Saline, green – EGCG. n = 5 – 8 in each groups. * p < 0.05 vs. Saline (Two-way repeated measures ANOVA).

3.4 Discussion

The main findings from this study were i) EGCG does not stimulate muscle glucose uptake directly, and ii) EGCG opposed 5-HT-, but not NE-, mediated vasoconstriction in the skeletal muscle vasculature. Therefore, EGCG possesses some direct vascular, but not metabolic, actions in skeletal muscle.

3.4.1 Metabolic studies

In the present study, the direct metabolic action of EGCG on skeletal muscle glucose uptake was assessed using the constant-flow perfused rat hindlimb system. The vasculature in the constant-flow perfused hindlimb system is fully dilated, making this an ideal preparation for studying muscle glucose uptake independent of the vascular actions of insulin or EGCG. While EGCG has been reported to activate PI3-K and promote GLUT4 translocation in myocytes (172; 173), it is reasonable to hypothesise that EGCG would mimic or sensitise insulin's metabolic action in the perfused rat hindlimb. This study demonstrated that EGCG at 10 μ M alone or after 4 increasing doses (up to 100 μ M) did not stimulate muscle glucose uptake or enhance insulin-stimulated muscle glucose uptake. This indicates that EGCG does not have a direct metabolic action in skeletal muscle *in situ* and does not alter insulin-stimulated glucose uptake in the absence of vascular actions of insulin.

The findings from this study are in contrast with the previous studies by Ueda *et al.* (172) and Jung *et al.* (173), which they reported that EGCG dose-dependently increased glucose uptake in L6 myotubes. One possible explanation for this difference could be that the effects of EGCG on glucose metabolism in muscle in previous

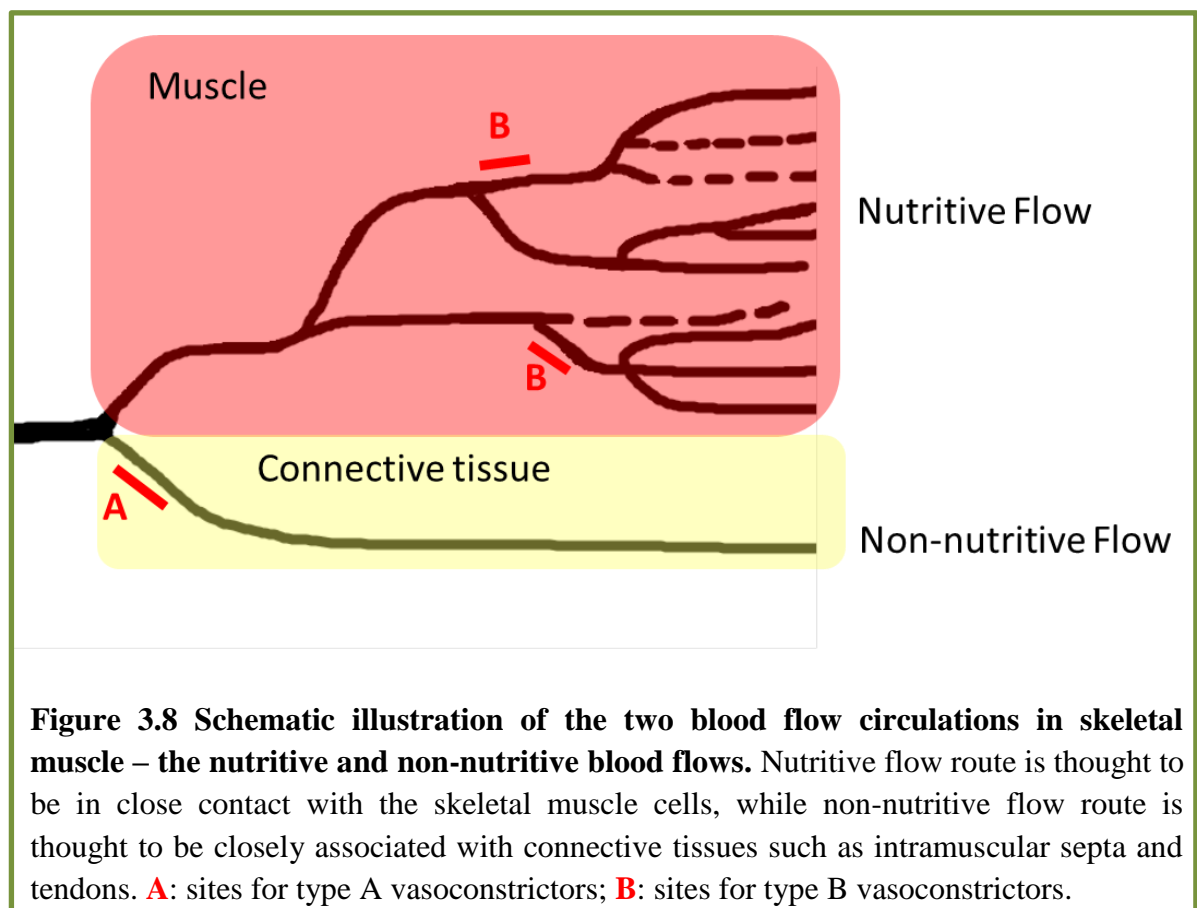
studies (157; 158; 172; 173) were assessed *in vitro* using L6 myotube culture systems. Metabolic effects observed in incubated muscles are likely to be the direct effects from the receptors on skeletal muscle sarcolemma as the nutrients and treatment substances are diffused to the myocytes (38; 196). Constant-flow perfused rat hindlimb preparation that was performed in the present study, as compared to the cell culture preparation, represents a closer approximation to that of an *in vivo* system. This present study showed that EGCG did not stimulate muscle glucose uptake in a perfused muscle system, indicating the vasculature might act as the barrier for EGCG. Thus higher concentrations of EGCG might be required to stimulate muscle glucose uptake when EGCG is being delivered via the vasculature.

3.4.2 Vascular studies

The direct vascular actions of EGCG in skeletal muscle were also characterised in this study using the constant-flow perfused rat hindlimb system. In this preparation, hindlimbs are fully vasodilated due to the absence of hormonal and neural input. Thus, this system allows the investigator to study the direct vascular effect of infused agents, such as EGCG, on the hindlimb vasculature. In protocol 1 and 2, EGCG (1 – 100 μ M) infusion alone (in the absence of vasoconstrictor) has not altered basal perfusion pressure (data not shown).

To determine whether EGCG is a vasodilator, the hindlimbs were pre-constricted to increase the perfusion pressure to 80 – 150 mmHg with NE or 5-HT. These vasoconstrictors were chosen as they constrict at different sites in the vascular tree and each causes blood flow re-distribution through a different vascular pathway termed

nutritive and non-nutritive (Figure 3.8). Type A vasoconstrictors increase muscle metabolism (increase perfusion through the nutritive flow route), while type B vasoconstrictors decrease muscle metabolism (increase perfusion through the non-nutritive flow route) (Figure 3.8) (See review by Clark *et al.* (38)). In the current study, vasodilator properties of EGCG in muscle vasculature were tested against a type A (low dose NE < 1 μ M), and type B (5-HT and high dose NE \geq 1 μ M) vasoconstrictor. Although the metabolic responses to each vasoconstrictor were not directly measured in this study, the characteristics of these vasoconstrictors have been extensively studied in the past (188; 200-204).



The present study showed that EGCG is a vasodilator in the 5-HT pre-constricted hindlimb. This is in accordance with other studies which showed that EGCG induced vasodilation in mesenteric vascular beds (119; 120) and aortic rings (178; 179; 182). The present study showed that EGCG at 10 μ M induced a slight, but significant vasodilation against high dose NE, but not low dose NE. However, the vasodilator properties of EGCG were larger in the presence of 5-HT, where 10 μ M EGCG stimulated 30% vasodilation in the 5-HT pre-constricted rat hindlimb. This study demonstrated that EGCG induces vasodilation in the 5-HT, but not NE pre-constricted hindlimb. Given that EGCG did not vasodilate against high dose NE, this implies that it is not specific to type A or type B vasoconstrictions. Therefore EGCG may dilate against soecific vasoconstrictors. 5-HT has been reported to reduce muscle metabolism in constant-flow perfused rat hindlimb (205) and can result in acute insulin resistance *in vivo* (206). The present study showed that EGCG induced vasodilation against 5-HT, suggesting that EGCG may increase muscle metabolism and overcome insulin resistance *in vivo*.

The mechanism of EGCG-induced vasodilation in skeletal muscle vasculature is unknown. Previous studies have reported that EGCG shares a common signalling pathway with insulin in vascular endothelial cells (119; 179). However this pathway has not been previously verified in the skeletal muscle vasculature. Thus the next chapter of this thesis reports on investigations of the mechanism of EGCG-mediated vasodilation in skeletal muscle.

In summary, this study has demonstrated that EGCG has some direct vascular but not metabolic actions in skeletal muscle. This study shows that EGCG did not directly stimulate muscle glucose uptake and did not enhance insulin-mediated muscle glucose

uptake. Furthermore, EGCG opposes 5-HT-mediated vasoconstriction. Given that EGCG is a vasodilator in skeletal muscle, whether this will in turn enhance nutrients delivery to skeletal muscle and thereby improve muscle glucose uptake is not known, and was investigated in studies reported in Chapter 5.

Chapter 4

Mechanism of EGCG-induced vasodilation in muscle vasculature

4.1 Introduction

The studies described in Chapter 3 showed that EGCG is a vasodilator in the muscle vasculature. In particular, EGCG vasodilated against 5-HT, the vasoconstrictor which results in increased non-nutritive perfusion of muscle (201) and can result in acute insulin resistance (206). The mechanism of EGCG-induced vasodilation in skeletal muscle has not been previously explored. Previous studies have reported that EGCG shares a common signalling pathway with insulin in cultured vascular endothelial cells (119; 179). However, whether this pathway is involved in EGCG-mediated dilation in the skeletal muscle vasculature is unknown.

Insulin stimulates nitric oxide (NO) production in vascular endothelial cells (17; 119). Quon and colleagues have elucidated the insulin signalling pathway in vascular endothelial cells leading to NO production. This pathway requires activation of IRS-1/PI3-K/PDK-1/Akt/eNOS pathway which leads to NO production (4; 8-10). Interestingly, EGCG also stimulates NO production in cultured vascular endothelial cells similar to insulin (119). Both insulin- and EGCG-mediated increases in NO production are dependent on the activation of PI3-K, since wortmannin blocks NO production (119; 179). Furthermore, like insulin, EGCG requires the activation of Akt and eNOS for NO production (119; 179; 181). However, activation of the PI3-K/Akt/eNOS pathway by EGCG does not require the activation of the insulin receptor (119). Interestingly, these results highlight that the EGCG signalling pathway shares features in common with the insulin signalling pathway leading to activation of eNOS and NO production in endothelial cells (119) (Figure 4.1). Studies have reported that EGCG-induced vasodilation in various tissues, including aortic ring (178; 179), bovine ophthalmic artery (180), coronary artery ring (181), and mesenteric vascular bed (119) is mediated by the PI3-K/Akt/NO pathway. In addition, several studies (119; 181) also

suggested that EGCG-mediated vasodilation required the activation of reactive oxygen species (ROS). Quon and colleagues reported that Fyn, a member of Src family tyrosine kinases (SFK) (207), is a signalling molecule upstream of PI3-K which is activated by ROS. SFK can activate PI3-K by binding the p85 regulatory subunit of PI3-K (208; 209) or directly activate eNOS independent of PI3-K (210), however, the mechanism by which Fyn stimulates NO production in vascular endothelial cells is not known. Alternatively, EGCG activates AMPK in bovine aortic endothelial cells (211). Studies have shown that AMPK can activate eNOS on Ser¹¹⁷⁷ and Ser⁶³³ (212; 213), in which phosphorylation of eNOS on Ser¹¹⁷⁷ can lead to NO production (214) and phosphorylation on Ser⁶³³ enhance NO production independent of intracellular Ca²⁺ level (215). The aim of this chapter was therefore to assess the molecular mechanism underlying the vascular actions of EGCG in skeletal muscle with enzyme inhibitory studies using the constant flow perfused rat hindlimb preparation (See Figure 4.1).

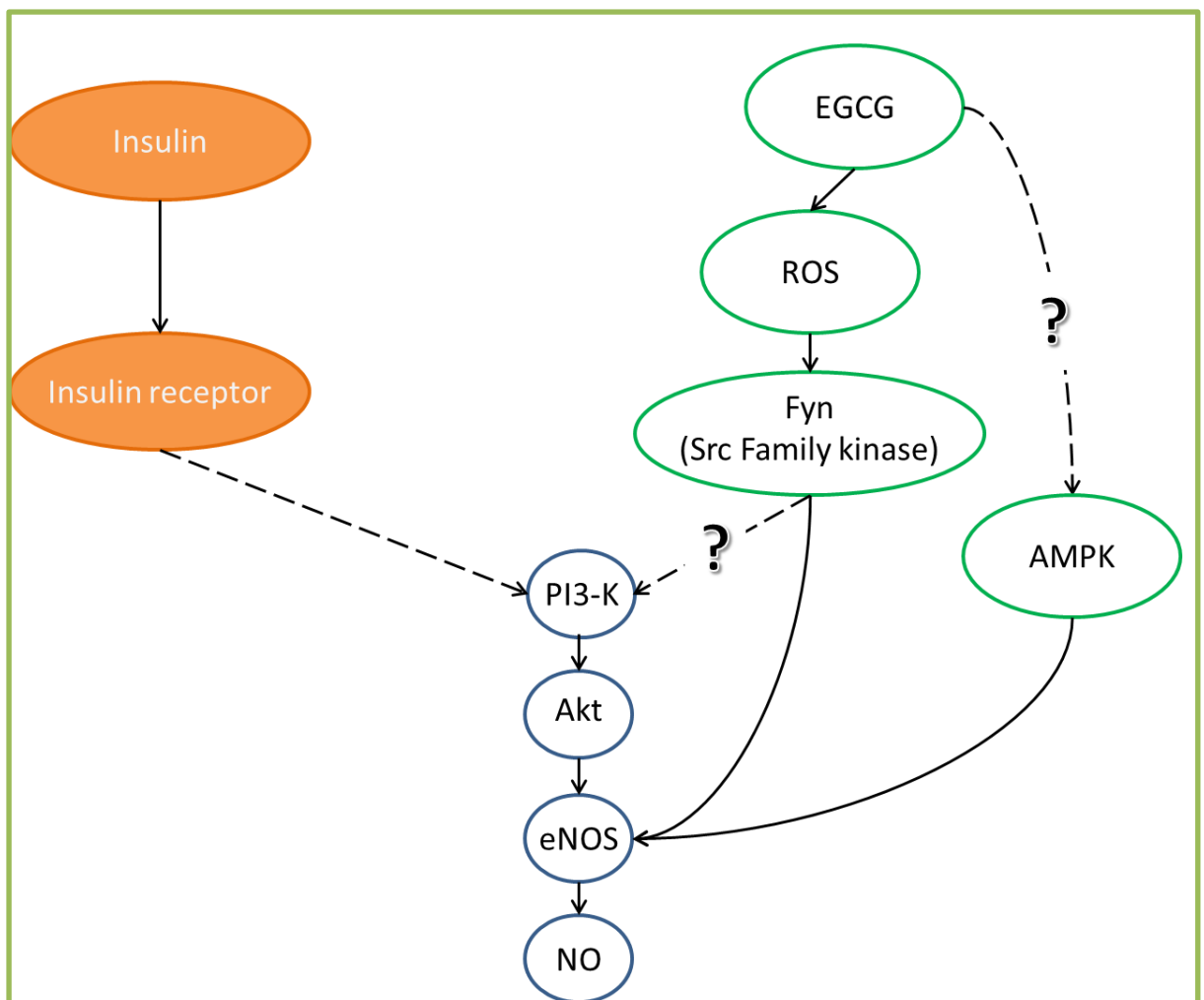


Figure 4.1 Potential pathways of EGCG mediated vasodilation in vascular endothelium of skeletal muscle. EGCG shares a common signalling pathway with insulin to mediated vasodilation in vascular endothelium. EGCG, like insulin, activates PI3-K/Akt pathway, phosphorylates, and activates eNOS to stimulate NO production. However, EGCG does not bind to insulin receptor. EGCG phosphorylates PI3-K via ROS and Fyn (a Src family kinase). EGCG could be activating AMPK, while AMPK is known to phosphorylate eNOS independent of PI3-K. Modified from Kim *et al.* (119)

4.2 Methods

4.2.1 Animals

Male Sprague-Dawley rats ($n = 53$) weighing 226 ± 4 g at 7 – 9 weeks old were used in this study. The rats were allowed free access to drinking water and food *ad libitum*. Rats were provided with normal chow from Specialty Feeds, Glen Forest, WA, Australia (5FD, see **Table 2.1**). All experimental procedures were approved by the University of Tasmania Animal Ethics Committee (A11282) and performed in accordance with the Australian Code of Practice for the Care and Use of Animals for Scientific Purposes – 2004, 7th Edition.

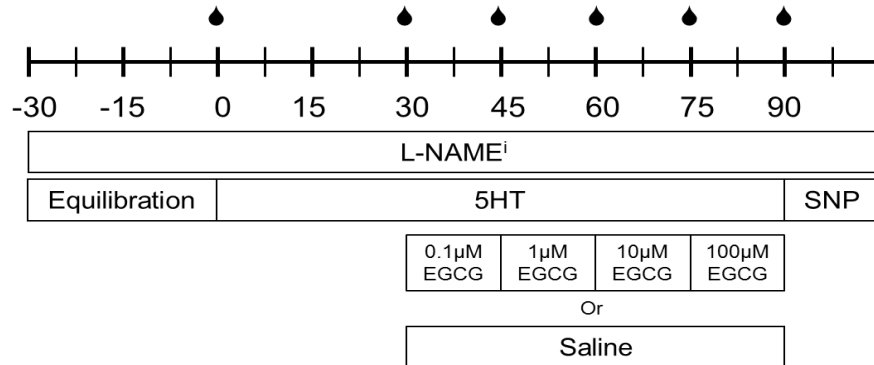
4.2.2 Experimental protocols

The mechanism of EGCG-mediated vasodilation was assessed using the constant flow perfused rat hindlimb preparation. Surgery was carried out in the rats as described in **2.3.2**. Vascular studies in hindlimbs were carried out according to the protocol outlined in Figure 4.2. Following the surgery, rats were connected to the perfusion apparatus (See **2.3.3**) and allowed a 30-min equilibration period to allow washout of red blood cells. The vasculature in the constant flow perfused hindlimb system is fully dilated. Therefore to study the potential vasodilatory response of EGCG, the hindlimb vasculature was pre-constricted with 5-HT ($0.06 - 0.3 \mu\text{M}$) or high dose NE ($5 \mu\text{M}$) to reach a perfusion pressure of ~80 and 150 mmHg respectively. EGCG was infused into the hindlimb to reach final concentrations of 0.1, 1, 10, and 100 μM in 15 min stepwise

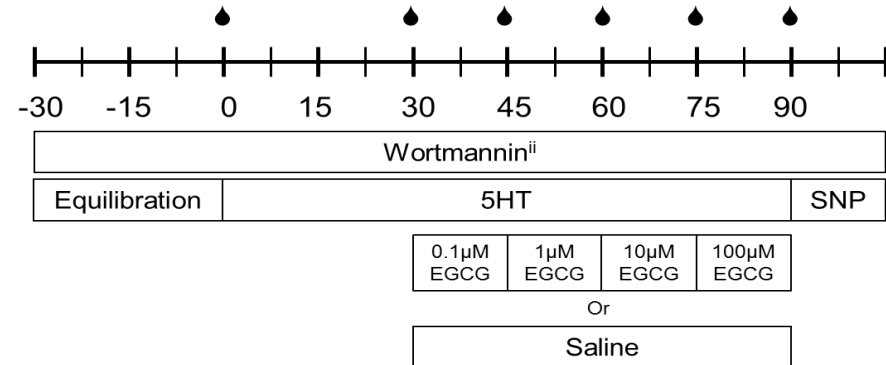
increments. Saline (vehicle) was infused in a separate group of animals for the same length of time (total of 60 min). The vasoconstrictor was infused 30 min prior to and during infusion of saline or EGCG. At the end of each experiment, 500 μ M SNP was infused to assess maximal vasodilatory capacity of the isolated hindlimb. Perfusion pressure was continually recorded using WinDaq data acquisition software (DataQ Instruments, Akron, OH, USA).

The mechanism of EGCG-induced vasodilation in skeletal muscle was assessed according to the protocols outlined in Figure 4.2. The vascular actions of EGCG were examined in the presence of i) Protocol 1: the NOS inhibitor N^o-Nitro-L-arginine methyl ester (L-NAME, 10 μ M), ii) Protocol 2: the PI3-K inhibitor wortmannin (100 nM), iii) Protocol 3: the SFK inhibitor 4-Amino-3-(4-chlorophenyl)-1-(t-butyl)-1H-pyrazolo[3,4-d]pyrimidine (PP2, 10 μ M), and iv) Protocol 4: the AMPK inhibitor Compound C (10 μ M) (Figure 4.3). L-NAME or wortmannin was present in perfusion buffer when the hindlimbs were connected to the perfusion apparatus, while PP2 or Compound C was infused via the infusion port directly into the arterial-line after the designated equilibration period. Wortmannin, PP2 and Compound C were dissolved in dimethyl sulfoxide (80% v/v) and infused at a rate of 1:200 to the perfusate flow rate. Given that EGCG produced the strongest vasodilatory effect against 5-HT (in Chapter 3), the vascular actions of EGCG in the presence of L-NAME, wortmannin, and Compound C were examined in 5-HT pre-constricted hindlimbs. However, because 5-HT mediated vasoconstriction is mainly mediated by the 5-HT_{2A} receptor, which is Src kinase dependent and therefore inhibited by PP2 (216), the effects of PP2 on EGCG-mediated vasodilation were examined in NE pre-constricted hindlimb, which is not SFK dependent.

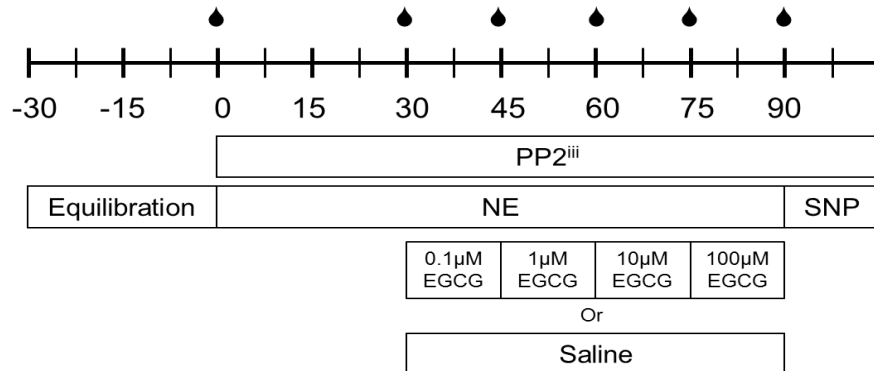
Protocol 1



Protocol 2



Protocol 3



Protocol 4

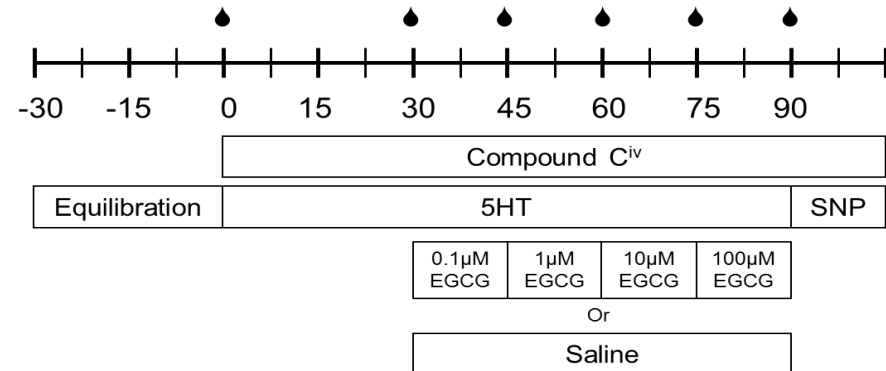
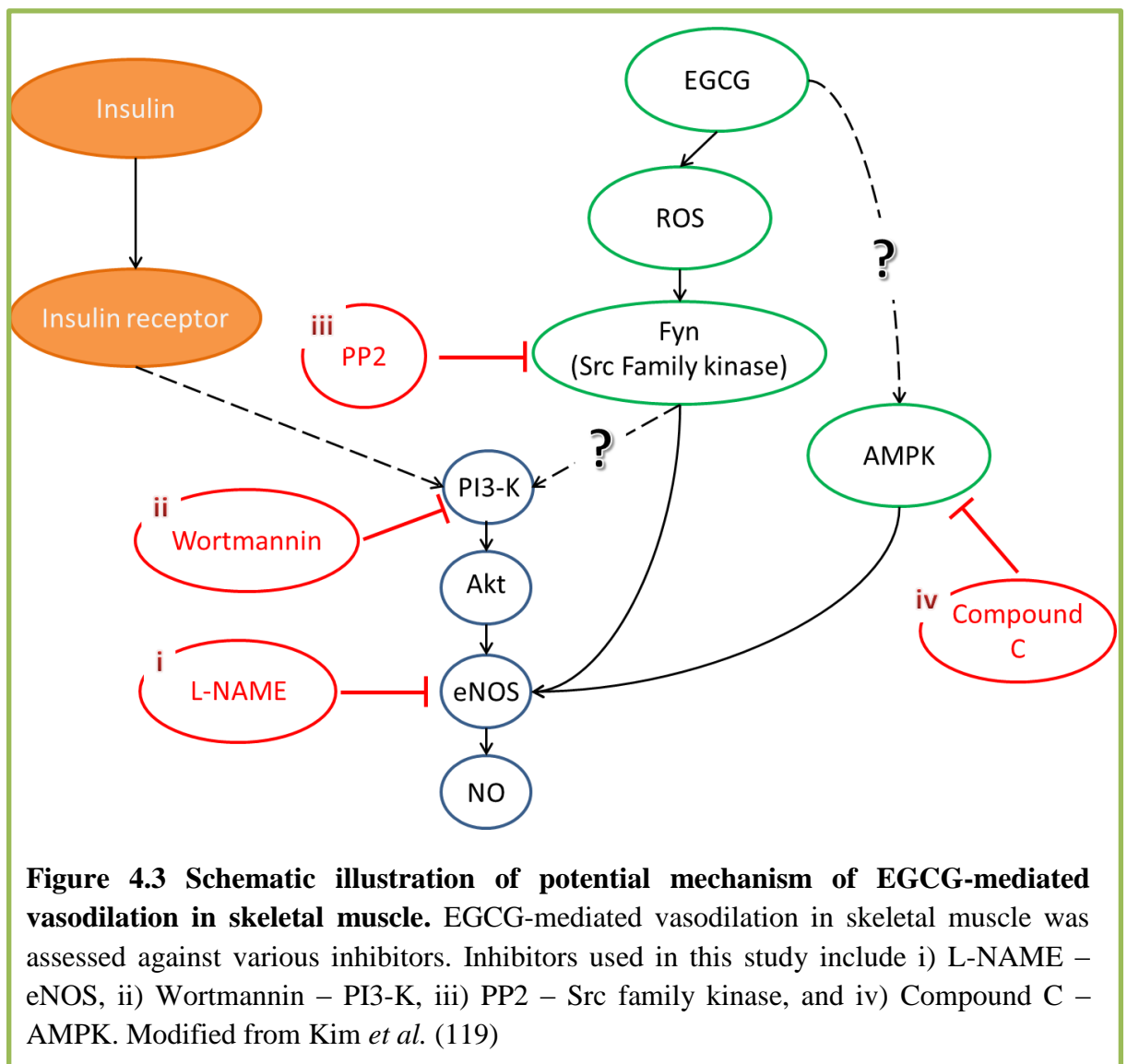
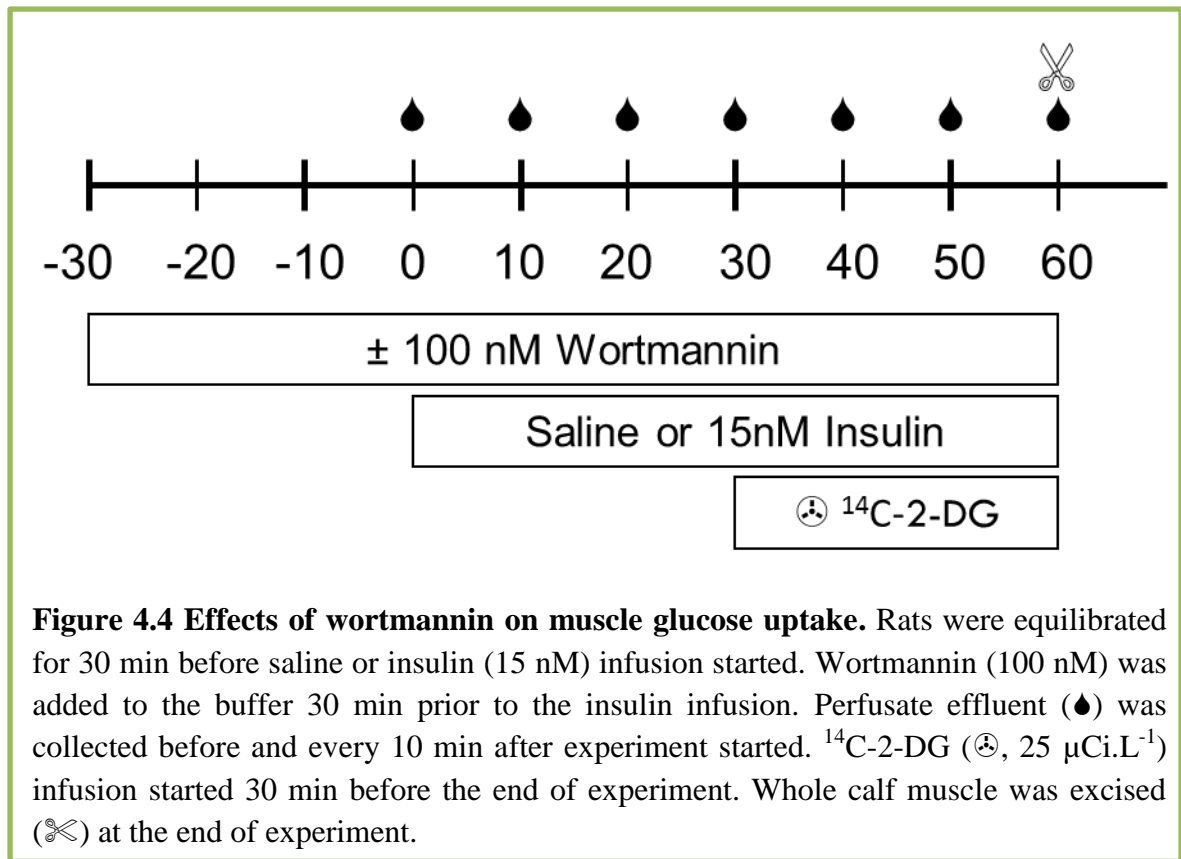


Figure 4.2 Experimental protocols. Protocol 1: Effects of L-NAME on EGCG-induced vasodilation; Protocol 2: Effects of wortmannin on EGCG-induced vasodilation; Protocol 3: Effects of PP2 on EGCG-induced vasodilation; Protocol 4: Effects of Compound C on EGCG-induced vasodilation. In all protocols, EGCG was infused to final concentrations of 0.1, 1, 10, and 100 µM in 15 min stepwise increments (See Figure 4.3). Perfusate effluent samples (●) were collected at times indicated in the figure. SNP (500 µM) was infused at the end of all experiment.



4.2.3 Metabolic actions of wortmannin in constant perfused rat hindlimbs

Wortmannin is known to block insulin-mediated glucose uptake in skeletal muscle (217). To confirm that the dose of wortmannin (100 nM) used in Protocol 2 was sufficient to inhibit PI3-K, the same dose of wortmannin was used to examine its effect on insulin-mediated muscle glucose uptake in isolated perfused rat hindlimb system. Surgery was carried out in overnight fasted rats as described in **2.3.2**. Experiments were carried out following the protocol shown in Figure 4.4. Following the surgery, rats were connected to the perfusion apparatus (See **2.3.3**) and allowed a 30-min equilibration period. Rat hindlimbs were perfused at a constant flow rate of $0.5 \text{ mL} \cdot \text{min}^{-1} \cdot \text{g}^{-1}$ of perfused muscle. Saline or insulin (15 nM) infusion started after the equilibration period. Wortmannin (100 nM) was added to the buffer 30 min prior to the insulin infusion. Perfusate effluents were collected before and every 10 min after experiment started. ^{14}C -2-DG ($25 \text{ nCi} \cdot \text{min}^{-1}$; American Radiolabeled Chemicals Inc.) infusion started 30 min before the end of experiment for the determination of muscle glucose uptake. Whole calf muscle was excised and freeze-clamped at the end of experiment. $R'g$ was then determined as described in **3.2.2.4**.



4.2.4 AMPK Western blot

To confirm that the dose of Compound C (10 μ M) used in Protocol 3 was sufficient to inhibit AMPK, perfused common iliac arteries were collected at the end of the experiment and stored in – 80 °C for Western blot analysis. AMPK Western blotting was performed as described in **2.5** with some modifications. Common iliac artery samples were snipped to fine sections in solubilising buffer (1:12.5 wt/vol) and sonicated. After blocking with 5% low fat milk in Tris-buffered saline plus 0.1% Tween 20, nitrocellulose membranes were incubated with 1:1000 rabbit anti-phospho-Thr¹⁷²-AMPK α (p-AMPK, Cell Signalling, Danvers, MA, USA) or 1:1000 rabbit anti-AMPK α (Cell Signalling) overnight at 4 °C. Following this, the membranes were probed with 1:1000 anti-rabbit secondary antibody (Cell Signalling) for 1 h at room temperature. To visualise the bands, equal volumes of West Pico Chemiluminescent Substrate (Thermo Fischer Scientific, Rockford, IL, USA) were mixed together and applied to the membrane. Band intensities were quantified by optical density using Image Station 4000mm Pro, Carestream Molecular Imaging (Carestream Health Inc., Rochester, NY, USA).

4.2.5 Statistical analysis

All data are expressed as means \pm S.E.M. Two-way repeated measures ANOVA with Student-Newman-Keuls post hoc test was used to compare treatment groups over the time course of experiment. An unpaired student's t-test or a one-way ANOVA with Student-Newman-Keuls post hoc test was used, where appropriate, to make comparisons of differences between endpoint values. All tests were performed using the SigmaPlot 11 (©Systat Software Inc. 2008).

4.3 Results

4.3.1 Effects of NOS inhibition on EGCG-mediated vasodilation

In the presence of L-NAME, 5-HT-induced vasoconstriction was augmented (218; 219), therefore a lower dose of 5-HT (0.06 μ M) was infused to raise perfusion pressure to a comparable 70 – 80 mmHg as in the non-LNAME treated experiments. Perfusion pressure following 30 min of 5-HT infusion represented 100% constriction (Figure 4.5), 5-HT-mediated vasoconstriction increased steadily over the course of the experiment in the presence of L-NAME. Due to upward drift of pressure with 5-HT in the presence of L-NAME, EGCG dose-response was time matched with saline perfusion pressure. When compared with saline infusion, EGCG-induced vasodilation was completely inhibited by L-NAME at 0.1, 1 and 10 μ M (Figure 4.5), indicating that EGCG at these doses vasodilates via a NOS-dependent process. However, 100 μ M EGCG-mediated dilation was only partially blocked by L-NAME (Figure 4.5) indicating that EGCG at this dose vasodilates, at least in part, by a NOS-independent mechanism. In all experiments, SNP reversed 5-HT mediated vasoconstriction by >95%, representing maximal vasodilation and return of perfusion pressures to basal levels.

4.3.2 Effects of PI3-K inhibition on EGCG-mediated vasodilation

EGCG-mediated vasodilation was not affected by PI3-K inhibition at any doses of EGCG (Figure 4.6). There was a slight decreased in perfusion pressure drift with

saline infusion in the presence of wortmannin, EGCG dose-response was time matched with saline perfusion pressure. In the presence of wortmannin, each dose of EGCG induced vasodilation to a similar extent to that in animals treated with 5-HT alone (i.e. without wortmannin) (Figure 3.7C). As shown in Figure 4.7, insulin-mediated R'g in the presence of 100 nM wortmannin was not different from saline R'g (5.07 ± 0.38 and $5.34 \pm 0.62 \mu\text{g.g}^{-1}.\text{min}^{-1}$ respectively), indicating that this dose of wortmannin completely inhibited insulin-mediated R'g. This implies that the failure of wortmannin to block EGCG-mediated vasodilation was not due to the lack of PI3-K inhibition. In all hindlimbs, SNP reversed 5-HT mediated vasoconstriction by >95%, representing maximal vasodilation and return of perfusion pressures to basal levels.

4.3.3 Effects of SFKs inhibition on EGCG-mediated vasodilation

5-HT mediated vasoconstriction is mainly mediated by the 5-HT_{2A} receptor, where c-Src tyrosine kinase is a key component for 5-HT_{2A} receptor-mediated vasoconstriction (216). In the presence of 10 μM PP2, 5-HT-mediated vasoconstriction in the perfused rat hindlimb was completely inhibited (data not shown) indicating that the dose of PP2 was sufficient to block SFK. Thus the involvement of SFKs in dilation by EGCG could not be assessed. However, some EGCG-mediated vasodilation occurred against high dose NE (Figure 3.7B). Therefore, effects of 10 μM PP2 on EGCG-mediated vasodilation were assessed in the NE (5 μM) pre-constricted hindlimbs which is not SFK-dependent. As detailed in Chapter 3 (Figure 3.7B), EGCG-mediated vasodilation against high dose NE (5 μM) is modest and only one dose of EGCG 10 μM was effective. Interestingly, vasodilation induced by 10 μM EGCG was not inhibited by PP2 (Figure 4.8), indicating EGCG-mediated vasodilation in skeletal muscle is

independent of SFKs. In all hindlimbs, SNP reversed NE mediated vasoconstriction by >95%, representing maximal vasodilation and return of perfusion pressures to basal levels.

4.3.4 Effects of AMPK inhibition on EGCG-mediated vasodilation

AMPK inhibition did not affect vasodilation at any EGCG doses (Figure 4.9). In the presence of Compound C, EGCG at all doses induced vasodilation to a similar extent compared to animals not treated with Compound C (Figure 3.7C). Activation of AMPK was assessed by Western blot to confirm that the dose of Compound C (10 μ M) used was sufficient to inhibit AMPK. Figure 4.10 showed an 80% reduction in pAMPK/AMPK_{total} ratio following 10 μ M Compound C treatment, indicating AMPK was markedly inhibited by Compound C. This implies that the failure of Compound C to block EGCG-mediated vasodilation was not due to the lack of AMPK inhibition. Effects of Compound C on AMPK inhibition were not different between the saline and EGCG treated samples (data not shown), therefore the pAMPK/AMPK_{total} ratio for the saline and EGCG samples were combined to increase the power of the statistics at testing. This indicates that the vasodilator action of EGCG in skeletal muscle is independent of AMPK. In all hindlimbs, SNP reversed 5-HT mediated vasoconstriction by >95%, representing maximal vasodilation and return of perfusion pressures to basal levels.

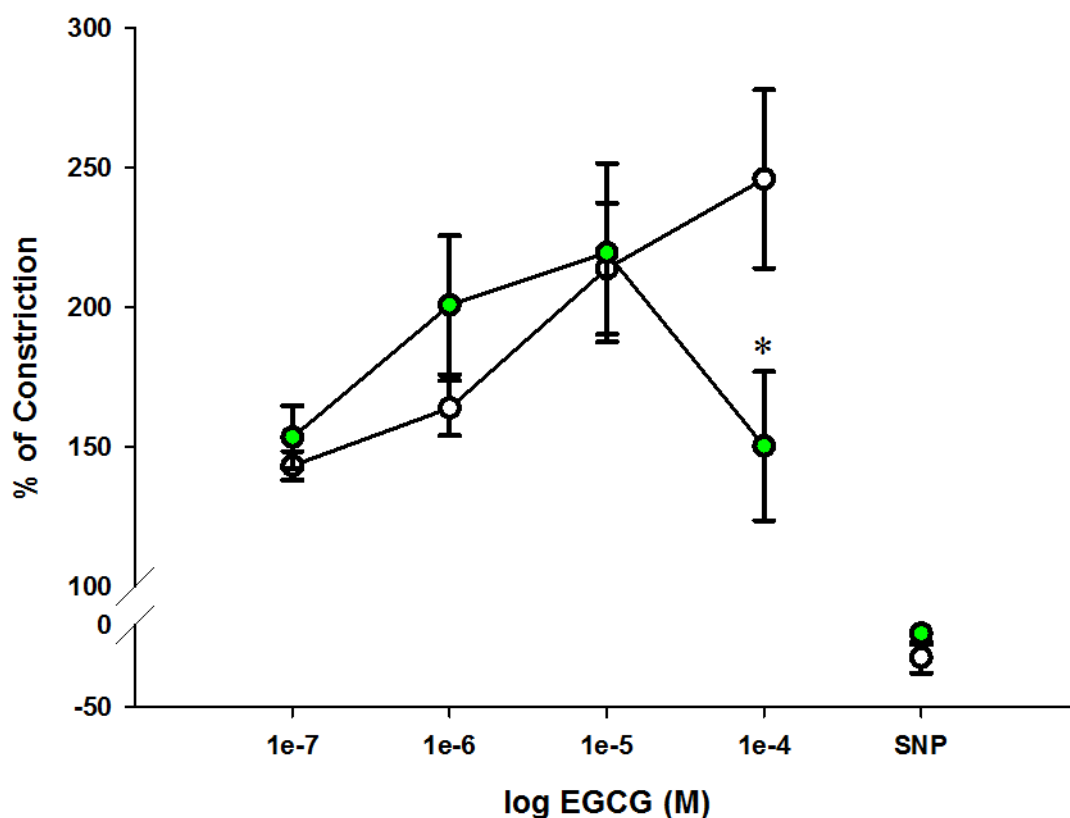
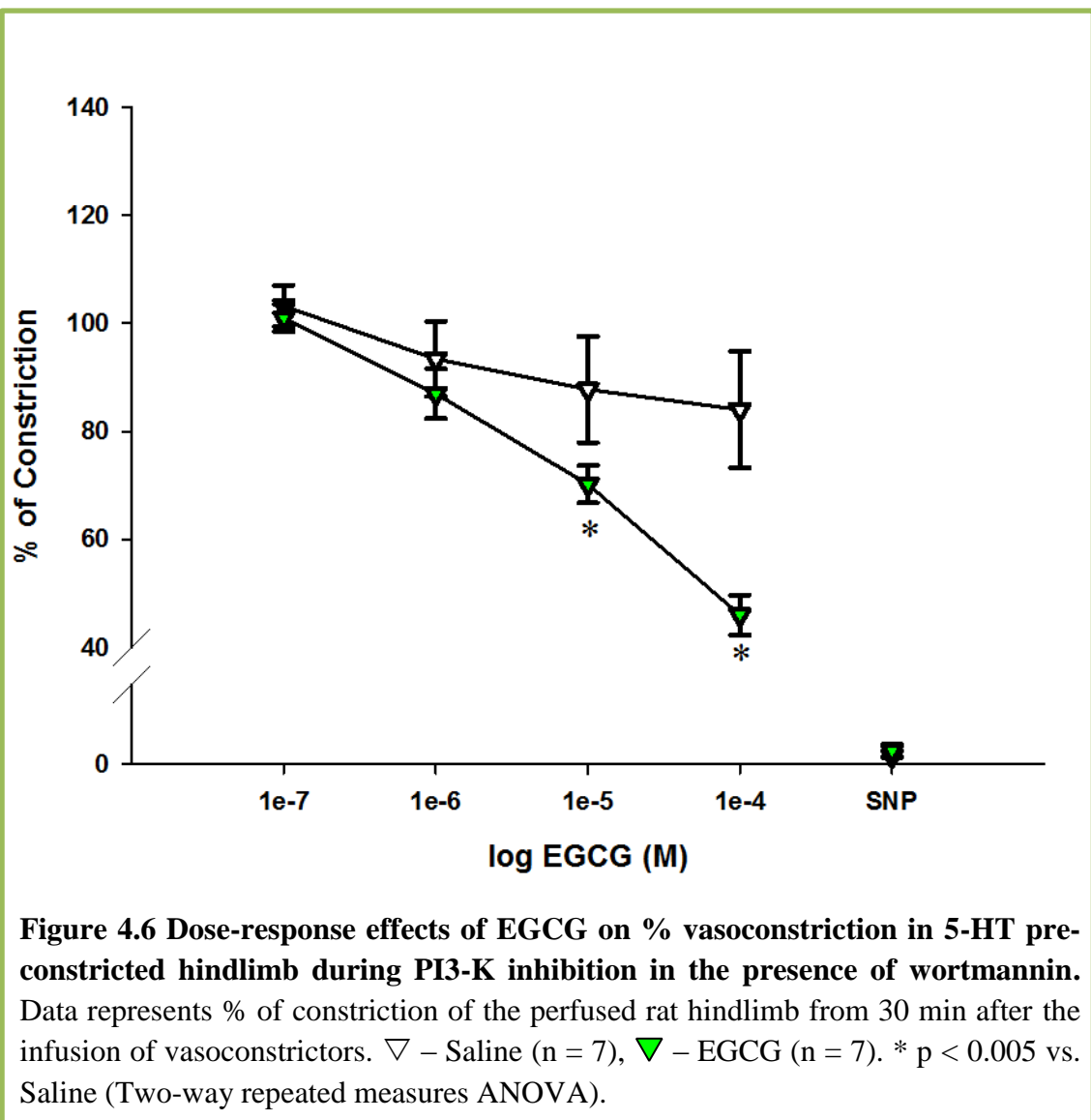


Figure 4.5 Dose-response effects of EGCG on % vasoconstriction in 5-HT pre-constricted hindlimb during NO synthase inhibition in the presence of L-NAME. Data represents % of constriction of the perfused rat hindlimb from 30 min after the infusion of vasoconstrictors. ○ – Saline (n = 7), ● – EGCG (n = 6). * p = 0.007 vs. Saline (Two-way repeated measures ANOVA).



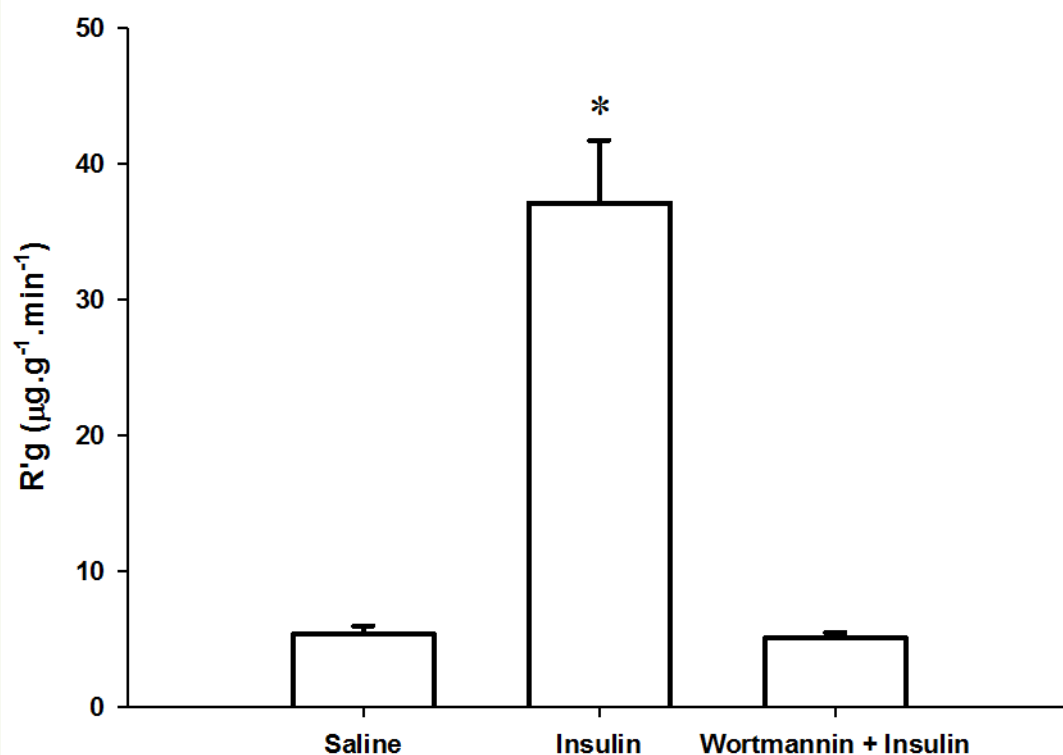


Figure 4.7 Effects of PI3-K inhibition by 100 nM wortmannin on muscle glucose uptake. Data represents R'g following 15 nM insulin infusion. n = 4 – 6 in each groups. * p < 0.001 vs. Saline and Wortmannin + Insulin (One-way ANOVA).

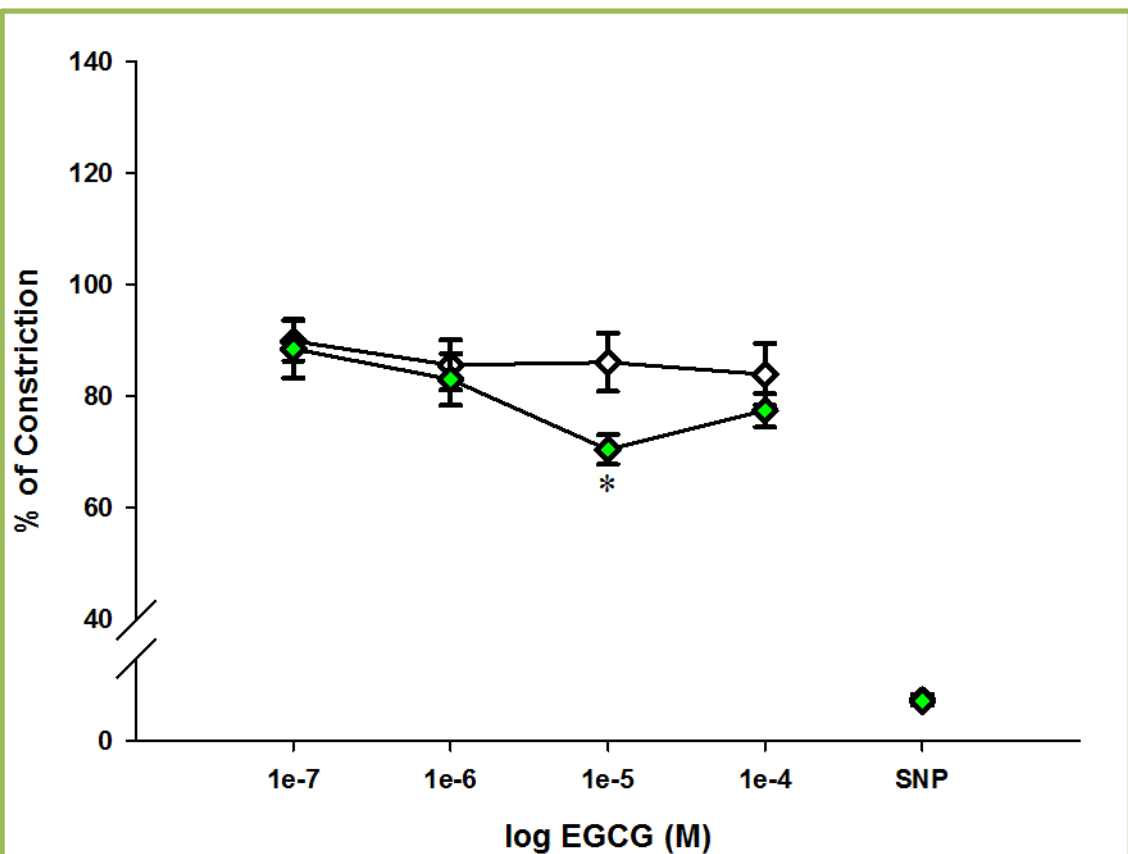
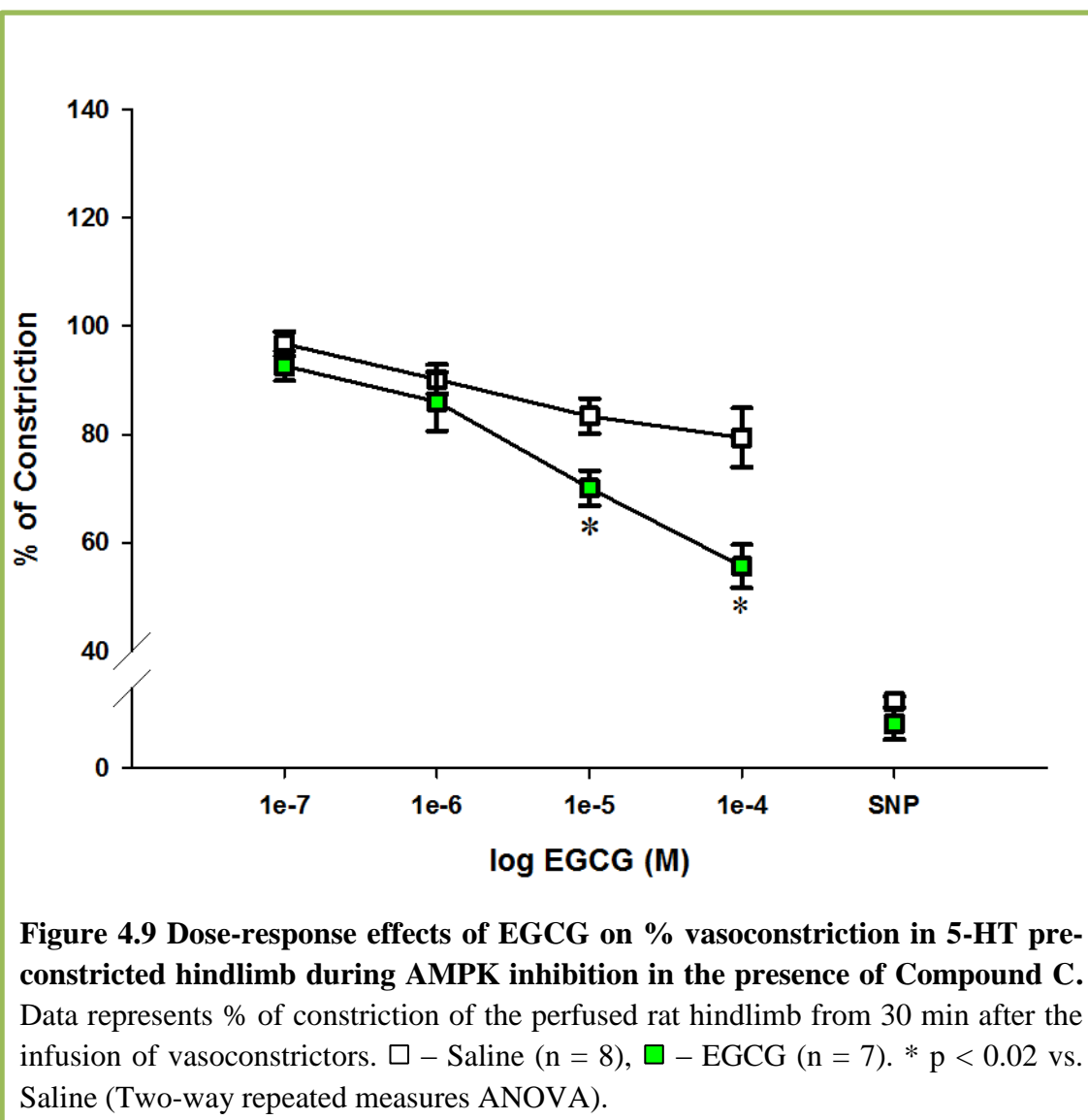
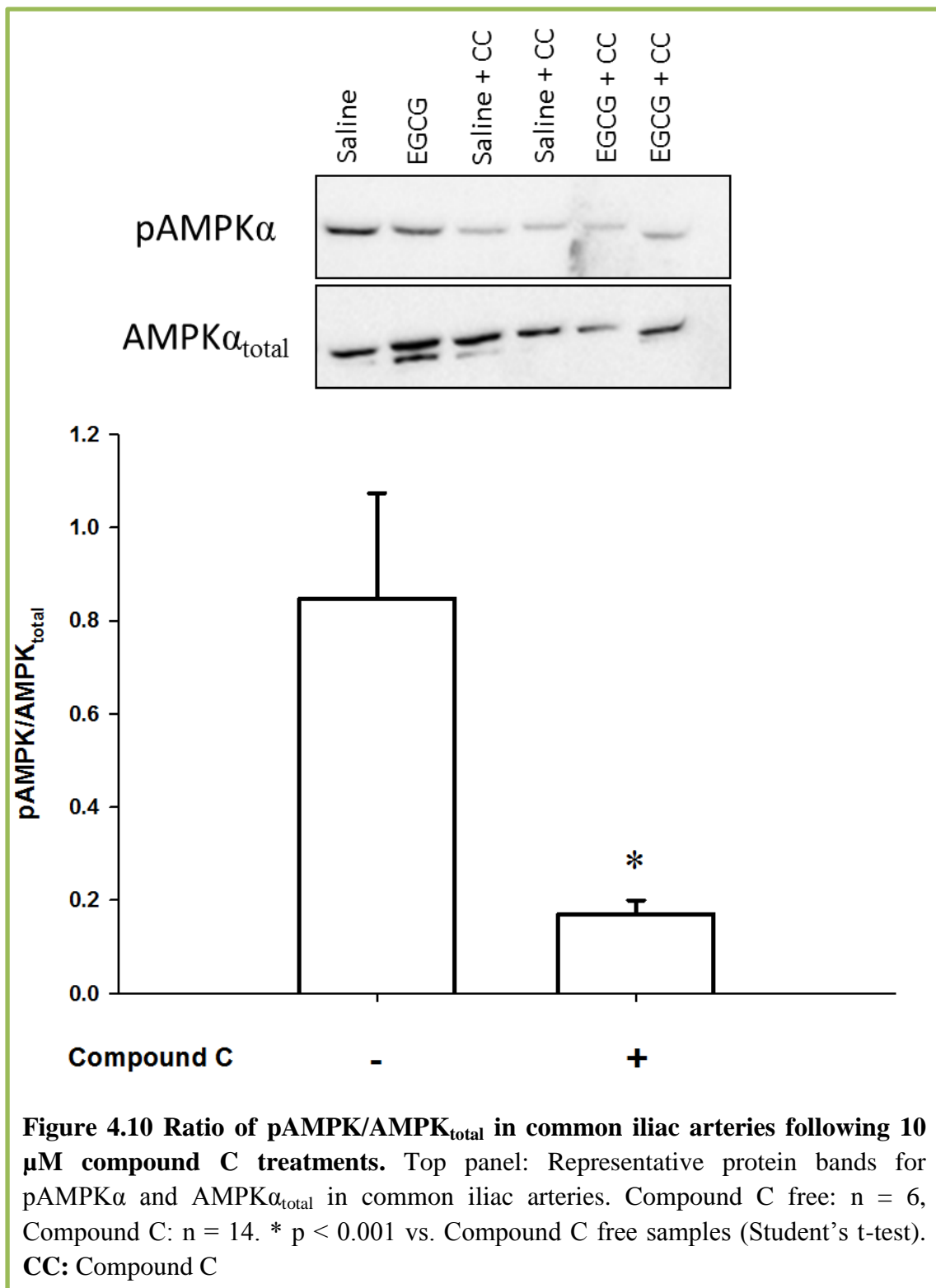


Figure 4.8 Dose-response effects of EGCG on % vasoconstriction in high dose NE pre-constricted hindlimb during SFK inhibition in the presence of PP2. Data represents % of constriction of the perfused rat hindlimb from 30 min after the infusion of vasoconstrictors. \diamond – Saline (n = 6), \blacklozenge – EGCG (n = 5). * p = 0.032 vs. Saline (Two-way repeated measure ANOVA).





4.4 Discussion

Previous studies have reported that vasodilator actions of EGCG are mediated by the PI3-K/Akt/NOS pathway in isolated aortic ring (178; 179), bovine ophthalmic artery (180), coronary artery ring (181), mesenteric vascular bed (119), and cultured vascular endothelial cells (119; 179; 181). Therefore, it was postulated that vasodilator actions of EGCG in skeletal muscle would be mediated by the same pathway. In contrast to the studies describe above, the main findings of this study were (i) EGCG, at low doses (0.1 – 10 μ M), vasodilates skeletal muscle vasculature in a NOS-dependent fashion and (ii) vasodilator actions of EGCG in skeletal muscle are independent of PI3-K, SFK and AMPK.

The present study showed that the vasodilatory effects of 1 and 10 μ M EGCG, but not 100 μ M EGCG, were inhibited by L-NAME. Similarly it was recently reported (178; 179) that vasodilation in rat thoracic aorta induced by low concentrations (0.01 - 10 μ M) of EGCG was abolished by NOS inhibition, but not higher doses of EGCG. Others have suggested that suprapharmacological doses of EGCG (>10 μ M) can induce vasodilation through different pathways by acting directly on smooth muscle cells (178), by activating the cAMP- (179; 182) or cGMP-dependent protein kinase pathway (182). Furthermore, polyphenols from grape seed (*Vitis Vinifera* L.) have been shown to dose-dependently induce vasodilation in human internal mammary aortic rings by stimulation of prostaglandin I₂ (PGI₂) release (220). EGCG has also been shown to increase PGI₂ production in bovine aortic endothelial cells (221). Thus, high dose (100 μ M) EGCG-induced vasodilation (NOS-independent) could involve PGI₂, however this was not tested in the current study.

The current study showed that EGCG-mediated vasodilation in skeletal muscle was not inhibited by wortmannin, indicating EGCG-mediated vasodilation in skeletal muscle is PI3-K-independent. The wortmannin dose that was used in this study inhibited insulin-mediated muscle glucose uptake. Therefore failure of wortmannin to inhibit the EGCG-mediated vasodilation is unlikely to be due to the lack of PI3-K inhibition.

As mentioned before, EGCG has been reported to activate Fyn, a member of SFK, which can lead to activation of the PI3-K/Akt/NO pathway in cultured vascular endothelial cells (119). Besides activating PI3-K (208; 209), SFK can directly activate eNOS independent of PI3-K (210). The current study showed that EGCG-mediated vasodilation in skeletal muscle was not inhibited by PP2, an inhibitor of SFK. Since the dose of PP2 used in the current study inhibited 5-HT mediated vasodilation, failure of PP2 to inhibit the EGCG-mediated vasodilation is unlikely due to lack of SFK inhibition. Furthermore, previous studies suggested that AMPK can be activated by EGCG in cultured vascular endothelial cells (211) and cultured hepatocytes (174). AMPK can directly activate eNOS (212; 213), and lead to NO production (214). However, this study showed that EGCG-mediated vasodilation is not inhibited by Compound C, indicating EGCG-mediated vasodilation in skeletal muscle is AMPK-independent. Immunoblot analysis showed that the dose of Compound C used in the present study reduced the pAMPK/AMPK_{total} ratio, indicating failure of Compound C to inhibit the EGCG-mediated vasodilation is unlikely to lack of AMPK inhibition.

Another pathway that EGCG could be operating through is the Ca²⁺/calmodulin-dependent kinase II (CaMKII)/eNOS pathway. Polyphenols from red wine have been shown to induce Ca²⁺-dependent production of NO from bovine aortic endothelial cells (222) and induce vasodilation in rat aortic rings through the same pathway (223).

Epicatechin, another polyphenol in green tea, has been shown to activate eNOS phosphorylation via Ca^{2+} /CaMKII pathway (224). This highlights the possibility that EGCG at low doses is activating NOS-dependent vasodilation via the Ca^{2+} /CaMKII/eNOS signalling pathway in skeletal muscle vasculature. On the other hand, studies showed that polyphenols from grapes and wines (resveratrol) (225; 226) and black tea (227) activate oestrogen receptors which lead to activation of p38 mitogen activated protein kinase (MAPK) and eNOS in endothelial cells. EGCG has also been shown to activate oestrogen receptor in the amyloid precursor protein overexpressing murine neuroblastoma N2a cells (228), suggesting that low doses EGCG-induced vasodilation in skeletal muscle could be mediated by the oestrogen receptor.

It is concluded that EGCG is a potent vasodilator in the skeletal muscle. EGCG vasodilates in skeletal muscle via NOS-dependent, and is in part NOS-independent at supra-pharmacological concentrations. Furthermore, EGCG vasodilates in skeletal muscle via a PI3K-, SFK- and AMPK-independent pathway. To date, the mechanism of EGCG-mediated vasodilation in skeletal muscle remains uncertain.

Chapter 5

Acute effects of EGCG in healthy rats *in vivo*

5.1 Introduction

Acute green tea consumption has been reported to enhance insulin sensitivity (148) and glucose tolerance (147) in healthy humans. In addition, chronic green tea treatment has been reported to improve glucose tolerance and insulin sensitivity in healthy (156; 158; 229) and insulin resistant (98; 147; 158-162; 164-167) animals. Taken together, these studies suggested that green tea treatment may be beneficial in managing metabolic health in animals, but the mechanism remains unknown.

Previously, studies have proposed that green tea or EGCG possesses insulin-mimetic effects *in vitro*, whereby green tea or EGCG stimulates GLUT4 translocation in isolated myocytes (157; 158; 172) and adipocytes (159), glucose uptake in skeletal muscle (157; 172) and adipocytes (156; 159), and suppresses hepatic glucose production (174; 175). Furthermore, EGCG has also been reported to be a potent vasodilator in isolated blood vessels (119; 178-182). However, the aforementioned studies were carried out *in vitro*, whether EGCG has insulin-mimetic actions *in vivo* has not been previously investigated. As shown in Chapter 3, EGCG is a vasodilator but does not have direct acute metabolic actions on skeletal myocytes. Importantly, Chapter 4 showed that EGCG-mediated vasodilation in skeletal muscle is NOS-dependent at doses up to 10 μM .

Barrett and colleagues have reported that the insulin increases microvascular perfusion in skeletal muscle in normal healthy animals (18; 53) and humans (230) via a NOS-dependent mechanism (18; 53). It is widely accepted that insulin-stimulated microvascular perfusion will increased delivery of nutrients, such as glucose and insulin, to skeletal muscle, resulting in increased muscle glucose uptake (231; 232). However, not all vasodilators can increase microvascular perfusion in skeletal muscle. Whether EGCG is a vasodilator that could increase microvascular perfusion and

thereby improve insulin sensitivity is not known. In this study, EGCG was intravenously infused to rats to acutely increase plasma EGCG to 10 μ M. The aim of this study was to determine whether acute EGCG treatment *in vivo* improved i) whole insulin sensitivity, ii) microvascular perfusion, and iii) muscle glucose uptake.

There are a number of techniques available for the measurement of microvascular perfusion, including the laser Doppler flowmetry (233), microdialysis (234), and intravital microscopy (235). While these are valuable methods, laser Doppler flowmetry, microdialysis, and intravital microscopy, are limited to blood flow measurement in small muscle regions. The application of microdialysis in humans may also be restricted due to invasive implantation of the measurement probe. Metabolism of 1-MX (21) is also widely used for the measurement of microvascular perfusion in rats. However, xanthine oxidase, which is required for the metabolism of 1-MX (see 1.1.2.3), is inhibited by EGCG (236; 237). Therefore, the use of 1-MX metabolism technique in the present study is not feasible. Measurement of muscle microvascular perfusion was made using the CEU technique in this study.

5.2 Methods

5.2.1 Animals

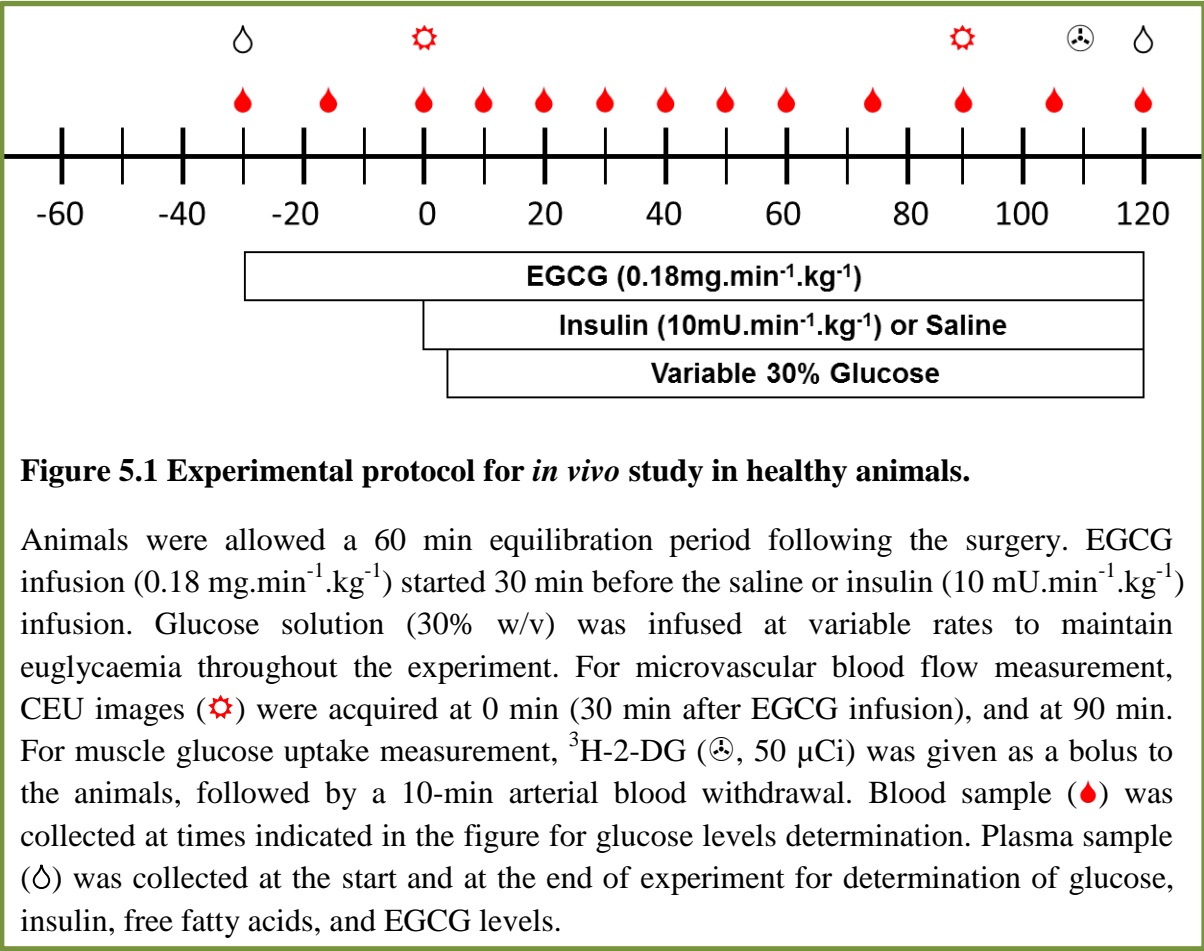
Male Sprague-Dawley rats (n = 32) weighing 246 ± 3 g at 9 – 10 weeks old were used in this study. The rats were allowed free access to drinking water and food *ad libitum*. Rats were provided with normal chow (5FD) from Specialty Feeds, Glen Forest, WA, Australia (Table 2.1). Rats were fasted overnight before the experiment was performed.

Rats were randomly allocated into 4 experimental groups- Saline, EGCG, Insulin and EGCG + Insulin groups. All experimental procedures were approved by the University of Tasmania Animal Ethics Committee (A11282) and performed in accordance with the Australian Code of Practice for the Care and Use of Animals for Scientific Purposes – 2004, 7th Edition.

5.2.2 Experiment protocol

Surgery was carried out in the overnight fasted rats as described in 2.4.1. Figure 5.1 shows the experimental protocol of this study. Rats were allowed a 60-min equilibration period following the surgery to stabilise MAP, heart rate, and anaesthetic level. Plasma samples were collected after equilibration for measurement of glucose, insulin, and free fatty acids levels. EGCG infusion of $0.18 \text{ mg} \cdot \text{min}^{-1} \cdot \text{kg}^{-1}$ (refer to 5.2.3) was started after equilibration period to raise plasma EGCG levels to $10 \text{ } \mu\text{M}$. Saline or insulin ($10 \text{ mU} \cdot \text{min}^{-1} \cdot \text{kg}^{-1}$) infusion was started 30 min after EGCG infusion. Glucose solution (30 %, w/v) was infused at variable rates to maintain the blood glucose levels at fasting levels. The glucose infusion rate (GIR), which is an indicator of the whole body insulin sensitivity, was recorded throughout the experiment. Microvascular blood flow measurement was made using CEU, as described in 2.4.7, at 0 min (30 min after EGCG infusion), and at 90min of the insulin clamp (Figure 5.1). Muscle glucose uptake were measured using 2-deoxy-D-[1,2- $^3\text{H}(\text{N})$]glucose (^3H -2-DG; specific activity 5 – 10 Ci.mmol⁻¹; Perkin Elmer Inc.), as described in 2.4.8. At 110 min during the insulin clamp, a bolus of ^3H -2-DG (50 μCi) was given to the rat via the jugular vein, immediately followed by a 10-min arterial blood withdrawal to assess average plasma ^3H -2-DG specific activity. Plasma samples were collected at the end of insulin clamp

for measurement of glucose, insulin, and EGCG levels. Whole calf muscle, liver, heart, epididymal fat pad, and aortic arch were collected and stored at -80 °C for further analysis.



5.2.3 Pharmacokinetics of intravenously administered EGCG

To determine the pharmacokinetics or clearance rate of EGCG in rat plasma, Sprague-Dawley rats ($n = 3$) weighing 328 ± 12 g were fasted overnight, anaesthetised and surgery carried out as described in 2.4.1. A bolus of EGCG (50 mg.kg^{-1}) was administered via the jugular vein as a bolus. Plasma samples ($200 \mu\text{L}$) were collected 5 min before the administration of EGCG, and at 2 min and every 15 min following the administration of EGCG bolus for 2 hours. Plasma EGCG concentrations were determined by HPLC as described in 2.4.6.

Plasma EGCG concentrations over the 2-hour period were fitted to the function $y = ae^{-bx}$ (Figure 5.2), where a is the initial plasma EGCG concentrations (following the administration of EGCG bolus), and b is the decay constant. Clearance rate of EGCG was determined from b multiplied by volume of distribution (V_D), where V_D was determined from the amount of EGCG administered divided by a . Infusion rate of EGCG solution was determined by multiplying the desired concentration ($10 \mu\text{M}$) and clearance rate of EGCG. An EGCG infusion rate was calculated to be $0.18 \text{ mg.min}^{-1}.\text{kg}^{-1}$ to maintain $10 \mu\text{M}$ EGCG in rat plasma.

5.2.4 Statistical Analysis

All data are expressed as means \pm S.E.M. Two-way repeated measures ANOVA with Student-Newman-Keuls *post hoc* test was used to compare treatment groups over the time course of experiment. One-way ANOVA with Student-Newman-Keuls *post hoc* test was used to make comparisons of differences between endpoint values. All tests were performed using the SigmaPlot 11 ($^{\circ}$ Systat Software Inc. 2008).

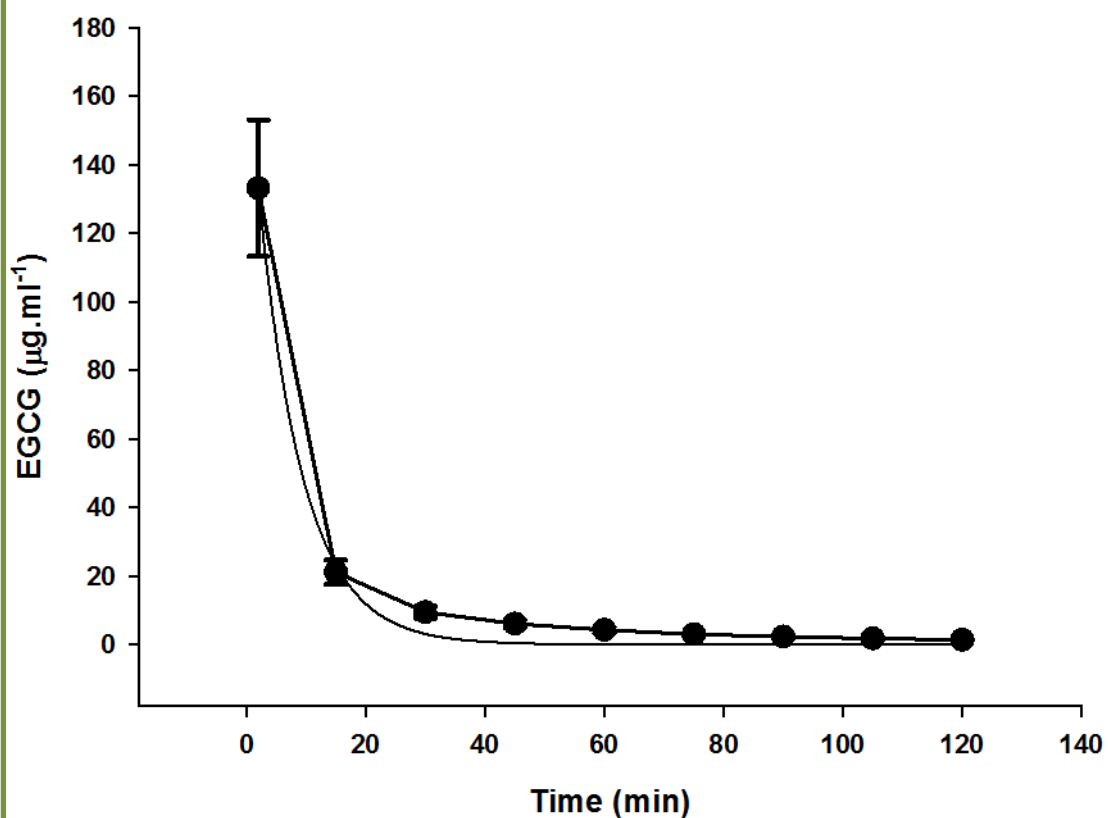


Figure 5.2 Plasma EGCG concentrations following the administration of 50 mg.kg^{-1} EGCG bolus. This was fitted to the exponential decay function $y = ae^{-bx}$, where $a = 174$, $b = 0.134$. $n = 3$.

5.3 Results

5.3.1 Animal characteristics

Fasting plasma glucose and insulin levels were 7.14 ± 0.11 mM ($n = 32$) and 70 ± 8 pM ($n = 32$) respectively. Fasting plasma free fatty acids were 0.64 ± 0.03 mM ($n = 17$). Epididymal fat pads weighed 0.48 ± 0.02 % ($n = 32$) of the rat body weight.

In the EGCG and EGCG + Insulin groups, EGCG was infused 30 min before and during the hyperinsulinaemic euglycaemic clamp. Plasma EGCG levels following 150 min of EGCG infusion in the EGCG and EGCG + Insulin groups were 10.79 ± 0.63 μ M and 9.73 ± 0.33 μ M respectively ($p = 0.131$) indicating that the target of 10 μ M was reached.

5.3.2 Whole body insulin sensitivity

The GIR (Figure 5.3 A) of the Insulin group during steady state of glucose infusion was 24.19 ± 1.10 mg.min⁻¹.kg⁻¹, and acute infusion of EGCG in the EGCG + Insulin group did not alter the GIR (24.04 ± 0.66 mg.min⁻¹.kg⁻¹). Plasma insulin levels post-insulin clamp of Insulin and EGCG + Insulin groups were 799 ± 57 pM and 800 ± 31 pM respectively ($p = 0.901$), indicating that EGCG did not affect plasma insulin levels. In the EGCG group, some glucose was required to maintain euglycaemia in the beginning of the experiment, however, this was not required through to the end of the experiment. Blood glucose (Figure 5.3B) measured throughout the experiments were not different between each group.

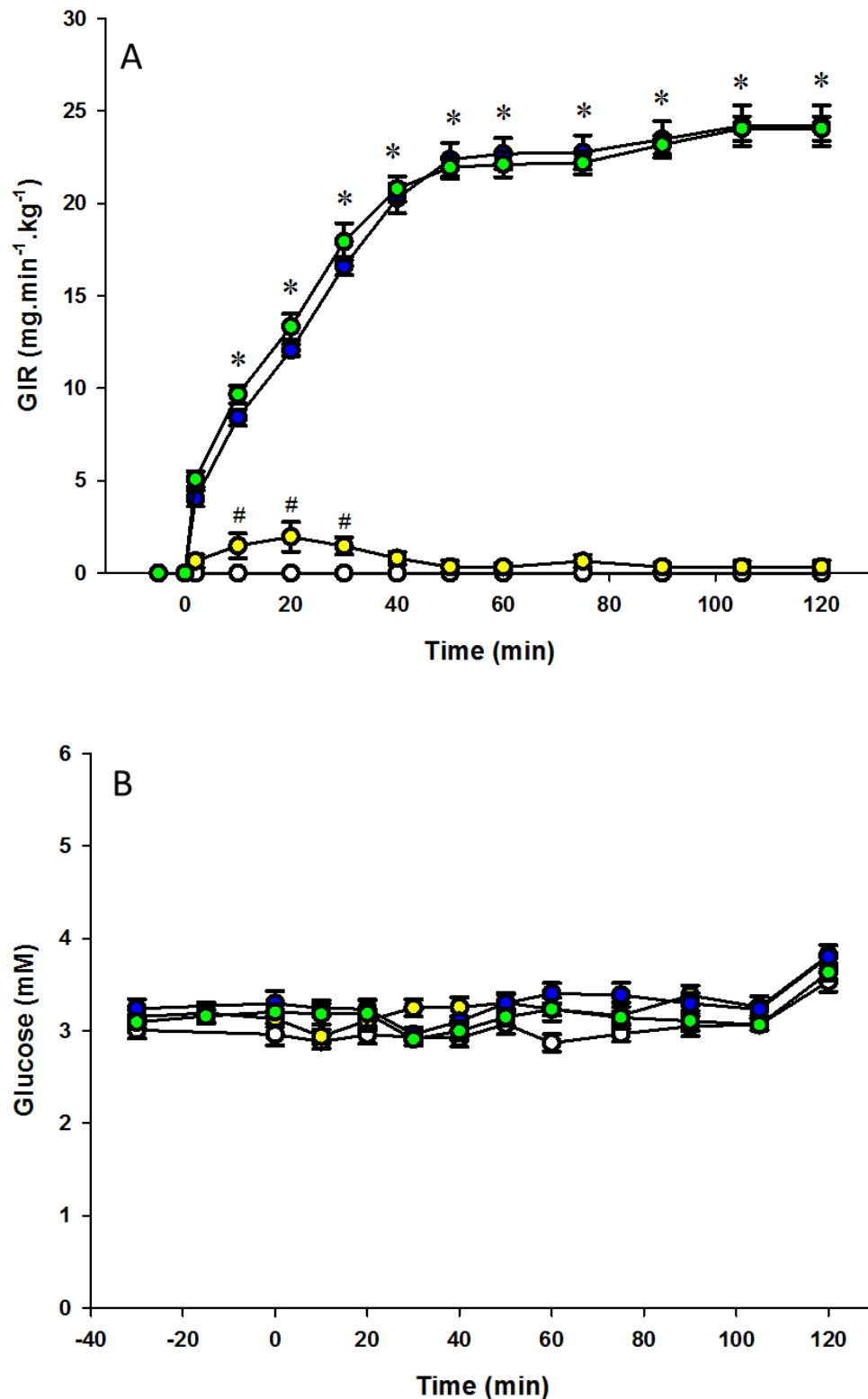
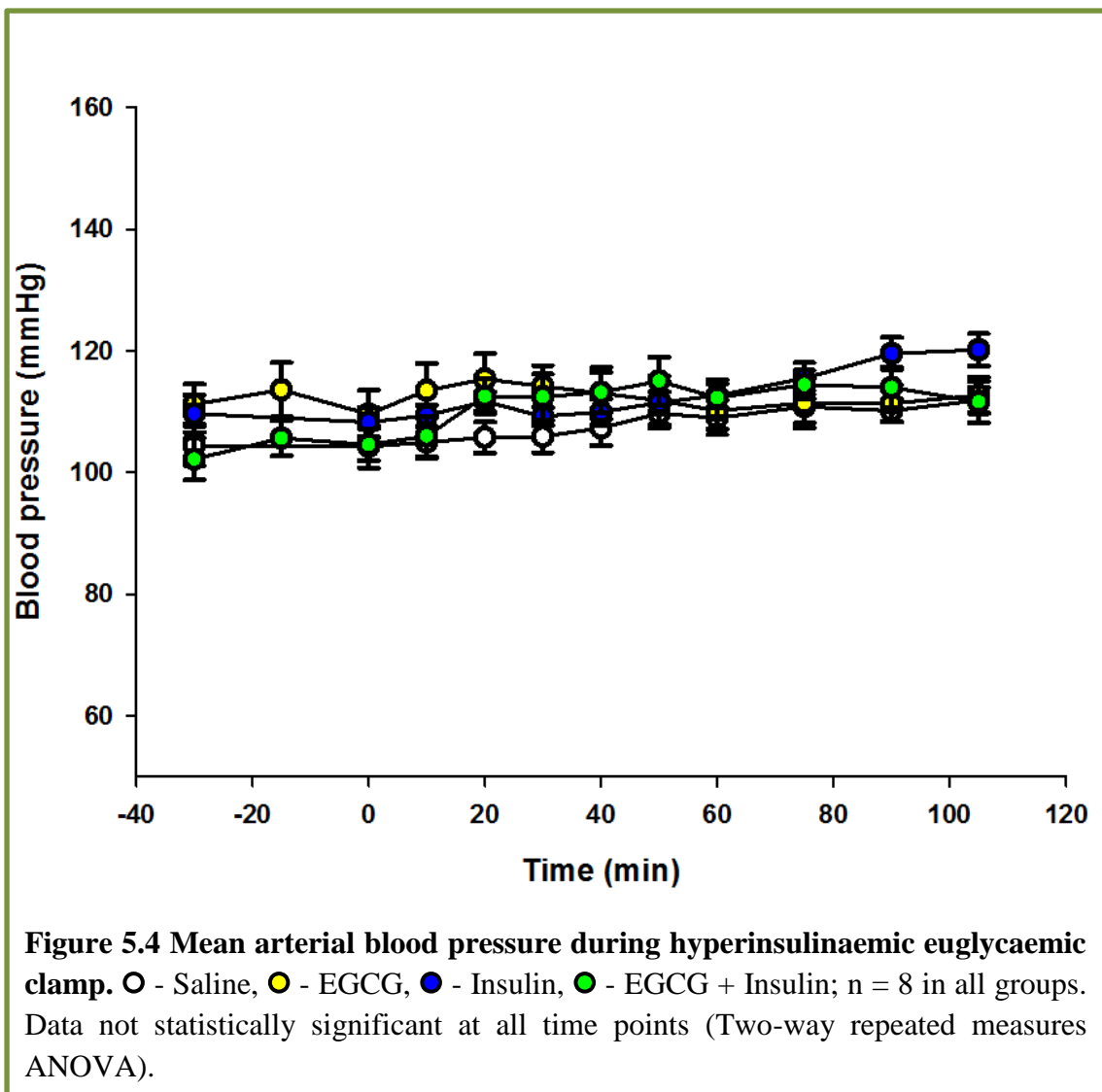


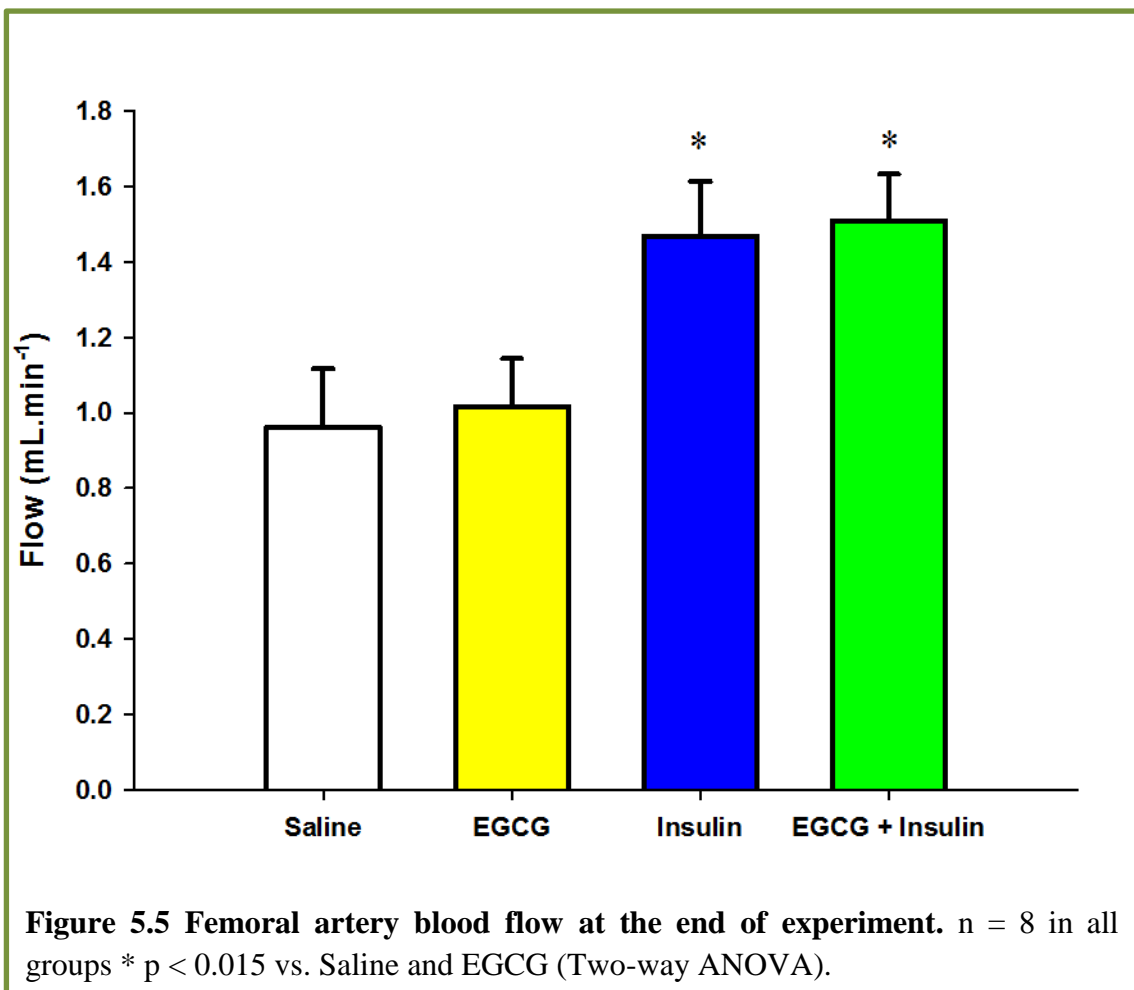
Figure 5.3 (A) Glucose infusion rate and (B) blood glucose levels during hyperinsulinaemic euglycaemic clamp. ○ - Saline, ● - EGCG, ● - Insulin, ● - EGCG + Insulin; n = 8 in all groups. * p < 0.001 vs. Saline and EGCG (Two-way repeated measures ANOVA); # p < 0.05 vs. Saline (Two-way repeated measures ANOVA).

5.3.3 Haemodynamic parameters

Figure 5.4 shows the mean arterial blood pressure (MAP) of the rats during the course of the experiment. MAP was not different between all groups indicating acute EGCG infusion has no effect on the MAP.

Femoral artery blood flow (FBF) was measured during the hyperinsulinaemic euglycaemic clamp (Figure 5.5). FBF before the experiments were not different between all groups (data not shown). As expected, at the end of hyperinsulinaemic euglycaemic clamp, FBF of the Insulin group ($1.47 \pm 0.15 \text{ ml.min}^{-1}$) was significantly higher than the Saline group ($0.96 \pm 0.16 \text{ ml.min}^{-1}$) (Figure 5.5). However, acute EGCG did not alter FBF ($1.02 \pm 0.13 \text{ ml.min}^{-1}$) or enhance insulin-stimulated FBF ($1.51 \pm 0.12 \text{ ml.min}^{-1}$)





5.3.4 Microvascular blood volume

CEU was used to measure the MBV before and 90 min after the hyperinsulinaemic euglycaemic clamp (Figure 5.6). At 0 min, MBV (Figure 5.6) were not different between groups. As expected, MBV of the Saline group was not different at 0 and 90 min (3.10 ± 0.21 and 2.92 ± 0.26 acoustic intensity units respectively, $p = 0.50$). At 90 min into the insulin clamp, MBV of the EGCG, Insulin and EGCG + Insulin groups had significantly increased from 0 min (Figure 5.6). This indicates that EGCG alone has stimulated microvascular perfusion to a similar extent as the insulin treatment. However, EGCG was not additive to insulin on its effect on MBV.

5.3.5 Muscle insulin sensitivity

Figure 5.7 shows results for muscle specific glucose uptake at the end of the experiment. Insulin stimulated muscle glucose uptake by 3.5-fold, where R'g of the Saline and Insulin groups were 2.81 ± 0.17 and $9.73 \pm 0.71 \mu\text{g}\cdot\text{g}^{-1}\cdot\text{min}^{-1}$ respectively. Acute EGCG did not alter muscle glucose uptake ($2.36 \pm 0.22 \mu\text{g}\cdot\text{g}^{-1}\cdot\text{min}^{-1}$) or enhance insulin-stimulated glucose uptake ($7.89 \pm 0.52 \mu\text{g}\cdot\text{g}^{-1}\cdot\text{min}^{-1}$).

Western blot analysis (Figure 5.8) showed that insulin stimulated phosphorylation of Akt in skeletal muscle by 6.4-fold, while EGCG did not stimulate or enhance Akt phosphorylation in skeletal muscle either in the absence or presence of insulin.

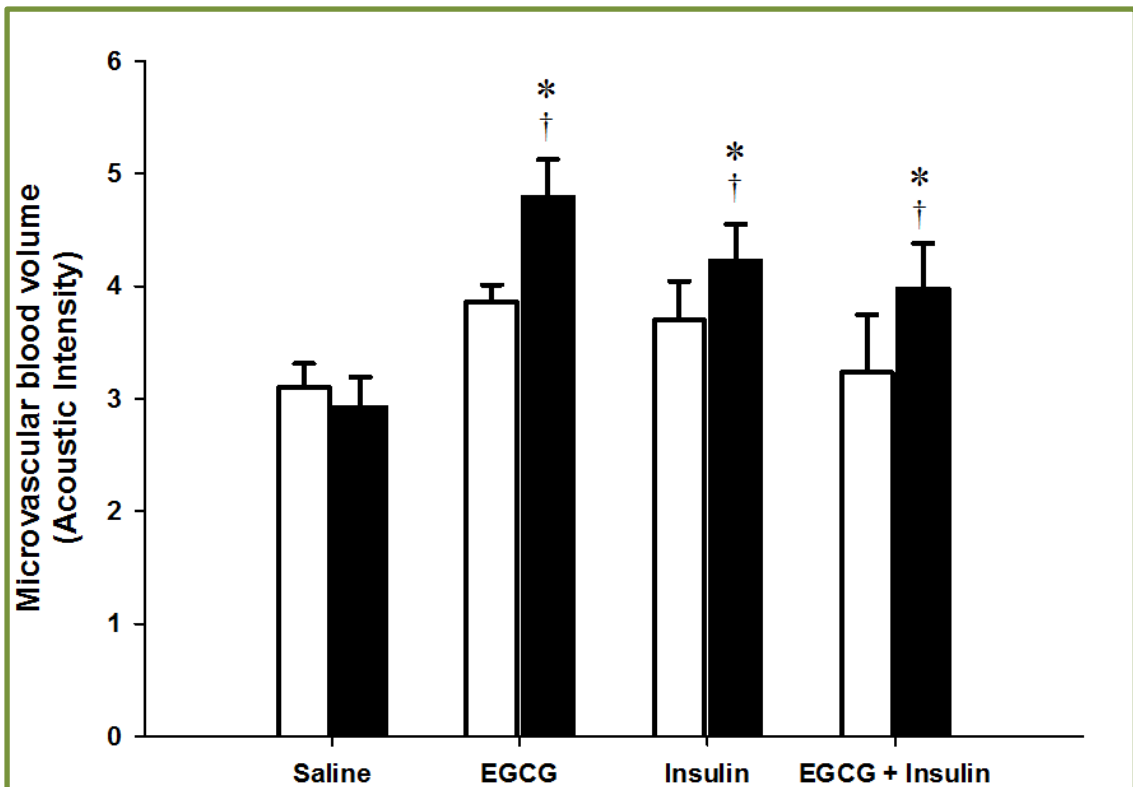
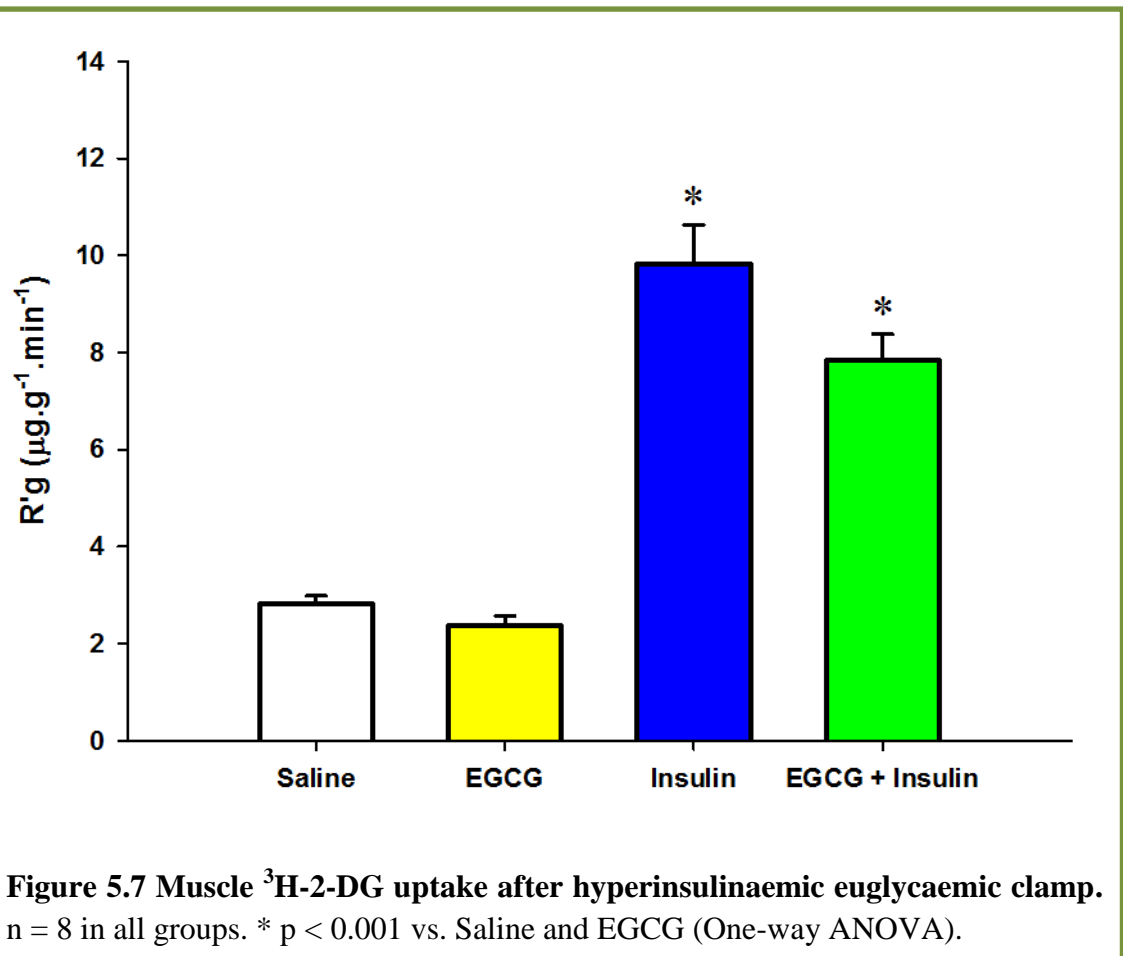
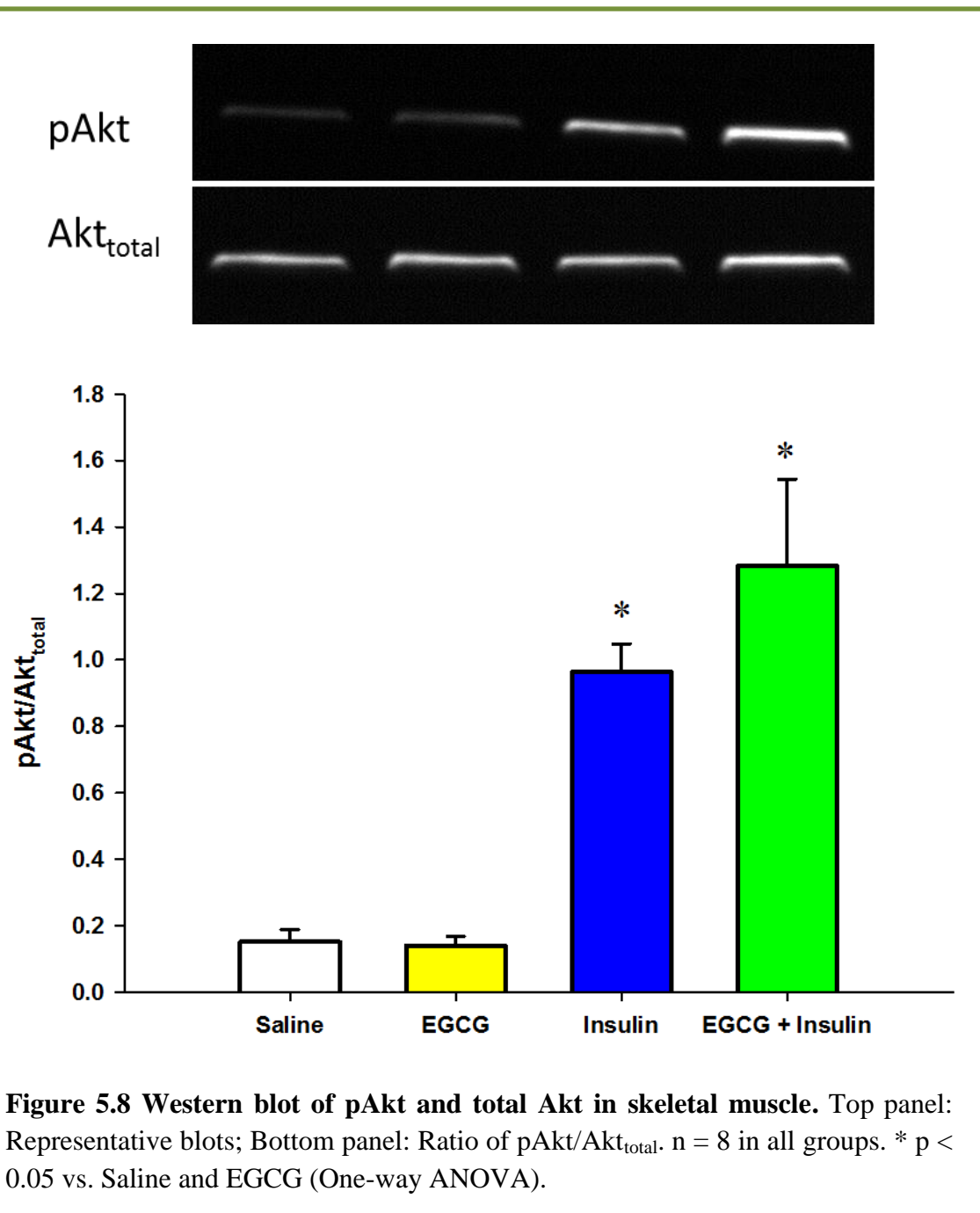


Figure 5.6 Microvascular blood volume before and during hyperinsulinaemic euglycaemic clamp. □ = 0 min, ■ = 90 min; n = 8 in all groups. * p < 0.05 vs. respective 0 min (Two-way repeated measures ANOVA); † p < 0.05 vs. 90 min Saline (Two-way repeated measures ANOVA).





5.4 Discussion

The main findings of the present study are that EGCG acutely increases MBV in skeletal muscle, but has no effect on muscle glucose uptake and whole body insulin sensitivity. Interestingly, EGCG alone increases MBV to a similar extent as raising plasma insulin to ~ 800 pM, however, EGCG did not further enhance insulin-stimulated increases in MBV. This indicates that EGCG mimics, but does not sensitize, insulin's action on microvascular perfusion.

The dose of EGCG used in this study raised plasma EGCG to 10 μ M. As shown in Chapters 3 and 4, 10 μ M EGCG induced an intermediate level of vasodilation in the perfused rat hindlimb. It was also the highest dose that vasodilated via a NOS-dependent process in skeletal muscle. This is crucial as Vincent and colleagues have previously demonstrated that insulin increases microvascular perfusion in normal healthy animals (18; 53) and humans (230) via a NOS-dependent mechanism (18; 53). It is important to note that 10 μ M EGCG is within the no-observed adverse effect level, as it has been shown previously that EGCG is not toxic to rats *in vivo* at doses up to 500 mg.kg⁻¹.d⁻¹ (197), which is equivalent to ~12 μ M EGCG in the plasma (197).

In the current study, 10 μ M EGCG stimulated microvascular perfusion, but not total blood flow in muscle. EGCG did not mimic or sensitize insulin's action on total hindleg blood flow indicating that EGCG acts on the microvasculature in skeletal muscle, with no effect on total blood flow. EGCG-stimulated microvascular perfusion was similar in magnitude to raising plasma insulin concentrations to 800 pM. However the microvascular actions of EGCG and insulin were not additive, suggesting that EGCG does not have insulin-sensitizing actions in the muscle microvasculature in normal healthy rats.

Previous studies have demonstrated that increased microvascular perfusion is associated with augmented muscle glucose uptake (18; 53; 80). The present study shows that EGCG increases MBV in skeletal muscle, but this was not accompanied by increased muscle glucose uptake. In contrast to studies by Ashida *et al.* (157) and Ueda *et al.* (172), the outcomes of this study showed that acute EGCG alone did not mimic insulin's action to stimulate glucose uptake in skeletal muscle. Similarly, EGCG does not alter muscle Akt phosphorylation, which is a downstream signalling molecule of PI3-K involved in the insulin signalling pathway leading to glucose uptake. This is in accordance with the results shown in Chapter 3, where EGCG does not have direct metabolic effects on skeletal muscle in perfused rat hindlimb.

The present study shows that whole body insulin sensitivity of the healthy rats was not significantly altered by acute EGCG treatment. Previously, regular green tea consumption has been reported to reduce the risk for developing type 2 diabetes (106; 125). Additionally, previous studies (156; 158; 229) have claimed that chronic green tea treatment improved glucose tolerance in rats. As demonstrated in Chapter 4, EGCG-mediated vasodilation in skeletal muscle through a separate (in part) signalling pathway to insulin, and therefore the unknown signalling pathway might be intact in insulin resistant rats. This suggests that acute EGCG treatment may be insufficient to improve whole body insulin sensitivity in healthy animals. However, there is still possibility that acute EGCG treatment may be effective in insulin resistant rats, which are lacking insulin-mediated microvascular recruitment or that chronic EGCG administration may be required to exert its health-promoting benefit.

In conclusion, this study shows that although 10 μ M EGCG increased microvascular blood volume *in vivo*, this was not sufficient to increase muscle glucose uptake in healthy insulin responsive animals. Previous studies by Shao *et al.* (238) and Tsuneki *et*

al. (147) reported that acute green tea or EGCG exerts opposite effects in healthy and insulin resistant mice. Green tea or EGCG acutely lowered blood glucose in *db/db* mice but not healthy mice (147), and improved glucose tolerance in insulin resistance but not healthy mice (238). The acute effects of EGCG on microvascular perfusion and muscle glucose uptake in an insulin resistant model, where both the microvasculature and myocyte are insulin resistant, are not known and thus were investigated in studies described in Chapter 6.

Chapter 6

Acute effects of EGCG in insulin resistant rats *in vivo*

6.1 Introduction

Animal models of insulin resistance and diabetes have been widely used to gain better understanding of the pathogenesis of insulin resistance and type 2 diabetes. Rodents fed a high fat diet (HFD) mimic the mechanisms responsible for the development of insulin resistance in humans (239). Kraegen *et al.* (240) showed that rats developed liver insulin resistance after 3 days of HFD feeding, followed by insulin resistance in other insulin sensitive tissues by 3 weeks. Studies showed that rats fed a HFD for ≥ 3 weeks developed whole body insulin resistance (82; 240-245), which is characterised by hyperinsulinaemia (241-244), impaired glucose uptake in skeletal muscle and adipose tissue (82; 242-245), and impaired insulin-mediated microvascular perfusion (82; 245).

As demonstrated in Chapter 5, acute administration of EGCG stimulated microvascular perfusion in skeletal muscle of healthy animals, but had no effects on muscle and whole body insulin sensitivity. Recent studies (147; 238) showed that acute administration of green tea or EGCG exerts opposite effects in healthy versus insulin resistant animals, in which acute green tea or EGCG treatment was metabolically beneficial for insulin resistant but not healthy animals.

In insulin resistant animals, studies have suggested that chronic green tea or EGCG treatment ameliorates insulin resistance by promoting GLUT4 translocation and glucose uptake in myocytes (157; 158) and adipocytes (159) in the absence of insulin. Furthermore, chronic EGCG treatment increases plasma adiponectin (120; 160), and reduces the gene expression of resistin (246) and peroxisome proliferator-activated receptor γ (PPAR γ) (98) in adipocytes of insulin resistant animals. The studies in Chapter 5 demonstrated that EGCG is a vasodilator that does not acutely alter muscle glucose uptake or enhance insulin's metabolic or vascular actions in healthy rats.

Chapter 4 demonstrated that EGCG vasodilates in skeletal muscle via NOS-dependent but PI3-K- and AMPK-independent pathway, which is a NOS-dependent pathway that is distinct from insulin. The use of a separate NOS-dependent vasodilation signalling pathway from insulin suggests the possibility that EGCG may still be able to recruit microvascular flow in insulin resistant animals. Whether EGCG administration can thus ameliorate insulin resistance in skeletal muscle, by bypassing a defect in delivery of glucose and/or insulin to myocytes, is not known and is the main purpose of the current chapter.

The aims of the present study were therefore to determine (i) whether EGCG has direct vascular actions in insulin resistant rat hindlimb and (ii) whether acute administration of EGCG (10 μ M) ameliorates insulin resistance by improving whole body insulin sensitivity, microvascular perfusion, and muscle glucose uptake.

6.2 Methods

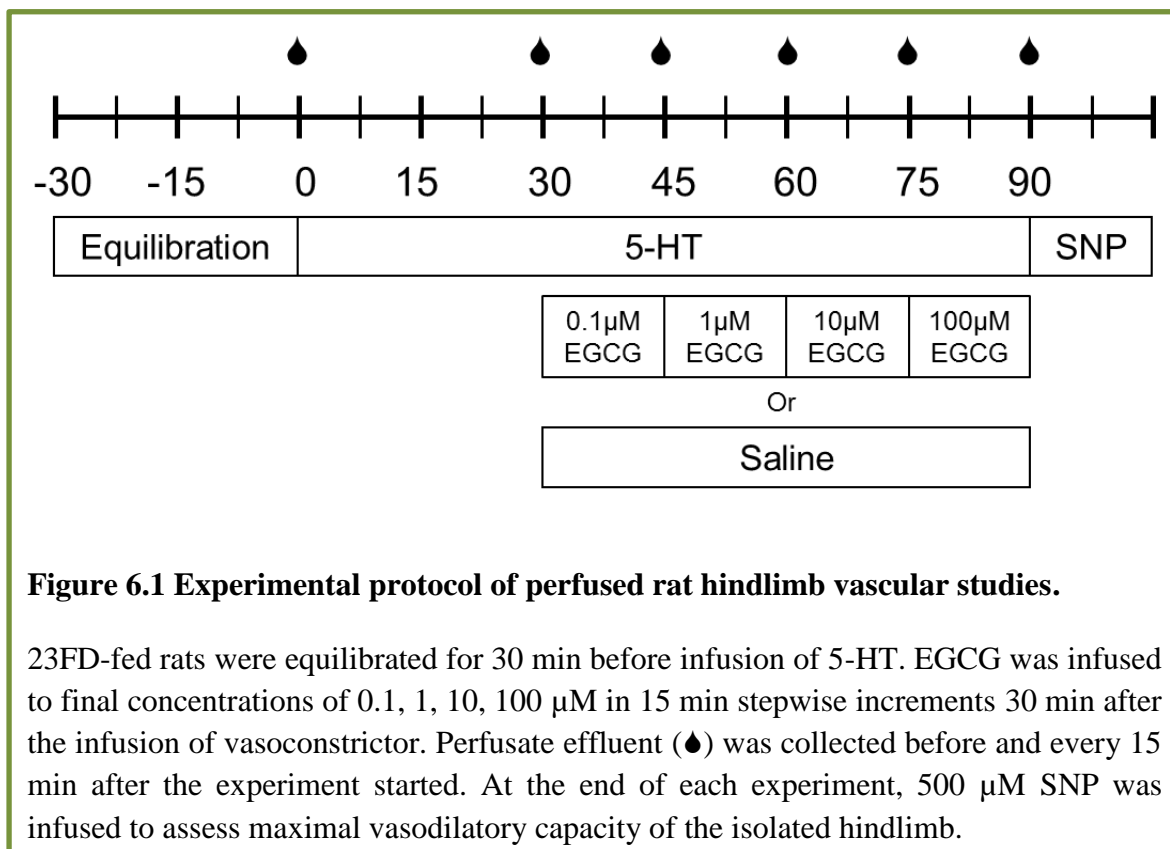
6.2.1 Animals

Male Sprague-Dawley rats ($n = 49$) at 6 – 7 weeks old were provided a 22.6% (w/w) fat semi-pure rodent diet (23FD) from Specialty Feeds, Glen Forest, WA, Australia (See Table 2.1) for 3 – 4 weeks. The rats were allowed free access to drinking water and food *ad libitum*. All experimental procedures were approved by the University of Tasmania Animal Ethics Committee (A11282 & A13384) and performed in accordance with the Australian Code of Practice for the Care and Use of Animals for Scientific Purposes – 2004, 7th Edition.

6.2.2 Experimental protocol

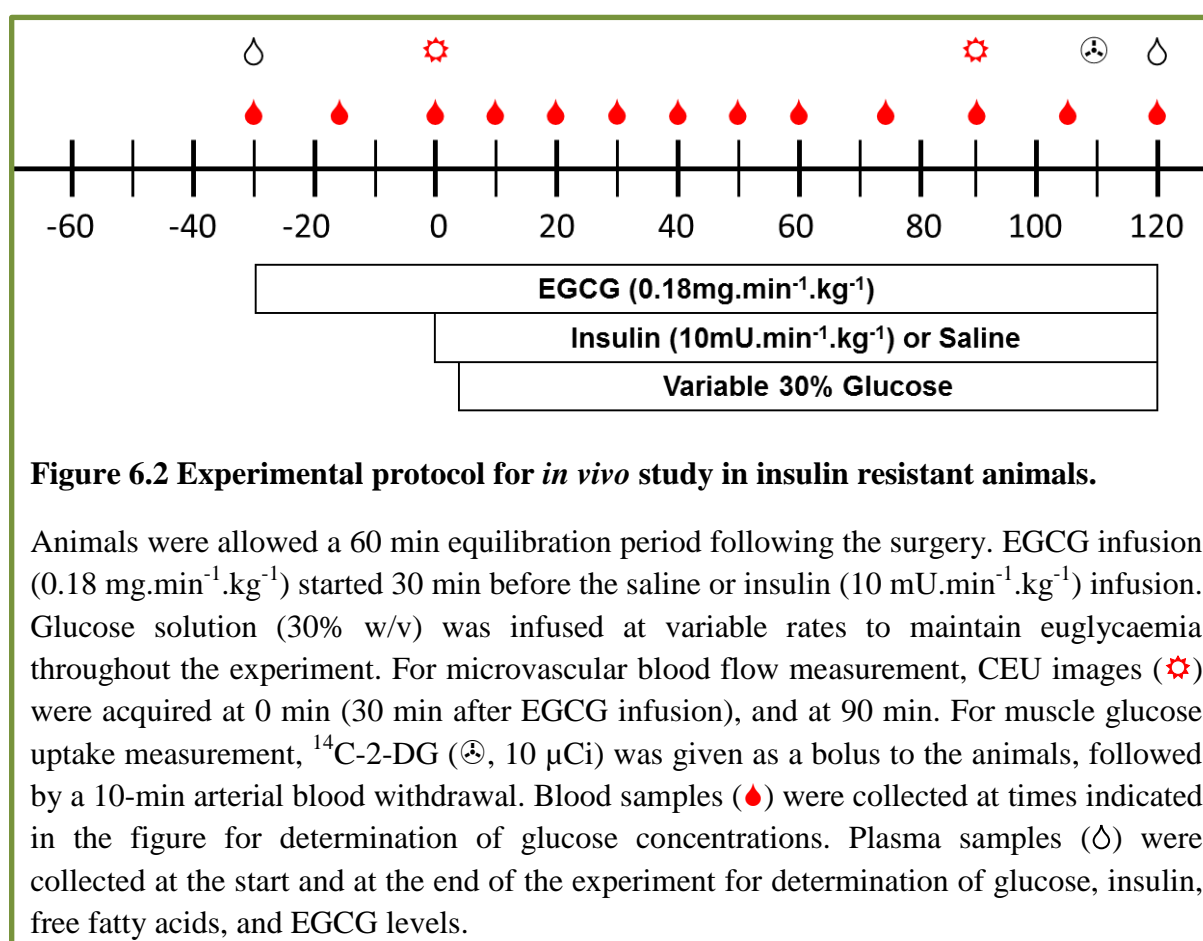
6.2.2.1 Constant-flow perfused rat hindlimb

Surgery was carried out in the rats as described in **2.3.2**. Vascular studies in hindlimbs were carried out according to the protocol outlined in **3.2.3** with some modifications (Figure 6.1). In the insulin resistant rats, the hindlimb vasculature was pre-constricted with 5-HT (0.15 – 0.24 μ M) to increase perfusion pressure to approximately 70 – 80 mmHg, perfusion pressure that is comparable with the pressure of 5-HT studies in Chapter 3. 5-HT was infused 30 min prior to and during infusion of saline or EGCG (0.1, 1, 10, 100 μ M in 15 min stepwise increments). At the end of each experiment, 500 μ M SNP was infused to assess maximal vasodilatory capacity of the isolated hindlimb, in order to determine the absence of oedema-mediated increase in perfusion pressure which may mask the vasodilation effects of EGCG.



6.2.2.2 *In vivo* study

Surgery was carried out in the overnight fasted rats as described in 2.4.1. The experimental protocol of this study was as described in 5.2.2 with some modifications (Figure 6.2). Muscle glucose uptake was measured using ^{14}C -2-DG (specific activity 50 – 60 mCi.mmol $^{-1}$, American Radiolabelled Chemicals, Saint Louis, MO, USA), as described in 2.4.8. A bolus of ^{14}C -2-DG (10 μCi) was given to the rat via jugular vein, followed by a 10-min arterial blood withdrawal.



6.2.3 Statistical Analysis

All data are expressed as means \pm S.E.M. Two-way repeated measures ANOVA with Student-Newman-Keuls *post hoc* test was used to compare treatment groups over the time course of experiment. One-way ANOVA with Student-Newman-Keuls *post hoc* test was used to make comparisons of differences between endpoint values. All tests were performed using the SigmaPlot 11 (©Systat Software Inc. 2008).

6.3 Results

6.3.1 Animal characteristics

Following 3 – 4 weeks of HFD feeding, body weight of the fasting rats was 265 ± 7 g (n = 35). Table 6.1 shows the basal metabolic characteristics of the rats fed with 5FD (Chapter 5) and 23FD. Following 4 weeks of dietary intervention, fasting plasma glucose of the 23FD rats was not different from the 5FD rats. As expected, fasting plasma insulin and free fatty acids, and epididymal fat pad weights were higher in the 23FD rats than the 5FD rats. Homeostatic model assessment of insulin resistance (HOMA-IR), a surrogate measure of insulin resistance, was higher in the 23FD rats. These indicate that rats developed insulin resistance following 4 weeks of 23FD treatment.

Table 6.1 Animal characteristics following 3 – 4 weeks of HFD treatment.

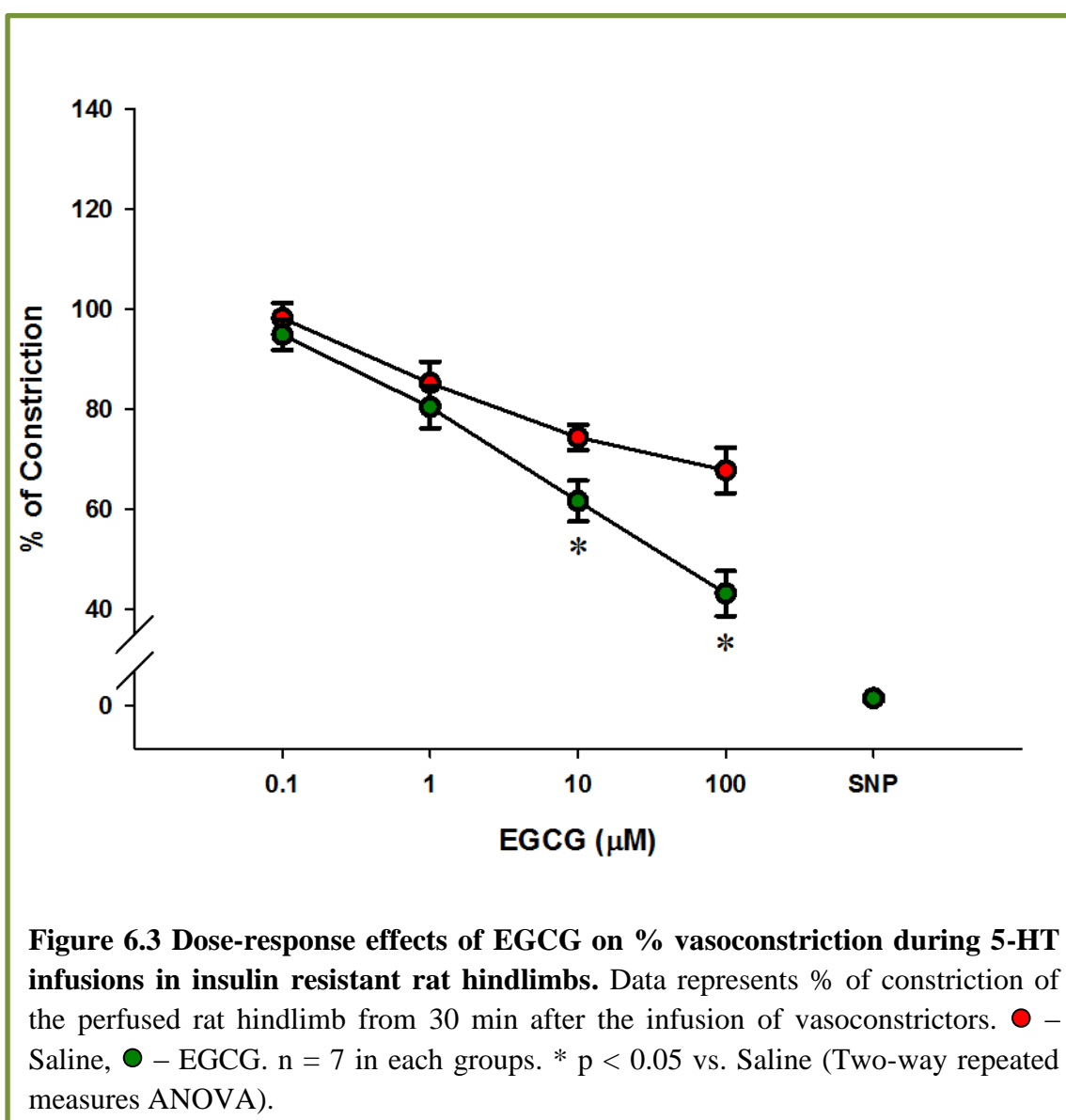
	5FD (n = 32)	23FD (n = 35)	P value
Fasting plasma glucose (mM)	7.14 ± 0.11	7.07 ± 0.14	0.720
Fasting plasma insulin (pM)	70 ± 8	205 ± 17	<0.001
Fasting plasma free fatty acids (mM)	0.64 ± 0.03	0.76 ± 0.02	0.001
Epididymal fat pad (% of body weight)	0.48 ± 0.02	0.86 ± 0.05	< 0.001
HOMA-IR	3.27 ± 0.04	9.50 ± 0.91	< 0.001

Data are expressed as Means ± SEM.

6.3.2 Vascular actions of EGCG in the perfused rat hindlimb

The direct vascular actions of EGCG in insulin resistant rat skeletal muscle were assessed in the constant-flow perfused rat hindlimb system. Hindlimb perfusion pressure under basal conditions at a flow rate of ~8 mL.min⁻¹ was 38.8 ± 1.0 mmHg (n = 14). The vascular preparation was pre-constricted with 5-HT (0.15 – 0.24 µM) to increase perfusion pressure to 79.4 ± 6.7 mmHg (n = 14), and this is comparable with the perfusion pressure induced by 5-HT in healthy rats (See 3.3.2.3). EGCG infused at 0.1, 1, 10, and 100 µM in 15 min step-wise increments caused dose-dependent vasodilation in 5-HT pre-constricted hindlimbs (Figure 6.3). Compared with saline, at 10 and 100 µM doses, EGCG infusion significantly (P < 0.05) reduced 5-HT-mediated vasoconstriction. At the highest dose tested (100 µM), EGCG opposed 5-HT mediated vasoconstriction by 43 ± 5 % (p < 0.001 vs. saline). Interestingly, the magnitude of EGCG-induced vasodilation in insulin resistant rat hindlimbs is similar to that of the normal healthy rat hindlimbs (Figure 3.7C), in which 100 µM EGCG opposed 5-HT

mediated vasoconstriction by 47 ± 6 %. In all hindlimbs, SNP reversed 5-HT mediated vasoconstriction by >95 %, representing maximal vasodilation and return of perfusion pressures to basal levels.

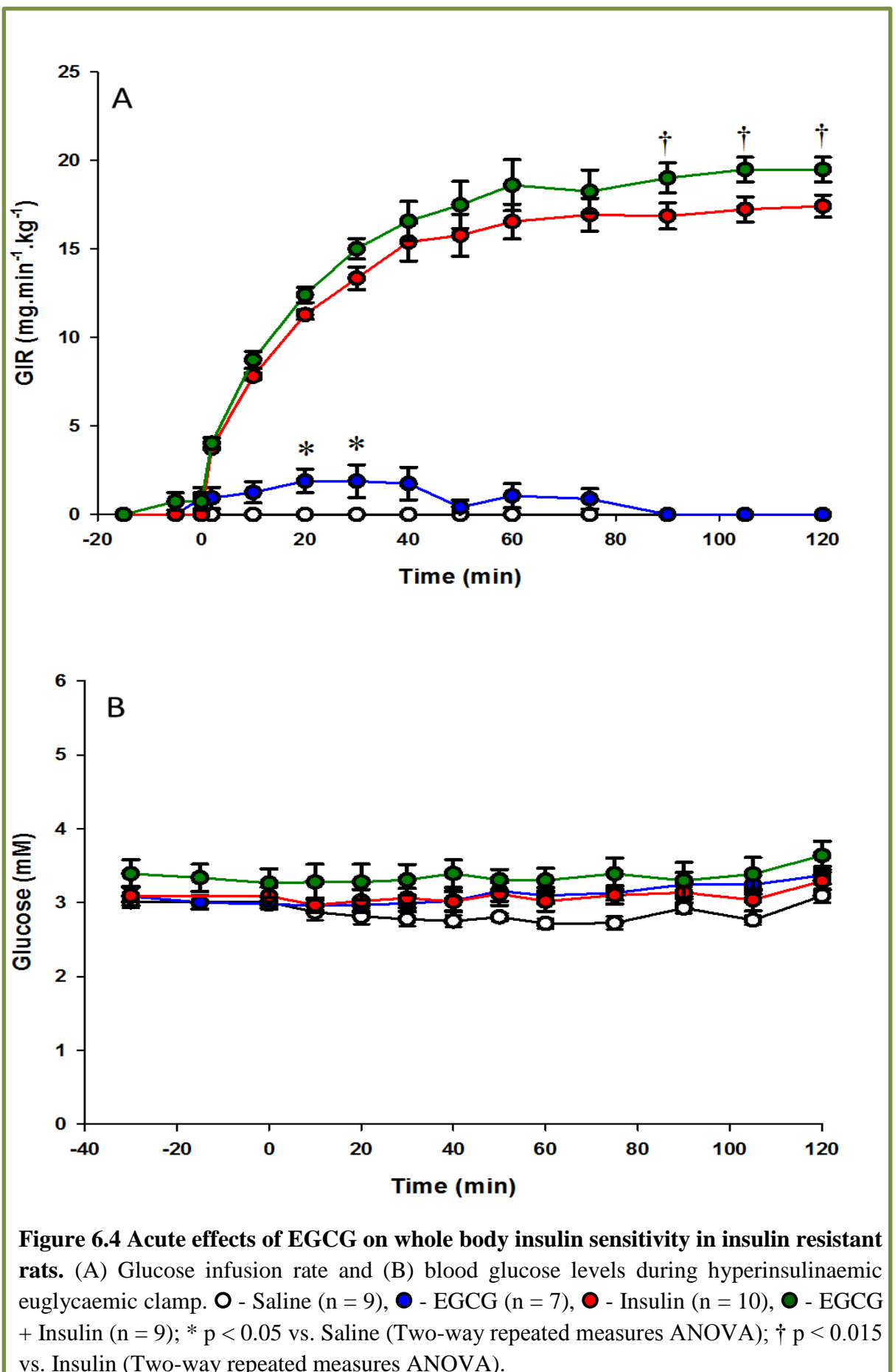


6.3.3 Acute effects of EGCG in insulin resistant rats *in vivo*

6.3.3.1 Whole body insulin sensitivity

The GIR (Figure 6.4A) of the Insulin group during steady state of glucose infusion was $17.42 \pm 0.63 \text{ mg} \cdot \text{min}^{-1} \cdot \text{kg}^{-1}$, and the GIR of the EGCG + Insulin group increased significantly ($19.48 \pm 0.70 \text{ mg} \cdot \text{min}^{-1} \cdot \text{kg}^{-1}$, $p < 0.015$) when compared to Insulin alone. This indicates that acute EGCG has improved whole body insulin sensitivity in the insulin resistant rats by 12%. Plasma insulin levels post-insulin clamp in the Insulin and EGCG + Insulin groups were $1495 \pm 113 \text{ pM}$ and $1337 \pm 63 \text{ pM}$ respectively ($p = 0.253$), indicating that EGCG did not significantly affect plasma insulin levels. In the EGCG group, some glucose was required to maintain euglycaemia in the beginning of the experiment, however, this was not required through to the end of experiment. Blood glucose (Figure 6.4B) measured throughout the experiments was not different between each group.

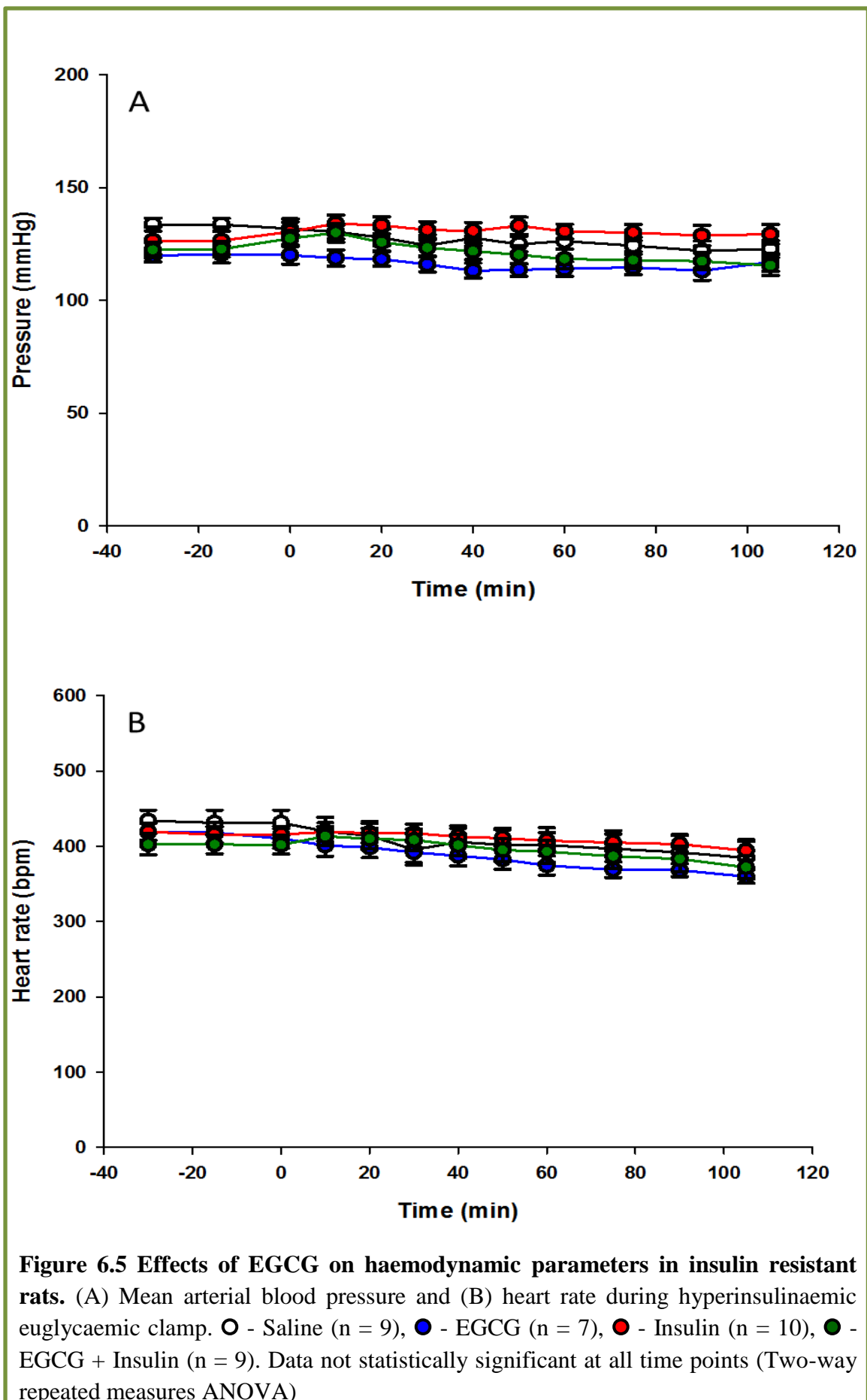
In the EGCG and EGCG + Insulin groups, EGCG was infused 30 min before the hyperinsulinaemic euglycaemic clamp. Plasma EGCG levels following 150 min EGCG infusion in the EGCG and EGCG + Insulin groups were $9.30 \pm 0.90 \text{ } \mu\text{M}$ and $10.88 \pm 0.44 \text{ } \mu\text{M}$ respectively ($p = 0.14$).



6.3.3.2 Haemodynamic parameters

Figure 6.5 shows the MAP and heart rate of the rats during the course of the experiments. MAP and heart rate were not different between groups during the course of experiments indicating acute EGCG infusion has no effect on these cardiovascular measures.

FBF was measured during the hyperinsulinaemic euglycaemic clamp (Figure 6.6). FBF before the experiments were not different between all groups (data not shown). In the 23FD rats, FBF of the Insulin group ($1.16 \pm 0.13 \text{ ml.min}^{-1}$) was not different from that of the Saline group ($1.16 \pm 0.13 \text{ ml.min}^{-1}$) at the end of experiment (Figure 6.6). Acute EGCG did not alter FBF ($1.17 \pm 0.03 \text{ ml.min}^{-1}$) or enhance insulin-stimulated FBF ($1.15 \pm 0.14 \text{ ml.min}^{-1}$) in the 23FD rats.



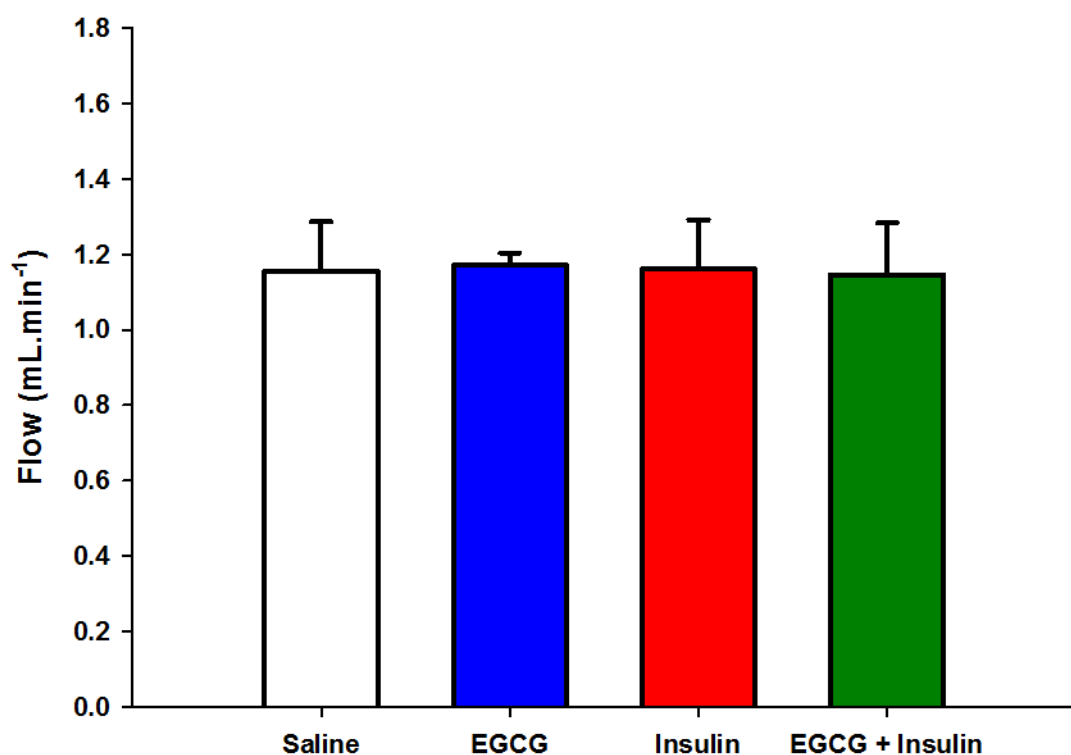


Figure 6.6 Femoral artery blood flow at the end of experiment in insulin resistant rats. - Saline (n = 9), - EGCG (n = 7), - Insulin (n = 10), - EGCG + Insulin (n = 9). Data not statistically significant (Two-way ANOVA).

6.3.3.3 Muscle microvascular perfusion

CEU was used to measure the MBV before and 90 min during the hyperinsulinaemic euglycaemic clamp (Figure 6.7). At 0 min (Figure 6.7), MBV of the EGCG and EGCG + Insulin groups were significantly higher than the Saline and Insulin groups (5.41 ± 0.34 and 5.33 ± 0.58 acoustic intensity units vs. 2.85 ± 0.09 and 3.54 ± 0.50 acoustic intensity units respectively, $p < 0.005$ vs. Saline and Insulin groups). In the EGCG and EGCG + Insulin groups, first CEU measurement was acquired 30 min after EGCG infusion, indicating acute EGCG infusion for 30 min has increased microvascular perfusion in skeletal muscle of the insulin resistant rats.

At 90 min, the Saline group had a modest but significant increase in MBV ($23 \pm 9 \%$, $p = 0.038$). The Insulin group also had a significant increase in the MBV by 90 min of insulin clamp ($45 \pm 12 \%$, $p < 0.001$), while MBV of EGCG and EGCG + Insulin groups remained unchanged from 0 min (Figure 6.7). MBV of the EGCG, Insulin and EGCG + Insulin groups at 90 min were not different, but significantly ($p < 0.05$) higher than the Saline group. This indicates that EGCG stimulated microvascular perfusion to a similar extent as insulin, but did not further enhance insulin's vascular action in skeletal muscle.

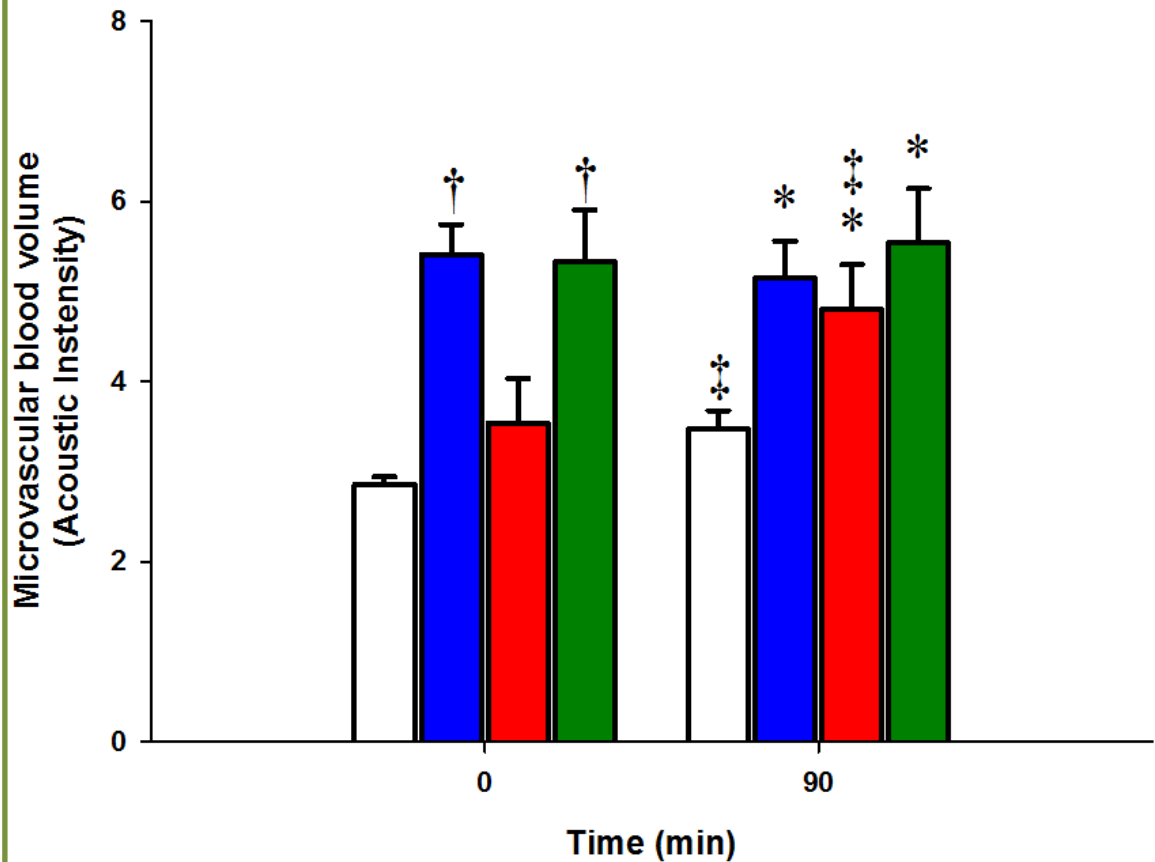


Figure 6.7 Microvascular blood volume before and during hyperinsulinaemic euglycaemic clamp in insulin resistant rats. - Saline (n = 9), - EGCG (n = 7), - Insulin (n = 10), - EGCG + Insulin (n = 9); [†] p < 0.005 vs. Saline and Insulin at 0 min (Two-way repeated measures ANOVA); [‡] p < 0.05 vs. respective 0 min (Two-way repeated measures ANOVA); * p < 0.05 vs. Saline at 90 min (Two-way repeated measures ANOVA).

6.3.3.4 Muscle insulin sensitivity

Muscle glucose uptake was assessed at the end of the experiment using an isotopic glucose tracer ^{14}C -2-DG. In insulin resistant rats, insulin stimulated muscle glucose uptake by 4.5-fold (Figure 6.8). Muscle glucose uptake was not different between the Insulin and EGCG + Insulin groups (8.18 ± 0.37 and $8.43 \pm 0.92 \mu\text{g}\cdot\text{g}^{-1}\cdot\text{min}^{-1}$ respectively). In addition, muscle glucose uptake was not different between Saline and EGCG groups (1.77 ± 0.19 and $1.95 \pm 0.24 \mu\text{g}\cdot\text{g}^{-1}\cdot\text{min}^{-1}$ respectively). In insulin resistant rats, EGCG did not improve muscle glucose uptake or enhance insulin-stimulated muscle glucose uptake.

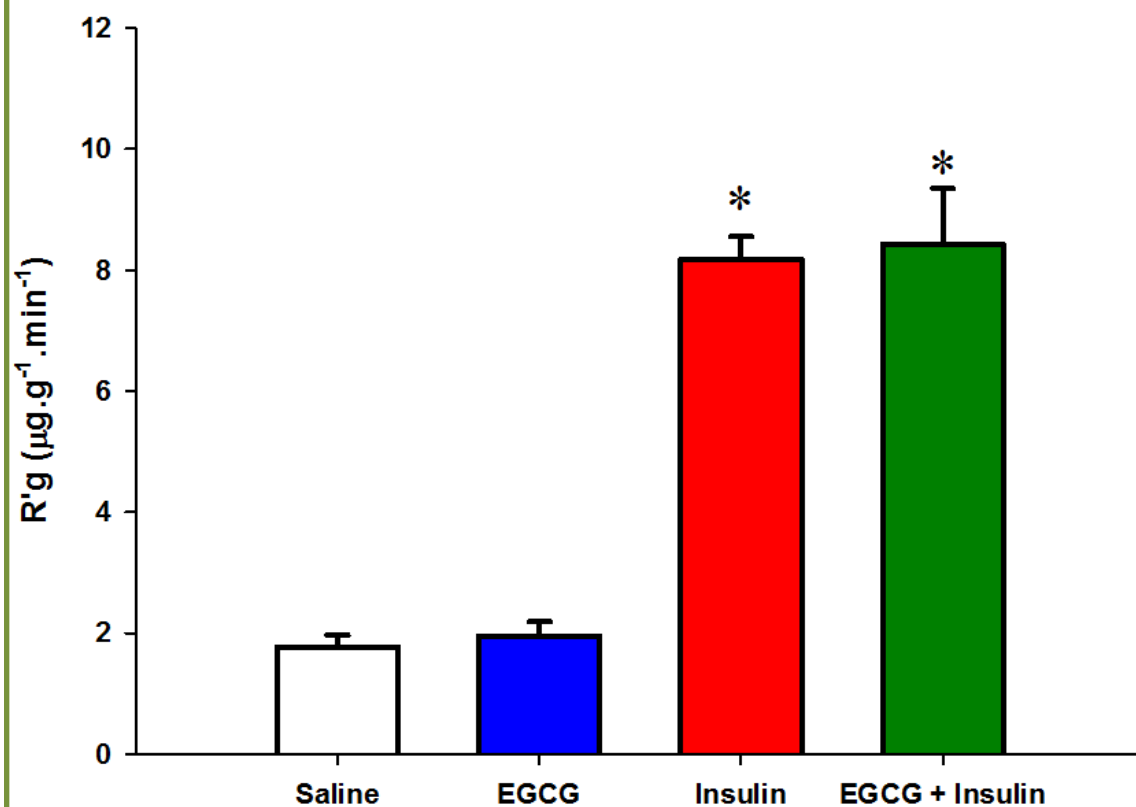


Figure 6.8 Muscle ¹⁴C-2-DG uptake at the end of hyperinsulinaemic euglycaemic clamp in insulin resistant rats. □ - Saline (n = 9), ■ - EGCG (n = 7), ■ - Insulin (n = 10), ■ - EGCG + Insulin (n = 9). * p < 0.001 vs. Saline and EGCG (One-way ANOVA).

6.4 Discussion

In the present chapter, the acute vascular and metabolic actions of EGCG were explored in skeletal muscle of HFD-induced insulin resistant rats. The main findings from the current study are i) EGCG vasodilates skeletal muscle vasculature *in situ*, ii) EGCG acutely stimulates skeletal muscle microvascular perfusion, but does not augment glucose uptake *in vivo*, and these effects are not additive to insulin, iii) however, EGCG acutely improves whole body insulin sensitivity of the insulin resistant rats. Therefore, EGCG possesses insulin-mimetic vascular, but not metabolic, actions in skeletal muscle of HFD-induced insulin resistant rats.

The present study shows that rats fed with 23FD for 4 weeks develop whole body insulin resistance, with a marked increase in epididymal fat pad weights, fasting plasma insulin and plasma free fatty acids. In recent years, Rattigan and colleagues have reported that insulin mediated increases in total blood flow and microvascular perfusion are impaired in obese humans (230) and HFD-induced insulin resistant rats (82; 245). In the perfused rat hindlimb preparations, EGCG dose-dependently vasodilated in 5-HT pre-constricted hindlimb of the insulin resistant rats. Interestingly, the magnitude of EGCG-induced vasodilation in rat hindlimb of insulin resistant rats was comparable to that observed in normal healthy rats (Chapter 3, Figure 6.3). Studies in Chapter 3 and 4 showed that EGCG is a NOS-dependent vasodilator in skeletal muscle. Similarly, microvascular perfusion mediated by insulin is NOS-dependent (18; 53), but this is impaired during insulin resistant states (80; 82). EGCG-induced vasodilation in muscle vasculature is mediated via a partially separate signalling pathway from that of the insulin, suggesting that vascular responses to acute EGCG are intact in the HFD-induced insulin resistant rats and this may in turn improve insulin sensitivity in the insulin resistant rats.

Chapter 5 showed that acute EGCG treatment had no effect on whole body insulin sensitivity in healthy rats. However, in the present study, acute EGCG treatment significantly increased the GIR in the insulin resistant rats by 12%, indicating improvement in whole body insulin sensitivity. This is in accordance with a recent study (238) which showed that acute administration of EGCG (50 mg.kg⁻¹) improved glucose tolerance and insulin sensitivity in macrophage-induced insulin resistant, but not normal, mice. Similarly, another study (147) showed that green tea acutely lowered blood glucose in diabetic, but not healthy, mice.

This study shows that acute EGCG infusion has no effect on the MAP or insulin-stimulated increase in FBF. However, acute EGCG infusion for 30 min increased MBV in the skeletal muscle of the insulin resistant rats. Interestingly, EGCG-stimulated microvascular perfusion was similar in magnitude to raising plasma insulin concentrations to 1.5 nM in insulin resistant rats. Nonetheless, acute infusion of EGCG did not further enhance insulin-mediated microvascular perfusion, indicating EGCG mimics but does not enhance insulin's action in muscle microvasculature. As compared to the healthy rats (Chapter 5), the microvasculature of the insulin resistant rats appeared to be more sensitive to EGCG, in which there was a significant increase in MBV following 30 min of EGCG infusion. Some (247; 248), but not all (249; 250), studies suggested an elevated ROS production following HFD treatment, and ROS have been implicated in EGCG-mediated NO production in endothelial cells (119; 181). This suggests that EGCG-mediated microvascular perfusion is more sensitive in the insulin resistant rats could be due to an elevation in ROS levels, however, further studies are required to determine this.

Despite the increase in whole body insulin sensitivity and microvascular perfusion, acute EGCG treatment did not cause glucose disposal by itself or enhance insulin-

stimulated glucose uptake in skeletal muscle. Previously, EGCG has been reported to stimulate glucose uptake in adipocytes (156; 159; 238) and inhibit hepatic gluconeogenesis (174; 175). Therefore, it is highly likely that acute EGCG treatment has improved insulin sensitivity in adipose tissue and/or liver, which resulted in increased GIR. However, adipose tissue and liver insulin sensitivity were not measured in the present study.

Insulin resistance in skeletal muscle is caused by the impairment in both delivery and extraction of glucose to skeletal muscle (243). While muscle microvascular perfusion plays a key role in determining the movement of glucose in blood to skeletal muscle (review by Barrett and Rattigan (251)), transmembrane glucose transport regulated by GLUT4 is an important rate-limiting step of glucose uptake into muscle and adipose tissue (252). HFD-induced muscle insulin resistance is characterised by elevated intracellular triglycerides in myocytes (253; 254), reduced muscle lipid oxidation (255; 256), reduced muscle GLUT4 content and insulin-stimulated GLUT4 translocation (257; 258), and reduced gene expressions of IRS-1 and PI3-K in skeletal muscle (259). Previous studies suggested that EGCG increased muscle lipid oxidation in HFD-fed mice *in vivo* (260; 261), reduced intracellular lipid accumulation (262) and stimulated GLUT4 translocation (158) in incubated myocytes *in vitro*. However, the present study showed that acute EGCG treatment stimulated muscle microvascular perfusion but not muscle glucose uptake in insulin resistant rats *in vivo*, suggesting that the GLUT4 translocation was not improved by acute EGCG treatment. This is in accordance with the findings from Chapter 3 where EGCG was shown to have direct vascular but not metabolic actions in skeletal muscle.

Studies in the past showed that chronic green tea or EGCG treatment improved glucose tolerance and insulin sensitivity in both healthy (156-158; 229) and insulin resistant (98;

158-167) animals. The present study showed that acute EGCG treatment improved whole body insulin sensitivity modestly in insulin resistant, but not healthy (Chapter 5) rats. Acute EGCG treatment has been shown to stimulate microvascular perfusion in healthy (Chapter 5) and HFD-induced insulin resistant rats. Whether chronic EGCG treatment could ameliorate insulin resistance by preventing the impairment of microvascular perfusion and muscle glucose uptake in HFD-fed rats is not known and was investigated in studies reported in Chapter 7.

Chapter 7

Chronic effects of EGCG in insulin resistant rats *in vivo*

7.1 Introduction

Several clinical studies (116; 128-149) have been carried out to investigate the anti-diabetic effects of green tea or EGCG. However, the outcome of these clinical trials was not conclusive. To date, there is mounting evidence (98; 120; 158-162; 164-167) that suggests that chronic green tea or EGCG treatment has anti-diabetic effects in insulin resistant mice and rats. However, the underlying mechanism of EGCG to ameliorate insulin resistance *in vivo* has not been fully elucidated.

Chapters 3 and 4 demonstrated that EGCG is a NOS-dependent vasodilator against 5-HT. Furthermore, Chapters 5 and 6 showed that acute administration of EGCG *in vivo* mimics insulin's action to stimulate muscle microvascular perfusion in healthy and insulin resistant rats. However, muscle glucose uptake was not improved following the increase in microvascular perfusion in the acute EGCG-treated rats. Acute administration of EGCG improved whole body insulin sensitivity of insulin resistant rat. This suggests that 10 μ M EGCG could acutely improve whole body insulin sensitivity in insulin resistant animals. In epidemiological studies, however, green tea/EGCG is present chronically. Therefore it is important to determine whether chronic administration of EGCG could prevent the development of insulin resistance.

Under normal healthy conditions, insulin stimulates microvascular perfusion to facilitate muscle glucose uptake (21; 263). However, in the presence of insulin resistance, insulin-mediated microvascular perfusion is impaired and leads to reduced insulin-stimulated muscle glucose uptake (245). Recently, a study (82) showed that impaired insulin-mediated microvascular perfusion could result in impaired insulin-stimulated muscle glucose uptake despite the myocytes being insulin sensitive. The reciprocal relationships between insulin-mediated microvascular perfusion and muscle

glucose uptake indicate that treatments to improve microvascular dysfunction may simultaneously improve muscle glucose uptake and insulin sensitivity. Thus the aim of this study was to determine whether chronic administration of EGCG prevents the development of insulin resistance by improving microvascular function and glucose metabolism in skeletal muscle of insulin resistant rats.

EGCG at the dose of $200 \text{ mg.kg}^{-1}.\text{d}^{-1}$ has been previously reported to improve cardiovascular and metabolic functions in SHR (120). In the present study, rats fed a high fat diet were treated with EGCG ($200 \text{ mg.kg}^{-1}.\text{d}^{-1}$) in drinking water for 4 weeks to determine the chronic effects of EGCG on whole body insulin sensitivity, insulin-mediated microvascular perfusion and insulin-mediated muscle glucose uptake.

7.2 Methods

7.2.1 Animals

Male Sprague-Dawley rats ($n = 13$) at 7 – 8 weeks old were provided a 22.6% (w/w) fat semi-pure rodent diet (23FD) from Specialty Feeds, Glen Forest, WA, Australia (See Table 2.1) for 4 weeks. The rats were allowed free access to drinking water and food *ad libitum*. During the dietary intervention period, EGCG ($200 \text{ mg.kg}^{-1}.\text{d}^{-1}$) was prepared freshly every 2 days and added to the drinking water. Food and water intake were monitored daily during the dietary intervention period. Following the dietary intervention, rats were fasted overnight before experiments were carried out, and EGCG water was removed and replaced with normal drinking water during the overnight fast. All experimental procedures were approved by the University of

Tasmania Animal Ethics Committee (A11282 & A13384) and performed in accordance with the Australian Code of Practice for the Care and Use of Animals for Scientific Purposes – 2004, 7th Edition.

7.2.2 Experimental protocol

Surgery was carried out in the overnight fasted rats as described in **2.4.1**. The experimental protocol of this study was as described in **6.2.2.2** (Figure 7.1). Importantly, EGCG was not infused into the rats intravenously.

In the present study, data from the rats fed with 23FD and EGCG water for 4 weeks (23FD + chEGCG) was compared with the 23FD rats (Saline group- 23FDsal and Insulin group- 23FDins) in Chapter 6 (Figure 7.2).

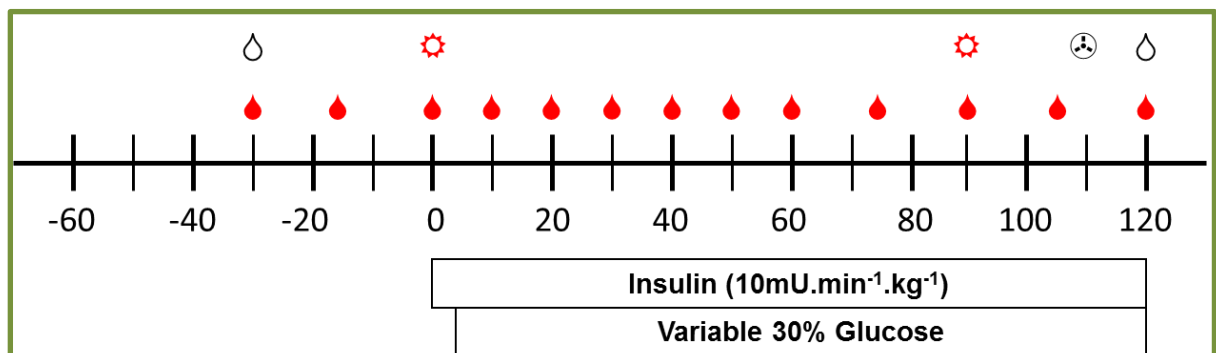
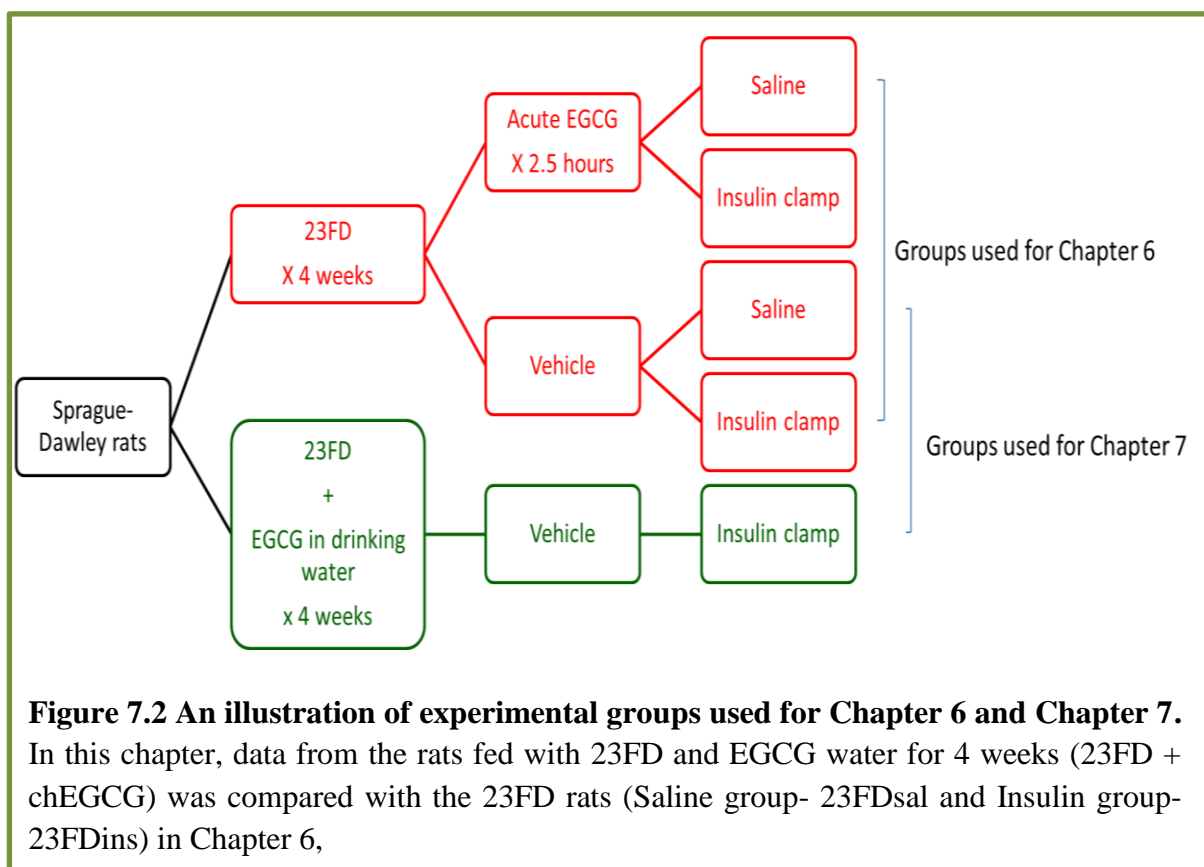


Figure 7.1 Experimental protocol for in vivo study in chronic EGCG-treated animals.

Animals were allowed a 60 min equilibration period following the surgery. Insulin (10 mU.min⁻¹.kg⁻¹) infusion started at 0 min. Glucose solution (30% w/v) was infused at variable rates to maintain euglycaemia throughout the experiment. For microvascular blood flow measurement, CEU images (⚙️) were acquired at 0 min, and at 90 min. For muscle glucose uptake measurement, ¹⁴C-2-DG (⊕, 10 µCi) was given as a bolus to the animals, followed by a 10-min arterial blood withdrawal. Blood samples (●) were collected at times indicated in the figure for glucose levels determination. Plasma samples (○) were collected at the start and at the end of the experiment to determine glucose, insulin, free fatty acids, and EGCG concentrations.



7.2.3 Western blot

Phosphorylation of Akt and TBC1D1^{Thr590}, both proteins involve in insulin signalling in skeletal muscle to stimulate glucose uptake, was assessed using Western blotting.

Western blot analysis of Akt was performed as described in 2.5. Western blot analysis of the TBC1D1^{Thr590} was performed as described in 2.5 with some modifications. Primary antibodies used were rabbit anti-phospho-Thr⁵⁹⁰-TBC1D1 (pTBC1D1, 1:1000; Cell Signalling) and rabbit-anti- α -tubulin (α -tubulin, 1:1000; Cell Signalling) as a loading control. Following incubation with primary antibody, the membranes were probed with 1:1000 anti-rabbit secondary antibody (Cell Signalling). To visualise the bands, equal volumes of West Pico Chemiluminescent Substrate (Thermo Fischer Scientific, Rockford, IL, USA) were mixed together and applied to the membrane. Band intensities were quantified by optical density using Image Station 4000mm Pro, Carestream Molecular Imaging (Carestream health Inc., Rochester, NY, USA).

7.2.4 Statistical analysis

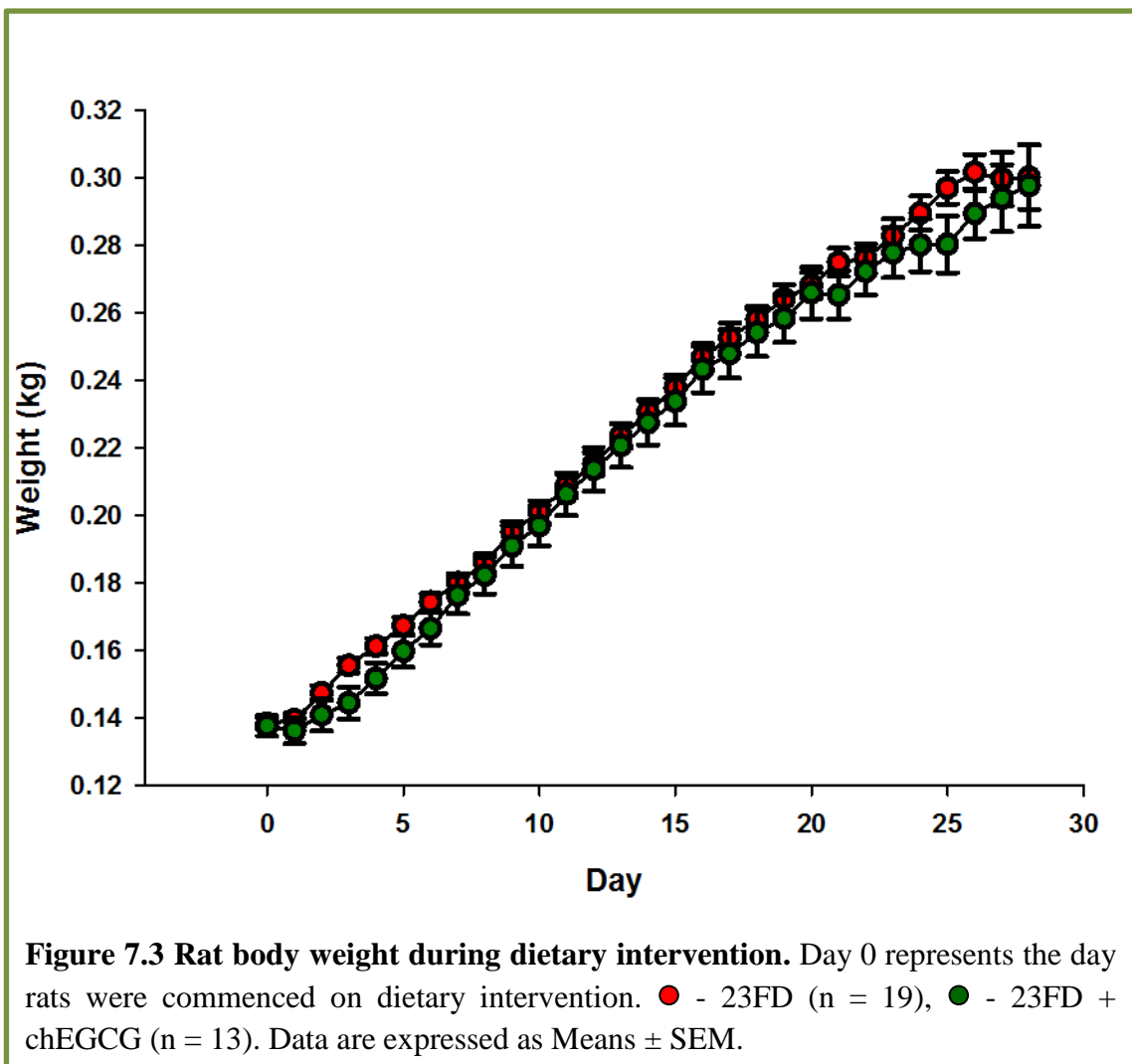
All data are expressed as means \pm S.E.M. Two-way repeated measures ANOVA with Student-Newman-Keuls *post hoc* test was used to compare treatment groups over the time course of experiment. An unpaired Student's t-test was used to make comparisons of differences between 2 groups. One-way ANOVA with Student-Newman-Keuls *post hoc* test was used to make comparisons of differences between endpoint values. All tests were performed using the SigmaPlot 11 ([©]Systat Software Inc. 2008).

7.3 Results

7.3.1 Animal characteristics

During dietary interventions, body weights of the rats fed with 23FD (23FD) were not different from that of the rats fed with 23FD and EGCG water (23FD + chEGCG) (Figure 7.3), indicating that EGCG treatment for 4 weeks had no effect on the rat's body weight. EGCG treatment did not alter food, energy and water intake of the rats (Figure 7.4 and 7.5A). During the dietary intervention, EGCG water was prepared fresh every 2 days to provide a dose up to $200 \text{ mg.kg}^{-1}.\text{d}^{-1}$. Accordingly, the actual average daily EGCG intake for the 23FD + chEGCG rats measured from water intake was $189 \pm 3 \text{ mg.kg}^{-1}.\text{d}^{-1}$ (Figure 7.5B).

Following 4 weeks of dietary intervention, body weight, epididymal fat pad weight, fasting plasma glucose, insulin and free fatty acids, and HOMA-IR were not different between the 23FD and 23FD + chEGCG rats (Table 7.1). Following an overnight fast, EGCG was not detected in the plasma of the 23FD + chEGCG rats. This indicates that chronic EGCG treatment for 4 weeks did not improve the abovementioned basal metabolic profiles of the insulin resistant rats.



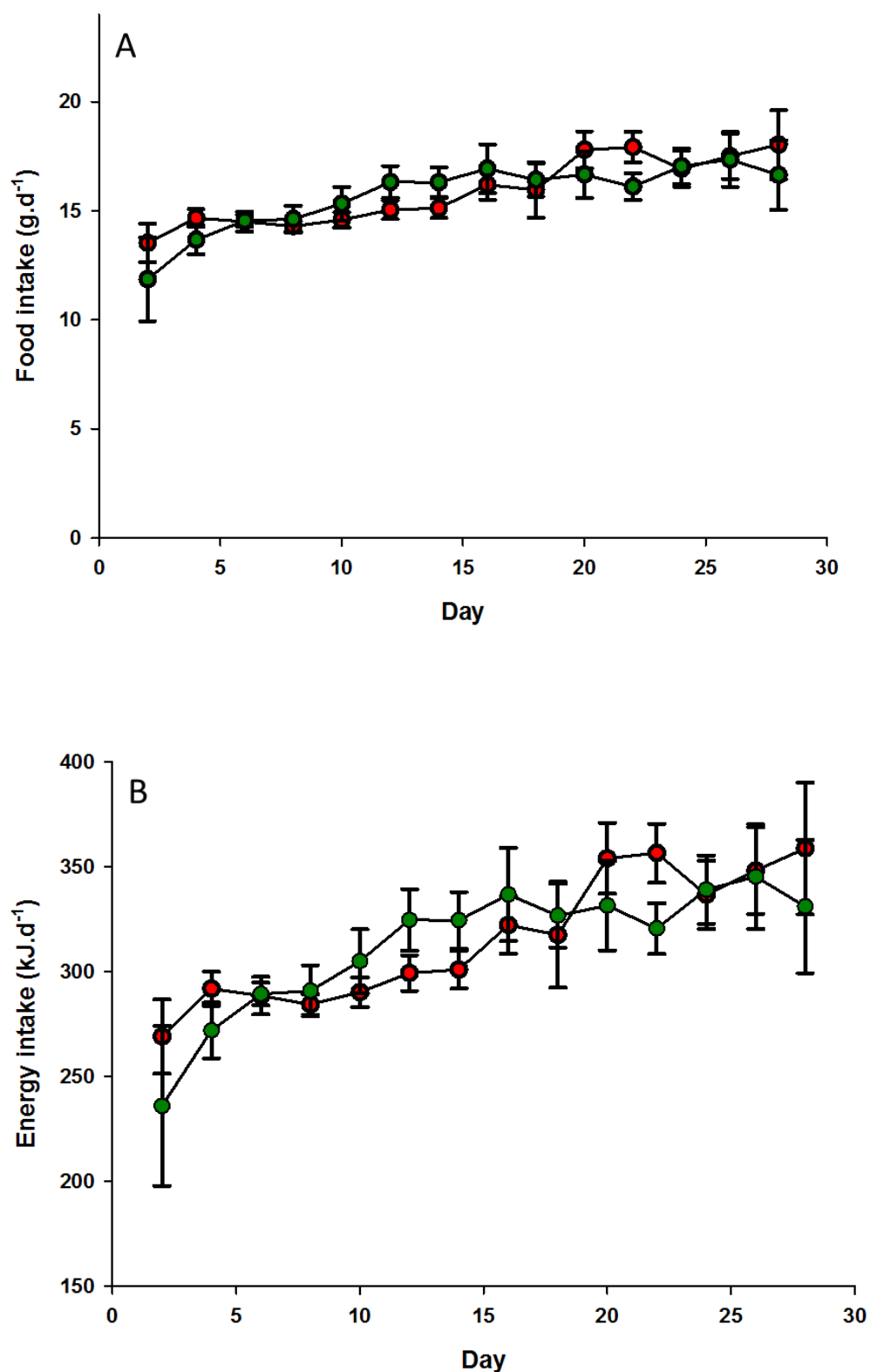


Figure 7.4 Food (A) and energy (B) intake of rats during dietary intervention. Day 0 represents the day rats were commenced on dietary intervention. ● - 23FD (n = 19), ● - 23FD + chEGCG (n = 13). Data are expressed as Means ± SEM.

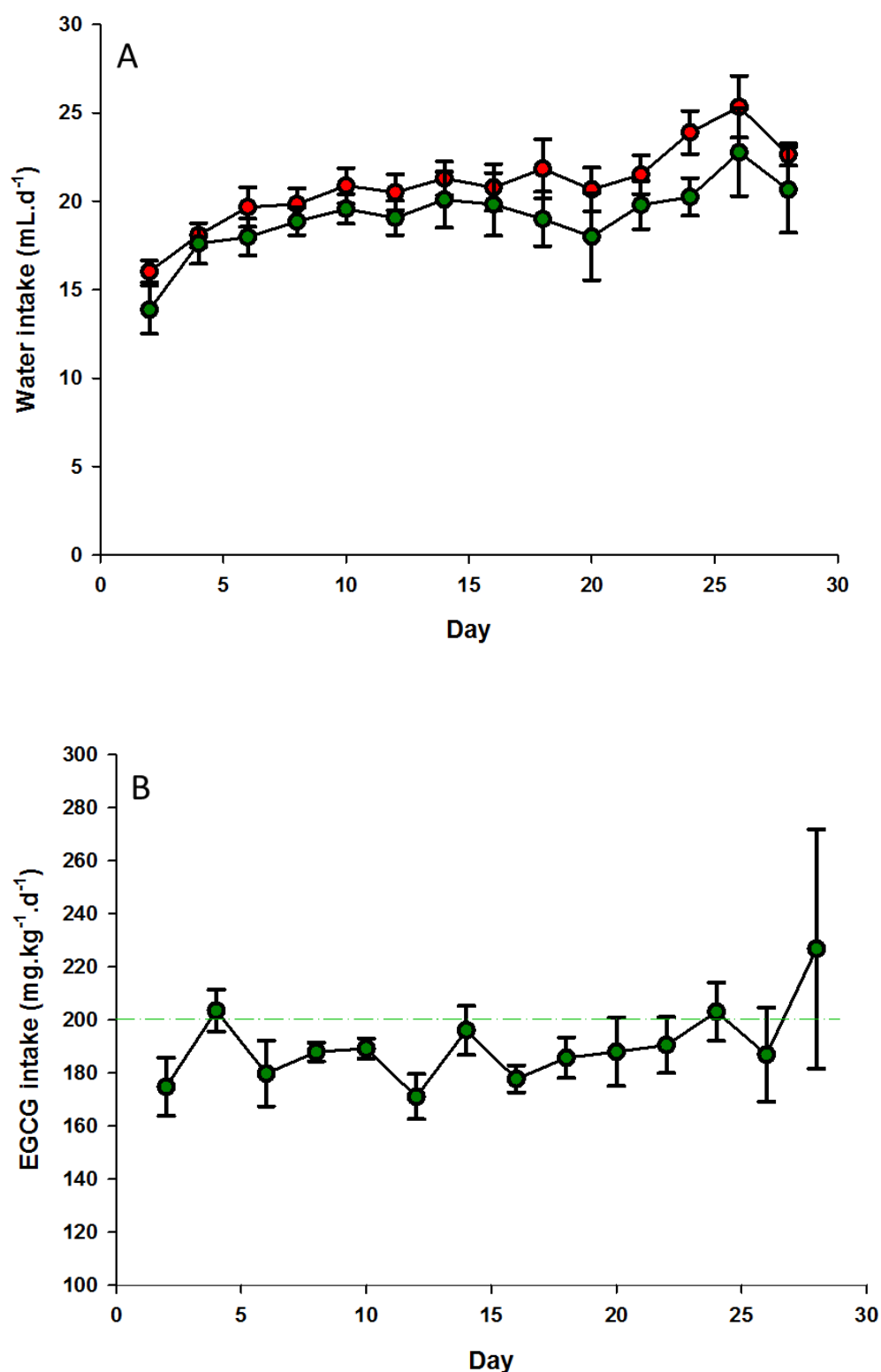


Figure 7.5 Water (A) and EGCG (B) intake of rats during dietary intervention. Day 0 represents the day rats were commenced on dietary intervention. ● - 23FD (n = 19), ● - 23FD + chEGCG (n = 13), green line: EGCG 200 mg.kg⁻¹.d⁻¹ target. Data are expressed as Means ± SEM.

Table 7.1 Chronic effects of EGCG on basal characteristics of the rats.

	23FD (n = 35)	23FD + chEGCG (n = 13)	P value
Body weight (g)	265 ± 7	289 ± 7	0.060
Fasting plasma glucose (mM)	7.07 ± 0.14	7.14 ± 0.21	0.795
Fasting plasma insulin (pM)	205 ± 17	233 ± 21	0.366
Fasting plasma free fatty acids (mM)	0.76 ± 0.02	0.75 ± 0.03	0.743
Epididymal fat pad (% of body weight)	0.86 ± 0.05	0.85 ± 0.03	0.927
HOMA-IR	9.50 ± 0.91	10.87 ± 1.14	0.411

Data are expressed as Means ± SEM.

7.3.2 Chronic effects of EGCG on whole body insulin sensitivity in insulin resistant rats.

Figure 7.6A shows the GIR of the 23FDins and 23FDins + chEGCG rats. GIR of the 23FDins rats during steady state glucose infusion was $17.42 \pm 0.63 \text{ mg} \cdot \text{min}^{-1} \cdot \text{kg}^{-1}$, while GIR of the 23FDins + chEGCG rats was $21.12 \pm 0.76 \text{ mg} \cdot \text{min}^{-1} \cdot \text{kg}^{-1}$ ($p < 0.001$ vs. 23FD). This indicates that the chronic EGCG treatment for 4 weeks has improved whole body insulin sensitivity of the insulin resistant rats. Plasma insulin concentrations post-insulin clamp of the 23FDins and 23FDins + chEGCG rats were 1495 ± 114 and $1522 \pm 78 \text{ pM}$ respectively ($p = 0.845$), indicating both groups were clamped with comparable amounts of insulin. Blood glucoses (Figure 7.6B) measured throughout the experiments were not different between groups.

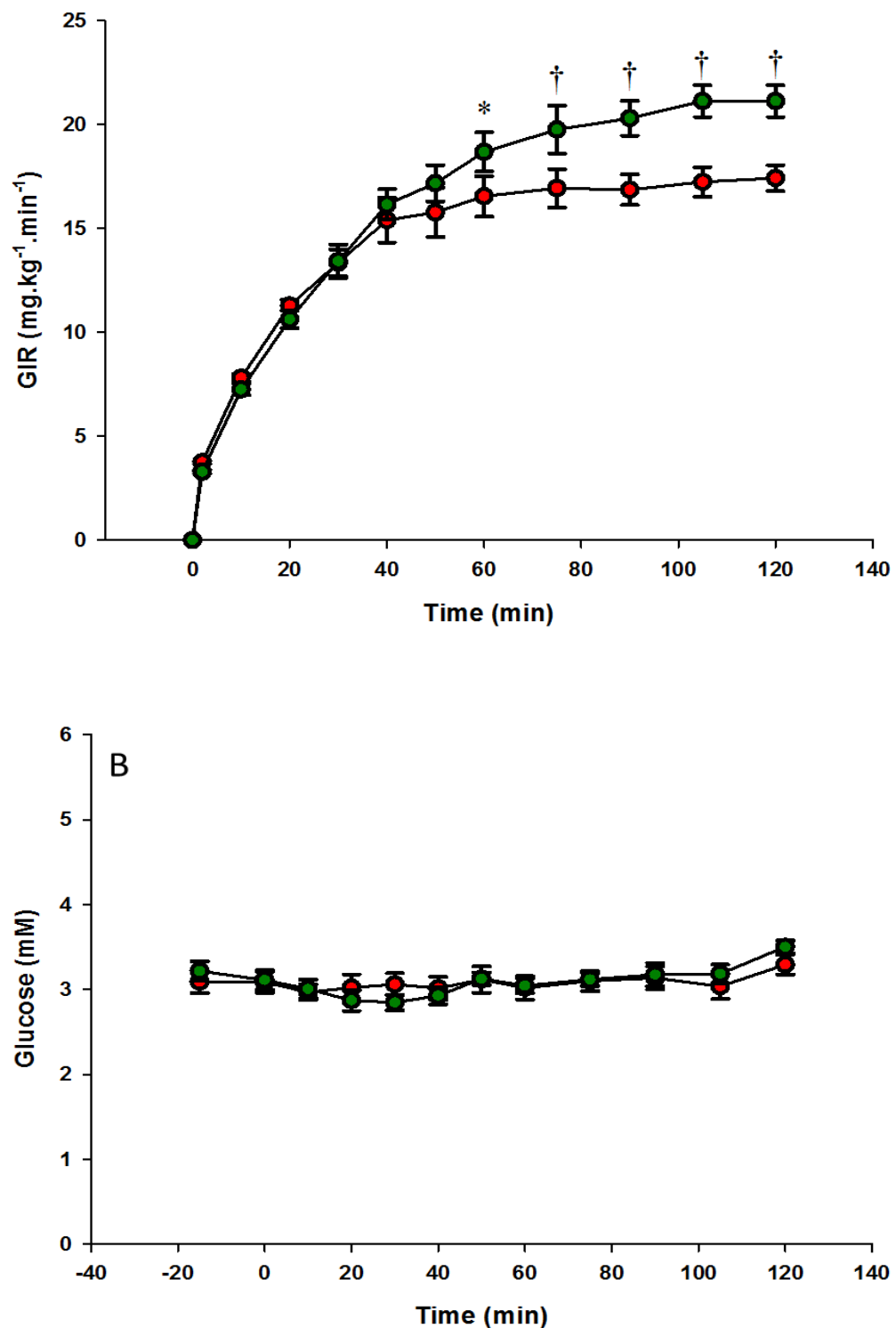


Figure 7.6 Chronic effects of EGCG on whole body insulin sensitivity in insulin resistance rats. (A) Glucose infusion rate and (B) blood glucose levels during hyperinsulinaemic euglycaemic clamp. ● - 23FDins (n = 10), ● - 23FDins + chEGCG (n = 13); * $p < 0.05$ vs. 23FDins (Two-way repeated measures ANOVA); † $p < 0.001$ vs. 23FDins (Two-way repeated measures ANOVA).

7.3.3 Chronic effects of EGCG on haemodynamic parameters *in vivo*.

Figure 7.7 shows the MAP and heart rate of the rats during the course of the experiments. MAP and heart rate were not different between groups during the course of the experiment indicating chronic EGCG treatment has no effect on these cardiovascular parameters.

FBF was measured during the experiments. At basal, FBF were not different between 23FDsal, 23FDins, and 23FDins + chEGCG rats (1.09 ± 0.12 , 0.97 ± 0.10 , and 0.96 ± 0.06 ml.min⁻¹ respectively). At the end of hyperinsulinaemic euglycaemic clamp, FBF was not different between treatment groups (Figure 7.8). This indicates that chronic EGCG treatment did not alter insulin-mediated increased in total blood flow in the insulin resistant rats.

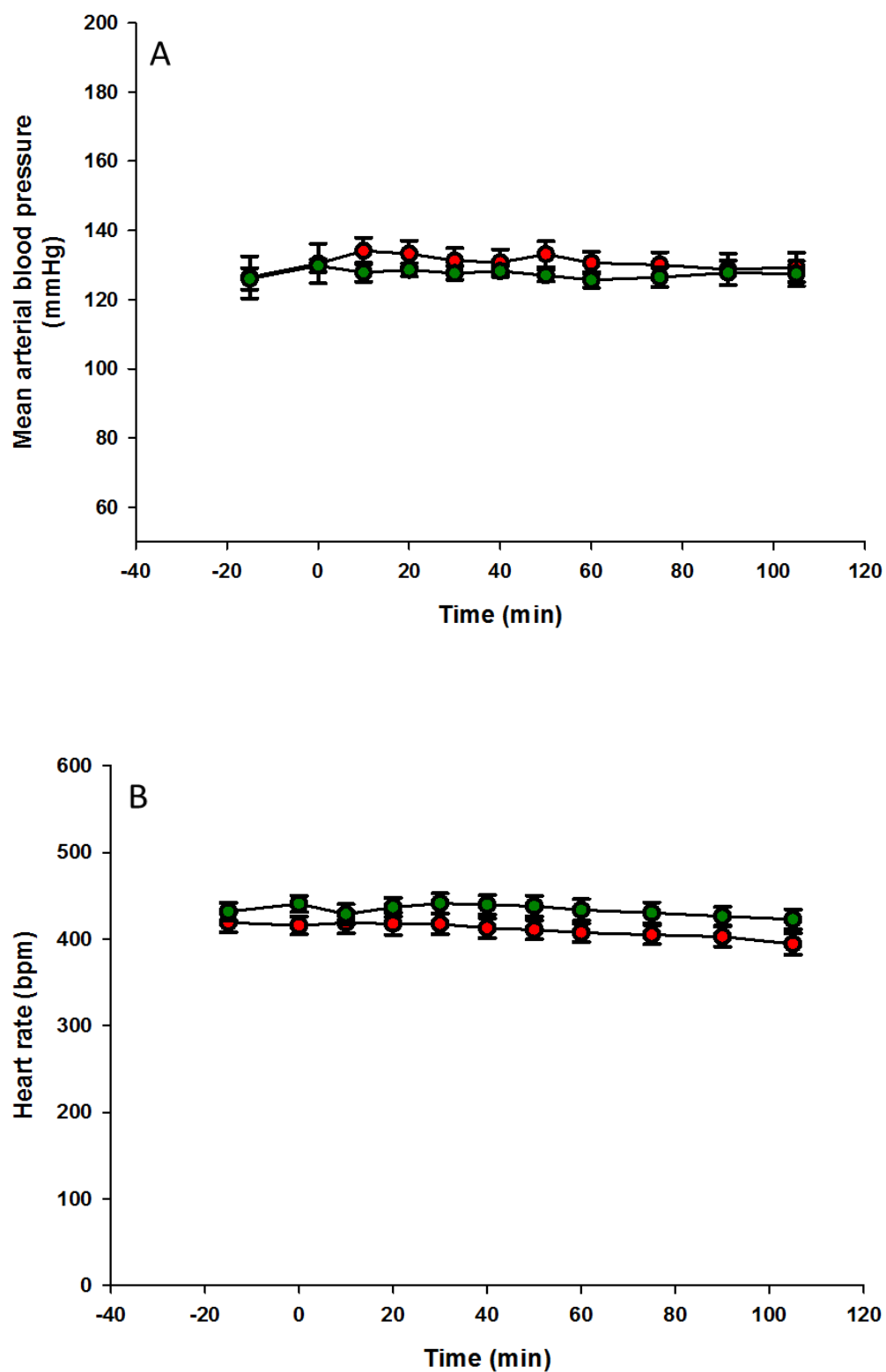
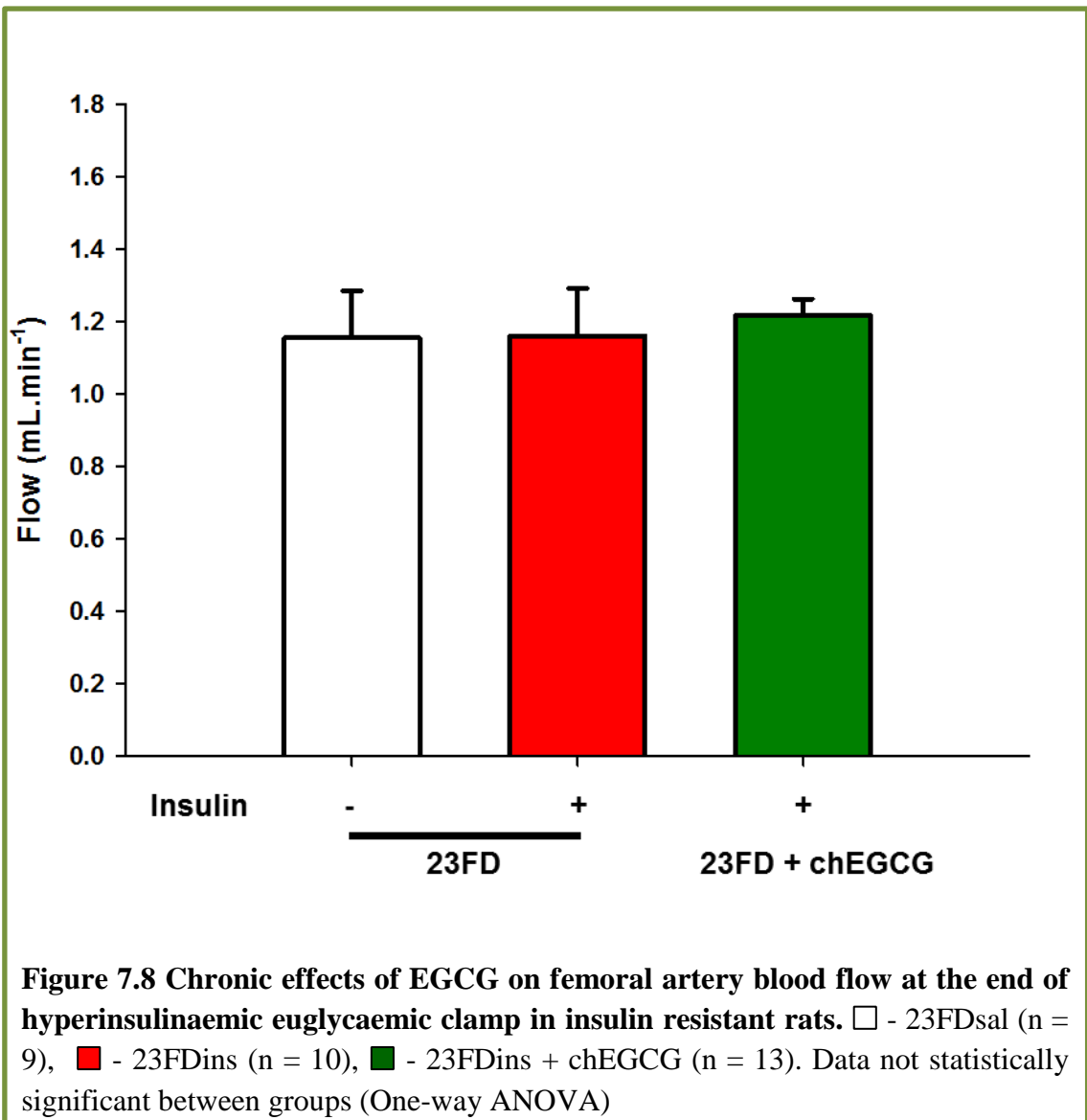


Figure 7.7 Chronic effects of EGCG on haemodynamic parameters. (A) Mean arterial blood pressure and (B) heart rate during hyperinsulinaemic euglycaemic clamp. ● - 23FDins (n = 10), ● - 23FDins + chEGCG (n = 13). Data not statistically significant at all times (Two-way repeated measures ANOVA).



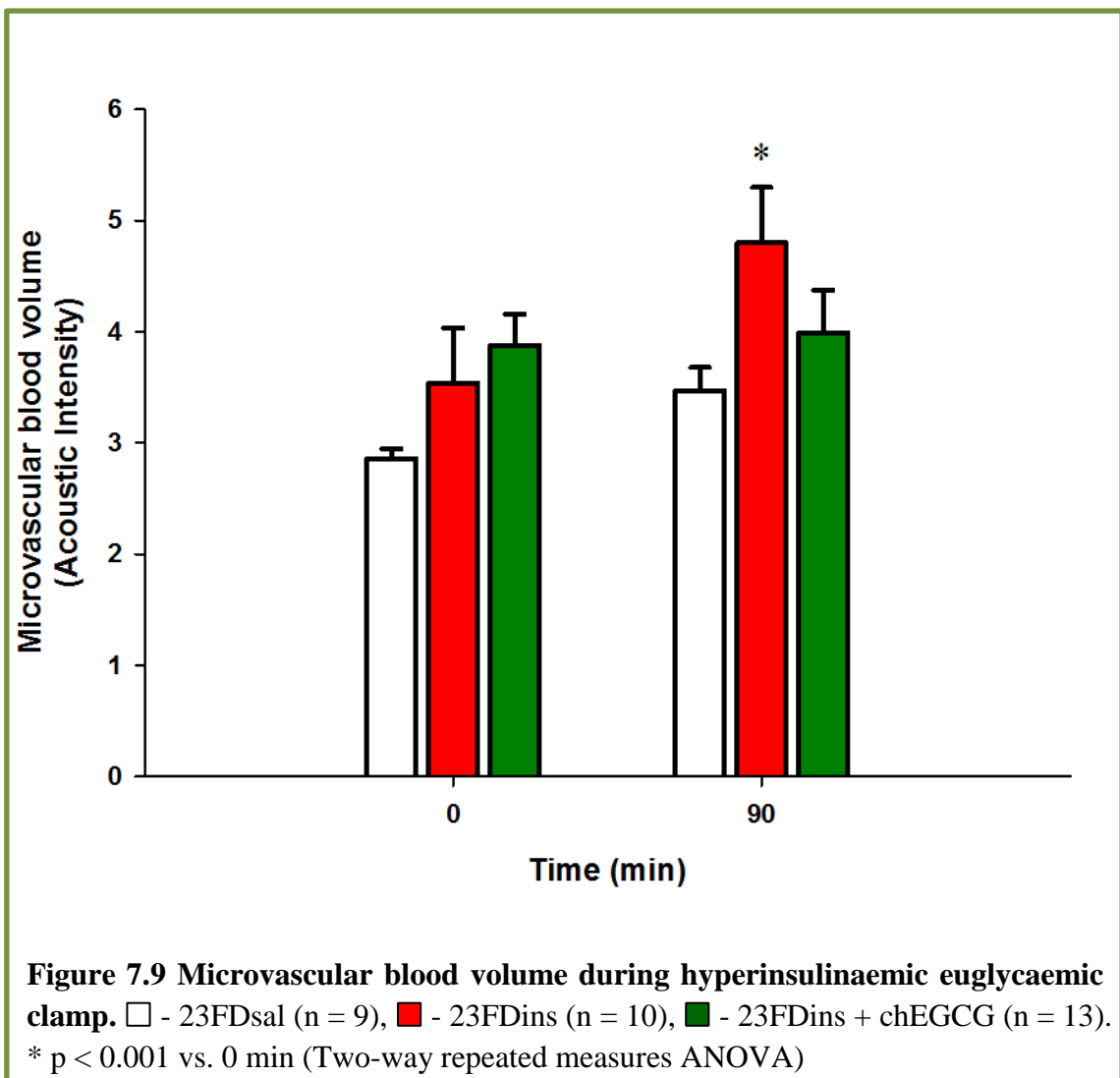
7.3.4 Chronic effects of EGCG on muscle microvascular perfusion *in vivo*.

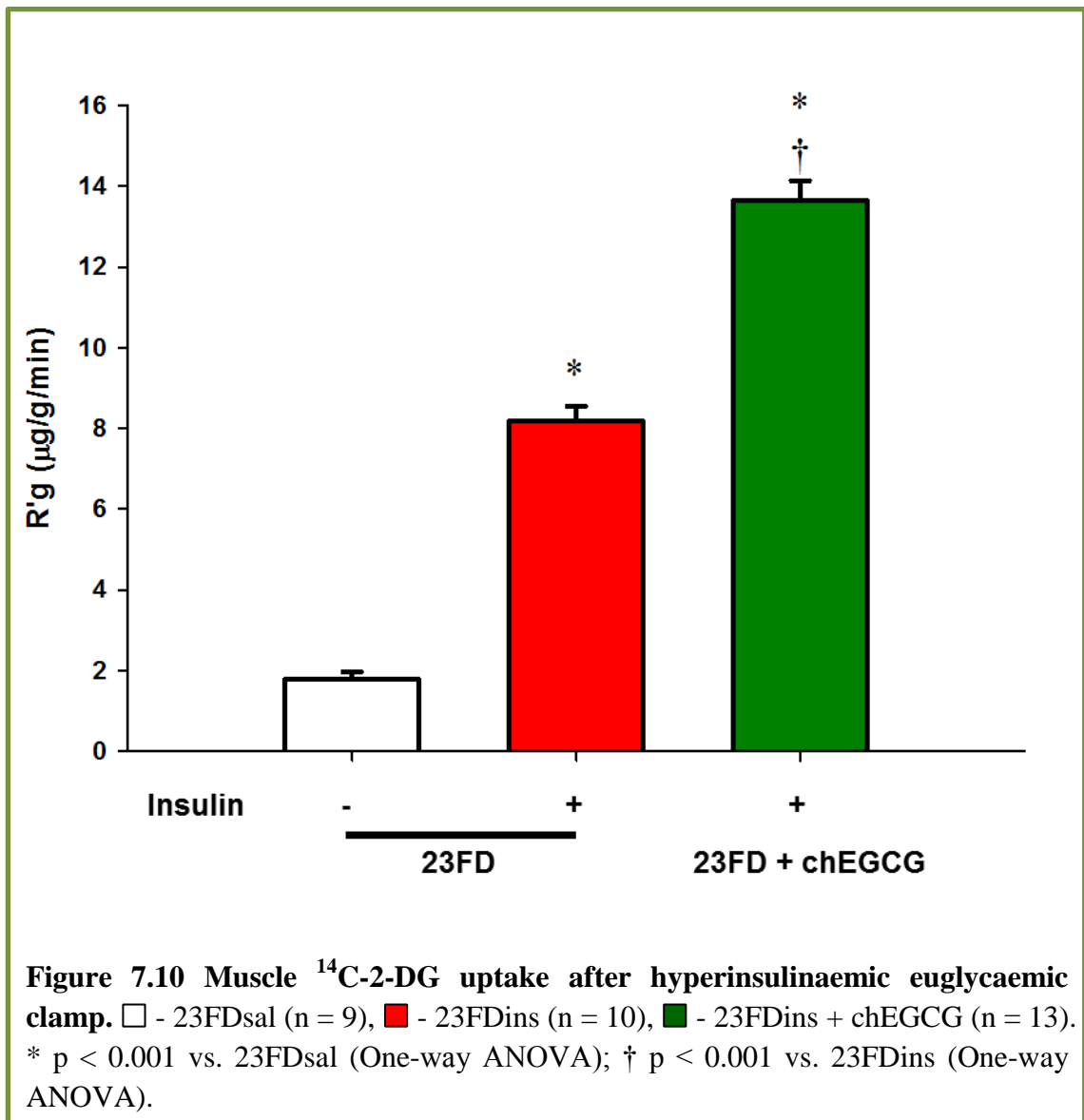
CEU was used to measure the MBV before and 90 min after the hyperinsulinaemic euglycaemic clamp (Figure 7.9). At basal, MBV was not different between the 23FDsal, 23FDins, and 23FDins + chEGCG rats (2.85 ± 0.09 , 3.54 ± 0.50 , and 3.65 ± 0.25 acoustic intensity respectively). In the 23FDins rats, insulin stimulated MBV by 1.44 fold at 90 min ($p < 0.001$). In the 23FDins + chEGCG, MBV at 90 min was not different from its basal (3.78 ± 0.36 acoustic intensity, $p = 0.632$), and was not different from the MBV of the 23FDsal and 23FDins rats at 90 min. This indicates that chronic EGCG treatment has blunted the effect of insulin to stimulate microvascular perfusion in muscle.

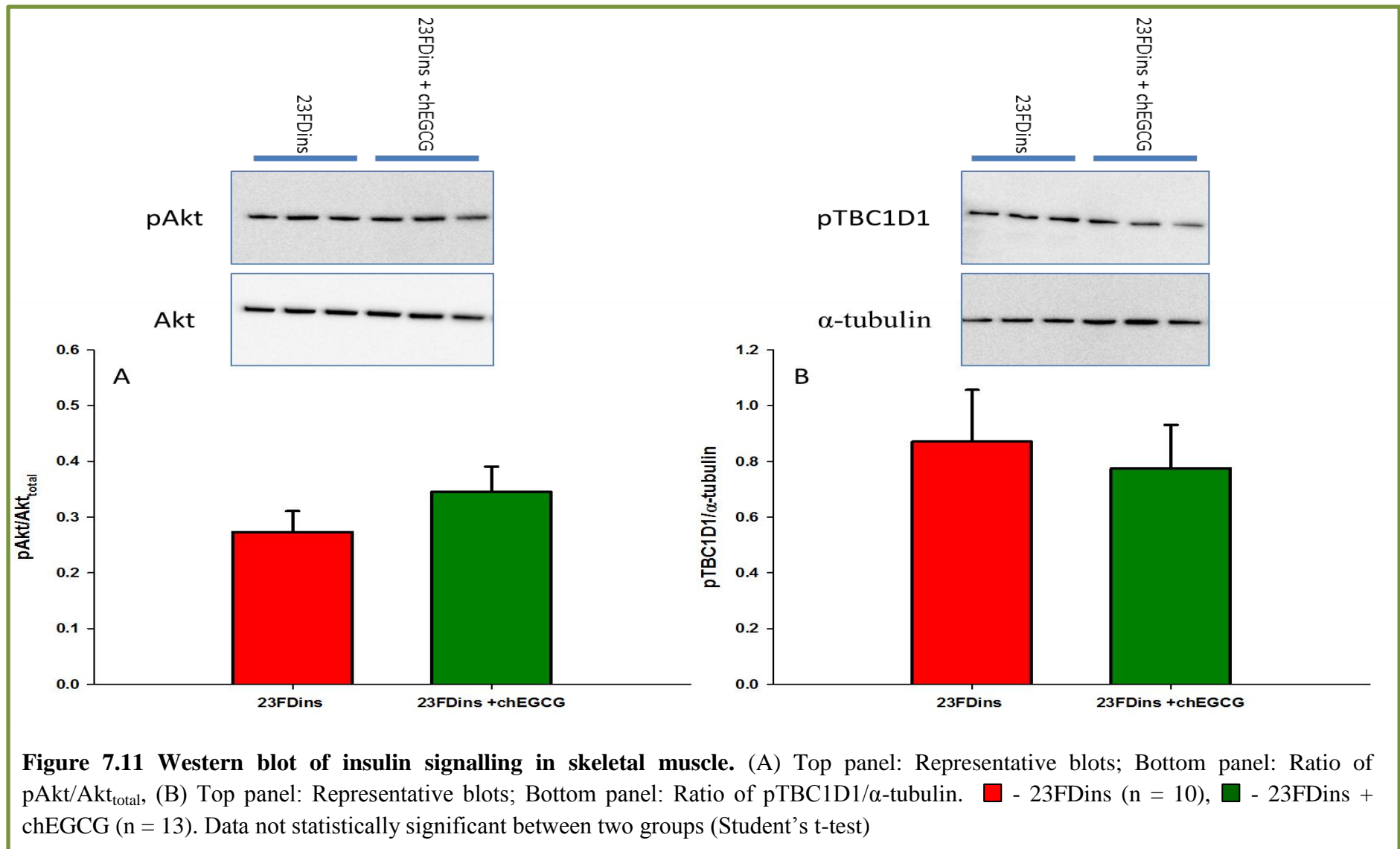
7.3.5 Chronic effects of EGCG on muscle insulin sensitivity *in vivo*.

Muscle glucose uptake was assessed using an isotopic glucose tracer which was measured at the end of the experiment. At the end of hyperinsulinaemic euglycaemic clamp, R'g of the 23FDins + chEGCG rats was significantly higher than the 23FDins rats (8.18 ± 0.37 vs. $13.64 \pm 0.50 \mu\text{g}\cdot\text{g}^{-1}\cdot\text{min}^{-1}$, $p < 0.001$, Figure 7.10). This indicates that chronic EGCG treatment has significantly improved muscle insulin sensitivity of the insulin resistant rats.

Western blot analysis (Figure 7.11) of the signalling pathway of insulin-stimulated glucose uptake in skeletal muscle showed that the phosphorylation of Akt and TBC1D1^{Thr590} were not different between the 23FDins and 23FDins + chEGCG rats following the insulin clamp. This indicates that chronic EGCG treatment has not improved insulin signalling in skeletal muscle at the end of the insulin clamp.







7.4 Discussion

The main findings of this study are that chronic EGCG treatment for 4 weeks improved whole body insulin sensitivity and insulin-stimulated muscle glucose uptake in insulin resistant rats, and this occurred in the absence of enhanced muscle microvascular perfusion. Chronic EGCG treatment in HFD-fed rats had no effect on basal metabolic profiles, including body weight, epididymal fat pad weight, HOMA-IR, and fasting plasma glucose, insulin and free fatty acids.

This is the first study that has assessed the chronic effects of EGCG treatment on whole body insulin sensitivity in insulin resistant rats using hyperinsulinaemic euglycaemic clamp. The hyperinsulinaemic euglycaemic clamp is the gold standard method to assess whole body insulin sensitivity (264). The present study showed that chronic EGCG treatment ($200 \text{ mg.kg}^{-1}.\text{d}^{-1}$) for 4 weeks significantly improved whole body insulin sensitivity. It is noted that the basal fasting plasma glucose and insulin levels, which were used for the calculations of the HOMA-IR index, were not improved following chronic EGCG treatment, indicating that the chronic EGCG treated rats were insulin resistant. This contrasts with the data from the hyperinsulinaemic euglycaemic clamp which showed improved whole body insulin sensitivity. However, the HOMA-IR, fasting plasma glucose and insulin at basal state are representations of the balance between hepatic glucose output and insulin secretion in the fasting state (265; 266), which reflect the liver insulin sensitivity and pancreatic β -cells function. Furthermore, the use of the HOMA model has not been previously validated in animal models (267). Therefore, the hyperinsulinaemic euglycaemic represents a more appropriate indication of whole body insulin sensitivity in rats.

As reported in Chapters 5 and 6, EGCG acutely stimulated MBV to a similar extent as the insulin. Unexpectedly, the present study showed that insulin-stimulated microvascular perfusion was blunted in the chronic EGCG-treated rats. A recent study (268) showed that chronic EGCG treatment ($50 - 100 \text{ mg.kg}^{-1}.\text{d}^{-1}$) for 4 weeks reduced capillary density in breast tumour tissue, but not in normal heart and skeletal muscle. Therefore it seems unlikely that the capillary density in the skeletal muscle of the rats has been affected by the chronic EGCG treatment. A previous study (120) has reported that chronic EGCG treatment ($200 \text{ mg.kg}^{-1}.\text{d}^{-1} \times 3 \text{ weeks}$) improves insulin's vascular action in mesenteric vascular bed of SHR *ex vivo*. The insulin dose ($3 \mu\text{M}$) used in Potenza's study (120) was suprapharmacological, while the present study showed that EGCG had no effect on vascular action of the more physiological 1.5 nM insulin dose *in vivo*.

Previous studies showed that insulin-stimulated microvascular perfusion is independent of total blood flow (21) and is NO-dependent (18; 53). It was somewhat surprising to see a blunted effect in insulin-stimulated increase in MBV of the chronic EGCG-treated rats. One possible explanation could be NO desensitisation in the muscle microvasculature following chronic EGCG treatment. As seen in Chapters 5 and 6, muscle microvasculature of the insulin resistant rats was more sensitive than in the healthy rats to acute EGCG treatment. In the insulin resistant rats, but not healthy rats, acute EGCG infusion increased MBV within 30 min. Furthermore, Chapter 4 showed that EGCG-mediated vasodilation in skeletal muscle is NOS-dependent. In the event that the insulin resistant rats were sensitive to EGCG-stimulated increases in MBV, there might be a chronic stimulation of NO in muscle microvasculature during the 4-week EGCG treatment in the insulin resistant rats. Studies suggested that NO desensitisation (similar to "nitrate tolerance") may occur following prolonged exposure

to NO (269-271). Following this chronic NO stimulation during EGCG treatment, the muscle microvasculature in the chronic EGCG-treated rats might have become insensitive to NO stimulated by insulin. Nonetheless, EGCG-stimulated NO production in the muscle microvasculature has not been measured in the present study, and whether the NO stimulated by EGCG has reached the level to induce NO desensitisation is not known.

Recently, Jang *et al.* (163) reported that high fat-fed mice treated with EGCG (50 mg.kg⁻¹.d⁻¹) for 10 weeks have lower fasting plasma glucose and insulin, indicating improved insulin sensitivity. Furthermore, they showed that chronic EGCG treatment improved insulin-stimulated vasodilation in the mesentery arteries in high fat-fed mice (163). This suggests that lower doses of EGCG might be beneficial to improve insulin sensitivity both vascularly and metabolically. However, whether chronic treatment with lower dose of EGCG can improve insulin-stimulated muscle microvascular perfusion and muscle glucose uptake is not known and will be important to investigate.

The present study is also the first study to assess the chronic effects of EGCG treatment on insulin-stimulated muscle glucose uptake *in vivo*. Despite the insulin-mediated microvascular perfusion being blunted following chronic EGCG treatment, insulin-stimulated muscle glucose uptake was significantly enhanced in the chronic EGCG-treated insulin resistant rats. This suggests that chronic EGCG treatment may have improved the muscle insulin sensitivity directly in the myocytes. Previous studies (172; 173) showed that EGCG stimulates GLUT4 translocation in cultured myotubes via the PI3-K/Akt pathway to promote glucose uptake. However, in the present study, the insulin signalling pathway that modulates glucose uptake in skeletal muscle, involving Akt and TBC1D1, was not enhanced in the chronic EGCG-treated rats. Therefore, the enhanced insulin-stimulated muscle glucose uptake following chronic EGCG treatment

may be mediated via an Akt-independent pathway. Studies have reported that insulin can stimulate GLUT4 translocation and glucose uptake in skeletal muscle via the Akt-independent pathway, which include the adapter protein with pleckstrin homology and Src homology 2 domains (APS) (272), PKC λ/ζ (273-275) and/or Munc18c (276). Furthermore, berberine (277; 278) and ginsenosides (279), which both are plant-derived naturally occurring products, have been shown to stimulate glucose uptake in cultured myocytes via the AMPK pathway. EGCG has also been reported to regulate its actions on inhibition of ET-1 production (211) and suppression of hepatic gluconeogenesis (174) via an AMPK-dependent pathway. This suggests that insulin-stimulated muscle glucose uptake in the chronic EGCG-treated rats might be mediated via the Akt-independent or AMPK-dependent pathways. However, whether glucose uptake in skeletal muscle following chronic EGCG treatment was mediated via the abovementioned pathway is yet to be confirmed.

In contrast, one study (261) showed that 0.5 % (w/w) EGCG treatment in HFD-fed mice for 8 days increased lipid oxidation and reduced incorporation of lipid into skeletal muscle, liver and adipose tissue. Interestingly, another study (260) has reported that HFD-fed mice treated with 0.32 % (w/w) EGCG for 15 weeks increased expressions of genes related to lipid oxidation in skeletal muscle, including nuclear respiratory factor (*nrf*) 1, medium chain acyl coA decarboxylase (*mcad*), uncoupling protein (*ucp*) 3, and peroxisome proliferator responsive element (*ppar*) α . These studies suggest that chronic EGCG treatment may have improved muscle insulin sensitivity by enhancing lipid oxidation and reducing intracellular lipid accumulation in skeletal muscle.

Other studies have shown that plasma adiponectin is elevated following chronic green tea or EGCG treatment in animals (120; 160; 280) and humans (144; 145). Adiponectin

is a metabolism stimulator adipokine secreted by adipocytes (281). Previous studies (282-284) have demonstrated that adiponectin stimulates GLUT4 translocation and glucose uptake in cultured myocytes via the AMPK pathway. Whether plasma adiponectin was elevated in the present study, which in turn resulted in increased muscle glucose uptake was not addressed.

It is important to note that following an overnight fast, EGCG was not detected in the plasma of the chronic EGCG-treated rats. Therefore the metabolic and vascular effects observed in the present study were due to the effects of long term green tea (EGCG) consumption. Although the underlying mechanisms of the chronic metabolic effects of EGCG have yet to be determined, it is concluded that chronic EGCG treatment ameliorates whole body and muscle insulin resistance in HFD-fed rats.

Chapter 8

Discussion

8.1 Summary of findings

The main hypothesis tested in this thesis was that EGCG has insulin-mimetic and/or insulin-sensitizing effects *in vivo* on vascular function to improve glucose metabolism in skeletal muscle. Prior to assessing the effects of EGCG *in vivo*, the direct vascular and metabolic actions of EGCG were characterised *in situ*. The data from the present thesis demonstrates that EGCG is a NOS-dependent, but PI3-K- and AMPK-independent vasodilator in skeletal muscle. In contrast, EGCG has no direct metabolic actions in skeletal muscle. While acute EGCG infusion increases microvascular blood volume in both healthy and insulin resistant rats *in vivo*, it does not stimulate muscle glucose uptake. However, acute EGCG infusion improves whole body insulin sensitivity in insulin resistant, but not healthy rats. Chronic EGCG treatment prevents the development of insulin resistance in rats, in which whole body insulin sensitivity and muscle glucose uptake are improved.

8.2 Vascular actions of EGCG in skeletal muscle

EGCG has been previously reported to be a vasodilator in various isolated blood vessels, including aortic ring (178; 179), bovine ophthalmic artery (180), coronary artery ring (181), and mesenteric vascular bed (119). The vascular actions of EGCG in skeletal muscle were characterised in Chapters 3 and 4 using the constant-flow perfused rat hindlimb system. Using this *in situ* preparation, the direct vascular effect of EGCG in the hindlimb vasculature can be assessed in the absence of humoral and neural input.

Since the hindlimb vasculature is free from humoral and neural input, the vasculature is fully dilated. Therefore, the hindlimb was pre-constricted using different

vasoconstrictors to study the potential vasodilatory response of EGCG. There are two distinct circulatory systems in skeletal muscle, designated as nutritive and non-nutritive flow routes (37-41). Two classes of vasoconstrictor, type A and B, have been identified based on the metabolic effects of each constrictor types. Type A vasoconstrictors (eg. low dose NE) induce vasoconstriction at the non-nutritive flow route directing flow through the nutritive route. These increase basal muscle metabolism, whereas type B vasoconstrictors (eg. 5-HT, high dose NE) stimulate vasoconstriction at the nutritive flow route and decrease muscle metabolism (Figure 3.8, see review by Clark et al. (38)). As EGCG did not dilate against high dose NE, indicating that EGCG-mediated vasodilation in skeletal muscle is not specific to type B vasoconstrictions. Data from Chapter 3 characterised a novel vascular action of EGCG to specifically oppose the vasoconstriction induced by 5-HT, but not NE. This is important as vasoconstriction induced by 5-HT acutely have been reported to reduce whole body and muscle insulin sensitivity *in vivo* (50).

The mechanism of EGCG's vascular actions in skeletal muscle was characterised in Chapter 4. Previous studies showed that EGCG mimics insulin to stimulate NO production in cultured vascular endothelial cells, via the PI3-K/Akt/eNOS pathway (119; 178-181). Studies showed that inhibition of PI3-K and NOS blunted the vasodilation induced by EGCG (119; 120; 179). However, data from Chapter 4 showed that EGCG-mediated vasodilation in skeletal muscle was blunted by L-NAME, but not wortmannin, indicating vascular action of EGCG in skeletal muscle is NOS-dependent, but PI3-K-independent. This implies that vasodilation induced by EGCG in skeletal muscle vasculature is mediated via a separate pathway from that of the other vascular tissues.

The mechanisms of EGCG-mediated vasodilation in skeletal muscle were assessed with other pathways that have been documented to stimulate a NOS-dependent vasodilation. One possible signalling pathway is via AMPK and activation of eNOS by phosphorylation on Ser¹¹⁷⁷ and Ser⁶³³ (212; 213). Previously, EGCG has been reported to activate AMPK in bovine aortic endothelial cells (211). However, data from Chapter 4 showed that vasodilation induced by EGCG in skeletal muscle is not inhibited by Compound C, an inhibitor of AMPK, indicating that EGCG-mediated vasodilation in skeletal muscle is AMPK-independent. Alternatively, Quon and colleagues (119) reported that Fyn, a member of SFK (207), is a signalling molecule upstream of PI3-K which resulted in eNOS activation and NO production. Interestingly, that study showed that SFK can directly activate eNOS independent of PI3-K (210). Data from Chapter 4 showed that PP2, an inhibitor of SFK, did not inhibit the vasodilation induced by EGCG, indicating EGCG-mediated vasodilation in skeletal muscle is SFK-independent.

The mechanism of EGCG-mediated vasodilation in skeletal muscle thus remains unknown. Other naturally occurring polyphenols (eg. epicatechin and resveratrol) have been reported to mediate vasodilation via the Ca²⁺/CaMK/eNOS (222-224) or MAPK (225-227) signalling pathway. Whether vasodilation induced by EGCG in the skeletal muscle is mediated through these signalling pathways is yet to be investigated.

Data from Chapters 5 and 6 showed that EGCG acutely stimulated microvascular perfusion, but had no effects on FBF, during hyperinsulinaemic euglycaemic clamp in both healthy and insulin resistant rats *in vivo*. The insulin resistant rats appeared to be more sensitive to EGCG-mediated microvascular perfusion, in which there was a significant increase in MBV following 30 min of EGCG infusion. Some (247; 248), but not all (249; 250), studies suggested an elevated ROS production following HFD

treatment, and ROS have been implicated in EGCG-mediated NO production in endothelial cells (119; 181). In the insulin resistant rat model used in the present study, whether there is an elevation in ROS production and the ROS level is sufficient to provoke a more sensitive response of EGCG-mediated microvascular perfusion in insulin resistant rats requires further investigation.

In another set of experiments, the chronic effects of EGCG on microvascular perfusion were assessed in insulin resistant rats. While there was no effect on insulin-stimulated FBF, microvascular perfusion responses to insulin were blunted following chronic EGCG treatment in the insulin resistant rats. This is in contrast to a study (120) which reported chronic EGCG treatment ($200 \text{ mg.kg}^{-1}.\text{min}^{-1} \times 3 \text{ weeks}$) improved insulin's vascular action in mesenteric vascular bed of SHR_s *ex vivo*. However, the effective insulin dose that was used in Potenza's study (120) was suprapharmacological ($3 \text{ } \mu\text{M}$), while the present study showed that EGCG had no effect on vascular action of 1.5 nM insulin *in vivo*. In Potenza's study (120), chronic EGCG treatment did not improve vascular action of insulin when a lower dose (1.5 nM) of insulin was tested. In contrast, EGCG has been reported to have anti-angiogenesis effects (285) and reduced capillary density in melanoma (286) and breast cancer (268) tissues. A recent study (268) showed that chronic EGCG treatment ($50 - 100 \text{ mg.kg}^{-1}.\text{d}^{-1}$) for 4 weeks reduced capillary density in breast tumour tissue, but not normal heart or skeletal muscle. Therefore it seems unlikely that the capillary density in the skeletal muscle of the rats has been affected by the chronic EGCG treatment, although this was not directly tested in the current study. One possible explanation for the blunted microvascular response following chronic EGCG treatment could be NO desensitisation. Some studies have suggested that NO desensitisation (similar to "nitrate tolerance") may occur following prolonged exposure to NO (269-271). EGCG is a NOS-dependent vasodilator in muscle

vasculature, suggesting that there might be a chronic stimulation of NO in muscle microvasculature during the 4-week EGCG treatment in the insulin resistant rats. Following this chronic NO stimulation during EGCG treatment, the muscle microvasculature in the chronic EGCG treated rats might have become insensitive to NO stimulated by insulin. Nonetheless, EGCG-stimulated NO production in the muscle microvasculature has not been measured in the present study, and whether the NO stimulated by EGCG has reached the level to induce NO desensitisation could be investigated in future.

It has been suggested that insulin-stimulated microvascular perfusion can increase delivery of nutrients, such as glucose and insulin, to skeletal muscle, resulting in increased muscle glucose uptake (231; 232). Because EGCG vasodilates in muscle vasculature and acutely stimulates microvascular perfusion in skeletal *in vivo*, it was postulated that EGCG could stimulate muscle microvascular perfusion and result in increased insulin-stimulated muscle glucose uptake *in vivo*.

8.3 Metabolic actions of EGCG in skeletal muscle

Skeletal muscle is the largest tissue in the human body responsible for storing 80 – 90 % of postprandial glucose as glycogen in healthy humans (62; 63). During insulin resistance, insulin-stimulated glucose uptake in skeletal muscle is impaired (80; 82; 239; 242). Previously, EGCG has been reported to mimic insulin's metabolic action to stimulate muscle glucose uptake *in vitro* via the PI3-K/Akt signalling pathway in cultured myotubes (172; 173; 176). In Chapter 3, the constant-flow perfused rat hindlimb preparation was used to assess the direct metabolic actions of EGCG in skeletal muscle. The direct metabolic actions of EGCG were assessed at four different

doses (0.1, 1, 10, and 100 μM). Plasma EGCG concentrations of 0.1 – 1 μM could be achieved by drinking 8 – 16 cups of green tea respectively (151; 186). Data from Chapter 3 showed that none of the EGCG doses tested have direct metabolic actions in skeletal muscle, and insulin-stimulated glucose uptake was not altered in perfused hindlimb. Another set of experiments was conducted to assess the metabolic effects of 10 μM EGCG for a longer period of time. However, muscle glucose uptake and insulin-stimulated muscle glucose uptake were not altered by 10 μM EGCG over the course of 60 min infusion. These findings contradict to previous studies in cultured myocytes (172; 173) in which EGCG dose-dependently stimulated GLUT4 translocation and glucose uptake. Furthermore, chronic green tea or EGCG treatment has been reported to promote GLUT4 translocation and glucose uptake in isolated myocytes in the absence of insulin in both healthy (157; 172) and insulin resistant (158) animals.

One possible explanation for this conflict could be that the metabolic actions of green tea or EGCG were assessed using myocyte incubations *in vitro* (157; 158; 172; 173), where glucose and EGCG were in direct contact with the myocytes rather than being delivered via vasculature (196). The constant-flow perfused rat hindlimb preparation that was employed in Chapter 3 more closely represents the *in vivo* system, in which nutrients and hormones (insulin, glucose and EGCG) are delivered to the skeletal muscle via the vasculature. Thus, the discrepancies between the *in vitro* and *in situ* studies suggest that the vasculature might act as a barrier for EGCG to stimulate glucose uptake in skeletal muscle. Cultured myocytes might be exposed to higher concentrations of EGCG without the vascular barrier, but microdialysis would need to be done to confirm this. Jung et al. (173) showed that 100 μM EGCG did not affect the viability of the cultured myocytes. However, it has been demonstrated that the highest tolerated dose of EGCG in rats *in vivo* was 12 μM (500 $\text{mg.kg}^{-1}.\text{d}^{-1}$) (197; 198), thus

assessing higher doses of EGCG is not physiologically relevant. Furthermore, plasma EGCG of 1 μ M can only be achieved with 16 cups of green tea per day, but health benefits are seen at much lower doses of green tea (> 3 cups) in humans (102; 123; 124). Therefore, it is not physiologically or even toxicologically possible to achieve doses like those used in isolated or cultured myocytes, and even less likely to be achieved if vascular system acts as a barrier. Thus, it is concluded that EGCG does not have direct metabolic actions in skeletal muscle.

Although EGCG acutely stimulated microvascular perfusion *in vivo*, this was not accompanied by increased muscle glucose uptake or insulin-stimulated muscle glucose uptake. While muscle microvascular perfusion plays a key role in determining the movement of glucose in blood to skeletal muscle (review by Barrett and Rattigan (251)), transmembrane glucose transport regulated by GLUT4 is also an important rate-limiting step of glucose uptake into muscle and adipose tissue (252). Chapter 3 showed that EGCG did not directly stimulate glucose uptake in the skeletal muscle *in situ*, suggesting that EGCG does not stimulate GLUT4 translocation into the plasma membrane of the muscle cell. Since EGCG does not stimulate GLUT4 translocation in skeletal muscle *in situ*, this may explain why the acute EGCG treatment *in vivo* stimulated muscle microvascular perfusion, but not muscle glucose uptake.

On the other hand, acute EGCG treatment resulted in a modest improvement (12%) in whole body insulin sensitivity of insulin resistant, but not healthy, rats. This is in accordance with findings by others (147; 238) which report acute green tea or EGCG treatment is metabolically beneficial for insulin resistant, but not healthy animals. EGCG has been reported to stimulate glucose uptake in adipocytes (156; 159; 238) and inhibit hepatic gluconeogenesis (174; 175) *in vitro*. Insulin-stimulated muscle glucose

uptake in the insulin resistant rats was not improved following the acute EGCG treatment, indicating that the acute EGCG treatment has improved insulin sensitivity in adipose tissue and/or liver. However, acute effects of EGCG on adipose tissue and liver insulin sensitivity *in vivo* have not been previously investigated. Therefore, more work is required before the acute effects of EGCG on whole body glucose metabolism can be fully understood.

Chronic EGCG treatments have been suggested to have anti-obesity effects (158; 161-163). Studies have suggested that EGCG treatment reduces food digestibility (261; 287) and fat absorption (161; 261) in HFD-fed mice. However, data from Chapter 7 showed that chronic EGCG treatment for 4 weeks did not alter the basal metabolic profile of the insulin resistant rats, including the body weight, epididymal fat pad weight, and fasting plasma glucose, insulin and free fatty acids. Previous studies (158; 161-163) showed that the effects of green tea or EGCG treatment on lowering body weight and fasting plasma glucose did not become apparent until week 7 of treatment. This indicates that longer EGCG treatment might be required to have apparent effects on the basal metabolic profiles. Compared to the acute EGCG treatment in insulin resistant rats, chronic EGCG treatment (200 mg.kg⁻¹.d⁻¹) resulted in a greater improvement in whole body insulin sensitivity within 4 weeks (improved GIR by 21% vs. 12%). This suggests that initially the benefits of EGCG are not mediated by improved metabolic profile. This supports the findings by other studies which showed that chronic green tea or EGCG treatment improved glucose tolerance or insulin sensitivity in both healthy (156-158; 229) and insulin resistant (98; 158-162; 164-167) animals.

In the chronic EGCG-treated rats, the improvement in whole body insulin sensitivity is, at least in part, attributable to an improvement in muscle insulin sensitivity. Data from Chapter 7 showed that insulin-stimulated muscle glucose uptake is enhanced without

increased in microvascular perfusion, suggesting that chronic EGCG treatment has improved myocyte insulin sensitivity rather than glucose or insulin delivery. Further supported by observation that in the chronic EGCG treated rats, insulin-stimulated muscle glucose uptake was improved without improving Akt-dependent muscle insulin signalling suggesting insulin delivery was not altered. Several proteins, including the APS (272), PKC λ/ζ (273-275), and Munc18c (276), have been found to stimulate GLUT4 translocation in skeletal muscle independent of Akt. Furthermore, berberine (277; 278) and ginsenosides (279), both plant-derived, naturally occurring products, have been shown to stimulate glucose uptake in cultured myocytes via the AMPK pathway. Whether chronic EGCG treatment improves the Akt-independent and/or AMPK-dependent signalling pathway in the skeletal muscle of insulin resistant rats requires further investigation.

Improvements in myocyte insulin sensitivity may have resulted from reduced intramyocellular lipid levels following chronic EGCG treatment. One study (261) showed that chronic EGCG treatment in HFD-fed mice had increased lipid oxidation and reduced lipid incorporation into skeletal muscle, liver and adipose tissue. Chronic EGCG treatment may have also improved myocyte insulin sensitivity by modulating lipid metabolism genes in skeletal muscle. Chronic EGCG treatment in HFD-mice increased expression of genes related to lipid oxidation in skeletal muscle, including the *inrf1*, *mcad*, *ucp2*, *ucp3*, and *ppara* (260; 287). These studies suggest that chronic EGCG treatment may have improved muscle insulin sensitivity by enhancing lipid oxidation and reducing intramyocellular lipid accumulation.

However, another possible mechanism of action of chronic EGCG is via reducing oxidative stress. Oxidative stress is one of the mechanisms postulated to have led to HFD-induced insulin resistance (288). Elevated fatty acids level during HFD is thought

to induce oxidative stress by increased mitochondrial uncoupling and β oxidation, which resulted in increased ROS production (289; 290). Several studies (291-294) showed that imbalance between the body antioxidant defence and ROS production resulted in insulin resistance, while restoration of this imbalance by antioxidants, such as α -lipoic acid, *N*-acetylcysteine, and taurine, ameliorates insulin resistance in rats and humans. Given that EGCG is a potent antioxidant *in vivo* (295; 296), whether chronic EGCG treatment ameliorated insulin resistance in HFD-induced insulin resistant rats by reducing oxidative stress requires further investigation.

8.4 Implications

Obesity, insulin resistance, and type 2 diabetes are growing to epidemic levels worldwide. It was estimated that in 2010, 50% of the Chinese population are pre-diabetic (297). During 2000 – 2010, prevalence of diabetes has doubled in Chinese population, increased from 5.5% to 11.6% (297; 298). Current medications and treatments for diabetes have side effects and often lose their effectiveness over time due to the progressive nature of the disease. Epidemiological studies (102; 106; 123-125) suggested long term green tea consumption of ≥ 3 cups.d⁻¹ may lower the risk of type 2 diabetes. This thesis explores the potential of EGCG to be used as an alternative medicine to prevent insulin resistance and type 2 diabetes. This thesis provides potential mechanisms between green tea consumption and reduced risk for type 2 diabetes (Figure 8.1). The overarching aim of this thesis was to explore the vascular and metabolic effects of EGCG in rats *in situ* and *in vivo*

The present study showed that acute administration of EGCG to raise plasma EGCG to 10 μ M had significantly increased insulin-mediated microvascular perfusion, but had

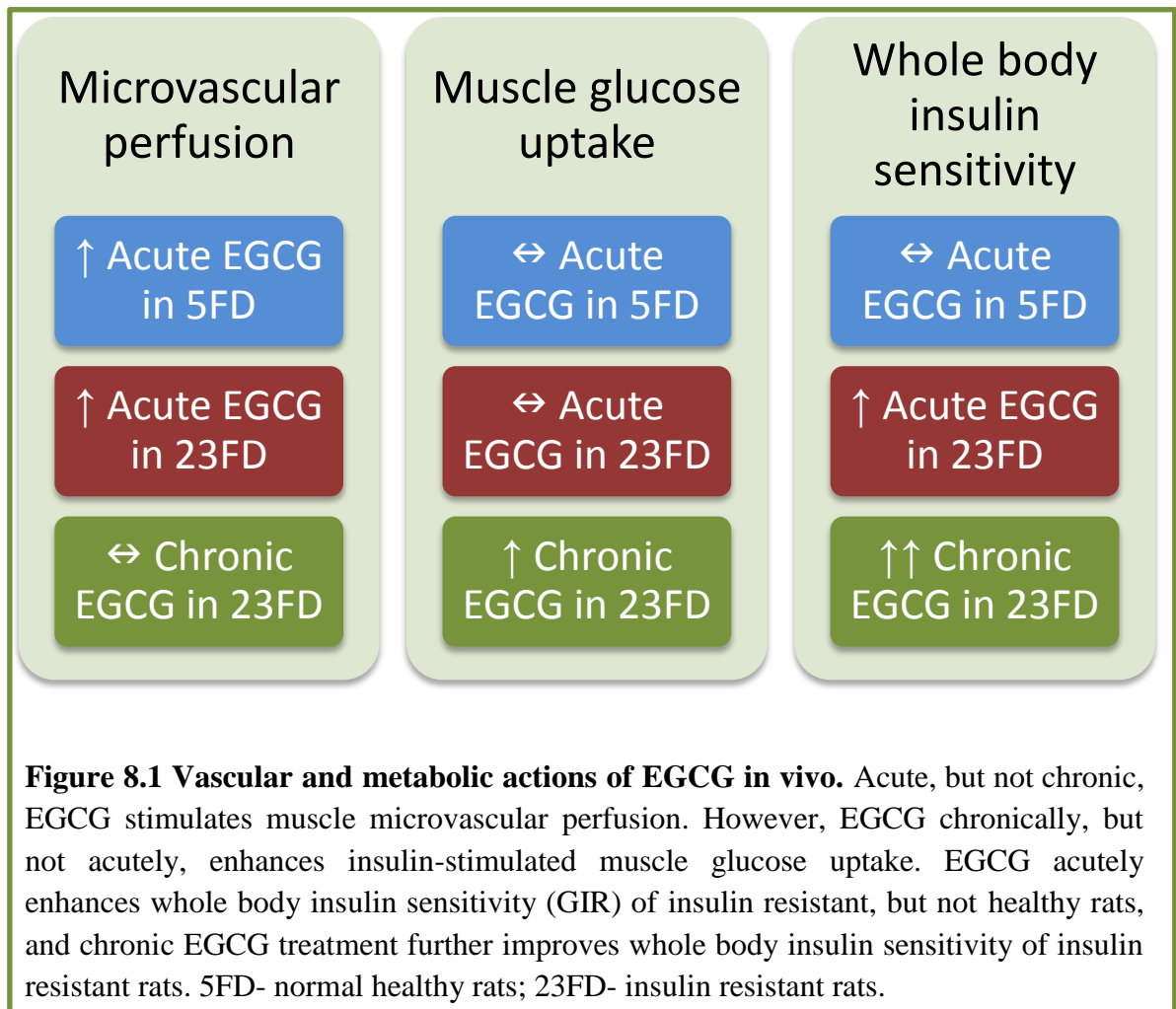
no effect on muscle glucose uptake. It has been recently reported that insulin resistance in muscle microvasculature can be developed independently of insulin resistance in myocytes (82), the current thesis suggests that acute EGCG treatment might be beneficial to subjects that display microvascular dysfunction but not myocyte insulin resistance.

However, the major benefit of EGCG is from chronic treatment, EGCG administration (200 mg.kg⁻¹.d⁻¹) for 4 weeks prevented the development of muscle insulin resistance with marked improvements in whole body insulin sensitivity in HFD insulin resistant rats. This suggests that EGCG is a prophylactic agent against insulin resistance, however, whether EGCG acts as a therapeutic agent to reverse insulin resistance requires further investigation. The most important outcome from animal data is its potential to be translated to human studies. It is noted that EGCG has poor oral bioavailability (186; 299-301), and extensive research has been undertaken to study approaches to improve the EGCG bioavailability. EGCG bioavailability could be enhanced by co-treatment of EGCG with ω 3 polyunsaturated fatty acids (302-304) or piperine (an alkaloid derived from black pepper) (305), EGCG encapsulation in chitosan nanoparticles (306; 307), and co-crystallization of EGCG (308). Nonetheless, further studies are required to assess the biological effects of these forms of EGCG.

It has been reported that EGCG undergoes high degree of glucuronidation in mice following oral administration, and only 10 – 50 % of free (unconjugated) EGCG is present in the plasma of mice (300). However, a study by Kim and colleagues (309) reported that there was 40 – 80 % of free (unconjugated) EGCG in the plasma of Sprague Dawley rats following oral administration of green tea catechins for 4 weeks. During green tea catechin administration in rats, most of the EGCG appeared to be in the colon, followed by the oesophagus and bladder (309). Kim and colleagues (309)

indicated that EGCG has low bioavailability in rats, in which EGCG is poorly absorbed and highly excreted through the faeces. However regardless of this low bioavailability, chronic EGCG administration to rats for 4 weeks in the present study produced profound effects on whole body and muscle insulin sensitivity indicating it is biologically potent.

The pharmacokinetics of EGCG in rats (299; 309) and humans (151; 186; 310) have been assessed under a variety of conditions. Furthermore, there is sufficient pharmacokinetic data in rats and humans to determine dietary versus pharmacological doses of plasma EGCG. It has been reported that in human, dietary relevant plasma doses of EGCG range from 0.1 to 1 μM (151; 186). Studies in the current thesis have been designed to test EGCG doses spanning the dietary (0.1 – 1 μM) to pharmacological (10 – 100 μM) range. EGCG levels in commercial tea leaves are approximately 20 mg.g^{-1} (107). Most tea bags have approximately 1.5 – 2 g of tea leaves per tea bag, indicating there is about 30 – 40 mg of EGCG in each tea bag. However, studies (186; 299; 310) reported that bioavailability of EGCG is higher in human than in Sprague-Dawley rats, in which maximum plasma EGCG concentrations following oral administration of 75 mg.kg^{-1} EGCG to rats and 2 mg.kg^{-1} EGCG to humans were 19.8 ng.mL^{-1} and 34.71 ng.mL^{-1} respectively. This suggests that humans might be able to drink fewer cups of green tea per day to achieve the plasma EGCG concentration found to be prophylactic in Chapter 7. However, further studies are required to determine the relevant dose for human use.



8.5 Limitations and future directions

In this thesis, EGCG treatment, both acutely and chronically, may have been more effective at lower insulin doses. In healthy rats, insulin dose-dependently ($1 - 10 \text{ mU} \cdot \text{min}^{-1} \cdot \text{kg}^{-1}$) stimulates muscle glucose uptake, while insulin-mediated microvascular perfusion reached maximal at the lowest dose of insulin ($1 \text{ mU} \cdot \text{min}^{-1} \cdot \text{kg}^{-1}$) (27). However, in HFD-induced (36% fat w/w) insulin resistant rats, while insulin-mediated microvascular perfusion was unresponsive to both physiological ($3 \text{ mU} \cdot \text{min}^{-1} \cdot \text{kg}^{-1}$) and pharmacological ($10 \text{ mU} \cdot \text{min}^{-1} \cdot \text{kg}^{-1}$) doses of insulin, loss of the skeletal muscle glucose uptake response to insulin was less evident at the higher insulin dose. The insulin dose used in this thesis was $10 \text{ mU} \cdot \text{min}^{-1} \cdot \text{kg}^{-1}$, so whole body and muscle insulin sensitivity of the acute EGCG-treated rats might have been masked and overlooked.

A number of questions have arisen from the current thesis that requires future studies. The mechanisms of EGCG-mediated vasodilation in skeletal muscle have not been fully elucidated. Determining the mechanisms may provide a better insight into the vascular actions of EGCG in skeletal muscle and identify potential therapeutic agents that may augment EGCG actions. Whilst EGCG-mediated vasodilation in skeletal muscle is NOS-dependent and PI3-K-independent, Ca^{2+} /CaMK or MAPK signalling pathways are potential pathways that activate NOS. Further studies using Western blot analysis are required to determine the activation of CaMK or MAPK by EGCG in the common iliac arteries of the perfused hindlimb. Besides that, inhibitory studies using a specific inhibitor of CaMK or MAPK, such as autocamtide-2 related inhibitory peptide and SB 202190 respectively, could be used to determine whether inhibition of these kinases inhibits EGCG-mediated vasodilation in the constant perfused rat hindlimb. Further studies are needed to assess liver and adipose tissue insulin sensitivity following acute and chronic EGCG treatment in insulin resistant rats. Furthermore,

acute EGCG treatment stimulates microvascular perfusion, indicating that EGCG might augment currently used anti-diabetic medications (eg. metformin and acarbose) that do not act on the muscle vasculature. Whether co-treatment of EGCG with current anti-diabetic medications can improve treatment outcome is not known and will be important to investigate.

The present study showed that chronic EGCG treatment for 4 weeks has improved muscle insulin sensitivity, however, the cellular mechanisms have not been fully elucidated. Some studies (260; 261) suggest that chronic treatment with EGCG may improve muscle lipid oxidation and reduce intracellular lipid accumulation in skeletal muscle. Therefore it is of important to assess the expression of genes related to muscle lipid oxidation as well as muscle lipid levels of rats treated with EGCG chronically. The present study indicated that chronic EGCG treatment might have led to NO desensitisation which led to blunted insulin-mediated microvascular perfusion. Studies have suggested that reduced activity of NO-sensitive guanylyl cyclase (271) and increased activity of phosphodiesterase (311) results in desensitisation of the NO/cGMP signalling pathway. This could be further examined and confirmed by assessing the activity of NO-sensitive guanylyl cyclase and phosphodiesterase to assess the effect of EGCG on NO sensitivity in the vasculature. Recently, one study (163) reported that chronic treatment with lower dose of EGCG ($50 \text{ mg.kg}^{-1}.\text{d}^{-1}$) improved insulin resistance and endothelial dysfunction in HFD-fed mice. If chronic EGCG treatment at $200 \text{ mg.kg}^{-1}.\text{d}^{-1}$ led to NO desensitisation in the muscle vasculature, it may be that a lower dose of EGCG preserves NO sensitivity and thereby further enhances muscle insulin sensitivity. Furthermore, it would be useful to determine whether acute and chronic actions of EGCG combine to give greater insulin sensitisation, since both vascular and metabolic (muscle glucose uptake) actions were improved by acute and

chronic EGCG administration, respectively. Similarly, whether chronic co-administration of EGCG with quinapril, an angiotensin converting enzyme inhibitor reported (52) to partially restore insulin-mediated microvascular perfusion in ZDF rats, could improve insulin sensitivity in both muscle microvascular and skeletal muscle requires further investigation. Finally, while this thesis has shown that chronic EGCG treatment prevented the development of insulin resistance in HFD-fed rats, it is important to establish whether chronic EGCG treatment reverses insulin resistance and diabetes.

8.6 Conclusion

The current thesis characterizes the direct metabolic and vascular effects of EGCG in skeletal muscle *in situ* using the constant-flow perfused rat hindlimb. EGCG is a NOS-dependent vasodilator in muscle vasculature, but had no direct metabolic actions on skeletal muscle *in situ*. For the first time, EGCG is demonstrated to induce vasodilation in skeletal muscle and more importantly oppose 5-HT, but not NE, vasoconstriction. When EGCG is administered acutely *in vivo*, whole body insulin sensitivity of insulin resistant, but not healthy rats is improved moderately. This thesis also showed that acute EGCG treatment stimulated muscle microvascular perfusion without enhancing muscle glucose uptake in both healthy and insulin resistant rats. This suggests that acute EGCG treatment might be beneficial for microvascular dysfunction in early stages of insulin resistance. On the other hand, chronic EGCG treatment improved insulin-stimulated muscle glucose uptake and ameliorated insulin resistance in insulin resistant rats. However, chronic EGCG treatment had no effects on insulin-stimulated microvascular perfusion. This was unexpected, and suggests that chronic EGCG

treatment might have led to NO-desensitization in the muscle microvasculature. Chronic EGCG treatment might have prevented insulin resistance in muscle via a non-vascular pathway. Collectively, the work presented in the current thesis showed that acute administration of EGCG is beneficial for microvascular dysfunction while chronic administration of EGCG may act as a new prophylactic agent against insulin resistance.

References

1. *IDF Diabetes Atlas*. International Diabetes Foundation, 2012
2. . *National Diabetes Fact Sheet: National estimates and general information on diabetes and prediabetes in the United States*. Atlanta, GA, 2011
3. Muniyappa R, Montagnani M, Koh KK, Quon MJ: Cardiovascular actions of insulin. *Endocr Rev* 2007;28:463-491
4. Vincent MA, Montagnani M, Quon MJ: Molecular and physiologic actions of insulin related to production of nitric oxide in vascular endothelium. *Current Diabetes Reports* 2003;3:279-288
5. Zeng GY, Quon MJ: Insulin-stimulated production of nitric oxide is inhibited by wortmannin - Direct measurement in vascular endothelial cells. *Journal of Clinical Investigation* 1996;98:894-898
6. Cardillo C, Nambi SS, Kilcoyne CM, Choucair WK, Katz A, Quon MJ, Panza JA: Insulin stimulates both endothelin and nitric oxide activity in the human forearm. *Circulation* 1999;100:820-825
7. Potenza MA, Marasciulo FL, Chieppa DM, Brigiani GS, Formoso G, Quon MJ, Montagnani M: Insulin resistance in spontaneously hypertensive rats is associated with endothelial dysfunction characterized by imbalance between NO and ET-1 production. *Am J Physiol-Heart Circul Physiol* 2005;289:H813-H822
8. Montagnani M, Chen H, Barr VA, Quon MJ: Insulin-stimulated activation of eNOS is independent of Ca²⁺ but requires phosphorylation by Akt at Ser(1179). *Journal of Biological Chemistry* 2001;276:30392-30398
9. Montagnani M, Golovchenko I, Kim I, Koh GY, Goalstone ML, Mundhekar AN, Johansen M, Kucik DF, Quon MJ, Draznin B: Inhibition of phosphatidylinositol 3-kinase enhances mitogenic actions of insulin in endothelial cells. *Journal of Biological Chemistry* 2002;277:1794-1799
10. Montagnani M, Ravichandran LV, Chen H, Esposito DL, Quon MJ: Insulin receptor substrate-1, and phosphoinositide-dependent kinase-1 are required for insulin-stimulated production of nitric oxide in endothelial. *Molecular Endocrinology* 2002;16:1931-1942
11. Formoso G, Chen H, Kim JA, Montagnani M, Consoli A, Quon MJ: Dehydroepiandrosterone mimics acute actions of insulin to stimulate production of both nitric oxide and endothelin 1 via distinct phosphatidylinositol 3-kinase- and mitogen-activated protein kinase-dependent pathways in vascular endothelium. *Molecular Endocrinology* 2006;20:1153-1163
12. Potenza MA, Marasciulo FL, Chieppa DM, Brigiani GS, Formoso G, Quon MJ, Montagnani M: Insulin resistance in spontaneously hypertensive rats is associated with endothelial dysfunction characterized by imbalance between NO and ET-1 production.

American Journal of Physiology Heart and Circulatory Physiology 2005;289:H813-H822

13. Potenza MA, Marasciulo FL, Tarquinio M, Quon MJ, Montagnani M: Treatment of Spontaneously Hypertensive Rats With Rosiglitazone and/or Enalapril Restores Balance Between Vasodilator and Vasoconstrictor Actions of Insulin With Simultaneous Improvement in Hypertension and Insulin Resistance. *Diabetes* 2006;55:3594-3603

14. Eringa EC, Stehouwer CD, Nieuw Amerongen GP, Ouwehand L, Westerhof N, Sipkema P: Vasoconstrictor effects of insulin in skeletal muscle arterioles are mediated by ERK1/2 activation in endothelium. *American Journal of Physiology Heart and Circulatory Physiology* 2004;287:H2043-H2048

15. Abramson DI, Schkloven N, Margolis MN, Mirsky IA: Influence of massive doses of insulin on peripheral blood flow in man. *American Journal of Physiology* 1939;128:124-132

16. Laakso M, Edelman SV, Brechtel G, Baron AD: Decreased effect of insulin to stimulate skeletal muscle blood flow in obese man. *Journal of Clinical Investigation* 1990;85:1844-1852

17. Steinberg HO, Brechtel G, Johnson A, Fineberg N, Baron AD: Insulin-mediated skeletal muscle vasodilation is nitric oxide dependent. A novel action of insulin to increase nitric oxide release. *Journal of Clinical Investigation* 1994;94:1172-1179

18. Vincent MA, Clerk LH, Lindner JR, Klibanov AL, Clark MG, Rattigan S, Barrett EJ: Microvascular recruitment is an early insulin effect that regulates skeletal muscle glucose uptake in vivo. *Diabetes* 2004;53:1418-1423

19. Roy D, Perreault M, Marette A: Insulin stimulation of glucose uptake in skeletal muscles and adipose tissues in vivo is NO dependent. *American Journal of Physiology* 1998;274:E692-E699

20. Natali A, Bonadonna R, Santoro D, Galvan AQ, Baldi S, Frascerra S, Palombo C, Ghione S, Ferrannini E: Insulin resistance and vasodilation in essential hypertension. Studies with adenosine. *Journal of Clinical Investigation* 1994;94:1570-1576

21. Rattigan S, Clark MG, Barrett EJ: Hemodynamic actions of insulin in rat skeletal muscle: evidence for capillary recruitment. *Diabetes* 1997;46:1381-1388

22. Nuutila P, Raitakari M, Laine H, Kirvela O, Takala T, Utriainen T, Makimattila S, Pitkanen OP, Ruotsalainen U, Iida H, Knuuti J, Yki-Jarvinen H: Role of blood flow in regulating insulin-stimulated glucose uptake in humans. Studies using bradykinin, [15O]water, and [18F]fluoro-deoxy- glucose and positron emission tomography. *Journal of Clinical Investigation* 1996;97:1741-1747

23. Mahajan H, Richards SM, Rattigan S, Clark MG: Local methacholine but not bradykinin potentiates insulin-mediated glucose uptake in muscle in vivo by augmenting capillary recruitment. *Diabetologia* 2004;47:2226-2234

24. Natali A, Quinones GA, Pecori N, Sanna G, Toschi E, Ferrannini E: Vasodilation with sodium nitroprusside does not improve insulin action in essential hypertension. *Hypertension* 1998;31:632-636
25. Pendergrass M, Fazoni E, Collins D, DeFronzo RA: IGF-I increases forearm blood flow without increasing forearm glucose uptake. *American Journal of Physiology* 1998;275:E345-E350
26. Baron AD, Steinberg H, Brechtel G, Johnson A: Skeletal muscle blood flow independently modulates insulin-mediated glucose uptake. *American Journal of Physiology* 1994;266:E248-E253
27. Zhang L, Vincent MA, Richards SM, Clerk LH, Rattigan S, Clark MG, Barrett EJ: Insulin sensitivity of muscle capillary recruitment in vivo. *Diabetes* 2004;53:447-453
28. Baron AD: Hemodynamic actions of insulin. *American Journal of Physiology* 1994;267:E187-E202
29. Delashaw JB, Duling BR: A study of the functional elements regulating capillary perfusion in striated muscle. *Microvascular Research* 1988;36:162-171
30. Murrant CL, Sarelius IH: Coupling of muscle metabolism and muscle blood flow in capillary units during contraction. *Acta Physiologica Scandinavica* 2000;168:531-541
31. Klitzman B, Damon DN, Gorczynski RJ, Duling BR: Augmented tissue oxygen supply during striated muscle contraction in the hamster. Relative contributions of capillary recruitment, functional dilation, and reduced tissue PO₂. *Circulation Research* 1982;51:711-721
32. Lindbom L, Arfors KE: Interrelationship between arteriolar blood flow distribution and capillary perfusion in skeletal muscle. *Progress in Applied Microcirculation* 1984;5:84-92
33. Honig CR, Odoroff CL, Frierson JL: Active and passive capillary control in red muscle at rest and in exercise. *American Journal of Physiology* 1982;243:H196-H206
34. Sweeney TE, Sarelius IH: Arteriolar control of capillary cell flow in striated muscle. *Circulation Research* 1989;64:112-120
35. Intaglietta M: Vasomotor activity, time-dependent fluid exchange and tissue pressure. *Microvascular Research* 1981;21:153-164
36. Rucker M, Strobel O, Vollmar B, Roesken F, Menger MD: Vasomotion in critically perfused muscle protects adjacent tissues from capillary perfusion failure. *Am J Physiol-Heart Circul Physiol* 2000;279:H550-H558
37. Clark MG, Rattigan S, Clerk LH, Vincent MA, Clark AD, Youd JM, Newman JM: Nutritive and non-nutritive blood flow: rest and exercise. *Acta Physiologica Scandinavica* 2000;168:519-530

38. Clark MG, Colquhoun EQ, Rattigan S, Dora KA, Eldershaw TP, Hall JL, Ye J: Vascular and endocrine control of muscle metabolism. *American Journal of Physiology* 1995;268:E797-E812
39. Ye JM, Colquhoun EQ, Hettiarachchi M, Clark MG: Flow-induced oxygen uptake by the perfused rat hindlimb is inhibited by vasodilators and augmented by norepinephrine: a possible role for the microvasculature in hindlimb thermogenesis. *Canadian Journal of Physiology and Pharmacology* 1990;68:119-125
40. Barlow TE, Haigh AL: Dual circulation in skeletal muscle. *Journal of Physiology* 1959;149:18P-19P
41. Barlow TE, Haigh AL, Walder DN: Evidence for two vascular pathways in skeletal muscle. *Clinical Science* 1961;20:367-385
42. Clark MG, Wallis MG, Barrett EJ, Vincent MA, Richards SM, Clerk LH, Rattigan S: Blood flow and muscle metabolism: a focus on insulin action. *American Journal of Physiology Endocrinology and Metabolism* 2003;284:E241-E258
43. Newman JM, Steen JT, Clark MG: Vessels supplying septa and tendons as functional shunts in perfused rat hindlimb. *Microvascular Research* 1997;54:49-57
44. Clerk LH, Smith ME, Rattigan S, Clark MG: Increased chylomicron triglyceride hydrolysis by connective tissue flow in perfused rat hindlimb. Implications for lipid storage. *Journal of Lipid Research* 2000;41:329-335
45. Grant RT, Wright HP: Anatomical basis for non-nutritive circulation in skeletal muscle exemplified by blood vessels of rat biceps femoris tendon. *Journal of Anatomy* 1970;106:125-133
46. Borgstrom P, Lindbom L, Arfors KE, Intaglietta M: Beta-adrenergic control of resistance in individual vessels in rabbit tenuissimus muscle. *American Journal of Physiology* 1988;254:H631-H635
47. Dawson D, Vincent MA, Barrett EJ, Kaul S, Clark A, Leong-Poi H, Lindner JR: Vascular recruitment in skeletal muscle during exercise and hyperinsulinemia assessed by contrast ultrasound. *American Journal of Physiology Endocrinology and Metabolism* 2002;282:E714-E720
48. Vincent MA, Dawson D, Clark AD, Lindner JR, Rattigan S, Clark MG, Barrett EJ: Skeletal muscle microvascular recruitment by physiological hyperinsulinemia precedes increases in total blood flow. *Diabetes* 2002;51:42-48
49. Rattigan S, Wallis MG, Youd JM, Clark MG: Exercise training improves insulin-mediated capillary recruitment in association with glucose uptake in rat hindlimb. *Diabetes* 2001;50:2659-2665
50. Rattigan S, Clark MG, Barrett EJ: Acute vasoconstriction-induced insulin resistance in rat muscle in vivo. *Diabetes* 1999;48:564-569
51. Rattigan S, Appleby GJ, Miller KA, Steen JT, Dora KA, Colquhoun EQ, Clark MG: Serotonin inhibition of 1-methylxanthine metabolism parallels its vasoconstrictor

activity and inhibition of oxygen uptake in perfused rat hindlimb. *Acta Physiologica Scandinavica* 1997;161:161-169

52. Clerk LH, Vincent MA, Barrett E, Lankford MF, Lindner JR: Skeletal muscle capillary responses to insulin are abnormal in late-stage diabetes and are restored by angiotensin converting enzyme inhibition. *American Journal of Physiology Endocrinology and Metabolism* 2007;293:E1804-E1809

53. Vincent MA, Barrett EJ, Lindner JR, Clark MG, Rattigan S: Inhibiting NOS blocks microvascular recruitment and blunts muscle glucose uptake in response to insulin. *American Journal of Physiology Endocrinology and Metabolism* 2003;285:E123-E129

54. Jarasch ED, Bruder G, Heid HW: Significance of xanthine oxidase in capillary endothelial cells. *Acta Physiologica Scandinavica Supplementum* 1986;548:39-46

55. Parks DA, Granger DN: Xanthine oxidase: biochemistry, distribution and physiology. *Acta Physiologica Scandinavica* 1986;548:87-99

56. Emmerson BT, Gordon RB, Cross M, Thomson DB: Plasma oxipurinol concentrations during allopurinol therapy. *British Journal of Rheumatology* 1987;26:445-449

57. Wei K, Jayaweera AR, Firoozan S, Linka A, Skyba DM, Kaul S: Quantification of myocardial blood flow with ultrasound-induced destruction of microbubbles administered as a constant venous infusion. *Circulation* 1998;97:473-483

58. Wei K, Le E, Bin JP, Coggins M, Thorpe J, Kaul S: Quantification of renal blood flow with contrast-enhanced ultrasound. *Journal of the American College of Cardiology* 2001;37:1135-1140

59. Jayaweera AR, Edwards N, Glasheen WP, Villanueva FS, Abbott RD, Kaul S: In vivo myocardial kinetics of air-filled albumin microbubbles during myocardial contrast echocardiography. Comparison with radiolabeled red blood cells. *Circulation Research* 1994;74:1157-1165

60. Wei K, Skyba DM, Firschke C, Jayaweera AR, Lindner JR, Kaul S: Interactions between microbubbles and ultrasound: in vitro and in vivo observations. *Journal of the American College of Cardiology* 1997;29:1081-1088

61. Coggins M, Lindner J, Rattigan S, Jahn L, Fasy E, Kaul S, Barrett E: Physiologic hyperinsulinemia enhances human skeletal muscle perfusion by capillary recruitment. *Diabetes* 2001;50:2682-2690

62. DeFronzo RA, Tripathy D: Skeletal Muscle Insulin Resistance Is the Primary Defect in Type 2 Diabetes. *Diabetes Care* 2009;32:S157-S163

63. Thiebaud D, Jacot E, DeFronzo RA, Maeder E, Jequier E, Felber JP: The effect of graded doses of insulin on total glucose uptake, glucose oxidation, and glucose storage in man. *Diabetes* 1982;31:957-963

64. Levine R, Goldstein MS: On the mechanism of action of insulin. *Hormoner* 1958;11:2-22

65. Park CR, Johnson LH: Effect of insulin on transport of glucose and galactose into cells of rat muscle and brain. *American Journal of Physiology* 1955;182:17-23
66. Birnbaum MJ: Identification of a novel gene encoding an insulin-responsive glucose transporter protein. *Cell* 1989;57:305-315
67. Charron MJ, Brosius FC, Alper SL, Lodish HF: A glucose transport protein expressed predominately in insulin-responsive tissues *Proc Natl Acad Sci U S A* 1989;86:2535-2539
68. Fukumoto H, Kayano T, Buse JB, Edwards Y, Pilch PF, Bell GI, Seino S: Cloning and characterization of the major insulin-responsive glucose transporter expressed in human skeletal muscle and other insulin-responsive tissues. *J Biol Chem* 1989;264:7776-7779
69. James DE, Strube M, Mueckler M: Molecular cloning and characterization of an insulin-regulatable glucose transporter. *Nature* 1989;338:83-87
70. Kaestner KH, Christy RJ, McLenithan JC, Braiterman LT, Cornelius P, Pekala PH, Lane MD: Sequence, tissue distribution, and differential expression of mRNA for a putative insulin-responsive glucose transporter in mouse 3T3-L1 adipocytes. *Proc Natl Acad Sci U S A* 1989;86:3150-3154
71. Leney SE, Tavaré JM: The molecular basis of insulin-stimulated glucose uptake: signalling, trafficking and potential drug targets. *Journal of Endocrinology* 2009;203:1-18
72. Ramm G, Larance M, Guilhaus M, James DE: A role for 14-3-3 in insulin-stimulated GLUT4 translocation through its interaction with the RabGAP AS160. *J Biol Chem* 2006;281:29174-29180
73. Dentin R, Liu Y, Koo SH, Hedrick S, Vargas T, Heredia J, Yates J, Montminy M: Insulin modulates gluconeogenesis by inhibition of the coactivator TORC2. *Nature* 2007;449:366-+
74. He L, Sabet A, Djedjos S, Miller R, Sun XJ, Hussain MA, Radovick S, Wondisford FE: Metformin and Insulin Suppress Hepatic Gluconeogenesis through Phosphorylation of CREB Binding Protein. *Cell* 2009;137:635-646
75. Zhou XY, Shibusawa N, Naik K, Porras D, Temple K, Ou HS, Kaihara K, Roe MW, Brady MJ, Wondisford FE: Insulin regulation of hepatic gluconeogenesis through phosphorylation of CREB-binding protein. *Nature Medicine* 2004;10:633-637
76. Herzig S, Long FX, Jhala US, Hedrick S, Quinn R, Bauer A, Rudolph D, Schutz G, Yoon C, Puigserver P, Spiegelman B, Montminy M: CREB regulates hepatic gluconeogenesis through the coactivator PGC-1. *Nature* 2001;413:179-183
77. Hunter SJ, Garvey WT: Insulin action and insulin resistance: Diseases involving defects in insulin receptors, signal transduction, and the glucose transport effector system. *American Journal of Medicine* 1998;105:331-345

78. Youd JM, Rattigan S, Clark MG: Acute impairment of insulin-mediated capillary recruitment and glucose uptake in rat skeletal muscle in vivo by TNF α . *Diabetes* 2000;49:1904-1909
79. Zhang L, Wheatley CM, Richards SM, Barrett EJ, Clark MG, Rattigan S: TNF- α acutely inhibits vascular effects of physiological but not high insulin or contraction. *American Journal of Physiology Endocrinology and Metabolism* 2003;285:E654-E660
80. St Pierre P, Genders AJ, Keske MA, Richards SM, Rattigan S: Loss of insulin-mediated microvascular perfusion in skeletal muscle is associated with the development of insulin resistance. *Diabetes, Obesity and Metabolism* 2010;12:798-805
81. Wallis MG, Wheatley CM, Rattigan S, Barrett EJ, Clark AD, Clark MG: Insulin-mediated hemodynamic changes are impaired in muscle of Zucker obese rats. *Diabetes* 2002;51:3492-3498
82. Premilovac D, Bradley EA, Ng HL, Richards SM, Rattigan S, Keske MA: Muscle insulin resistance resulting from impaired microvascular insulin sensitivity in Sprague Dawley rats. *Cardiovascular Research* 2013;
83. Cefalu WT: Animal models of type 2 diabetes: Clinical presentation and pathophysiological relevance to the human condition. *Ilar Journal* 2006;47:186-198
84. Medications for type 2 diabetes. *Diabetes Australia*, 2010
85. Ganmaa D, Willett WC, Lit TY, Feskanich D, van Dam RM, Lopez-Garcia E, Hunter DJ, Holmes MD: Coffee, tea, caffeine and risk of breast cancer: A 22-year follow-up. *International Journal of Cancer* 2008;122:2071-2076
86. Luo HT, Tang LL, Tang M, Billam M, Huang TR, Yu JH, Wei ZL, Liang YQ, Wang KB, Zhang ZQ, Zhang LS, Wang JS: Phase IIa chemoprevention trial of green tea polyphenols in high-risk individuals of liver cancer: modulation of urinary excretion of green tea polyphenols and 8-hydroxydeoxyguanosine. *Carcinogenesis* 2006;27:262-268
87. Bettuzzi S, Brausi M, Rizzi F, Castagnetti G, Peracchia G, Corti A: Chemoprevention of human prostate cancer by oral administration of green tea catechins in volunteers with high-grade prostate intraepithelial neoplasia: A preliminary report from a one-year proof-of-principle study. *Cancer Res* 2006;66:1234-1240
88. Bravo L: Polyphenols: Chemistry, dietary sources, metabolism, and nutritional significance. *Nutrition Reviews* 1998;56:317-333
89. Scalbert A, Williamson G: Dietary intake and bioavailability of polyphenols. *J Nutr* 2000;130:2073S-2085S
90. Lattanzio V, Lattanzio VMT, Cardinali A: Role of phenolics in the resistance mechanisms of plants against fungal pathogens and insects. In *Phytochemistry: Advances in Research* F I, Ed. Kerala, India, Research Signpost, 2006, p. 23-68

91. Haminiuk CWI, Maciel GM, Plata-Oviedo MSV, Peralta RM: Phenolic compounds in fruits - an overview. *International Journal of Food Science and Technology* 2012;47:2023-2044
92. Ferguson PJ, Kurowska E, Freeman DJ, Chambers AF, Koropatnick DJ: A flavonoid fraction from cranberry extract inhibits proliferation of human tumor cell lines. *J Nutr* 2004;134:1529-1535
93. Gao YT, McLaughlin JK, Blot WJ, Ji BT, Dai Q, Fraumeni JF: Reduced risk of esophageal cancer associated with green tea consumption. *J Natl Cancer Inst* 1994;86:855-858
94. Komori A, Yatsunami J, Okabe S, Abe S, Hara K, Suganuma M, Kim SJ, Fujiki H: Anticarcinogenic activity of green tea polyphenols. *Jpn J Clin Oncol* 1993;23:186-190
95. Wang ZY, Agarwal R, Bickers DR, Mukhtar H: Protection against ultraviolet B radiation-induced photocarcinogenesis in hairless mice by green tea polyphenols. *Carcinogenesis* 1991;12:1527-1530
96. Darvesh AS, Carroll RT, Bishayee A, Geldenhuys WJ, Van der Schyf CJ: Oxidative stress and Alzheimer's disease: dietary polyphenols as potential therapeutic agents. *Expert Rev Neurother* 2010;10:729-745
97. Silva AR, Pinheiro AM, Souza CS, Freitas SRVB, Vasconcellos V, Freire SM, Velozo ES, Tardy M, El-Bacha RS, Costa MFD, Costa SL: The flavonoid rutin induces astrocyte and microglia activation and regulates TNF-alpha and NO release in primary glial cell cultures. *Cell Biology and Toxicology* 2008;24:75-86
98. Chen N, Bezzina R, Hinch E, Lewandowski PA, Cameron-Smith D, Mathai ML, Jois M, Sinclair AJ, Begg DP, Wark JD, Weisinger HS, Weisinger RS: Green tea, black tea, and epigallocatechin modify body composition, improve glucose tolerance, and differentially alter metabolic gene expression in rats fed a high-fat diet. *Nutrition Research* 2009;29:784-793
99. Li HG, Forstermann U: Red Wine and Cardiovascular Health. *CircRes* 2012;111:959-961
100. Stoclet JC, Chataigneau T, Ndiaye M, Oak MH, El Bedoui J, Chataigneau M, Schini-Kerth VB: Vascular protection by dietary polyphenols. *European Journal of Pharmacology* 2004;500:299-313
101. Greenberg JA, Axen KV, Schnoll R, Boozer CN: Coffee, tea and diabetes: the role of weight loss and caffeine. *Int J Obes* 2005;29:1121-1129
102. Hamer M, Witte DR, Mosdol A, Marmot MG, Brunner EJ: Prospective study of coffee and tea consumption in relation to risk of type 2 diabetes mellitus among men and women: The Whitehall II study. *Br J Nutr* 2008;100:1046-1053
103. Song YQ, Manson JE, Buring JE, Sesso HD, Liu SM: Associations of dietary flavonoids with risk of type 2 diabetes, and markers of insulin resistance and systemic inflammation in women: A prospective study and cross-sectional analysis. *Journal of the American College of Nutrition* 2005;24:376-384

104. Polychronopoulos E, Zeimbekis A, Kastorini CM, Papairakleous N, Vlachou I, Bountziouka V, Panagiotakos DB: Effects of black and green tea consumption on blood glucose levels in non-obese elderly men and women from Mediterranean Islands (MEDIS epidemiological study). *Eur J Nutr* 2008;47:10-16
105. van Woudenberg GJ, Kuijsten A, Droogan D, Van Der A DL, Romaguera D, Ardanaz E, Amiano P, Barricarte A, Beulens JWJ, Boeing H, Bueno-De-Mesquita HB, Dahm CC, Chirlaque MD, Clavel FC, Crowe FL, Eomois PP, Fagher-Azzi G, Franks PW, Halkjaer J, Khaw KT, Masala G, Mattiello A, Nilsson P, Overvad K, Quiros JR, Rolandsson O, Romieu I, Sacerdote C, Sanchez MJ, Schulze MB, Slimani N, Sluijs I, Spijkerman AMW, Tagliabue G, Teucher B, Tjonneland A, Tumino R, Forouhi NG, Sharp S, Langenberg C, Feskens EJM, Riboli E, Wareham NJ, InterAct C: Tea Consumption and Incidence of Type 2 Diabetes in Europe: The EPIC-InterAct Case-Cohort Study. *PLoS One* 2012;7
106. Iso H, Date C, Wakai K, Fukui M, Tamakoshi A, Grp JS: The relationship between green tea and total caffeine intake and risk for self-reported type 2 diabetes among Japanese adults. *Ann Intern Med* 2006;144:554-562
107. Lin YS, Tsai YJ, Tsay JS, Lin JK: Factors affecting the levels of tea polyphenols and caffeine in tea leaves. *J Agric Food Chem* 2003;51:1864-1873
108. Vuong QV, Golding JB, Nguyen M, Roach PD: Extraction and isolation of catechins from tea. *Journal of Separation Science* 2010;33:3415-3428
109. Wang ZY, Cheng SJ, Zhou ZC, Athar M, Khan WA, Bickers DR, Mukhtar H: Antimutagenic activity of green tea polyphenols *Mutation Research* 1989;223:273-285
110. Lambert JD, Yang CS: Mechanisms of cancer prevention by tea constituents. *J Nutr* 2003;133:3262S-3267S
111. De Bacquer D, Clays E, Delanghe J, De Backer G: Epidemiological evidence for an association between habitual tea consumption and markers of chronic inflammation. *Atherosclerosis* 2006;189:428-435
112. Katiyar SK, Matsui MS, Elmets CA, Mukhtar H: Polyphenolic antioxidant (-)-epigallocatechin-3-gallate from green tea reduces UVB-induced inflammatory responses and infiltration of leukocytes in human skin. *Photochem Photobiol* 1999;69:148-153
113. Fassina G, Buffa A, Benelli R, Varnier OE, Noonan DM, Albini A: Polyphenolic antioxidant (-)-epigallocatechin-3-gallate from green tea as a candidate anti-HIV agent. *Aids* 2002;16:939-941
114. Weber JM, Ruzindana-Umunyana A, Imbeault L, Sircar S: Inhibition of adenovirus infection and adenain by green tea catechins. *Antiviral Res* 2003;58:167-173
115. Yu JX, Jia YQ, Guo YS, Chang G, Duan WS, Sun MM, Li B, Li CY: Epigallocatechin-3-gallate protects motor neurons and regulates glutamate level. *FEBS Lett* 2010;584:2921-2925

116. Basu A, Sanchez K, Leyva MJ, Wu MY, Betts NM, Aston CE, Lyons TJ: Green Tea Supplementation Affects Body Weight, Lipids, and Lipid Peroxidation in Obese Subjects with Metabolic Syndrome. *Journal of the American College of Nutrition* 2010;29:31-40
117. Hininger-Favier I, Benaraba R, Coves S, Anderson RA, Roussel AM: Green Tea Extract Decreases Oxidative Stress and Improves Insulin Sensitivity in an Animal Model of Insulin Resistance, the Fructose-Fed Rat. *Journal of the American College of Nutrition* 2009;28:355-361
118. Ou HC, Song TY, Yeh YC, Huang CY, Yang SF, Chiu TH, Tsai KL, Chen KL, Wu YJ, Tsai CS, Chang LY, Kuo WW, Lee SD: EGCG protects against oxidized LDL-induced endothelial dysfunction by inhibiting LOX-1-mediated signaling. *Journal of Applied Physiology* 2010;108:1745-1756
119. Kim JA, Formoso G, Li YH, Potenza MA, Marasciulo FL, Montagnani M, Quon MJ: Epigallocatechin gallate, a green tea polyphenol, mediates NO-dependent vasodilation using signaling pathways in vascular endothelium requiring reactive oxygen species and Fyn. *J Biol Chem* 2007;282:13736-13745
120. Potenza MA, Marasciulo FL, Tarquinio M, Tiravanti E, Colantuono G, Federici A, Kim JA, Quon MJ, Montagnani M: EGCG, a green tea polyphenol, improves endothelial function and insulin sensitivity, reduces blood pressure, and protects against myocardial I/R injury in SHR. *Am J Physiol-Endocrinol Metab* 2007;292:E1378-E1387
121. Oba S, Nagata C, Nakamura K, Fujii K, Kawachi T, Takatsuka N, Shimizu H: Consumption of coffee, green tea, oolong tea, black tea, chocolate snacks and the caffeine content in relation to risk of diabetes in Japanese men and women. *Br J Nutr* 2010;103:453-459
122. Odegaard AO, Pereira MA, Koh WP, Arakawa K, Lee HP, Yu MC: Coffee, tea, and incident type 2 diabetes: the Singapore Chinese Health Study. *American Journal of Clinical Nutrition* 2008;88:979-985
123. Huxley R, Lee CMY, Barzi F, Timmermeister L, Czernichow S, Perkovic V, Grobbee DE, Batty D, Woodward M: Coffee, decaffeinated coffee, and tea consumption in relation to incident type 2 diabetes mellitus A systematic review with meta-analysis. *Arch Intern Med* 2009;169:2053-2063
124. Jing YL, Han GJ, Hu Y, Bi Y, Li LR, Zhu DL: Tea Consumption and Risk of Type 2 Diabetes: A Meta-Analysis of Cohort Studies. *Journal of General Internal Medicine* 2009;24:557-562
125. Zheng XX, Xu YL, Li SH, Hui RT, Wu YJ, Huang XH: Effects of green tea catechins with or without caffeine on glycemic control in adults: a meta-analysis of randomized controlled trials. *American Journal of Clinical Nutrition* 2013;97:750-762
126. Shimada K, Kawarabayashi T, Tanaka A, Fukuda D, Nakamura Y, Yoshiyama M, Takeuchi K, Sawaki T, Hosoda K, Yoshikawa J: Oolong tea increases plasma adiponectin levels and low-density lipoprotein particle size in patients with coronary artery disease. *Diabetes Res Clin Pract* 2004;65:227-234

127. Hosoda K, Wang MF, Liao ML, Chuang CK, Iha M, Clevidence B, Yamamoto S: Antihyperglycemic effect of oolong tea in type 2 diabetes. *Diabetes Care* 2003;26:1714-1718
128. Basu A, Du M, Sanchez K, Leyva MJ, Betts NM, Blevins S, Wu MY, Aston CE, Lyons TJ: Green tea minimally affects biomarkers of inflammation in obese subjects with metabolic syndrome. *Nutrition* 2011;27:206-213
129. Brown AL, Lane J, Coverly J, Stocks J, Jackson S, Stephen A, Bluck L, Coward A, Hendrickx H: Effects of dietary supplementation with the green tea polyphenol epigallocatechin-3-gallate on insulin resistance and associated metabolic risk factors: randomized controlled trial. *Br J Nutr* 2009;101:886-894
130. Brown AL, Lane J, Holyoak C, Nicol B, Mayes AE, Dadd T: Health effects of green tea catechins in overweight and obese men: a randomised controlled cross-over trial. *Br J Nutr* 2011;106:1880-1889
131. Chan CCW, Koo MWL, Ng EHY, Tang OS, Yeung WSB, Ho PC: Effects of Chinese green tea on weight, and hormonal and biochemical profiles in obese patients with polycystic ovary syndrome - A randomized placebo-controlled trial. *Journal of the Society for Gynecologic Investigation* 2006;13:63-68
132. Hill AM, Coates AM, Buckley JD, Ross R, Thielecke F, Howe PRC: Can EGCG reduce abdominal fat in obese subjects? *Journal of the American College of Nutrition* 2007;26:396S-402S
133. Hursel R, Westerterp-Plantenga MS: Green tea catechin plus caffeine supplementation to a high-protein diet has no additional effect on body weight maintenance after weight loss. *American Journal of Clinical Nutrition* 2009;89:822-830
134. Diepvens K, Kovacs EMR, Vogels N, Westerterp-Plantenga MS: Metabolic effects of green tea and of phases of weight loss. *Physiol Behav* 2006;87:185-191
135. Frank J, George TW, Lodge JK, Rodriguez-Mateos AM, Spencer JPE, Minihihan AM, Rimbach G: Daily Consumption of an Aqueous Green Tea Extract Supplement Does Not Impair Liver Function or Alter Cardiovascular Disease Risk Biomarkers in Healthy Men. *J Nutr* 2009;139:58-62
136. Fukino Y, Shimbo M, Aoki N, Okubo T, Iso H: Randomized controlled trial for an effect of green tea consumption on insulin resistance and inflammation markers. *Journal of Nutritional Science and Vitaminology* 2005;51:335-342
137. Hsu CH, Tsai TH, Kao YH, Hwang KC, Tseng TY, Chou P: Effect of green tea extract on obese women: A randomized, double-blind, placebo-controlled clinical trial. *Clinical Nutrition* 2008;27:363-370
138. Hsu C-H, Liao Y-L, Lin S-C, Tsai T-H, Huang C-J, Chou P: Does supplementation with green tea extract improve insulin resistance in obese type 2 diabetics? A randomized, double-blind, and placebo-controlled clinical trial. *Alternative medicine review : a journal of clinical therapeutic* 2011;16:157-163

139. Josic J, Olsson AT, Wickeberg J, Lindstedt S, Hlebowicz J: Does green tea affect postprandial glucose, insulin and satiety in healthy subjects: a randomized controlled trial. *Nutr J* 2010;9
140. Kovacs EMR, Lejeune M, Nijs I, Westerterp-Plantenga MS: Effects of green tea on weight maintenance after body-weight loss. *Br J Nutr* 2004;91:431-437
141. Nagao T, Hase T, Tokimitsu I: A green tea extract high in catechins reduces body fat and cardiovascular risks in humans. *Obesity* 2007;15:1473-1483
142. Stendell-Hollis NR, Thomson CA, Thompson PA, Bea JW, Cussler EC, Hakim IA: Green tea improves metabolic biomarkers, not weight or body composition: a pilot study in overweight breast cancer survivors. *Journal of Human Nutrition and Dietetics* 2010;23:590-600
143. Westerterp-Plantenga MS, Lejeune M, Kovacs EMR: Body weight loss and weight maintenance in relation to habitual caffeine intake and green tea supplementation. *Obesity Research* 2005;13:1195-1204
144. Mirzaei K, Hossein-Nezhad A, Karimi M, Hosseinzadeh-Attar MJ, Jafari N, Najmafshar A, Larijani B: Effect of green tea extract on bone turnover markers in type 2 diabetic patients; A double-blind, placebo-controlled clinical trial study. *Daru-Journal of Faculty of Pharmacy* 2009;17:38-44
145. Nagao T, Meguro S, Hase T, Otsuka K, Komikado M, Tokimitsu I, Yamamoto T, Yamamoto K: A Catechin-rich Beverage Improves Obesity and Blood Glucose Control in Patients With Type 2 Diabetes. *Obesity* 2009;17:310-317
146. Ryu OH, Lee J, Lee KW, Kim HY, Seo JA, Kim SG, Kim NH, Baik SH, Choi DS, Choi KM: Effects of green tea consumption on inflammation, insulin resistance and pulse wave velocity in type 2 diabetes patients. *Diabetes Res Clin Pract* 2006;71:356-358
147. Tsuneki H, Ishizuka M, Terasawa M, Wu J, Sasaoka T, Kimura I: Effect of green tea on blood glucose levels and serum proteomic patterns in diabetic (db/db) mice and on glucose metabolism in healthy humans. *BMC Pharmacology* 2008;4
148. Venables MC, Hulston CJ, Cox HR, Jeukendrup AE: Green tea extract ingestion, fat oxidation, and glucose tolerance in healthy humans. *American Journal of Clinical Nutrition* 2008;87:778-784
149. Suliburska J, Bogdanski P, Szulinska M, Stepień M, Pupek-Musialik D, Jablecka A: Effects of Green Tea Supplementation on Elements, Total Antioxidants, Lipids, and Glucose Values in the Serum of Obese Patients. *Biological Trace Element Research* 2012;149:315-322
150. Bogdanski P, Suliburska J, Szulinska M, Stepień M, Pupek-Musialik D, Jablecka A: Green tea extract reduces blood pressure, inflammatory biomarkers, and oxidative stress and improves parameters associated with insulin resistance in obese, hypertensive patients. *Nutrition Research* 2012;32:421-427

151. Chow HHS, Hakim IA, Vining DR, Crowel JA, Ranger-Moore J, Chew WM, Celaya CA, Rodney SR, Hara Y, Alberts DS: Effects of dosing condition on the oral bioavailability of green tea catechins after single-dose administration of Polyphenon E in healthy individuals. *Clinical Cancer Research* 2005;11:4627-4633
152. Henning SM, Choo JJ, Heber D: Nongallated compared with gallated flavan-3-ols in green and black tea are more bioavailable. *J Nutr* 2008;138:1529-1534
153. Henning SM, Niu YT, Lee NH, Thames GD, Minutti RR, Wang HJ, Go VLW, Heber D: Bioavailability and antioxidant activity of tea flavanols after consumption of green tea, black tea, or a green tea extract supplement. *American Journal of Clinical Nutrition* 2004;80:1558-1564
154. Leenen R, Roodenburg AJC, Tijburg LBM, Wiseman SA: A single dose of tea with or without milk increases plasma antioxidant activity in humans. *European Journal of Clinical Nutrition* 2000;54:87-92
155. Peters CM, Green RJ, Janle EM, Ferruzzi MG: Formulation with ascorbic acid and sucrose modulates catechin bioavailability from green tea. *Food Research International* 2010;43:95-102
156. Wu LY, Juan CC, Ho LT, Hsu YP, Hwang LS: Effect of green tea supplementation on insulin sensitivity in Sprague-Dawley rats. *J Agric Food Chem* 2004;52:643-648
157. Ashida H, Furuyashiki T, Nagayasu H, Bessho H, Sakakibara H, Hashimoto T, Kanazawa K: Anti-obesity actions of green tea: Possible involvements in modulation of the glucose uptake system and suppression of the adipogenesis-related transcription factors. *Biofactors* 2004;22:135-140
158. Nishiumi S, Bessyo H, Kubo M, Aoki Y, Tanaka A, Yoshida K-i, Ashida H: Green and Black Tea Suppress Hyperglycemia and Insulin Resistance by Retaining the Expression of Glucose Transporter 4 in Muscle of High-Fat Diet-Fed C57BU6J Mice. *J Agric Food Chem* 2010;58:12916-12923
159. Wu LY, Juan CC, Hwang LS, Hsu YP, Ho PH, Ho LT: Green tea supplementation ameliorates insulin resistance and increases glucose transporter IV content in a fructose-fed rat model. *Eur J Nutr* 2004;43:116-124
160. Li RW, Douglas TD, Maiyoh GK, Adeli K, Theriault AG: Green tea leaf extract improves lipid and glucose homeostasis in a fructose-fed insulin-resistant hamster model. *J Ethnopharmacol* 2006;104:24-31
161. Bose M, Lambert JD, Ju J, Reuhl KR, Shapses SA, Yang CS: The major green tea polyphenol, (-)-epigallocatechin-3-gallate, inhibits obesity, metabolic syndrome, and fatty liver disease in high-fat-fed mice. *J Nutr* 2008;138:1677-1683
162. Axling U, Olsson C, Xu J, Fernandez C, Larsson S, Strom K, Ahrne S, Holm C, Molin G, Berger K: Green tea powder and *Lactobacillus plantarum* affect gut microbiota, lipid metabolism and inflammation in high-fat fed C57BL/6J mice. *Nutrition & Metabolism* 2012;9

163. Jang HJ, Ridgeway SD, Kim JA: Effects of the Green Tea Polyphenol, Epigallocatechin-3-Gallate (EGCG), on High Fat Diet-Induced Insulin Resistance and Endothelial Dysfunction. *Am J Physiol Endocrinol Metab* 2013;
164. Wolfram S, Raederstorff D, Preller M, Wang Y, Teixeira SR, Riegger C, Weber P: Epigallocatechin gallate supplementation alleviates diabetes in rodents. *J Nutr* 2006;136:2512-2518
165. Ortsater H, Grankvist N, Wolfram S, Kuehn N, Sjöholm A: Diet supplementation with green tea extract epigallocatechin gallate prevents progression to glucose intolerance in db/db mice. *Nutrition & Metabolism* 2012;9
166. Ihm SH, Jang SW, Kim OR, Chang K, Oak MH, Lee JO, Lim DY, Kim JH: Decaffeinated green tea extract improves hypertension and insulin resistance in a rat model of metabolic syndrome. *Atherosclerosis* 2012;224:377-383
167. Ihm SH, Lee JO, Kim SJ, Seung KB, Schini-Kerth VB, Chang K, Oak MH: Catechin prevents endothelial dysfunction in the prediabetic stage of OLETF rats by reducing vascular NADPH oxidase activity and expression. *Atherosclerosis* 2009;206:47-53
168. Matsumoto T, Kakami M, Noguchi E, Kobayashi T, Kamata K: Imbalance between endothelium-derived relaxing and contracting factors in mesenteric arteries from aged OLETF rats, a model of Type 2 diabetes. *Am J Physiol-Heart Circul Physiol* 2007;293:H1480-H1490
169. Galleano M, Bernatova I, Puzserova A, Balis P, Sestakova N, Pechanova O, Fraga CG: (-)-Epicatechin reduces blood pressure and improves vasorelaxation in spontaneously hypertensive rats by NO-mediated mechanism. *IUBMB life* 2013;65:710-715
170. Picchi A, Gao X, Belmadani S, Potter BJ, Focardi M, Chilian WM, Zhang C: Tumor necrosis factor-alpha induces endothelial dysfunction in the prediabetic metabolic syndrome. *CircRes* 2006;99:69-77
171. Sukumar P, Viswambharan H, Imrie H, Cubbon RM, Yuldasheva N, Gage M, Galloway S, Skromna A, Kandavelu P, Santos CX, Gatenby VK, Smith J, Beech DJ, Wheatcroft SB, Channon KM, Shah AM, Kearney MT: Nox2 NADPH Oxidase Has a Critical Role in Insulin Resistance-Related Endothelial Cell Dysfunction. *Diabetes* 2013;62:2130-2134
172. Ueda M, Nishiumi S, Nagayasu H, Fukuda I, Yoshida K, Ashida H: Epigallocatechin gallate promotes GLUT4 translocation in skeletal muscle. *Biochemical and Biophysical Research Communications* 2008;377:286-290
173. Jung KH, Choi HS, Kim DH, Han MY, Chang UJ, Yim SV, Song BC, Kim CH, Kang SA: Epigallocatechin gallate stimulates glucose uptake through the phosphatidylinositol 3-kinase-mediated pathway in L6 rat skeletal muscle cells. *Journal of Medicinal Food* 2008;11:429-434

174. Collins QF, Liu HY, Pi JB, Liu ZQ, Quon MJ, Cao WH: Epigallocatechin-3-gallate (EGCG), a green tea polyphenol, suppresses hepatic gluconeogenesis through 5'-AMP-activated protein kinase. *J Biol Chem* 2007;282:30143-30149
175. Waltner-Law ME, Wang XHL, Law BK, Hall RK, Nawano M, Granner DK: Epigallocatechin gallate, a constituent of green tea, represses hepatic glucose production. *J Biol Chem* 2002;277:34933-34940
176. Zhang ZF, Li Q, Liang J, Dai XQ, Ding Y, Wang JB, Li Y: Epigallocatechin-3-O-gallate (EGCG) protects the insulin sensitivity in rat L6 muscle cells exposed to dexamethasone condition. *Phytomedicine* 2010;17:14-18
177. Zhang Z, Dai X, Ding y: Epigallocatechin-3-O-gallate inhibits tumour necrosis factor- α induced insulin resistance in rat skeletal muscle cells. *Chinese Preventive Medicine* 2009;10:973-975
178. Aggio A, Grassi D, Onori E, D'Alessandro A, Masedu F, Valenti M, Ferri C: Endothelium/nitric oxide mechanism mediates vasorelaxation and counteracts vasoconstriction induced by low concentration of flavanols. *Eur J Nutr* 2012;
179. Lorenz M, Wessler S, Follmann E, Michaelis W, Dusterhoft T, Baumann G, Stangl K, Stangl V: A constituent of green tea, epigallocatechin-3-gallate, activates endothelial nitric oxide synthase by a phosphatidylinositol-3-OH-kinase-, cAMP-dependent protein kinase-, and Akt-dependent pathway and leads to endothelial-dependent vasorelaxation. *J Biol Chem* 2004;279:6190-6195
180. Romano MR, Lograno MD: Epigallocatechin-3-gallate relaxes the isolated bovine ophthalmic artery: Involvement of phosphoinositide 3-kinase-Akt-nitric oxide/cGMP signalling pathway. *European Journal of Pharmacology* 2009;608:48-53
181. Auger C, Kim JH, Chabert P, Chaabi M, Anselm E, Lanciaux X, Lobstein A, Schini-Kerth VB: The EGCg-induced redox-sensitive activation of endothelial nitric oxide synthase and relaxation are critically dependent on hydroxyl moieties. *Biochemical and Biophysical Research Communications* 2010;393:162-167
182. Alvarez E, Toimil MC, Justiniano-Basaran H, Lugnier C, Orallo F: Study of the mechanisms involved in the vasorelaxation induced by (-)-epigallocatechin-3-gallate in rat aorta. *Br J Pharmacol* 2006;147:269-280
183. Alvarez-Castro E, Campos-Toimil M, Orallo F: (-)-Epigallocatechin-3-gallate induces contraction of the rat aorta by a calcium influx-dependent mechanism. *Naunyn-Schmiedeberg's Archives of Pharmacology* 2004;369:496-506
184. Li Z, Wang Y, Vanhoutte PM: Epigallocatechin Gallate Elicits Contractions of the Isolated Aorta of the Aged Spontaneously Hypertensive Rat. *Basic & Clinical Pharmacology & Toxicology* 2011;109:47-55
185. Shen JZ, Zheng XF, Wei EQ, Kwan CY: Green tea catechins evoke a phasic contraction in rat aorta via H₂O₂-mediated multiple-signalling pathways. *Clinical and Experimental Pharmacology and Physiology* 2003;30:88-95

186. Chow HHS, Cai Y, Hakim IA, Crowell JA, Shahi F, Brooks CA, Dorr RT, Hara Y, Alberts DS: Pharmacokinetics and safety of green tea polyphenols after multiple-dose administration of epigallocatechin gallate and Polyphenon E in healthy individuals. *Clinical Cancer Research* 2003;9:3312-3319
187. Ruderman NB, Houghton CR, Hems R: Evaluation of the isolated perfused rat hindquarter for the study of muscle metabolism. *Biochemical Journal* 1971;124:639-651
188. Colquhoun EQ, Hettiarachchi M, Ye JM, Richter EA, Hnati AJ, Rattigan S, Clark MG: Vasopressin and angiotensin II stimulate oxygen uptake in the perfused rat hindlimb. *Life Sciences* 1988;43:1747-1754
189. Dora KA. Characterization of the vascular control of hindlimb metabolism. University of Tasmania, 1993
190. Fu T, Liang J, Han GZ, Lv L, Li N: Simultaneous determination of the major active components of tea polyphenols in rat plasma by a simple and specific HPLC assay. *J Chromatogr B* 2008;875:363-367
191. St-Pierre P, Keith LJ, Richards SM, Rattigan S, Keske MA: Microvascular blood flow responses to muscle contraction are not altered by high-fat feeding in rats. *Diabetes Obes Metab* 2012;14:753-761
192. Ross RM, Wadley GD, Clark MG, Rattigan S, McConell GK: Local NOS inhibition reduces skeletal muscle glucose uptake but not capillary blood flow during in situ muscle contraction in rats. *Diabetes* 2007;56:2885-2892
193. Kraegen EW, James DE, Jenkins AB, Chisholm DJ: Dose-response curves for in vivo insulin sensitivity in individual tissues in rats. *American Journal of Physiology* 1985;248:E353-E362
194. Kraegen EW, James DE, Storlien LH, Burleigh KM, Chisholm DJ: In vivo insulin resistance in individual peripheral tissues of the high fat fed rat: assessment by euglycaemic clamp plus deoxyglucose administration. *Diabetologia* 1986;29:192-198
195. Wasserman DH, Kang L, Ayala JE, Fueger PT, Lee-Young RS: The physiological regulation of glucose flux into muscle in vivo. *Journal of Experimental Biology* 2011;214:254-262
196. Bonen A, Clark MG, Henriksen EJ: Experimental approaches in muscle metabolism: hindlimb perfusion and isolated muscle incubations. *American Journal of Physiology* 1994;266:E1-16
197. Isbrucker RA, Edwards JA, Wolz E, Davidovich A, Bausch J: Safety studies on epigallocatechin gallate (EGCG) preparations. Part 2: Dermal, acute and short-term toxicity studies. *Food and Chemical Toxicology* 2006;44:636-650
198. Nakagawa K, Miyazawa T: Absorption and distribution of tea catechin, (-)-epigallocatechin-3-gallate, in the rat. *Journal of Nutritional Science and Vitaminology* 1997;43:679-684

199. Miles PD, Levisetti M, Reichart D, Khoursheed M, Moossa AR, Olefsky JM: Kinetics of insulin action in vivo - Identification of rate-limiting steps. *Diabetes* 1995;44:947-953
200. Hettiarachchi M, Colquhoun EQ, Ye JM, Rattigan S, Clark MG: Norephedrine (phenylpropanolamine) stimulates oxygen consumption and lactate production in the perfused rat hindlimb. *International Journal of Obesity and Related Metabolic Disorders* 1991;15:37-43
201. Dora KA, Richards SM, Rattigan S, Colquhoun EQ, Clark MG: Serotonin and norepinephrine vasoconstriction in rat hindlimb have different oxygen requirements. *American Journal of Physiology* 1992;262:H698-H703
202. Ye JM, Steen JT, Matthias A, Clark MG, Colquhoun EQ: Effects of noradrenaline and flow on lactate uptake in the perfused rat hindlimb. *Acta Physiologica Scandinavica* 1998;163:49-57
203. Cote C, Thibault MC, Vallieres J: Effect of endurance training and chronic isoproterenol treatment on skeletal muscle sensitivity to norepinephrine. *Life Sciences* 1985;37:695-701
204. Grubb B, Folk GE: Effect of cold acclimation on norepinephrine stimulated oxygen consumption in muscle. *Journal of Comparative Physiology* 1976;110:217-226
205. Newman JM, Clark MG: Stimulation and inhibition of resting muscle thermogenesis by vasoconstrictors in perfused rat hind limb. *Canadian Journal of Physiology and Pharmacology* 1998;76:867-872
206. Rattigan S, Dora KA, Colquhoun EQ, Clark MG: Serotonin-mediated acute insulin resistance in the perfused rat hindlimb but not in incubated muscle: a role for the vascular system. *Life Sciences* 1993;53:1545-1555
207. Resh MD: Fyn, a Src family tyrosine kinase. *Int J Biochem Cell Biol* 1998;30:1159-1162
208. Pleiman CM, Clark MR, Gauen LKT, Winitz S, Coggeshall KM, Johnson GL, Shaw AS, Cambier JC: Mapping of sites on the Src family protein tyrosine kinases p55blk, p59fyn, and p56lyn which interact with the effector molecules phospholipase C-gamma 2, microtubule-associated protein kinase, GTPase-activating protein, and phosphatidylinositol 3-kinase. *Molecular and Cellular Biology* 1993;13:5877-5887
209. Pleiman CM, Hertz WM, Cambier JC: Activation of phosphatidylinositol-3' kinase by Src-family kinase SH3 binding to the p85 subunit. *Science* 1994;263:1609-1612
210. Fulton D, Church JE, Ruan L, Li CY, Sood SG, Kemp BE, Jennings IG, Venema RC: Src kinase activates endothelial nitric-oxide synthase by phosphorylating Tyr-83. *J Biol Chem* 2005;280:35943-35952
211. Reiter CEN, Kim JA, Quon MJ: Green Tea Polyphenol Epigallocatechin Gallate Reduces Endothelin-1 Expression and Secretion in Vascular Endothelial Cells: Roles for AMP-Activated Protein Kinase, Akt, and FOXO1. *Endocrinology* 2010;151:103-114

212. Chen Z, Peng IC, Sun W, Su M-I, Hsu P-H, Fu Y, Zhu Y, Defea K, Pan S, Tsai M-D, Shyy JYJ: AMP-Activated Protein Kinase Functionally Phosphorylates Endothelial Nitric Oxide Synthase Ser633. *CircRes* 2009;104:496-U159
213. Chen ZP, Mitchelhill KI, Michell BJ, Stapleton D, Rodriguez-Crespo I, Witters LA, Power DA, de Montellano PRO, Kemp BE: AMP-activated protein kinase phosphorylation of endothelial NO synthase. *FEBS Lett* 1999;443:285-289
214. Fulton D, Gratton JP, McCabe TJ, Fontana J, Fujio Y, Walsh K, Franke TF, Papapetropoulos A, Sessa WC: Regulation of endothelium-derived nitric oxide production by the protein kinase Akt. *Nature* 1999;399:597-601
215. Boo YC, Sorescu GP, Bauer PM, Fulton D, Kemp BE, Harrison DG, Sessa WC, Jo H: Endothelial NO synthase phosphorylated at Ser(635) produces no without requiring intracellular calcium increase. *Free Radical Biology and Medicine* 2003;35:729-741
216. Lu R, Alioua A, Kumar Y, Kundu P, Eghbali M, Weisstaub NV, Gingrich JA, Stefani E, Toro L: c-Src tyrosine kinase, a critical component for 5-HT(2A) receptor-mediated contraction in rat aorta. *J Physiol-London* 2008;586:3855-3869
217. Bradley EA, Clark MG, Rattigan S: Acute effects of wortmannin on insulin's hemodynamic and metabolic actions in vivo. *American Journal of Physiology Endocrinology and Metabolism* 2007;292:E779-E787
218. Budzyn K, Ravi RM, Miller AA, Sobey CG: Mechanisms of augmented vasoconstriction induced by 5-hydroxytryptamine in aortic rings from spontaneously hypertensive rats. *Br J Pharmacol* 2008;155:210-216
219. Datte JY, Yapo PA, Offoumou MA: Nitric oxide effect on 5-hydroxytryptamine-induced vasoconstrictions of isolated smooth muscle. *Pharmacol Rep* 2005;57:113-120
220. Aldini G, Carini M, Piccoli A, Rossoni G, Facino RM: Procyanidins from grape seeds protect endothelial cells from peroxynitrite damage and enhance endothelium-dependent relaxation in human artery: new evidences for cardio-protection. *Life Sciences* 2003;73:2883-2898
221. Mizugaki M, Ishizawa F, Yamazaki T, Hishinuma T: Epigallocatechin gallate increase the prostacyclin production of bovine aortic endothelial cells. *Prostaglandins & Other Lipid Mediators* 2000;62:157-164
222. Martin S, Andriambeloson E, Takeda K, Andriantsitohaina R: Red wine polyphenols increase calcium in bovine aortic endothelial cells: a basis to elucidate signalling pathways leading to nitric oxide production. *Br J Pharmacol* 2002;135:1579-1587
223. Stoclet JC, Kleschyov A, Andriambeloson E, Diebolt M, Andriantsitohaina R: Endothelial NO release caused by red wine polyphenols. *Journal of Physiology and Pharmacology* 1999;50:535-540

224. Ramirez-Sanchez I, Maya L, Ceballos G, Villarreal F: (-)-Epicatechin Activation of Endothelial Cell Endothelial Nitric Oxide Synthase, Nitric Oxide, and Related Signaling Pathways. *Hypertension* 2010;55:1398-U1198
225. Hien TT, Oh WK, Quyen BT, Dao TT, Yoon JH, Yun SY, Kang KW: Potent vasodilation effect of amurensin G is mediated through the phosphorylation of endothelial nitric oxide synthase. *Biochemical Pharmacology* 2012;84:1437-1450
226. Klinge CM, Blankenship KA, Risinger KE, Bhatnagar S, Noisin EL, Sumanasekera WK, Zhao L, Brey M, Keynton RS: Resveratrol and estradiol rapidly activate MAPK signaling through estrogen receptors alpha and beta in endothelial cells. *J Biol Chem* 2005;280:7460-7468
227. Anter E, Chen K, Shapira OM, Karas RH, Keaney JF: p38 Mitogen-activated protein kinase activates eNOS in endothelial cells by an estrogen receptor alpha-dependent pathway in response to black tea polyphenols. *CircRes* 2005;96:1072-1078
228. Fernandez JW, Rezai-Zadeh K, Obregon D, Tan J: EGCG functions through estrogen receptor-mediated activation of ADAM10 in the promotion of non-amyloidogenic processing of APP. *FEBS Lett* 2010;584:4259-4267
229. Serrano JCE, Gonzalo-Benito H, Jove M, Fourcade S, Cassanye A, Boada J, Delgado MA, Espinel AE, Pamplona R, Portero-Otin M: Dietary intake of green tea polyphenols regulates insulin sensitivity with an increase in AMP-activated protein kinase content and changes in mitochondrial respiratory complexes. *Mol Nutr Food Res* 2013;57:459-470
230. Clerk LH, Vincent MA, Jahn LA, Liu Z, Lindner JR, Barrett EJ: Obesity blunts insulin-mediated microvascular recruitment in human forearm muscle. *Diabetes* 2006;55:1436-1442
231. Liu Z: Insulin at physiological concentrations increases microvascular perfusion in human myocardium. *American Journal of Physiology Endocrinology and Metabolism* 2007;293:E1250-E1255
232. Clark MG: Impaired microvascular perfusion: a consequence of vascular dysfunction and a potential cause of insulin resistance in muscle. *AmJPhysiol EndocrinolMetab* 2008;295:E732-E750
233. de Jongh RT, Clark AD, Ijzerman RG, Serne EH, De Vries G, Stehouwer CD: Physiological hyperinsulinaemia increases intramuscular microvascular reactive hyperaemia and vasomotion in healthy volunteers. *Diabetologia* 2004;47:978-986
234. Gudbjornsdottir S, Sjostrand M, Strindberg L, Wahren J, Lonnroth P: Direct measurements of the permeability surface area for insulin and glucose in human skeletal muscle. *Journal of Clinical Endocrinology and Metabolism* 2003;88:4559-4564
235. Renaudin C, Michoud E, Rapin JR, Lagarde M, Wiernsperger N: Hyperglycaemia modifies the reaction of microvessels to insulin in rat skeletal muscle. *Diabetologia* 1998;41:26-33

236. Aucamp J, Gaspar A, Hara Y, Apostolides Z: Inhibition of xanthine oxidase by catechins from tea (*Camellia sinensis*). *Anticancer Research* 1997;17:4381-4385
237. Lin JK, Chen PC, Ho CT, Lin-Shiau SY: Inhibition of xanthine oxidase and suppression of intracellular reactive oxygen species in HL-60 cells by theaflavin-3,3'-digallate, (-)-epigallocatechin-3-gallate, and propyl gallate. *J Agric Food Chem* 2000;48:2736-2743
238. Shao L, Liu K, Huang F, Guo XD, Wang M, Liu BL: Opposite Effects of Quercetin, Luteolin, and Epigallocatechin Gallate on Insulin Sensitivity Under Normal and Inflammatory Conditions in Mice. *Inflammation* 2013;36:1-14
239. Han DH, Hancock C, Jung SR, Holloszy JO: Is "fat-induced" muscle insulin resistance rapidly reversible? *American Journal of Physiology Endocrinology and Metabolism* 2009;297:E236-E241
240. Kraegen EW, Clark PW, Jenkins AB, Daley EA, Chisholm DJ, Storlien LH: Development of muscle insulin resistance after liver insulin resistance in high-fat-fed rats. *Diabetes* 1991;40:1397-1403
241. Kim JK, Wi JK, Youn JH: Metabolic impairment precedes insulin resistance in skeletal muscle during high-fat feeding in rats. *Diabetes* 1996;45:651-658
242. Han DH, Hansen PA, Host HH, Holloszy JO: Insulin resistance of muscle glucose transport in rats fed a high-fat diet: a reevaluation. *Diabetes* 1997;46:1761-1767
243. Halseth AE, Bracy DP, Wasserman DH: Limitations to basal and insulin-stimulated skeletal muscle glucose uptake in the high-fat-fed rat. *American Journal of Physiology Endocrinology and Metabolism* 2000;279:E1064-E1071
244. Kim JY, Nolte LA, Hansen PA, Han DH, Ferguson K, Thompson PA, Holloszy JO: High-fat diet-induced muscle insulin resistance: relationship to visceral fat mass. *American Journal of Physiology Regulatory, Integrative and Comparative Physiology* 2000;279:R2057-R2065
245. St-Pierre P, Genders AJ, Keske MA, Richards SM, Rattigan S: Loss of insulin-mediated microvascular perfusion in skeletal muscle is associated with the development of insulin resistance. *Diabetes Obes Metab* 2010;12:798-805
246. Liu HS, Chen YH, Hung PF, Kao YH: Inhibitory effect of green tea (-)-epigallocatechin gallate on resistin gene expression in 3T3-L1 adipocytes depends on the ERK pathway. *Am J Physiol-Endocrinol Metab* 2006;290:E273-E281
247. Bonnard C, Durand A, Peyrol S, Chanseaux E, Chauvin M-A, Morio B, Vidal H, Rieusset J: Mitochondrial dysfunction results from oxidative stress in the skeletal muscle of diet-induced insulin-resistant mice. *J Clin Invest* 2008;118:789-800
248. Matsuzawa-Nagata N, Takamura T, Ando H, Nakamura S, Kurita S, Misu H, Ota T, Yokoyama M, Honda M, Miyamoto K-i, Kaneko S: Increased oxidative stress precedes the onset of high-fat diet-induced insulin resistance and obesity. *Metabolism-Clinical and Experimental* 2008;57:1071-1077

249. Hoeks J, Briede JJ, de Vogel J, Schaart G, Nabben M, Moonen-Kornips E, Hesselink MKC, Schrauwen P: Mitochondrial function, content and ROS production in rat skeletal muscle: Effect of high-fat feeding. *FEBS Lett* 2008;582:510-516
250. Iossa S, Mollica MP, Lionetti L, Crescenzo R, Botta M, Liverini G: Skeletal muscle oxidative capacity in rats fed high-fat diet. *Int J Obes* 2002;26:65-72
251. Barrett EJ, Rattigan S: Muscle perfusion: its measurement and role in metabolic regulation. *Diabetes* 2012;61:2661-2668
252. Cline GW, Petersen KF, Krssak M, Shen J, Hundal RS, Trajanoski Z, Inzucchi S, Dresner A, Rothman DL, Shulman GI: Impaired glucose transport as a cause of decreased insulin-stimulated muscle glycogen synthesis in type 2 diabetes. *N Engl J Med* 1999;341:240-246
253. Manco M, Mingrone G, Greco AV, Capristo E, Gniuli D, De Gaetano A, Gasbarrini G: Insulin resistance directly correlates with increased saturated fatty acids in skeletal muscle triglycerides. *Metabolism-Clinical and Experimental* 2000;49:220-224
254. Storlien LH, Jenkins AB, Chisholm DJ, Pascoe WS, Khouri S, Kraegen EW: Influence of dietary fat composition on development of insulin resistance in rats. *Diabetes* 1991;40:280-289
255. Corcoran MP, Lamon-Fava S, Fielding RA: Skeletal muscle lipid deposition and insulin resistance: effect of dietary fatty acids and exercise. *American Journal of Clinical Nutrition* 2007;85:662-677
256. Kim JY, Hickner RC, Cortright RL, Dohm GL, Houmard JA: Lipid oxidation is reduced in obese human skeletal muscle. *Am J Physiol-Endocrinol Metab* 2000;279:E1039-E1044
257. Kahn BB, Pedersen O: Suppression of GLUT4 expression in skeletal muscle of rats that are obese from high fat feeding but not from high carbohydrate feeding or genetic obesity. *Endocrinology* 1993;132:13-22
258. Zierath JR, Houseknecht KL, Gnudi L, Kahn BB: High-fat feeding impairs insulin-stimulated GLUT4 recruitment via an early insulin-signaling defect. *Diabetes* 1997;46:215-223
259. Kim YB, Nakajima R, Matsuo T, Inoue T, Sekine T, Komuro M, Tamura T, Tokuyama K, Suzuki M: Gene expression of insulin signal-transduction pathway intermediates is lower in rats fed a beef tallow diet than in rats fed a safflower oil diet. *Metabolism-Clinical and Experimental* 1996;45:1080-1088
260. Sae-tan S, Grove KA, Kennett MJ, Lambert JD: (-)-Epigallocatechin-3-gallate increases the expression of genes related to fat oxidation in the skeletal muscle of high fat-fed mice. *Food & Function* 2011;2:111-116
261. Friedrich M, Petzke KJ, Raederstorff D, Wolfram S, Klaus S: Acute effects of epigallocatechin gallate from green tea on oxidation and tissue incorporation of dietary lipids in mice fed a high-fat diet. *Int J Obes* 2012;36:735-743

262. Deng YT, Chang TW, Lee MS, Lin JK: Suppression of Free Fatty Acid-Induced Insulin Resistance by Phytopolyphenols in C2C12 Mouse Skeletal Muscle Cells. *J Agric Food Chem* 2012;60:1059-1066
263. Vincent MA, Clerk LH, Rattigan S, Clark MG, Barrett EJ: Active role for the vasculature in the delivery of insulin to skeletal muscle. *Clinical and Experimental Pharmacology and Physiology* 2005;32:302-307
264. Kim JK: Hyperinsulinemic-euglycemic clamp to assess insulin sensitivity in vivo. *Methods in molecular biology (Clifton, NJ)* 2009;560:221-238
265. Matthews DR, Hosker JP, Rudenski AS, Naylor BA, Treacher DF, Turner RC: Homeostasis model assessment: insulin resistance and beta-cell function from fasting plasma glucose and insulin concentrations in man. *Diabetologia* 1985;28:412-419
266. Turner RC, Holman RR, Matthews D, Hockaday TDR, Peto J: Insulin deficiency and insulin resistance interaction in diabetes: estimation of their relative contribution by feedback analysis from basal plasma insulin and glucose concentrations. *Metabolism-Clinical and Experimental* 1979;28:1086-1096
267. Wallace TM, Levy JC, Matthews DR: Use and abuse of HOMA modeling. *Diabetes Care* 2004;27:1487-1495
268. Gu J-W, Makey KL, Tucker KB, Chinchar E, Mao X, Pei I, Thomas EY, Miele L: EGCG, a major green tea catechin suppresses breast tumor angiogenesis and growth via inhibiting the activation of HIF-1alpha and NFkappaB, and VEGF expression. *Vascular cell* 2013;5:9-9
269. Ohashi Y, Kawashima S, Hirata K, Yamashita T, Ishida T, Inoue N, Sakoda T, Kurihara H, Yazaki Y, Yokoyama M: Hypotension and reduced nitric oxide-elicited vasorelaxation in transgenic mice overexpressing endothelial nitric oxide synthase. *Journal of Clinical Investigation* 1998;102:2061-2071
270. Yamashita T, Kawashima S, Ohashi Y, Ozaki M, Ueyama T, Ishida T, Inoue N, Hirata K, Akita H, Yokoyama M: Resistance to endotoxin shock in transgenic mice overexpressing endothelial nitric oxide synthase. *Circulation* 2000;101:931-937
271. Yamashita T, Kawashima S, Ohashi Y, Ozaki M, Rikitake Y, Inoue N, Hirata K, Akita H, Yokoyama M: Mechanisms of reduced nitric oxide/cGMP-mediated vasorelaxation in transgenic mice overexpressing endothelial nitric oxide synthase. *Hypertension* 2000;36:97-102
272. Rea R, Gray S, Donnelly R: Contrasting effects of insulin and cellular differentiation on expression of the novel insulin receptor substrate APS in skeletal muscle. *Biochemical Pharmacology* 2005;70:1309-1311
273. Bandyopadhyay G, Kanoh Y, Sajan MP, Standaert ML, Farese RV: Effects of adenoviral gene transfer of wild-type, constitutively active, and kinase-defective protein kinase C-lambda on insulin-stimulated glucose transport in L6 myotubes. *Endocrinology* 2000;141:4120-4127

274. Kim YB, Kotani K, Ciaraldi TP, Henry RR, Kahn BB: Insulin-stimulated protein kinase C lambda/zeta activity is reduced in skeletal muscle of humans with obesity and type 2 diabetes - Reversal with weight reduction. *Diabetes* 2003;52:1935-1942
275. Standaert ML, Ortmeier HK, Sajan MP, Kanoh Y, Bandyopadhyay G, Hansen BC, Farese RV: Skeletal muscle insulin resistance in obesity-associated type 2 diabetes in monkeys is linked to a defect in insulin activation of protein kinase C-zeta/lambda/iota. *Diabetes* 2002;51:2936-2943
276. Jewell JL, Oh E, Ramalingam L, Kalwat MA, Tagliabracci VS, Tackett L, Elmendorf JS, Thurmond DC: Munc18c phosphorylation by the insulin receptor links cell signaling directly to SNARE exocytosis. *Journal of Cell Biology* 2011;193:185-199
277. Cheng Z, Pang T, Gu M, Gao A-H, Xie C-M, Li J-Y, Nan F-J, Li J: Berberine-stimulated glucose uptake in L6 myotubes involves both AMPK and p38 MAPK. *Biochimica Et Biophysica Acta-General Subjects* 2006;1760:1682-1689
278. Liu L-Z, Cheung SCK, Lan L-L, Ho SKS, Xu H-X, Chan JCN, Tong PCY: Berberine modulates insulin signaling transduction in insulin-resistant cells. *Molecular and Cellular Endocrinology* 2010;317:148-153
279. Lee MS, Hwang JT, Kim SH, Yoon S, Kim MS, Yang HJ, Kwon DY: Ginsenoside Rc, an active component of Panax ginseng, stimulates glucose uptake in C2C12 myotubes through an AMPK-dependent mechanism. *J Ethnopharmacol* 2010;127:771-776
280. Tian C, Ye XL, Zhang R, Long J, Ren WY, Ding SB, Liao D, Jin X, Wu HM, Xu SQ, Ying CJ: Green Tea Polyphenols Reduced Fat Deposits in High Fat-Fed Rats via erk1/2-PPAR gamma-Adiponectin Pathway. *PLoS One* 2013;8
281. Scherer PE, Williams S, Fogliano M, Baldini G, Lodish HF: A novel serum protein similar to C1q, produced exclusively in adipocytes. *J Biol Chem* 1995;270:26746-26749
282. Ceddia RB, Somwar R, Maida A, Fang X, Bikopoulos G, Sweeney G: Globular adiponectin increases GLUT4 translocation and glucose uptake but reduces glycogen synthesis in rat skeletal muscle cells. *Diabetologia* 2005;48:132-139
283. Tomas E, Tsao TS, Saha AK, Murrey HE, Zhang CC, Itani SI, Lodish HF, Ruderman NB: Enhanced muscle fat oxidation and glucose transport by ACRP30 globular domain: acetyl-CoA carboxylase inhibition and AMP-activated protein kinase activation. *Proceedings of the National Academy of Sciences of the United States of America* 2002;99:16309-16313
284. Yamauchi T, Kamon J, Minokoshi Y, Ito Y, Waki H, Uchida S, Yamashita S, Noda M, Kita S, Ueki K, Eto K, Akanuma Y, Froguel P, Foufelle F, Ferre P, Carling D, Kimura S, Nagai R, Kahn BB, Kadowaki T: Adiponectin stimulates glucose utilization and fatty-acid oxidation by activating AMP-activated protein kinase. *Nature Medicine* 2002;8:1288-1295

285. Cao YH, Cao RH: Angiogenesis inhibited by drinking tea. *Nature* 1999;398:381-381
286. Gu J-W, Tucker KB, Young E, Wells J, Chawla S: Oral Administration of EGCG, a Green Tea Antioxidant, Reduces Growth and Capillary Density of Melanoma but does not affect those of the Heart and Skeletal Muscles in Mice. *Faseb Journal* 2009;23
287. Klaus S, Pultz S, Thone-Reineke C, Wolfram S: Epigallocatechin gallate attenuates diet-induced obesity in mice by decreasing energy absorption and increasing fat oxidation. *Int J Obes* 2005;29:615-623
288. Evans JL, Goldfine ID, Maddux BA, Grodsky GM: Are oxidative stress-activated signaling pathways mediators of insulin resistance and beta-cell dysfunction? *Diabetes* 2003;52:1-8
289. Wojtczak L, Schonfeld P: Effect of fatty acids on energy coupling processes in mitochondria. *Biochimica et biophysica acta* 1993;1183:41-57
290. Yamagishi SI, Edelstein D, Du XL, Kaneda Y, Guzman M, Brownlee M: Leptin induces mitochondrial superoxide production and monocyte chemoattractant protein-1 expression in aortic endothelial cells by increasing fatty acid oxidation via protein kinase A. *J Biol Chem* 2001;276:25096-25100
291. Haber CA, Lam TKT, Yu ZW, Gupta N, Goh T, Bogdanovic E, Giacca A, Fantus IG: N-acetylcysteine and taurine prevent hyperglycemia-induced insulin resistance in vivo: possible role of oxidative stress. *Am J Physiol-Endocrinol Metab* 2003;285:E744-E753
292. Jacob S, Ruus P, Hermann R, Tritschler HJ, Maerker E, Renn W, Augustin HJ, Dietze GJ, Rett K: Oral administration of RAC-alpha-lipoic acid modulates insulin sensitivity in patients with type-2 diabetes mellitus: A placebo-controlled pilot trial. *Free Radical Biology and Medicine* 1999;27:309-314
293. Khamaisi M, Potashnik R, Tirosh A, Demshchak E, Rudich A, Tritschler H, Wessel K, Bashan N: Lipoic acid reduces glycemia and increases muscle GLUT4 content in streptozotocin-diabetic rats. *Metabolism-Clinical and Experimental* 1997;46:763-768
294. Konrad T, Vicini P, Kusterer K, Hoflich A, Assadkhani A, Bohles HJ, Sewell A, Tritschler HJ, Cobelli C, Usadel KH: alpha-lipoic acid treatment decreases serum lactate and pyruvate concentrations and improves glucose effectiveness in lean and obese patients with type 2 diabetes. *Diabetes Care* 1999;22:280-287
295. Uchida S, Ozaki M, Suzuki K, Shikita M: Radioprotective effects of (-)-epigallocatechin 3-O-gallate (green-tea tannin) in mice. *Life Sciences* 1992;50:147-152
296. Wiseman SA, Balentine DA, Frei B: Antioxidants in tea. *Critical Reviews in Food Science and Nutrition* 1997;37:705-718
297. Xu Y, Wang L, He J, Bi Y, Li M, Wang T, Wang L, Jiang Y, Dai M, Lu J, Xu M, Li Y, Hu N, Li J, Mi S, Chen C-S, Li G, Mu Y, Zhao J, Kong L, Chen J, Lai S, Wang W, Zhao W, Ning G, China Noncommunicable Dis S: Prevalence and Control of

Diabetes in Chinese Adults. *Jama-Journal of the American Medical Association* 2013;310:948-958

298. Gu D, Reynolds K, Duan X, Xin X, Chen J, Wu X, Mo J, Whelton PK, He J, Inter ACG: Prevalence of diabetes and impaired fasting glucose in the Chinese adult population: International Collaborative Study of Cardiovascular Disease in Asia (InterASIA). *Diabetologia* 2003;46:1190-1198

299. Chen LS, Lee MJ, Li H, Yang CS: Absorption, distribution, and elimination of tea polyphenols in rats. *Drug Metabolism and Disposition* 1997;25:1045-1050

300. Lambert JD, Lee MJ, Lu H, Meng XF, Ju J, Hong J, Seril DN, Sturgill MG, Yang CS: Epigallocatechin-3-gallate is absorbed but extensively glucuronidated following oral administration to mice. *J Nutr* 2003;133:4172-4177

301. Mereles D, Hunstein W: Epigallocatechin-3-gallate (EGCG) for Clinical Trials: More Pitfalls than Promises? *International Journal of Molecular Sciences* 2011;12:5592-5603

302. Bose M, Hao X, Ju J, Husain A, Park S, Lambert JD, Yang CS: Inhibition Of Tumorigenesis in Apc(Min/+) Mice by a Combination of (-)-Epigallocatechin-3-gallate and Fish Oil. *J Agric Food Chem* 2007;55:7695-7700

303. Giunta B, Hou H, Zhu Y, Salemi J, Ruscin A, Shytle RD, Tan J: Fish oil enhances anti-amyloidogenic properties of green tea EGCG in Tg2576 mice. *Neuroscience Letters* 2010;471:134-138

304. Shirai N, Suzuki H: Effects of simultaneous intakes of fish oil and green tea extracts on plasma, glucose, insulin, C-peptide, and adiponectin and on liver lipid concentrations in mice fed low- and high-fat diets. *Annals of Nutrition and Metabolism* 2008;52:241-249

305. Lambert JD, Hong JG, Kim DH, Mishin VM, Yang CS: Piperine enhances the bioavailability of the tea polyphenol (-)-epigallocatechin-3-gallate in mice. *J Nutr* 2004;134:1948-1952

306. Dube A, Nicolazzo JA, Larson I: Chitosan nanoparticles enhance the intestinal absorption of the green tea catechins (+)-catechin and (-)-epigallocatechin gallate. *European Journal of Pharmaceutical Sciences* 2010;41:219-225

307. Hu B, Ting Y, Zeng X, Huang Q: Bioactive Peptides/Chitosan Nanoparticles Enhance Cellular Antioxidant Activity of (-)-Epigallocatechin-3-gallate. *J Agric Food Chem* 2013;61:875-881

308. Smith AJ, Kavuru P, Arora KK, Kesani S, Tan J, Zaworotko MJ, Shytle RD: Crystal Engineering of Green Tea Epigallocatechin-3-gallate (EGCg) Cocrystals and Pharmacokinetic Modulation in Rats. *Molecular pharmaceutics* 2013;10:2948-2961

309. Kim SB, Lee MJ, Hong JI, Li C, Smith TJ, Yang GY, Seril DN, Yang CS: Plasma and tissue levels of tea catechins in rats and mice during chronic consumption of green tea polyphenols. *Nutrition and Cancer-an International Journal* 2000;37:41-48

310. Lee MJ, Maliakal P, Chen LS, Meng XF, Bondoc FY, Prabhu S, Lambert G, Mohr S, Yang CS: Pharmacokinetics of tea catechins after ingestion of green tea and (-)-epigallocatechin-3-gallate by humans: formation of different metabolites and individual variability. *Cancer Epidemiology Biomarkers & Prevention* 2002;11:1025-1032
311. Mullershausen F, Russwurm M, Thompson WJ, Liu L, Koesling D, Friebe A: Rapid nitric oxide-induced desensitization of the cGMP response is caused by increased activity of phosphodiesterase type 5 paralleled by phosphorylation of the enzyme. *Journal of Cell Biology* 2001;155:271-278